A Study of Biomarkers for Cancer Immune Checkpoint Inhibitor Therapy

Brian Richard James Bird
MB BCh BAO FRCPI

University of Dublin, Ireland
School of Medicine

A thesis submitted to Trinity College Dublin , the University of Dublin, for the Degree of Doctor of Medicine (M.D.)

June 2026

Department of Medical Oncology
Bon Secours Hospital Cork

Supervisor: Dr Stephen Finn MB BAO BCh FDS PhD FRCPath FFPATH Associate Professor, Department of Histopathology and Morbid Anatomy, TCD Consultant Histopathologist, Department of Histopathology, St James's Hospital Dublin

DECLARATION

I, Brian Bird, declare that this thesis has not been submitted as an exercise for a degree at this or any other university and it is entirely my own work.

I agree to deposit this thesis in the University's open access institutional repository or allow the Library to do so on my behalf, subject to Irish Copyright Legislation and Trinity College Library conditions of use and acknowledgement. I consent to the examiner retaining a copy of the thesis beyond the examining period, should they so wish (EU GDPR May 2018).

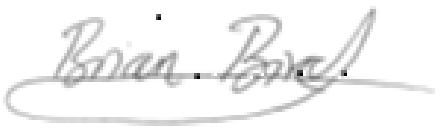

Brian Bird

Summary

Immune Checkpoint Inhibitors (ICI) have revolutionised the treatment of solid tumours and brought in a new era of oncology. However, only 40% of patients derive a significant benefit and an equal number develop autoimmune related adverse events (irAE). Current biomarkers such as Programmed Death Ligand 1 positivity (PD-L1) and Tumour Mutational Burden (TMB) lack predictive power in most cases.

The APC125 study aimed to identify novel biomarkers of immune checkpoint inhibitor response in blood, faecal microbiome, and tumour tissue in patients with unresectable solid tumours treated with PD-1/PD-L1 inhibitors. This was a single institution observational study.

Patients were also treated with standard of care combination cytotoxics where appropriate. Patients aged over 18 years with unresectable or metastatic solid tumours measurable by iRECIST criteria and scheduled to start first line anti PD-1/PD-L1 ICI therapy with or without cytotoxic chemotherapy or tyrosine kinase inhibitors (TKIs) were invited to enrol in an observational study.

Baseline white cell count (WCC) and differential, platelet count, LDH, ESR and C-Reactive Protein (CRP) were recorded as were serial WCC and differential at the second treatment visit (3 to 6 weeks later) and at the 3-month treatment and restaging Computed Tomography (CT) scan visit. The Systemic Inflammatory Index (SII) was calculated from the Full Blood Count (FBC). (SII = Neutrophils x Platelets/Lymphocytes). Serum samples were collected at all 3 time points for proteomic analysis and Kynurenine/Tryptophan ratio. PAXgene® peripheral blood mRNA tubes were collected at baseline and at the second visit only. Faecal samples were collected at baseline and second visit for microbiome analysis. Archived FFPE samples were tested for transcriptome mRNA expression. Pre-specified clinical endpoints included disease response rates as assessed by CT scans reported to iRECIST, progression free survival (PFS), overall survival (OS), and Grade 2-5 irAE.

The FACT-ICM questionnaire was used to measure changes in Quality of Life (QoL) between baseline and restaging CT visit (Visit 3). Some patients used digital tablets to

complete baseline and Visit 3 Cambridge Neuropsychological Test Automated Battery (CANTAB) testing.

Between August 2021 and December 2022, 20 patients were enrolled. The breakdown was as follows: 12 Non-Small Cell Lung Cancer (NSCLC) (7 adenocarcinoma, 5 squamous cell), 3 Extensive Stage Small Cell Lung Cancer (ES-SCLC), 2 oesophageal adenocarcinoma, 1 malignant melanoma, 1 endometrial carcinoma and 1 with triple negative breast cancer (TNBC). The median PFS and OS were 20.9 weeks and 34 weeks for the entire population and 20.1 weeks and 35.9 weeks for the NSCLC cohort. Four patients experienced Grade 3-4 irAE. Two patients with ongoing response had ICI held for multiple Grade 2 toxicities.

Higher baseline levels of CRP correlated with worse PFS ($p = 0.01$,) as did Systemic Inflammatory Index ($p = 0.20$) when analysed as single variables. Using multivariate analysis Neutrophil to Lymphocyte Ratio correlated with worse OS with a Hazard Ratio of 1.69 (95% C.I. 1.05 to 3.21). When outliers were removed using Grub's test there was a significant rise ($p= 0.03$) in Kynurenine/Tryptophan Ratio (K/T) between the pooled average of baseline and second visit blood draws which may enable identification of patients who would benefit from modification of T cell metabolism. Principle component analysis (PCA) of baseline serum immune proteins using the 96 Immune-Oncology Olink Proximity Extension Assay identified candidate biomarkers of worse OS including elevated levels of circulating Platelet Derived Growth Factor Subunit Beta (PDGF BB) and Vascular Endothelial Growth Factor Receptor 2 (VEGF R2). Although not significant it is possible that patients with high levels of serum PDGF BB and VEGF R2 would benefit from simultaneous targeting of angiogenesis and immune checkpoints. mRNA analysis suggests that upregulation of Extracellular Membrane gene pathways and downregulation of immune activation correlated with better response as per first restaging CT scan imaging measured by iRECIST. Faecal microbiome alpha diversity increased on treatment and beta diversity decreased but did not correlate with clinical outcomes.

Acknowledgements

I would like to thank each of the patients who took part in this research and their families. They taught me about how to live with adversity and find meaning through the possibility of helping others. A unique and larger than life patient who sadly died before this work started donated generously to the Trinity Foundation which enabled it and I think of them often. A great lady, Mrs Ita McEnery, raised money during her illness for Cúnamh, which helped with research nurse funding.

I wish to thank my supervisor, Prof Stephen Finn, for his kind and wise support, guidance, and encouragement. He helped me navigate the challenges posed by scientific collaboration across sites and countries.

This work was inspired by meeting Dr Ken Nally APC UCC and our shared fascination with the immune system and a belief in harnessing it to help people. Prof Richard Flavin TCD was unfailingly encouraging, practical and patient. They both helped me to understand how best to turn ideas into academic reality. I would like to thank all the skilled and compassionate Oncology Research Nurses in Bon Secours Cork who worked so hard on patient education and recruitment, gathering samples, and collecting clinical data during the COVID pandemic. Clinical data and patient samples were gathered by Oncology Research Nurses in Bon Secours Cork, including Ms. Evelyn O'Sullivan Greene, Ms Lisa Stack, Ms Lucia Moloney and Mr Richard O'Callaghan.

The staff in the Alimentary Pharmaceutical Centre, University College Cork who helped greatly with protocol writing, data sharing agreements and gaining ethical approval as we met online are superb. Dr James Boyle and Ms. Akshaya Moktur (both medical students in UCC) tabulated the Quality-of-Life Survey data. Dr Karine Ronan is a talented physician and illustrator and her artwork which is included in this thesis appeared on the front cover of *Diagnostics*. Dr Aine O'Reilly encouraged me to use PRISM and to write a thesis properly.

I am grateful to Dr Cristina Rosell-Cardona undertook the measurements of tryptophan and kynurenine pathway metabolites and performed statistical analysis supervised by Prof Gerard Clarke (both at APC Microbiome Ireland/Department of Psychiatry and

Neurobehavioural Science, University College Cork). Dr Jason Martin set up and remotely supervised CANTAB psychomotor assessments. Dr Cian Hurley and Dr Dara Meehan at the O'Toole Lab UCC and Dr Ciaran Devoy at the Tangney Lab in UCC were instrumental in arranging storage, processing and analysis of the microbiome samples which were sequenced by Novogene. mRNA analysis was carried out by Mr Mohammed Alkhatib of GenXPro GmbH, Frankfurt Germany in consultation with me for clinical guidance. Dr Darren Dahly, UCC who endeavoured to help me understand some statistics and assisted with analysis of data is to be commended for his tolerance. I would like to thank Dr Anne-Marie Baird (Trinity Translational Medicine Institute) for her detailed reading and invaluable scientific feedback.

I dedicate this thesis to my wife, Janice, who believed I could do it, and my daughters Suzanne and Anabel who continually inspire me. Thanks, are also due to my terriers Marco and Pickles for walks along the River Lee.

FUNDING

This investigator-initiated study was made possible by patient donations to the St James's Foundation, Cúnamh and an unrestricted research grant from Roche Ireland.

scientia vincere tenebra

OUTPUT OF THESIS RESEARCH

The work has contributed to two peer -reviewed journal publications and was presented at the 2022 Irish Lung Cancer Alliance Meeting. Details of research outputs are below:

Healey Bird, B., Nally, K., Ronan, K., Clarke, G., Amu, S., Almeida, A.S., Flavin, R. and Finn, S. (2022) 'Cancer Immunotherapy with Immune Checkpoint Inhibitors – Biomarkers of Response and Toxicity; Current Limitations and Future Promise', *Diagnostics 12(1):124*.

Leigh, S.J., Lynch, C.M.K., Healey Bird, B., Griffin, B.T., Cryan, J.F. and Clarke, G. (2022) 'Gut microbiota-drug interactions in cancer pharmacotherapies: implications foe efficacy and adverse effects', *Expert opinion on Drug Metabolism and Toxicity, 18(1), 5-26*.

Healey Bird, B. (2022) 'Update on APC125 Biomarker study, interim survival data and clinical details of first 10 patients', *Presentation (online) to Meeting of Irish Lung Cancer Alliance, June 2022*.

TABLE OF CONTENTS

LIST OF FIGURES

LIST OF TABLES

List of Abbreviations

AC:	Adenocarcinoma
ALK:	Anaplastic Lymphoma Kinase
APC:	Alimentary Pharmaceuticals Centre
APC(s):	Antigen Presenting Cell(s)
ATRA:	All-trans Retinoic Acid
B2M:	Beta 2 Microglobulin
BMI:	Body Mass Index
bTMB:	Blood Tumour Mutational Burden
CAF:	Cancer Associated Fibroblast
CANTAB:	Cambridge Neuropsychological Test Automated Battery
CCND1:	Cyclin Dependant Kinase 1
CD:	Cluster of Differentiation
CI:	Confidence Interval
CPS:	Combined Positivity Score
CRC:	Colorectal Cancer
CREC:	Clinical Research Ethics Committee
CRP:	C-reactive Protein
ctDNA:	Circulating tumour DNA
CTLA-4:	Cytotoxic T-Cell Antigen 4
CXCR2:	CXC motif chemokine receptor 2
DNA:	Deoxyribonucleic Acid
EGFR:	Epidermal Growth Factor Receptor
EMA:	European Medicines Agency
ES-SCLC:	Extensive Stage Small Cell Lung Cancer
FACT-ICM:	Functional Assessment of Cancer Therapy – Immune Checkpoint Modulator
FDA:	Food and Drug Administration (USA)
FBC:	Full Blood Count
FFPE:	Formalin Fixed Paraffin Embedded
FMT:	Faecal Microbial Transplant

GEP:	Gene Expression Profiling
GSEA:	Gene Set Enrichment Analysis
HLA I:	Human Leukocyte Antigen I
HR:	Hazard Ratio
H&E:	Haematoxylin and Eosin
HMT:	Faecal Human Microbiota Transplant
HNPCC:	Hereditary Non-Polyposis Colon Cancer
IBD:	Inflammatory Bowel Disease
ICI:	Immune Checkpoint Inhibitor(s)
ICM:	Immune Checkpoint Modulator
ICOS:	Inducible T-cell costimulator
ICOSLG:	Inducible T cell co-stimulator ligand
IDO (1):	Indoleamine 2,3-dioxygenase (1)
IFNα:	Interferon alpha
IFNβ:	Interferon beta
IFNy:	Interferon gamma
IHC:	Immunohistochemistry
IL-1β:	Interleukin 1 beta
IL-6:	Interleukin 6
IL-9:	interleukin 9
IL2ra:	Interleukin-2 receptor alpha chain
IQR:	Interquartile Range
iRAE:	Immune Related Adverse Events
ISF:	Immunoglobulin Super Family
JAK-STAT:	Janus Associated Kinase-Signal Transducers and Activators of Transcription
Ki67:	Antigen Kiel 67
KEAP:	Kelch-like ECH-associated protein
K/T:	Kynurenine to Tryptophan
LAG3:	Lymphocyte-associated gene 3
lfcSE:	log2 fold change standard error
LS-SCLC;	Limited Stage Small Cell Lung Cancer
LDH:	Lactate Dehydrogenase
MDSC:	Myeloid Derived Suppressor Cell
MHC I:	Major Histocompatibility Complex I

MLH1:	DNA mismatch repair protein 1
MMP:	Matrix Metalloproteinase
MMR:	Mismatch Repair
Mut/Mb:	Mutations per Megabase
RNA:	Ribo Deoxynucleic Acid
mRNA:	messenger RNA
MSAF:	Maximum Somatic Allele Frequency
MSI:	Microsatellite Instability
MSI-high:	Microsatellite Instability-high
Mφ:	Macrophage
NE:	Not Estimable
NES:	Normalised Enrichment Score
NGS:	Next Generation Sequencing
NR:	Not Reached
NPX:	Normalised Protein Expression
n.s.;	Not statistically significant
NSCLC:	Non-Small Cell Lung Cancer
OS:	Overall Survival
OTU:	Operational Taxonomic Units
PMBCs:	Peripheral Blood Mononuclear Cells
PCR:	Polymerase Chain Reaction
PD-1:	Programmed Death 1 Receptor
PD-L1:	Programmed Death Ligand 1
PDGF BB:	Platelet Derived Growth Factor Subunit Beta
PFS:	Progression Free Survival
PLC:	Protein Loading Complex
PMS2:	Postmeiotic Segregation Increased 2
PTEN:	Phosphatase and Tensin Deleted
QA:	Quality Assurance
QC:	Quality Control
RAS:	Rat sarcoma virus protein gene
ROC:	Receiver Operating Characteristic
SCFA:	Short Chain Fatty Acid
SGB:	Subgroup Bin

SCC:	Squamous Cell Carcinoma
SCLC:	Small Cell Lung Cancer
SD:	Standard Deviation
SII:	Systemic Immune Inflammatory Index
SJH:	St James's Hospital, Dublin 8.
sPD-L1:	soluble PD-L1
STK11:	Serine/Threonine Kinase 11
TAM:	Tumour-associated Macrophages
TMB:	Tumour Mutational Burden
TCD:	Trinity College Dublin
TCR:	T Cell Receptor
TDO2:	Tryptophan 2,3-Dioxygenase
Tex:	exhausted T cell
TGF-β:	Transforming growth factor beta
Th1:	T helper cell Th1 subtype
Th9:	T helper cell Th9
TIGIT:	T cell immunoreceptor with immunoglobulin and ITIM domain
TIM3:	T-cell immunoglobulin and mucin domain-containing molecule 3
TKI;	Tyrosine Kinase Inhibitor
TME:	Tumour Microenvironment
TPM:	Transcripts Per Million
TNBC:	Triple Negative Breast Cancer
TNF-α:	Tumour Necrosis factor-alpha
TPS:	Tumour Proportion Score
TRAIL:	Tumour Necrosis Factor-related apoptosis-inducing ligand
Treg:	CD4+ regulatory T cell
Trp:	Tryptophan
WES:	Whole Exome Sequencing
UCC:	University College Cork
UMI:	Unique Molecular Identifier
VEGF:	Vascular Endothelial Growth Factor
VICM:	Citrullinated and Matrix Metalloproteinase Degraded Vimentin

1 INTRODUCTION

1.1 General Introduction

Immune Checkpoint Inhibitors (ICI) are monoclonal antibodies that are used to treat over one in three cancer patients (Haslam et al. 2020; Prasad et al. 2024). While they have changed the natural history of certain cancers by prolonging life and preserving quality of life, they are highly active in less than 40% of patients (Sharma et al. 2017). ICI, even in the most responsive malignancies such as melanoma, can cause significant autoimmune side effects. Approved companion diagnostic tests for use of ICI include tumour PD-L1 expression, microsatellite instability (MSI) and Tumour Mutational Burden (TMB), none of which are particularly sensitive or specific. Emerging tumour and immune tissue biomarkers of ICI response include those such as novel immunohistochemistry scores of PD-L1 expression on tumour, immune and stromal cells, tumour, stromal and immune cell gene expression profiling, and are promising areas of research (Haddad et al. 2022). Liquid biomarkers such as systemic inflammatory markers, kynurenine/tryptophan ratio, circulating immune cells, cytokines and circulating cell free tumour DNA (ctDNA) are all under investigation (Duchemann et al. 2020; Zou et al. 2021; Bratman et al. 2020). Modern analysis of ctDNA may include not only sequencing looking for mutations and copy number amplification but also DNA methylation patterns, also termed methylomics, and fragmentomics where the various sizes and the genomic location of fragments of DNA can reflect the chromatin structure of tumour cells and improve sensitivity to detect very low levels of ctDNA (Nguyen et al. 2023). In addition, the faecal microbiome is a promising biomarker of response and toxicity and it may be possible to alter its composition with beneficial effects (Simpson et al. 2022). While all currently approved biomarkers are based on pre-treatment analysis of the tumour by Immunohistochemistry (IHC) or genetic sequencing, dynamic biomarkers which evaluate changes in the immune response during treatment but prior to the clinical standard restaging Computer Tomography (CT) scan are of great importance. The most promising of

these dynamic biomarkers is changes in the K/T ratio post first dose ICI (Haoxin Li et al. 2019).

1.1.1 Overview

ICI are monoclonal antibodies that inhibit negative feedback signals in tumour specific T cells (Mc Neil and Lee 2025). However, most patients do not benefit from these expensive drugs, and a substantial minority experience immune-related autoimmune adverse event (irAE). These adverse events are caused by the unleashed immune system targeting other organs (Chhabra and Kennedy 2021). Patients who experience irAE are more likely to have a clinical benefit but the relationship is not absolute (Shankar et al. 2020). There are three approved tissue biomarkers in clinical practice but they lack predictive value of benefit, have low negative predictive value, and do not predict toxicity (Ganesan and Mehnert 2020; Meng et al. 2015).

There are three classes of licenced ICI. Ipilimumab and Tremelimumab both target the Cytotoxic T- Lymphocyte Associated 4 (CTLA-4) immune checkpoint molecule on T cells activated after encountering professional antigen-presenting cells (APCs) bearing tumour antigens in lymph nodes, leading to clonal expansion of T cells (Buchbinder and Desai 2016). The second type of ICI targets either Programmed Death Receptor-1 (PD-1) on mature cytotoxic CD8+ T cells or its ligands PD-L1 and PD-L2 expressed by cancer cells, stromal cells, and immune cells in the tumour microenvironment. These drugs include the PD-1 antagonists Cemiplimab, Dostarlimab, Pembrolizumab, and Nivolumab, as well as the PD-L1 antagonists Atezolizumab, Avelumab, and Durvalumab. PD-L1 and PD-L2 on binding to PD-1 on CD8+ T cells can trigger apoptosis or T cell exhaustion. Inhibition of PD-1 signalling by ICI allows the tumour-specific T cell to become fully activated and attack the tumour cell. This is a simplified reduction of a complicated process. CTLA-4 is also expressed by activated and regulatory T cells, PD-L1 is found on APCs and PD-1 can be found on CD4+ T helper cells and B lymphocytes (Bagchi et al. 2021). More recently a LAG-3 targeting antibody (Relatimab) has come to the market which may act by restoring exhausted T-cell function and is synergistic when combined with anti-PD-1 therapy in melanoma (Davar et al. 2025; Lipson et al. 2025).

Cancer cells which express high levels of PD-L1 are more vulnerable to ICI. There is, however, substantial variation in response rates between patients with the same type of cancer which may be partially explained by differences in the tumour microenvironment

(TME) (Yuan et al. 2025). Each TME is uniquely heterogeneous both in terms of the composition and spatial distribution of diverse cell populations - which include tumour, stromal and immune cells - and the tumour extracellular matrix (Figure 1.1). Tumour stromal cells include cancer associated fibroblasts and mesenchymal stromal cells and provide nutrition to cancer cells (Valkenburg et al. 2018). Stromal cells may inhibit tumour specific T cells from infiltrating the tumour or parts of the tumour creating a 'cold' or immune-excluded tumour, less likely to benefit from ICI (Jenkins et al. 2022).

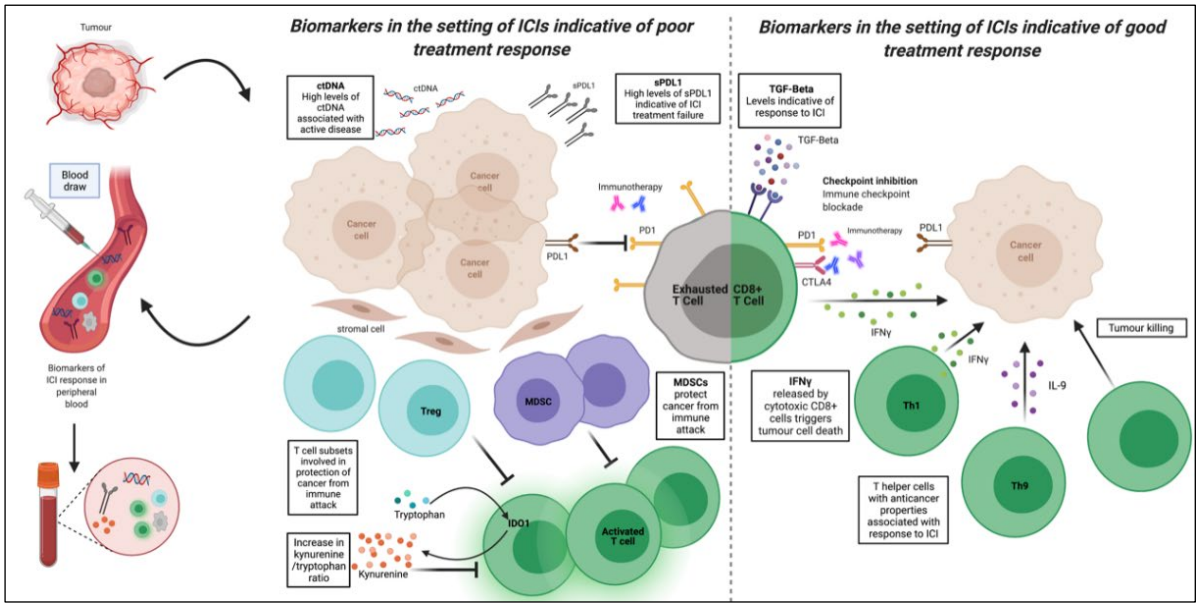

Figure 1.1 Tumour Microenvironment and Novel Potential Biomarkers *sPDL1 = soluble PDL1; ctDNA = circulating tumour DNA; TGF-β = transforming growth factor beta; Trp = tryptophan; IDO = indoleamine 2,3-dioxygenase; Treg = regulatory T cell; Tex = exhausted T cell; MDSC = myeloid derived suppressor cell; Th1 = T helper cell Th1 subtype; Th9 = T helper cell Th9 subtype; IFNy = interferon gamma; IL-9 = interleukin 9; ICI = immune checkpoint inhibitor* (Adapted from Healey Bird 2022).

Immunosuppressive cells such as tumour-associated macrophages (TAMs), myeloid-derived suppressor cells (MDSCs), CD4+ regulatory T cells (Tregs), and stromal cells can block T-cell infiltration and activation and can directly inhibit cytotoxic T-cells from attacking cancer cells. This is mediated through the combinatorial action of cell surface and secreted molecules such as immunoregulatory cytokines, chemokines, and prostaglandins. Each cell in the tumour microenvironment including tumour cells can be considered immunomodulatory. Each TME cell expresses and secretes a wide variety of pro- or anti-inflammatory signalling molecules (Abdul-Rahman et al. 2024). Cytokines and chemokines are small, secreted proteins, that immune cells use to communicate with each other through specific and cell type selective ligand-receptor interactions creating a complex and dynamic

cell-cell interaction network. Cytokines can have activating and inhibitory effects on immune cells and non-immune cells in the TME, and can through their collective effects determine the overall chemokine contexture of the TME affecting the recruitment and migration of either immunosuppressive immune cell populations or anti-tumour effector T-cell populations (Peng et al. 2012; Bridge et al. 2018). Chemokines, are a subset of cytokines which direct chemotaxis or the migration of (immune) cells in and out of tissues and are emerging as key determinants of the overall immune contexture of the TME and the likelihood of a positive response to ICI (Rivas-Fuentes et al. 2015; Ji et al. 2020). Indeed, circulating cytokines and chemokines can be measured in serum or plasma and may be predictive of response to ICI (Y. Wang et al. 2021; Boutsikou et al. 2018).

The complexity of the interactions between cancer cells, stromal cells, immune cells, the extracellular matrix, the tumour microbiome and the spatial and temporal variation of gene and protein expression within different parts of the sampled tumour - which may change with treatment - make the development of a single pre-treatment tissue biomarker challenging and perhaps unrealistic (Yamaguchi et al. 2024). Pragmatically, it is easier to obtain repeated blood samples, and blood may provide an averaged snapshot of the interplay between all cellular components of the TME at multiple sites (Nejman et al. 2020; Mildner et al. 2020). It is possible that the most active site of metastatic disease will contribute most to detectable components in blood such as circulating tumour DNA (ctDNA) (Cresswell et al. 2020).

1.1.2 Approved Predictive Biomarkers of Response

1.1.2.1 Immunohistochemistry for PD-L1

Tumours with high PD-L1 expression by IHC have a higher chance of responding to ICI, especially in non-small cell lung cancer (NSCLC) (X.-J. Chen et al. 2020). However a meta-analysis of six randomized controlled trials (1432 NSCLC patients treated with ICI) found that it had no prognostic or predictive effect of OS or PFS (Zhang et al. 2020). Technical limitations include interobserver variation, which can be improved by training and limiting PD-L1 reporting to pathologists who are experts in cancers of the organ in question i.e. thoracic pathologists to score lung tissue and genitourinary pathologists to score bladder (Troncone and Gridelli 2017; C. Wang et al. 2018). It is still essential for the pathologist to decide what the tissue of origin and the cell type of the cancer is. In NSCLC, the choice of cytotoxic chemotherapy to partner immunotherapy relies on accurate histological diagnosis

and has remained unchanged for nearly two decades with adenocarcinomas receiving platinum and pemetrexed and squamous cell carcinomas receiving platinum and gemcitabine or platinum and paclitaxel (Scagliotti et al. 2008; Schiller et al. 2002).

The Tumour Proportion Score (TPS) is the number of tumour cells with positive membranous staining for PD-L1 divided by the total number of viable tumour cells, expressed as a percentage. The TPS cut-off value of ≥50% was derived using training and validation sets in a large single-arm trial of patients with metastatic NSCLC treated with Pembrolizumab monotherapy (Garon et al. 2015). The area under the ROC curve was 0.743, sensitivity 70.4%, and specificity 79%. Its use is rendered more complicated by different drug companies and trials using different proprietary companion diagnostic monoclonal antibodies to PD-L1, which are not interchangeable (Torlakovic et al. 2020). In general, first-line Pembrolizumab monotherapy is considered in NSCLC with a PD-L1 TPS score greater than 50%, especially in elderly patients. Pembrolizumab and cytotoxic chemotherapy is used in patients whose PD-L1 score ranges from 0-100% in non-driver mutation driven NSCLC (Reck et al. 2016; Mok et al. 2019) (Figure 1.2). PD-L1 TPS is useful when deciding on first-line monotherapy *vs* combination therapy with cytotoxics in NSCLC (Gandhi et al. 2018; Gadgeel et al. 2020; Paz-Ares et al. 2018).

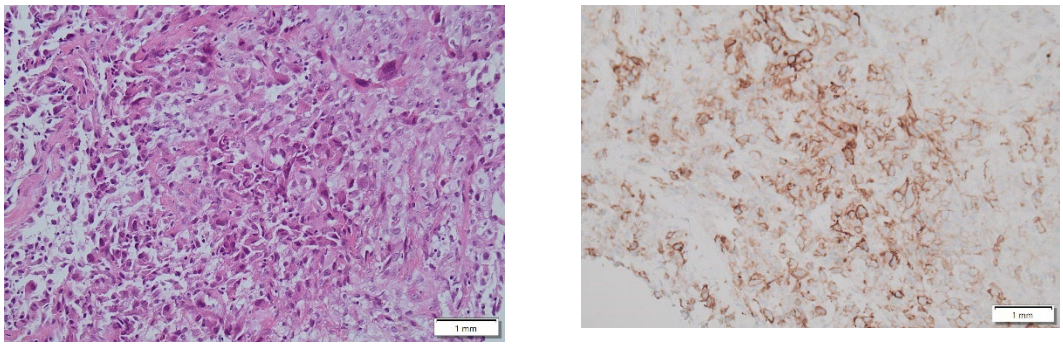

(a) (b)

Figure 1.2 Example of Haematoxylin and Eosin and PD-L1 Immunohistochemistry in NSCLC; (a) Non-Small Cell Lung Cancer stained with Haematoxylin and Eosin (20x) (b) Same specimen stained for PD-L1. Tumour Proportion Score = 100% (20x) Provided by R.F., SJH

NSCLC patients with a high PD-L1 TPS and adverse prognostic features such as recent use of steroids, malignant pleural effusion and elevated CRP may be considered for first-line cytotoxic and ICI combination, especially if fit for conventional chemotherapy (Jørgensen 2020; Morita et al. 2020). The net effect is that most patients with Stage IV NSCLC will receive first-line Pembrolizumab whether alone or in combination.

Another IHC method of assessing PD-L1 is the combined positivity score (CPS, also known as composite proportion score). The CPS (Eqn.1) incorporates PD-L1 expression on tumour infiltrating immune cells as well as cancer cells and has been shown to be of value in predicting response in cancers of the stomach and oesophagus (Kojima et al. 2020):

$$CPS = \frac{\#\ PD{-}L1\ staining\ cells\ (tumour\ cells,\ \ lymphocytes,\ \ macrophages)}{Total\ \#\ of\ viable\ tumour\ cells} \times 100 \qquad \textbf{Eqn. 1}$$

Pembrolizumab, in combination with chemotherapy is licenced in metastatic or unresectable Triple Negative Breast Cancer with a CPS score of 10 or higher (Cortes et al. 2020).

PD-L1 score can vary depending on whether the primary tumour or metastasis is sampled and whether the edge of the tumour or centre is present. Core biopsies taken from lung cancer resection specimens show significant intra-tumoural heterogeneity both of tumour and immune cells (Munari et al. 2018; Casadevall et al. 2017). PD-L1 staining may also vary over time and with treatment. PD-L1 staining is relatively cheap (100-200 euro per specimen) and readily available in most cancer centres. The future of PD-L1 as a biomarker lies in its incorporation into multi-parametric models. Artificial Intelligence may be used to interpret digitized images of tumour tissue including PD-L1 staining which may yield more accurate TPS and CPS (Echle et al. 2021).

1.1.2.1.1 Tumour Mutational Burden

Tumour Mutational Burden (TMB) is a measure of how many mutations per one million bases or Megabase (Mb) of DNA are found in the tumour genome. It is expressed as the total number of somatic or acquired mutations per coding area of a tumour genome in mutations per Megabase (Mut/Mb). The more mutations, the more neo-antigens are potentially coded for, and presented to the immune system by the tumour cell via Major Histocompatibility Complex I (MHC I, also known as Human Leukocyte Antigen I (HLA I)) (Snyder et al. 2014; Cristescu et al. 2022). TMB can be calculated using Whole Exome Sequencing (WES) or by looking at the mutational frequency in a smaller panel of affected genes using Next Generation Sequencing (NGS) but with at least 1 Mb genomic coverage. TMB correlates with ICI response, is independent of PD-L1 expression, and has been approved by the USFDA as a tissue agnostic biomarker for the PD-L1 inhibitor Pembrolizumab (TMB > 10 mt/Mb). Tumours with high TMB (>20 mt/Mb) have an

approximately 45% response rate to immunotherapy (Goodman et al. 2020). TMB based on analysis of tumour tissue is not routinely available outside of clinical trials although is offered as part of a NGS package by several companies. When three commercially available platforms (TruSight Oncology 500 (TSO500) and Oncomine Tumour Mutation Load (OTML) versus a reference assay (Foundation One, FO)) were used to evaluate 96 samples, good concordance was evident, especially in PD-L1 low samples, although cut-offs had to be altered to increase sensitivity when compared with the gold standard assay (FO) (Ramos-Paradas et al. 2021). TMB identifies a population of NSCLC patients who respond to dual immunotherapy rather than conventional first line chemotherapy (Hellmann et al. 2018). Tissue TMB suffers from the same issues of spatial and temporal heterogeneity as tissue PD-L1. It is hoped that blood TMB of cell-free tumour DNA (ctDNA) may provide a better biomarker (Scagliotti et al. 2008; Z. Wang et al. 2019). Blood TMB has been shown to differentiate between responders and non-responders to first line Atezolizumab in NSCLC (Horn et al. 2018; Socinski et al. 2019). A complete review of the challenges in using TMB as a biomarker of ICI response demonstrates that nonsynonymous mutations which lead to frameshifts and accumulation of multiple abnormal amino acid sequences when transcribed and translated are much more immunogenic than synonymous point mutations (Jardim et al. 2021). Clonal TMB, i.e. nonsynonymous mutations, found in at least 95% of cancer cells is a better predictor of ICI response than sub-clonal TMB. Clonal TMB can be combined with other genetic biomarkers of favourable response such as low genetic heterogeneity, dinucleotide variants and loss of TNF signalling gene (*via* TRAF2) (Litchfield et al. 2021; Gao et al. 2020). The relatively high cost of TMB, the complicated laboratory and computational analysis required, and its lack of predictive value have limited its widespread clinical adaptation outside the USA. A recent review of TMB as an ICI biomarker highlights the variable success of high TMB in predicting response with huge variation between different tumour types (Strickler et al. 2021). High TMB is of value in lung cancer, where a subset of patients with absent PD-L1 expression will respond to ICI, but of no discriminatory value in anal cancer (Marabelle et al. 2020) . In glioma, high TMB, which develops post exposure to alkylating cytotoxic chemotherapy may predict resistance to ICI (Samstein et al. 2019). Some cancers respond well to ICI despite having low TMB such as Merkel Cell Carcinoma and renal cell carcinoma. TMB does not take into account that frameshift and insertion deletion mutations are more immunogenic than nonsynonymous point mutations (Turajlic et al. 2017).

1.1.2.2 Microsatellite Instability

Microsatellites are short sequences of base pair repeats which may become elongated or duplicated during DNA replication in the absence of the DNA mismatch repair (MMR) complex which repairs these errors (Yamamoto and Imai 2019). Tumours with loss of MMR genes, whether inherited as in Hereditary Non-Polyposis Colon Cancer (HNPCC or Lynch Syndrome), or sporadically acquired, exhibit genetic microsatellite instability (MSI). These MSI-high tumours are vulnerable to treatment with ICI with high response rates and durable clinical benefit (Le et al. 2015). Fifteen percent of sporadic colon, endometrial and gastric cancers are MSI-H. IHC to detect loss of any of the four MMR proteins is quick, cheap, and readily available (Figure 1.3). IHC detection of MMR deficiency is reliable in colon, gastric and endometrial cancers but may be less reliable in less common MSI-H cancers such as urothelial. Polymerase Chain Reaction (PCR) analysis is used to compare microsatellites in tumour and normal tissue from the same patient. Patients with MSI-high cancers will have a higher number of microsatellite repeats detected by PCR. PCR detection of MSI-high status is reliable across tumour types (Stelloo et al. 2017; Smyth et al. 2017). PCR testing for MSI may detect an extra 5-11% of MSI-high malignancies without loss of MMR protein expression. NGS can also be used to detect MSI and other predictive mutations, but is expensive (Yamamoto and Imai 2019). However, this is changing rapidly and NGS for MSI may become standardised and readily available (Bonneville et al. 2020). As expected, MSI-H tumours tend to have high TMB scores (Chalmers et al. 2017). There is also interest in using ctDNA to detect MSI-H cancers (Tieng et al. 2021).

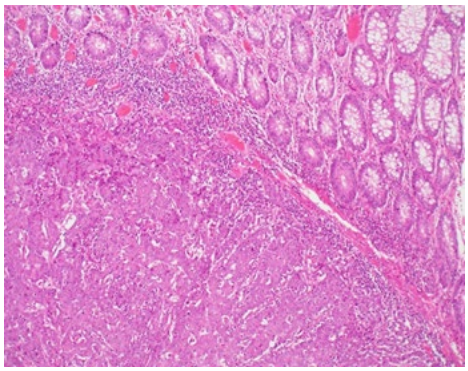

(a)

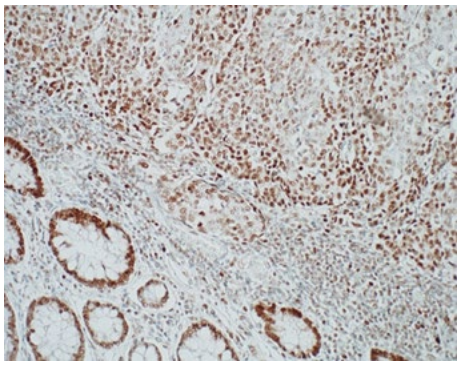

(b)

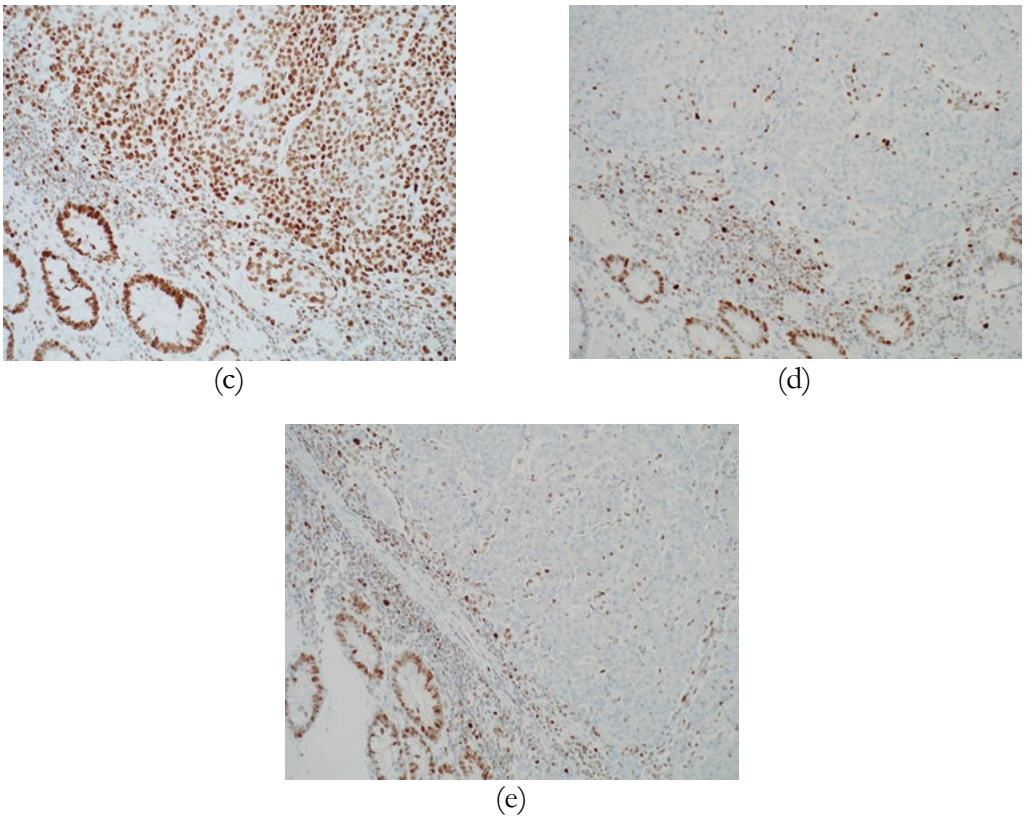

Figure 1.3 (a) Colorectal Cancer H&E x 10 magnification; (b)CRC Intact expression of MSH2 x20; (c) MSH6 expression x20; (d) Loss of MLH1 x20; (e)Loss of PMS2 x20. Micrographs provided by R.F. SJH (Healey Bird et al. 2022).

1.1.3 Novel Biomarkers of Response, Resistance, and Toxicity

1.1.3.1 Novel Immunohistochemistry Biomarkers

The presence of different populations of immune cells and their spatial location can be determined using IHC. Tumours which "exclude" CD8+ T cells, keeping them at the edge of tumoral tissue are more likely to be resistant to ICIs than those where the T cells freely infiltrate the tumour (P. Ouyang et al. 2024). The Immunoscore uses digital pathology to quantify CD3+ and CD8+ T cells in the tumour and in the invasive margin of cancers. It is prognostic and predicts benefit to adjuvant cytotoxic chemotherapy. While it is best described in colorectal cancer (CRC) it has been used to predict outcomes in other malignancies (Zhuge et al. 2020; Nassif et al. 2021; Mlecnik et al. 2020). It is unknown whether Immunoscore can predict benefit of ICI therapy. The phase II POCHI trial uses Immunoscore to select patients with metastatic CRC microsatellite stable tumours and a high immune infiltrate for treatment with chemotherapy, bevacizumab and ICI (Federation Francophone de Cancerologie Digestive 2020). Preliminary results suggest that this may be

a successful strategy, with CT scans showing 25% of 55 patients having a complete response (Tougeron et al. 2024). IHC has been used to examine PD-L2 staining especially in lung cancer (Yearley et al. 2017). Lymphocyte-associated gene 3 (LAG3), a CD4 homologue, is another checkpoint implicated in T cell exhaustion and a therapeutic target under investigation, usually combined with anti-PDL1 treatments (Lecocq et al. 2021; Triebel et al. 1990). It is unknown whether IHC for LAG3 on tumour infiltrating lymphocytes is an effective biomarker. Tumour cells resistant to PD-1 blockade produce IFNβ and ATRA (all-trans retinoic acid), increasing CD38 expression on the tumour cell surface. This in turn leads to production of adenosine which inhibits CD8+ T cells in the TME (L. Chen et al. 2018). While monoclonal antibodies targeting CD38 are used in multiple myeloma, they have not proved successful in solid tumours when combined with ICI in early phase trials (Pillai et al. 2021). However, agents targeting the adenosinergic pathway may hold promise, especially in tumours with high CD38 expression detected by IHC. As therapies targeting other immune checkpoints such as TIM3 and TIGIT enter clinical practice, IHC for markers in tumour and immune tissue may play a role (Anderson, Joller, and Kuchroo 2016).

1.1.3.2 Systemic Markers of Inflammation

It is hypothesized that patients with a low burden of disease, whose immune system is already attempting to attack the tumour will have the best outcomes (Joseph et al. 2018; Lim et al. 2024). There are several routine blood tests that can be used to estimate tumour burden (e.g. Lactate Dehydrogenase) and beneficial immune activation (e.g. elevated lymphocyte count) (Kelderman et al. 2014). There are also markers of systemic inflammation which portend worse outcomes including elevated neutrophil and platelet counts and C-Reactive Protein (CRP), which primarily reflects interleukin-6 (IL-6) levels (Capone et al. 2018; Fu et al. 2019)). These can be combined to create Systemic Inflammatory Scores and possibly guide treatment decisions (Liu et al. 2019). One example is the Systemic immune-inflammation index (SII), calculated as Neutrophils × Platelets/Lymphocytes). Elevated SII is associated with poor outcomes in patients with pancreatic cancer treated with ICI and other therapies (Shang et al. 2021). Studies have shown that male obese melanoma patients did better than non-obese patients with ICI (McQuade et al. 2018). Obesity (BMI over 30) drives tumorigenesis and PD-L1 expression but makes these tumours vulnerable to ICI without an increase in irAE (Ziming Wang et al. 2019). Neutrophils may contribute to an inflammatory pro-angiogenic tumour microenvironment (Ozel et al. 2022). Neutrophil extracellular traps (NET), webs of DNA and proteins, are known to contribute to the dissemination of

metastases (Park et al. 2016; Kaltenmeier et al. 2021). While acute infection and steroids both increase the peripheral blood neutrophil count it seems clear that elevated Neutrophil to Lymphocyte Ratio (NLR) portends a poor response to ICI in a wide variety of malignancies (Criscitiello et al. 2020). One study of 239 NSCLC patients found that serial changes in NLR and Neutrophil to Eosinophil Ratio (NER) outperformed both PD-L1 TPS and TMB as a predictor of response to ICI (Hwang et al. 2022).

1.1.3.3 Cytokines, Chemokines, and other Soluble Immune Markers

Different cytokine and chemokine cell-cell interaction networks in the TME, tumour draining lymph nodes and tertiary lymphoid structures will dictate the overall spatial composition of the immune cell component of the TME, and its contribution to the overall tumour Immunoscore and the classification of the tumour as 'hot', 'cold' or 'immune excluded'. This in turn may predict different therapeutic outcomes depending on the type of tumour and therapy used (F. Wei et al. 2023). Many studies are contradictory and large data sets will be needed to elucidate how best to use baseline tumour and systemic cytokine levels, gene expression signatures, or on treatment changes as indicated by a renal cancer study (Chehrazi-Raffle et al. 2021). Tumour necrosis factor-alpha (TNFα) and Interferon-gamma (IFN-γ) released by CD4+ Th1 T cells and CD8+ cytotoxic T cells, trigger senescence and cell death in tumour cells, and efficacy of ICI in melanoma is dependent on tumour cell responsiveness to IFN-γ, as evidenced by the emergence of adaptive resistance to ICI in some patients mediated through accumulated mutations in genes coding for JAK-STAT signalling and antigen processing and presentation (Grasso et al. 2020; J. Gao et al. 2016; Frangieh et al. 2021; Hoekstra, Vijver, and Schumacher 2021). Transforming Growth Factor Beta (TGF-β) is an immunomodulator thought to restrain the immune system. Pre-treatment levels of cytokines in melanoma patients treated with neoadjuvant Ipilimumab (CTLA4 inhibitor) have different predictive values. High levels of IL-17 predict elevated incidence of irAE. Patients with baseline low levels of TGF-β and high levels of IL-10 have worse responses to ICI. In metastatic melanoma, responders to Nivolumab had elevated baseline TGF-β compared to non-responders (Tarhini et al. 2015; Nonomura et al. 2016). Another study has found that high baseline TGF-β predicts poor outcomes in hepatocellular carcinoma treated with Pembrolizumab (Feun et al. 2019). Circulating cytokines and chemokines (CXCL2 and CXCL5) have been shown to predict response and immune toxicity in patients treated with anti-PD-L1 therapy (Lim et al. 2019; Davids et al. 2016). CXCR2 and IL2ra increased from baseline in a patient treated with Nivolumab who

developed radiation pneumonitis and levels of these cytokines declined on initiation of corticosteroids (Schoenfeld et al. 2019). While serial changes in cytokine levels can be observed in patients treated with Atezolizumab (rise in IL-18, fall in IL-6), they do not appear to segregate responders from non-responders (Herbst et al. 2014). Splice variants of PD-L1 are shed from cell surfaces and can be measured in blood samples (Cheng et al. 2015). High soluble PD-L1 (sPD-L1) is associated with worse outcomes in lung, but not gastric cancer (Zhang et al. 2015; Zheng et al. 2014). A meta-analysis of multiple non immunotherapy trials (anti-VEGF therapies, cytotoxic chemotherapy) in multiple tumour types (lung, gastric, hepatocellular) found sPD-L1-high to be associated with worse OS (Wei et al. 2018). There is much debate in the literature as to the role of sPD-L1 in health and disease and whether it impairs ICI treatment by acting as a decoy receptor (Ng et al. 2019). In the setting of ICI therapy for NSCLC, low baseline sPD-L1 is associated with better outcomes and high or increased levels at two months with treatment failure (Okuma et al. 2018; Costantini et al. 2018). Other immune checkpoint transmembrane receptors can be cleaved by metalloproteinases and shed into the circulation such as CTLA-4, LAG-3, and TIM-3. These are all targets for established ICI such as Ipilimumab (anti-CTLA4) and novel agents (anti-LAG3, anti-TIM-3) in clinical trials. One melanoma study of patients treated with Ipilimumab showed that high sCTLA4 levels were associated with both improved response rates and increased irAE (Pistillo et al. 2019). Early clinical data suggest that high levels of circulating cleaved LAG3 (sLAG3) may predict immunotherapy response in gastric cancer (N. Li et al. 2018). The role of sTIM-3 as a biomarker of inflammation, immunosuppression and cancer progression is as yet unclear (Bailly et al. 2023).

1.1.3.4 Immune Metabolism

Activated T cells are highly metabolically active and consume tryptophan to generate kynurenine which is an immunosuppressant (Platten et al. 2019). Increases in kynurenine/tryptophan (K/T) ratio at 4-6 weeks, but not the baseline K/T ratio, have been shown to predict resistance to ICI in renal cell carcinoma (RCC) and melanoma (H. Li et al. 2019). Melanoma patients treated with Nivolumab, whose K/T ratio increased >50% from baseline, had a median OS of 15.7 months compared to >38 months in those with falling K/T ratio. In RCC patients treated with Nivolumab (ICI), but not with Everolimus, a mammalian target of rapamycin (mTOR) inhibitor, rises in K/T ratio correlated with increased PD-L1 expression and worse OS. This suggests that changes in T cell metabolism reflected in the K/T ratio are a potential immunotherapy resistance mechanism. Li et al.

suggest that a high baseline K/T ratio is a prognostic marker of reduced survival reflecting disease bulk. They also postulate that dynamic changes in K/T ratio reflect a predictive biomarker of ICI response. The enzyme, indoleamine-2,3 dioxygenase (IDO1) is the first step of tryptophan catabolism. It was hoped that drugs such as Epacadostat which inhibit IDO1 would be synergistic with ICI but to date, this approach has failed in clinical trials (Van den Eynde, van Baren, and Baurain 2020; Long et al. 2019). These drugs should possibly be reserved for patients with rising K/T ratio post ICI exposure. It remains to be seen whether manipulating immune and tumour metabolism is a useful therapeutic target, albeit changes in the K/T ratio may still be a useful biomarker in terms of ICI response. Changes in the K/T ratio have been associated with depression and impaired psychomotor function in Crohn's autoimmune colitis (Clarke et al. 2020). Elevated Kynurenine levels may lead to the production of quinolinic acid with depressive effects (Sforzini et al. 2019). In breast and colon cancer survivors, elevated K/T ratio has been associated with depression and difficulty completing psychomotor tasks (Hongjin Li et al. 2023; Holthuijsen, van Roekel, Bours, Ueland, Breukink, Janssen-Heijnen, Keulen, Gigic, et al. 2024).

1.1.3.5 Flow Cytometry of Circulating Immune Cells

Immune cells constantly move in and out of the TME and circulate in peripheral blood and lymph nodes. It is challenging to perform flow cytometry of tissue specimens that require rapid processing of fresh or frozen samples and, therefore, the perennial sampling issues of all tissue biomarkers apply. Peripheral blood may hold greater utility than tumour samples, especially when comparing baseline to early treatment samples (C. Wei et al. 2022). The dynamic changes in immune cell populations in peripheral blood post ICI exposure may be of greater importance than the baseline population's composition (Ma et al. 2023). Flow cytometry assays have been used to identify different populations of immune cells both in the TME and in peripheral blood (Rusdi and Pawitan 2019; Cossarizza et al. 2019). TME cells which protect the tumour from immune cell attack include both MDSC and Tregs. CD4+ T regs also express surface CD25 and the transcription factor FOXP3. Other T helper cells (Th1 subtype (secretes IFN-γ and IL-2)) and IL-9 and IL-10 producing T cells (Th9 cells) have anticancer properties (T. Chen et al. 2020). A rise in Th9 circulating cells is associated with melanoma response to Nivolumab (Nonomura et al. 2016). The complexity of analysing Peripheral Blood Mononuclear Cells (PMBCs) can be seen in the case of CD14+ monocytes. Pre-treatment levels of HLA-DR expression on the monocyte surface appear to have a predictive effect with low levels indicating an immunosuppressive phenotype and

worse outcomes, whereas HLA-DRhi cells correlate with improved outcomes (Mengos, Gastineau, and Gustafson 2019; Krieg et al. 2018). Huang et al. described how early changes in circulating T cell populations were a powerful predictor of response in melanoma patients, especially combined with imaging estimates of tumour burden (Huang et al. 2017). In lung cancer, circulating lymphocytes with high-level PD-1, PD-L1 and PD-L2 expression were associated with poorer prognosis whether patients were treated with cytotoxics or in the Epidermal Growth Factor Receptor (EGFR) mutated population appropriate TKI (Arrieta et al. 2017). CD8+ T cells attempt to bind to, and destroy, tumour cells but are inhibited by PD-1/PDL-1 signalling. These frustrated CD8+ T cells become dormant or exhausted T cells, expressing PD-1, TIM, ICOS and LAG3 (Jo et al. 2024). Prior work has mostly investigated the pre-treatment ratio of effector (CD8+) to inhibitory cells (Tregs and MDSCs) as a predictor of outcome. Some studies have shown that early increases in circulating effector T cells (Ki67+, PD-1+, CD8+) post ICI are predictive of response in lung cancer (Kamphorst et al. 2017). Other work has examined reactivation of exhausted T cells as measured by Ki67 expression. Autoimmune toxicity of combined (anti-CTLA4 and PD-1) ICI is associated with early activation (Ki67+) of CD8+ effector and memory cells (Andrews et al. 2021). CD27 and CD28 are expressed by activated T cells and expression normally decreases as cells mature. Low pre-treatment levels of these surface markers at baseline are associated with decreased risk of irAE (Andrews et al. 2021).

1.1.3.6 Novel tumour and blood genetic biomarkers

ctDNA can be used to quantitate tumour burden, and its early fall at 3-6 weeks is an on-treatment predictor of lung cancer ICI response (Goldberg et al. 2018). Patients whose ctDNA remains detectable at 12 weeks have a worse prognosis (Lee et al. 2017). In melanoma patients who are responding to treatment, rises in ctDNA may precede clinical progression and potentially identify resistance mechanisms (Braune et al. 2020). The maximum somatic allele frequency (MSAF), or proportion of total circulating DNA derived from cancer, combined with bTMB, retrospectively predicted response to Atezolizumab versus docetaxel in two large trials of Atezolizumab in NSCLC. In particular, a group with worse outcomes when treated with immunotherapy (bTMB low and MSAF-high) could be defined (Y. Chen et al. 2019). Methylomics and fragmentomics have emerged as promising new approaches in ctDNA analysis of liquid biopsies (Lo et al. 2021). Fragmentomics permits identification of very low levels of tumour derived cfDNA and even enables cell of

origin to be assigned, holding promise for detection of minimal residual disease and cancer screening (Cristiano et al. 2019) .

Copy number loss in tumour biopsies is associated with ICI resistance probably due to decreased expression of genes involved in antigen expression and tumour cell IFN-γ signalling (Roh et al. 2017; Andrews et al. 2021). Tumour tissue NGS can identify genes predictive of ICI response and resistance (mutations in STK11 and KEAP1 in RAS-mutated NSCLC, loss of MHC Class I expression, impaired IFN receptor signalling) (Schabath et al. 2016; Singh et al. 2016). One small study found that *TP53* mutated NSCLC was more responsive to ICI (Assoun et al. 2019). Gene Expression Profiling (GEP) of tumour tissue, looking for differing levels of mRNA, especially IFN signalling pathways, holds great promise (Yu et al. 2020). Early changes in tissue gene expression have been shown to predict response in mouse models (Lesterhuis et al. 2017). It may be possible to use GEP of TME across different solid tumour types (Nielsen et al. 2021). GEP of tumour cells has been shown to predict benefit of ICI in Small Cell Lung Cancer (SCLC) (Gay et al. 2021).

EGFR mutated NSCLC is resistant to ICI, albeit a recent study suggested that patients whose tissue GEP indicated an inflamed TME may derive some benefit (Hayashi et al. 2021). In the CheckMate 275 study of Nivolumab in urothelial cancer, high expression of genes associated with Epithelial to Mesenchymal Transition (EMT) predicted an adverse outcome, whereas high expression of genes associated with Type I Interferon immune response predicted favourable outcomes (Sharma et al. 2017; L. Wang et al. 2018). The promise of mRNA is not confined to tissue and GEP of circulating tumour and immune RNA can also be used (Brueckl et al. 2021). Acquired resistance to ICI can be mediated by mutations in cancer cells that are selected under immune pressure. These mutations include loss of interferon receptor downstream signalling by loss of function mutations in *JAK1* and *JAK2*. Beta 2 Microglobulin (B2M) is essential for MCH I function and presentation of antigen to T cells by tumour cells (Restifo et al. 1996). Loss of *B2M* is associated with immunotherapy resistance. *PTEN* loss predicts ICI resistance (Peng et al. 2016). *Cyclin D1* (CCND1) amplification down-regulates PD-L1 expression and is associated with reduced ICI response (Litchfield et al. 2021). T cell receptor diversity or repertoire (the variation in the binding region of different T cell clones) can be measured using NGS in tumour tissue and in blood (Kidman et al. 2020). Early increased diversification of the T cell repertoire from pre-treatment values when resampled at two weeks post treatment is associated with irAE in patients treated with anti-CTLA-4 (Oh et al. 2017). Clonal expansion of CD8+ T cells

measured by sequencing TCR beta chains also precedes Ipilimumab toxicity (Subudhi et al. 2016). Drugs which enhance thymic function and TCR diversity may play a role in improving response rates to ICI (Cardinale et al. 2021).

1.1.3.7 Microbiome mediators as Biomarkers and Therapeutic Targets

Humans live in harmony with trillions of bacteria in our gut, which influences the immune system in a dynamic fashion (Zheng et al. 2020) (Figure 1.4). Circulating CD8+ T cells are primed by CD68+ APC in the gut lymph nodes, which in turn are influenced by interactions with gut bacteria and bacterial metabolites. Gut microbiota release metabolites with immunomodulatory activities such as vitamin B and short-chain fatty acids (SCFAs). Several studies have shown that patients who have not received antibiotics one to three months prior to treatment and who have a healthy diverse faecal microbiome have a better response to ICI in melanoma, RCC, urothelial and lung cancer (Chaput et al. 2017; Routy et al. 2016). Chaput et al. examined 26 metastatic melanoma patients treated with Ipilimumab and showed that increased alpha diversity of the faecal microbiome was associated with an increased likelihood of ICI response. Routy et al. found that recent antibiotic use prior to starting ICI was associated with shorter PFS and OS in NSCLC (n=140) and RCC (67) patients, unlike baseline clinical variables. Jin et al. analysed 37 NSCLC patients and found that alpha diversity and smoking status corresponded with favourable Nivolumab response but there was no impact on response from the clinical variables of sex, disease history or disease stage (Jin et al. 2019). They did not find any detriment from antibiotic use in the two months prior to starting treatment.

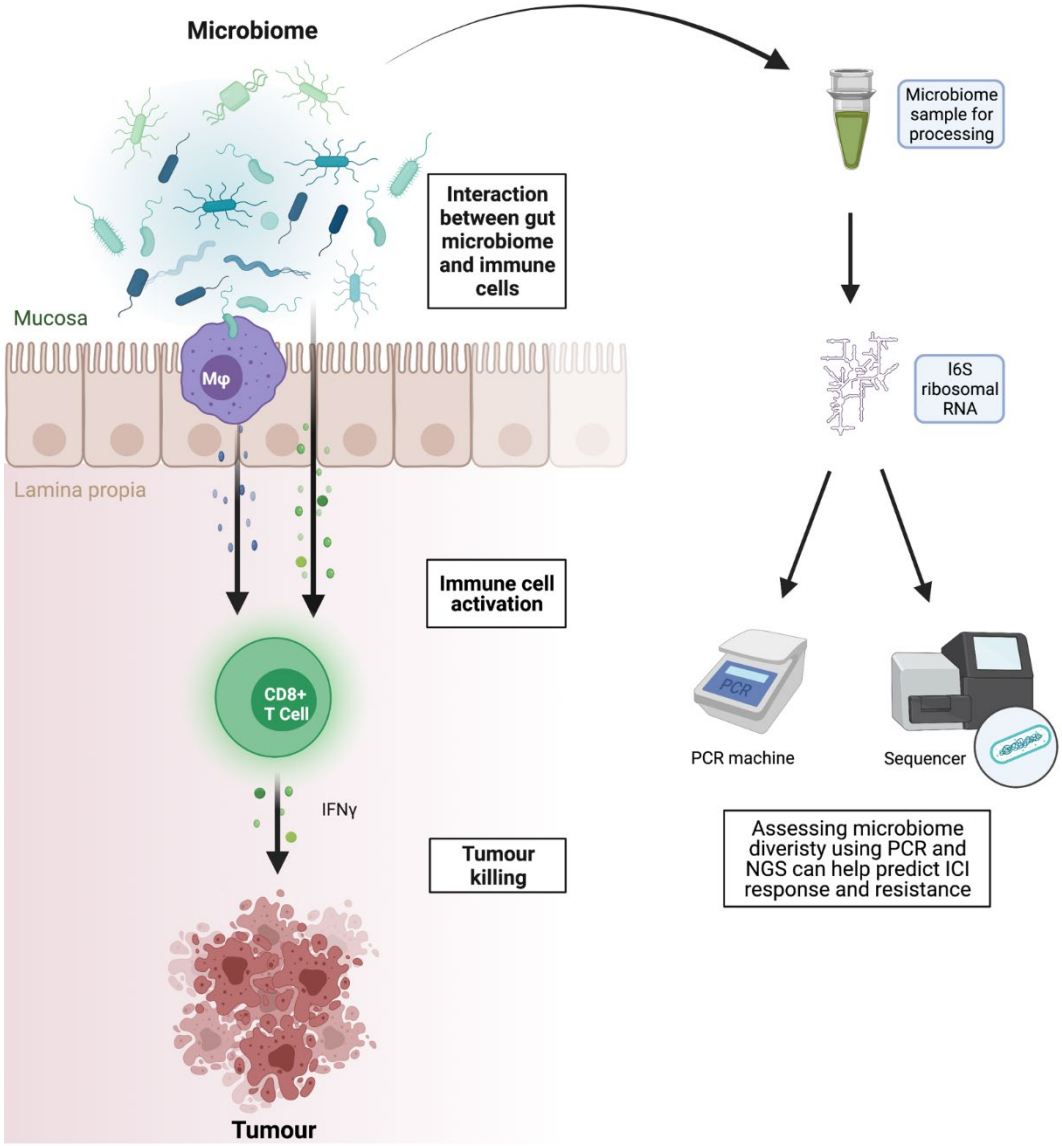

Figure 1.4 Assessing faecal microbiome diversity and composition as a biomarker of response and toxicity (Healey Bird et al. 2022).

Depiction of the interaction between the gut microbiome, immune cells and the TME. Cytokines released from activated immune cells promote tumour killing. Targeted PCR and NGS of microbiome samples can be used to assess microbiome diversity, which may predict response to immune checkpoint inhibition. Mφ = macrophage; IFNγ = interferon gamma; PCR = polymerase chain reaction; NGS = next generation sequencing.

Antibiotics prior to ICI therapy appear to reduce the incidence of ICI-mediated colitis but may make colitis more severe if initiated post ICI (Abu-Sbeih et al. 2019). Immune-mediated colitis resulting from ICI treatment has successfully been treated with Faecal Microbiota

Transplant (FMT) in humans (Yinghong Wang et al. 2018). Tumour samples from cervical cancer patients with a more diverse microbiome are more heavily infiltrated by T lymphocytes (Sims et al. 2021). In mouse models, faecal human microbiota transplant (HMT) from human responders to germ-free mice caused tumour shrinkage compared to HMT from non-responders (Vétizou et al. 2015). In mouse models of cancer, intestinal *Bifidobacterium pseudolongum* produced inosine, which could leak into the circulation and activate cytotoxic T cells via adenosine receptors when ICI caused decreased gut barrier function (Mager et al. 2020). Certain bacterial genera such as *Akkermansia, Faecalibacterium, Ruminococcaceae,* and *Bacteroides* are associated with a positive ICI response, whereas *Bacteroidales thetaoitaomicron* and *Escherichia coli* are associated with resistance (Shui et al. 2020; Routy et al. 2018). Patients treated with dual ICI with a higher abundance of *Bacteroides intestinalis* had more severe irAE. In those patients with ICI colitis, and in mouse models, IL-1β was upregulated in colonic biopsies (Andrews et al. 2021). Different groups have reported varying positive and negative associations with individual species but there appears to be clear differences in the faecal microbiota of responders and non-responders (Matson et al. 2018). It is unlikely that a single microbiome score will be prognostic or predictive, but it may well be incorporated into multiparametric models. FMT clinical trials in humans were placed on hold after adverse events but have recently been shown to provide benefit in some non-responders (Baruch et al. 2020; Davar et al. 2021). Probiotics and faecal viral transfer may play a role in therapeutic modulation of the microbiome but this is under investigation and should not be attempted outside clinical trials (T. Wang et al. 2019; Draper et al. 2020; Gopalakrishnan et al. 2020). Geographic location, genetics, ethnicity, diet, age, medication and environment all influence the microbiome and will have to be taken into account if the faecal microbiome is to be used as a biomarker or manipulated therapeutically (Gupta, Paul, and Dutta 2017; Clooney et al. 2021). The microbiome is usually characterised using 16S ribosomal RNA sequencing but more information can be obtained using metagenomics, which is becoming standard in microbiome research (Malla et al. 2019). The enormous amount of data generated by metagenomics looking at which bacterial metabolic pathways are activated, can be analysed using machine learning tools such as Random Forest analysis (Gharaibeh and Jobin 2019).

1.1.4 Hypothesis and Aims

Multi-parametric models which combine some or all of the above may enable clinicians to choose which patients are treated with anti-PD-1 or PD-L1 monotherapy (low total ctDNA,

high bTMB, favourable immune profile) or combined anti-CTLA4 and anti-PD-1 or PD-L1 (high ctDNA, low bTMB, unfavourable immune profile). Immune-PET may also play a role (Chatterjee et al. 2017). ICI have deepened our knowledge of the immune system in health and disease (Perez-Ruiz et al. 2019; Alvarez et al. 2019). As novel agents targeting other checkpoints, such as TIGIT and LAG3, make their way out of trials and into practice, patients need accurate biomarkers to guide their use (Chauvin and Zarour 2020; Puhr and Ilhan-Mutlu 2019; Tawbi et al. 2022). To make this a reality, it is imperative that scientists and clinicians standardize how they measure and report clinical data, wherever possible (Altman et al. 2012; Mildner et al. 2020).

This thesis describes a series of measurements and experiments on blood, stool and tissue derived from patients with a variety of advanced solid tumours who participated in a single site observational study while treated with standard of care ICI targeting Programmed Death Ligand 1 (PD-L1) and its receptor (PD-1).

The hypothesis of this work is that circulating blood biomarkers can predict response measured by CT scan, OS and PFS and irAE. In order to test the hypothesis that serial measurements of circulating immune cells, cytokines and immune mRNA could better predict clinical outcomes than any current baseline tissue biomarker, a prospective observational study of patients receiving standard of care ICI with and without other licenced agents (cytotoxic chemotherapy and TKIs) for incurable solid tumours measurable by iRECIST, was undertaken.

Following this first chapter, Chapter 2 of the thesis outlines the specific aims and objectives of the research presented. Chapter 3 expands on the clinical, scientific and statistical methodologies that underpin the work and. Chapter 4 presents the biomarker data gathered, with the final section (correlations) examining the success, if any, of various biomarkers in predicting clinical outcomes. These results are discussed in Chapter 5 with the conclusions and future directions for research in this area being presented in Chapter 6. The thesis concludes with the cited references that supported the research and the thesis appendices that contain additional material relevant to the work.

2 AIMS AND OBJECTIVES

2.1 Hypothesis

The overall aim of this thesis is to search for baseline and early dynamic biomarkers of response and toxicity to immune checkpoint inhibitors used to treat solid tumours.

2.1.1 Specific Objectives

In the context of the thesis hypothesis, the specific objectives are:

- To measure markers of systemic inflammation such as (i) Neutrophil to Lymphocyte Ratio and Systemic Inflammatory Index, (ii) their changes during the first three months of ICI treatment and (iii) explore their correlation with clinical outcomes (response rates, Progression Free and Overall Survival, Durable clinical benefit (alive without progression at six months) and iatrogenic autoimmune side effects (iRAE).

- To measure a panel of circulating cytokines, chemokines and soluble cell surface receptors, and their changes, during the first three months of treatment and to explore correlation with clinical outcomes.

- To measure key markers of immune metabolism such as serum Kynurenine and Tryptophan during the first three months of treatment and explore the correlation with clinical outcomes including Quality of Life as measured by validated instruments and psychomotor testing.

- To explore changes in psychomotor testing during the first three months of ICI treatment

- To measure whole transcriptomic mRNA expression in stored tumour samples as well as matched blood sample changes in circulating mRNA during treatment and correlate recorded data with clinical outcomes.

- To explore changes in the faecal microbiome in terms of diversity and species at pre-treatment (baseline) and the second treatment visit.

3 METHODS

3.1 Study Design and Ethical Approval

In testing the hypothesis that novel biomarkers of ICI response and toxicity could be found, a biomarker study was designed. This study was titled Biomarker Prediction of Response to Immune Checkpoint Inhibitors and given the designation APC125.

Ethical Approval was obtained from the Clinical Research Ethics Committee (CREC) of UCC and the Ethics Committee of the Bon Secours Group (Ireland). It was designed as a Human Observational Study. Patients were recruited from Bon Secours Cork. All patients starting standard of care immunotherapy for unresectable or metastatic disease were identified at Cancer Multidisciplinary Team meetings and chemotherapy planning meetings in Bon Secours, Cork (see Figure 3.1 for flow diagram of study).

Suitable patients were invited to take part by their treating clinician or by non-consultant hospital doctors (NCHD) trained to take part in this study as co-investigators. They were given (or if contacted by phone, posted out or e-mailed) a Patient Information Leaflet (PIL) which contained an Informed Consent Form (ICF), and as mandated by UCC, were also provided with a separate Genetics ICF (See Appendices A, B, and C) to read before they attended for immunotherapy treatment. When they attended for immunotherapy, they discussed the PIL with the Oncology Research Nurse and signed consent in the presence of the Investigator (includes co-investigators). A period of at least 24 hours was allowed between patients receiving PIL and signing onto the study. Patients who had treatment held for irAE or who withdrew from study had an off-study blood draw taken on withdrawal if they agreed. Patients who withdrew from study or transferred to another institution were followed for PFS and OS with their agreement.

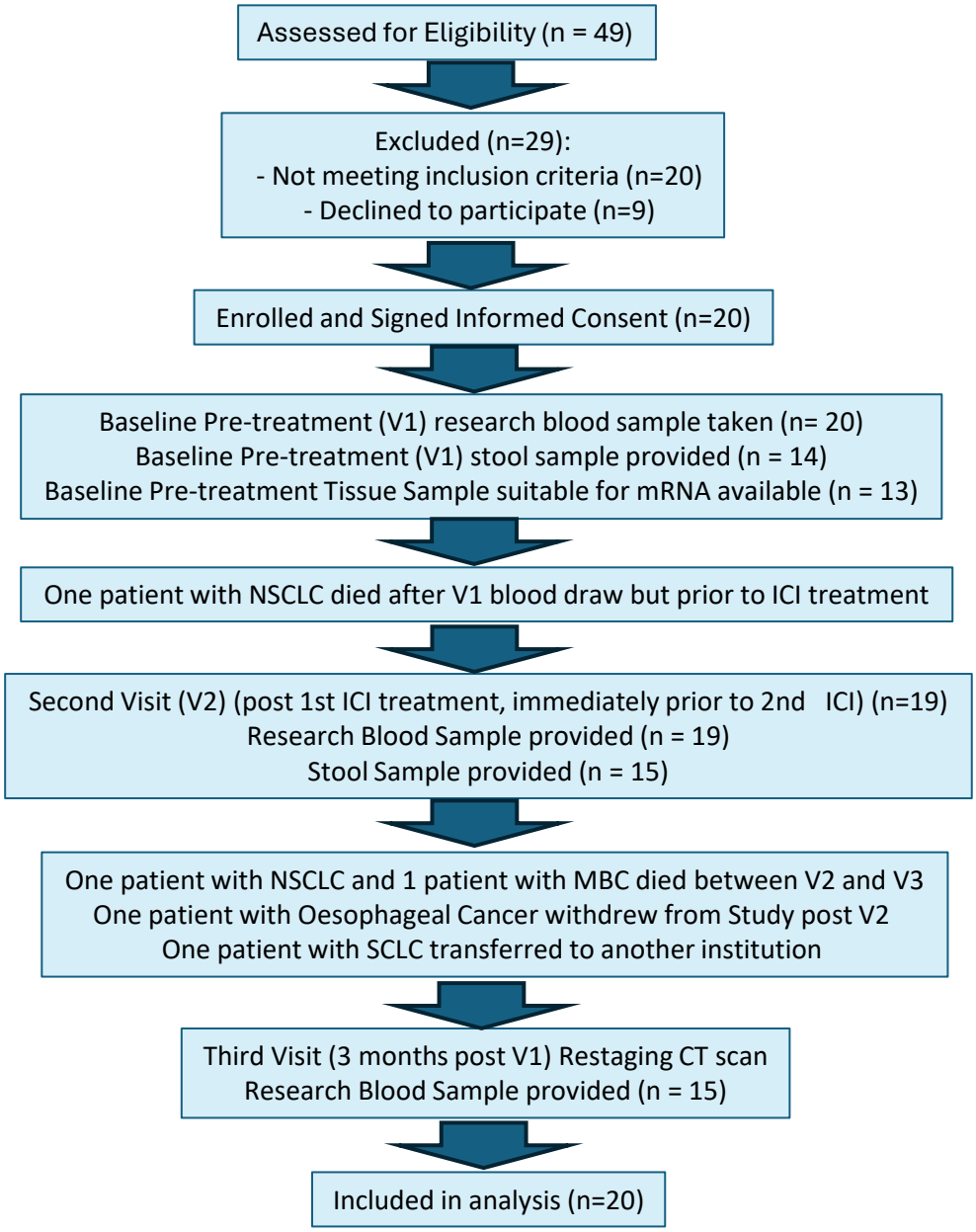

Figure 3.1 Flow Diagram of APC 125 Study.

Study participation involved two extra blood draws of 20-40 millilitres prior to commencing immunotherapy and either at 3-6 weeks (usual timing of second dose ICI) or when immunotherapy was stopped, if earlier than 3-6 weeks. Patients were asked to provide a stool sample at baseline and at second study visit. They were invited to undergo the Cambridge Neuropsychological Test Automated Battery (CANTAB) test before the commencement of treatment and again, 3-6 weeks later, when they arrived for their second treatment. (See Appendix D Schedule of Trial Activities and Blood Sample Instructions).

Appropriate inclusion and exclusion criteria underpinned participation in the study. For eligibility and enrolment in the study, subjects must:

1. Have been able to give written informed consent.
2. Have been over 18 years of age.
3. Have been diagnosed with unresectable/metastatic disease (solid tumour).
4. Been fit for first line anti PD-1 or PD-L1 immunotherapy as assessed by the treating physician (Concurrent treatment with cytotoxic chemotherapy or Tyrosine Kinase Inhibitor is allowed).
5. Have had measurable disease by iRECIST

Subjects were excluded from the study if they:

1. Had previously been treated with immune checkpoint inhibitors in any setting (neoadjuvant, adjuvant or metastatic).
2. Were receiving concomitant treatment with Ipilimumab or any anti-CTLA4 therapy.
3. Were patients who were on clinical trials of immunotherapy, unless the study sponsor gave written permission for their participation in this study.

Ethics Approval was sought from the Clinical Research Ethics Committee (CREC) of UCC (received 13 Jan 2021) and from the Clinical Ethics Committee of the Bon Secours Health System (received 5 March 2021).

3.2 Sample Collection and Analysis, Quality of Life Questionnaires and Psychomotor testing

3.2.1 Blood Samples

Full Blood Count including Total White Cell Count, Neutrophil Count and Lymphocyte Count and Platelets were obtained from patients' standard of care baseline (pre-treatment, Visit 1 or Timepoint 1) blood draws. Where possible, ESR and LDH were also measured at baseline visit in the Bon Secours Hospital Cork Laboratory.

Three EDTA tubes were used to collect blood for future flow cytometry analysis at first and second visits. These were then collected by APC staff, centrifuged and frozen at -80°C in the Nally Lab as detailed in Appendix D and Appendix E SepMate^{TM}-50 protocol.

Serum tubes were taken at visits one, two and three for measurements of the immune metabolites L-Kynurenine (K), L-Tryptophan (T), Kynurenic Acid (KA) and for proteomic analyses.

3.2.2 Analysis of Serum Samples for Immune Metabolites

Serum Samples were taken at all three study visits (baseline, second treatment visit and final restaging CT scan and treatment visit (at 3 months)) and were analysed in the Clarke Lab in UCC by Dr Cristina Rosell Cardona as per a previously published methodology (Ratsika et al. 2024) (Detailed in Appendix F, Analysis of Serum Samples for Immune Metabolites). The three metabolites measured were L-Kynurenine (K), L-Tryptophan (T), and Kynurenic Acid (KA). The ratios of L-Kynurenine to L-Tryptophan (K/T) and Kynurenic Acid to L-Kynurenine (KA/K) were calculated.

3.2.3 Analysis of Serum Samples for Cytokine, Interleukin and soluble cell surface receptors

Serum samples were analysed for cytokine, interleukin and soluble receptor expression using Olink® dual recognition Proximity Extension Assay (PEA). The PEA assays work by using two antibodies which bind to different epitopes of the same antigen. Each antibody carries a single stranded DNA oligonucleotide which is complimentary to the other antibody's oligo DNA sequence. When the antibodies bind to the target protein the DNA strands join to form double stranded dsDNA. This unique dsDNA can be amplified by PCR leading to a signal which identifies the target antigen and correlates with its concentration (Assarsson et al. 2014). Ninety-two different soluble proteins were measured at V1 and V2 (baseline pre-ICI treatment and first post-ICI visit). Olink® PEA assays are reported in terms of normalised protein expression (NPX) compared to internal controls on a $\log_2$ scale, where high NPX value equals a high protein concentration. NPX is a relative quantification unit. Spiked internal controls were used at each step of the process for quality assurance. Two non-human antigens were added at the first step of incubation of sample with appropriate ssDNA tagged antibodies; paired DNA-tags were added at the second step (extension of the hybridizing oligonucleotide by 3' Exonuclease capable DNA polymerase). The final QA step was detection control where a dsDNA amplicon is added to the sample prior to PCR

amplification of sample and control amplicons. If the controls differ from acceptance criteria by more than ± 0.3 NPX then the sample was deemed to have failed QC and was not included in analysis. (See Appendix G Olink® Target Immuno Oncology Assay and Appendix H Olink® Assay Technical Details)

3.2.4 Analysis of PAXgene® blood samples and pre-treatment tumour tissue for mRNA expression

PAXgene® mRNA blood tubes were collected at baseline and at second visits (3-6 weeks later) and were frozen for future mRNA analysis. These were divided into aliquots, frozen at -80°C Celsius and shipped to GenXPro for analysis. Where pretreatment tissue samples of tumour biopsies were available, these were sent to St. James's Hospital for review and suitable fixed unstained slides were sent to GenXPro.

The aim of the mRNA analysis was to discover if mRNA expression profiles of tissue and matched paired sequential blood samples could identify genes or pathways predictive of response to ICI treatment. GenXPro uses 3' massive analysis of complementary-DNA (c-DNA) ends (MACE) which overcomes some of the disadvantages of traditional mRNA sequencing. It is highly effective at generating mRNA profiles from small and degraded samples (Boneva et al. 2020) and relies on Unique Molecular Identifiers (UMI) which are short unique nucleotide sequences attached to individual unique c-DNA sequences prior to PCR amplification. UMIs can be used to reduce PCR bias where some molecules are preferentially amplified by ensuring that each read is only counted once.

Library Preparation and Sequencing; The 3'-RNA libraries were prepared using the MACE-Seq Kit (GenXPro GmbH) according to manufacturer's instructions. Briefly, mRNA was fragmented, and the 3' ends were reverse transcribed, and cDNA was generated after template switching and incorporation of UMIs (TrueQuant; GenXPro), followed by PCR amplification with a minimal number of cycles and silica-bead purification. Sequencing was performed on an Illumina NEXTSEQ instrument with 1x76 bps.

Data Processing: Unprocessed sequencing reads were adapter-trimmed and quality-trimmed using Cutadapt (version 4.6) with the arguments "-e 0.1 -O 3 -q 20 -m 20 -n 8" (Martin 2011). Additional sequencing artifacts were removed from the reads with the arguments "-m 20 -u 4 -a 'A{300}X' -a 'A{10};o=10'". FastQC (0.11.9) ("Babraham Bioinformatics - FastQC A Quality Control Tool for High Throughput Sequence Data" 2025)) was used to assess the quality of sequencing reads. Processed sequencing reads were

mapped to ENSEMBL_dna of hg38 (Homo sapiens) using Bowtie2 (2.4.4, (Langmead and Salzberg 2012)) with the arguments "--sensitive --local". Quantification of mapped reads to each gene was performed using HTSeq (version 2.0.2, (Anders et al. 2015)) with the arguments "-i gene_id -r pos -a 0" and setting strandedness to "yes". Raw counts were geometric-mean-normalized using DESeq2 (version 1.38, (Love et al. 2014)) and Transcripts Per Million (TPM)-normalized by dividing each count with the sum of all counts for each sample multiplied by one million. MultiQC (version 1.25.1 (Ewels et al. 2016)) was used to create a single report visualising output from multiple tools across many samples, enabling global trends and biases to be quickly identified(Ewels et al. 2016).

Differential Expression Analysis (DEA): DEA was performed using DESeq2 (version 1.38). Only entries having at least a raw count of 5 in at least 2 samples were used in the DEA. Log2FoldChange values were shrinked using "ashr" ((Stephens 2017)). DEA results with an FDR-adjusted p-value lesser or equal than 0.05 and an absolute log2FoldChange greater or equal than 1 were deemed significant.

Gene Set Enrichment Analysis (GSEA): Gene set enrichment analysis (GSEA) is a computational method used to determine whether predefined groups of genes, such as those involved in specific biological pathways or functions, show statistically significant differences in expression between two conditions. Instead of focusing on individual genes, GSEA evaluates gene sets collectively, increasing sensitivity and biological interpretability, especially when changes in single genes are modest but coordinated. This approach uses ranked gene expression data to assess whether members of a gene set are overrepresented at the extremes of the list. GSEA is widely used to identify affected pathways, infer functional mechanisms, and interpret results from high-throughput experiments like RNA-seq or microarrays. We used *R* and *clusterProfiler* for gene set enrichment analysis and visualization (Xu et al. 2024). As per standard practice only gene sets having a minimum size of 5 and a maximum size of 500 were used for the analysis (Subramanian et al. 2005; "GSEA User Guide" 2025). P-values and FDR-values are based on 1,000 permutations and a p-value cutoff of 0.05 was used. WikiPathways images were coloured and rendered using CanvasXpress10.

3.3 Stool Samples and Faecal Microbiome Analysis

Faecal Samples were provided prior to visit one and visit two and frozen in the O'Toole Lab in UCC. Microbial DNA was extracted (see Appendix I Isolation of Microbial DNA from Faecal Samples). Aliquoted stocks were diluted to 100 ng/ul, total volume 50 ul for

Novogene Library preparation. Where the stock concentration was below 100 ng/ul, 50 ul of the stock was used instead. 16S amplicon sequencing was carried out by Novogene. Short (less than 500 base pair) hypervariable regions of interest (V3-V4) were amplified by PCR and analysed using Next Generation Sequencing (NGS) as outlined in Table 3.1 (Klindworth et al. 2013).

Table 3.1 cDNA Primers Applied to Amplicon Metagenomic Sequencing (Downloaded from Novogene Website Feb 1st 2025. Nucleotide symbols: R = A or G; Y = C or T; N = any nucleotide; W = A or T; M = A or C; K = T or G; S = C or G; and H = A/C/T (Yang et al. 2015)).

Amplified Region			
V3-V4	470 bp	341F	CCTAYGGGRBGCASCAG
		806R	GGACTACNNGGGTATCTAAT

Microbiome diversity was assessed using common microbial statistics. Briefly alpha diversity looks at how diverse a single population or stool sample is in terms of how many different species exist in the sample and how numerous or abundant each species is. Richness is defined as the number of different species or Operational Taxonomic OTU in each sample and evenness measures the relative abundance distribution across species. Standard metrics of alpha diversity include Chao1, Simpson, Shannon Index and Pielou's Evenness (Chao 1987; Kim et al. 2017). Each of these has advantages and disadvantages. Chao1 gives a good estimate of species richness but assumes the distribution of rare taxa and is sensitive to outliers. It is affected by sequencing depth (deeper sequencing will detect more rare species inflating Chao1) and, therefore, may not be a good cross study comparator (Reese and Dunn 2018). The Shannon Index combines richness and evenness and is useful in cross-study comparisons. Simpson's Index measures the probability that two randomly chosen individuals belong to the same species which gives a good measure of evenness but underrepresents rare species. Pielou's Evenness measures evenness but not richness (Lutz et al. 2022). Beta diversity measures the difference in diversity between different populations or samples and was used to compare pre and post treatment samples. In this study, beta diversity was measured using the Unifrac method. Unifrac incorporates phylogenetic information which may provide better biological comparison between populations. The Unweighted Unifrac focuses on presence/absence and is sensitive to rare taxa whereas the Weighted Unifrac is affected by abundance and can be affected by a few dominant taxa (Lozupone and Knight 2005).

Notes on Statistical Test Used in the Volcano Plots

The volcano plots were generated using EdgeR, which applies a negative binomial model to analyse differential abundance (Robinson et al. 2010). Specifically, the test used is the exactTest() function in EdgeR, which is similar to a Fisher's exact test but adapted for count data using a negative binomial distribution.

Breakdown of the Statistical Analysis used for Volcano Plot Analysis:

1. Normalization → EdgeR first applies TMM normalization (Trimmed Mean of M-values) to account for sequencing depth differences.

2. Dispersion Estimation → As there are no replicates (multiple samples from the same patient at the same timepoint) a fixed dispersion of 0.01 was chosen as EdgeR requires a dispersion value for testing.

3. Exact Test (Fisher-like) → EdgeR's exactTest() compares the two timepoints for each patient, testing whether bacterial genus abundance is significantly different.

4. P-values & FDR Correction → The raw p-values are adjusted using False Discovery Rate (FDR) correction (p.adjust(method = "fdr")).

Y-Axis Threshold for P-Value Significance

The y-axis in the volcano plot represents -log10 (P-value). The threshold for significance is typically set at $p < 0.05$. Since $p = 0.05$, then, Log 10 (0.05) ≈ 1.3 −log 10 (0.05) ≈ 1.3. The dashed horizontal line at 1.3 (-log10(0.05)) indicates statistical significance (Above this line → Significant bacterial genera; Below this line → Not statistically significant).

Summary

Test Used → EdgeR's exactTest (Negative Binomial Model, similar to Fisher's Exact Test). Not ANOVA → ANOVA assumes normality, which is not valid for count data. Significance Threshold → Dashed line at -log10(0.05) = 1.3 on the y-axis indicates significance.

3.4 FACT-ICM Questionnaire

The FACT-ICM was created in 2020 and is a validated quality of life questionnaire, specifically tailored to patients who are on immune checkpoint inhibitors. The FACT-ICM consists of the validated FACT-G and a 25-item toxicity checklist that is specific to immune

checkpoint inhibitors. The 25-item checklist was created by descriptive thematic analysis of interviews from patient focus groups and patient interviews. The form takes approximately 10 minutes to complete (A. R. Hansen et al. 2020) (See Appendix J for FACT-ICM Questionnaire).

FACT-ICM is divided into five subscales. Four of these are Physical Well Being (PWB), Social/Family Well Being (SWB), Emotional Well Being (EWB) and Functional Well Being (FWB), and are general components of the FACT-G QoL questionnaire. The Additional Concerns section asks patients about common side effects of ICI treatment. In each section, each item is given a score (for some items a reversal score is indicated). Individual items were summed to obtain a score. The sum of the item scores were then multiplied by the number of items in the subscale and divided by the number of items answered. This produced the subscale score. The higher the score the greater the quality of life, with scores being in the range from 0 to 208.

All participant responses to the FACT-ICM quality of life questionnaire were recorded and scored. Both FACT-ICM scores and relevant patient outcome measures were anonymised and stored in Excel on a password protected computer in Bons Secours, Cork. All data was then analysed using Excel and Graph Pad Prism 10.2.3 (403). Summary statistics were performed, including descriptive statistics such as mean values and standard deviations. The median and interquartile range were also calculated for this dataset. Histogram and boxplots were used to display means and interquartile ranges, respectively. The statistics package SPSS was used to analyse changes in K/T ratios and these were correlated with clinical outcomes. Graphs were produced using GraphPad PRISM.

3.5 CANTAB Psychomotor Testing

Cognitive Testing using the CANTAB (Cambridge Neuropsychological Test Automated Battery) was carried out using PC tablets during patients' visits to the hospital for treatment at pre-treatment visits and three months. Due to COVID restrictions, trained test administrators could not attend the hospital in person but instead, guided Research Nurses and patients using iPad video calls. CANTAB is a computerised battery of psychomotor tests which measures processing speed and attention (Fray and Robbins 1996; Sahakian and Owen 1992).

Table 3.2 Summary of CANTAB Tasks Completed at Pre-Treatment and 3-month study visits.

Task Name	CANTAB Name
Motor screening task (MOT)	MOT Tone 2.0
Reaction Time (RTI)	RTI Simple and Five-Choice
Match to sample visual search (MTS)	MTS Recommended Standard Tone
Spatial Working Memory (SWM)	SWM Recommended Standard 2.0 Extended
Paired Associates Learning (PAL)	PAL Recommended Standard Extended
Rapid Visual Information Processing (RVP)	RVP 3 Targets

Cognitive assessments typically lasted approximately 1 h and 15 min. At each testing session, participants first completed the motor screening task (MOT) to get accustomed to using the touch screen monitor. The following tests were then administered in a counterbalanced fashion: Paired Associates Learning (PAL), Delayed Match to Sample (DMS), Rapid Visual Information Processing (RVP) and Simple Reaction Time (SRT) (Kennedy et al. 2015).

Motor Screening Task (MOT): General screen on whether sensorimotor or comprehension deficits will affect valid data collection. This evaluates accuracy measured by the distance between where the patient's finger touches the screen and the location of a target, as well as response time.

Simple Reaction Time (SRT): The SRT is a basic measure of reaction time to a simple stimulus (white box) which appears on screen over a number of repeated trials. The outcome measure assessed at each testing session was latency (measured in milliseconds (ms)).

RTI Mean Five-Choice Movement Time: The mean time taken for a subject to select the target stimulus after releasing the response button. (measured in milliseconds (ms)).

Delayed Match to Sample (DMS): The DMS is a forced choice recognition memory test and assesses simultaneous and short-term (delay of 0, 4 or 12 s) recognition memory of complex patterns which appear on-screen. Overall performance on the DMS has been shown to activate a range of the brain regions including the anterior cingulate, the medial frontal gyrus region and posterior cortical regions. Notably, longer delay trials more heavily engage temporal regions and ventrolateral frontal cortices (Elliott and Dolan 1999). The outcome measures assessed at each testing session were the total percent correct and total correct latency.

Spatial Working Memory (SWM): The SWM task is a computerized assessment designed to evaluate an individual's ability to retain and manipulate visuospatial information over short periods - a key component of executive function. In this task, participants were shown a number of coloured boxes on the screen and asked to find hidden blue tokens by searching inside these boxes. The challenge lies in remembering which boxes have already been checked to avoid returning to the same location, especially as the number of boxes increases. This task requires both working memory and strategic planning, as participants must monitor their search patterns and update information in real time. Errors are categorized into *between-search errors* (returning to a box where a token was already found in a previous search) and *within-search errors* (rechecking the same box during a single search). The SWM task is widely used in both clinical and research settings to assess frontal lobe function and is sensitive to deficits seen in conditions such as schizophrenia, ADHD, and traumatic brain injury (Owen et al. 1990).

Paired Associates Learning (parallel mode): PAL is a test of visuospatial episodic memory and assesses new learning, list learning and list memory. PAL has shown sensitivity to changes in the function of hippocampal brain regions and engages a fronto-parietal network during encoding phases and posterior cingulate and left cuneus regions during retrieval stages (Blackwell et al. 2003). Outcome measures assessed at each experimental session were total errors (adjusted) and mean trials to success and first trial memory score.

Rapid Visual Information Processing (RVP): The RVP assesses visual sustained attention and has been shown to engage a fronto-parietal network of brain regions (Coull et al. 1996). The outcomes measures assessed at each testing session were total hits, total false alarms and latency. Participants watch a stream of digits (from 2 to 9) appearing in the center of a screen at a rate of 100 digits per minute. They're required to detect target sequences of digits (e.g., 2-4-6, 3-5-7) and respond when they see them.

3.6 Statistics

GraphPad PRISM was used to calculate ANOVA to compare serial sample values and Cox Proportional Hazards results that correlated clinical and laboratory results with the outcomes PFS and OS. Durable clinical benefit (DCB) was defined as alive and without progressive disease or Grade 3 to 4 irAE at 6 months. Where there were skewed distributions of pre-treatment laboratory variables, such as LDH, the natural log was investigated to see if it was a predictor of outcomes.

4 RESULTS

4.1 Baseline Characteristics

Between August 2021 and December 2022, 20 patients were enrolled in the study. This was broken down as follows: Twelve had Non-Small Cell Lung Cancer (NSCLC) (7 adenocarcinoma, 5 squamous cell), three had Extensive Stage Small Cell Lung Cancer (ES-SCLC), two had oesophageal adenocarcinoma, one had metastatic malignant melanoma, one had endometrial carcinoma and one had triple negative breast cancer (TNBC). Patients were followed until August 29th 2023 when the Excel database was locked. Figure 4.1 shows pre-treatment Body Mass Index (BMI) and Body Surface Area (BSA). Table 4.1 and Table 4.2 summarise the baseline clinical characteristics of the study population. Seven of 20 patients were female (35%) and 13 (65%) were male. The average patient age was 67 years (range 52 -81). The mean Body Mass Index was 23 (Standard Deviation 4.9), Median 23 [Interquartile Range 20, 26], Range 13 to 32. The mean Body Surface Area was 1.9 m^2 (SD 0.29) [IQR 1.7, 2.1] Range 1.3 to 2.3).

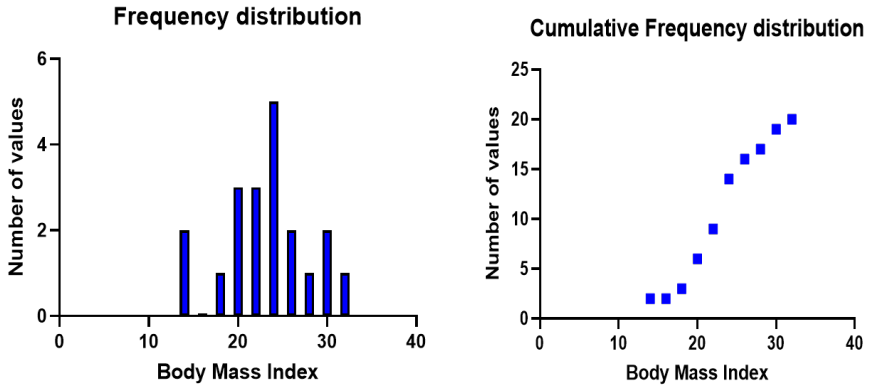

(a)

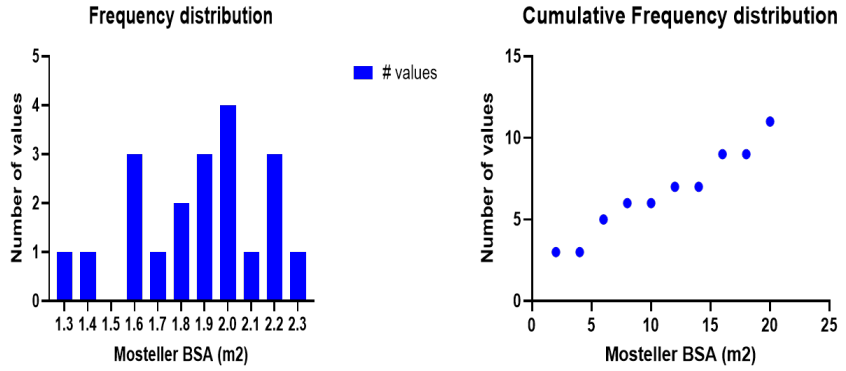

(b)

Figure 4.1 Graphical Representation of Baseline Body Mass Index and Body Surface Area (m2) calculated using Mosteller Method.

Table 4.1 Gender (Male/Female) Baseline Body Mass Index and Body Surface Area (m^2 (meters squared)) calculated using Mosteller Method (n (%); Mean (SD); Median [IQR]; (Range)).

Characteristic	**n (=20)**
Gender	
Male	7 (35%)
Female	13 (65%)
Height (m)	1.66 (0.09); 1.68 [1.62, 1.73]; (1.45 to 1.79)
Weight (kg)	77 (19); 78 [64, 88]; (39 to 111)
BMI (kg/m^2)	23.0 (4.9); 23.2 [19.9, 25.4]; (13.5 to 31.8)
BSA (m^2)	1.9 (0.29); 1.9 [1.7, 2.1]; (1.3 to 2.3)

Table 4.2 Cancer Diagnoses, Pre-treatment ECOG Performance Status (PS) (n (%)).

Diagnosis	n (=20)
Ad Lung	7 (35%)
Ad Oesophageal	2 (10%)
Endometrial	1 (5%)
Melanoma	1 (5%)
Met Breast	1 (5%)
SCLC	3 (15%)
Sq Lung	5 (25%)

ECOG PS	n (=20)
0	4 (20%)
1	14 (70%)
2	2 (10%)

4.1.1 Treatments Received and Clinical Outcomes

All lung cancer patients were scheduled to receive appropriate concurrent cytotoxic chemotherapy with their ICI for at least the first four cycles of treatment. All NSCLC cases received the anti PD-1 inhibitor, Pembrolizumab, while those with SCLC received the PD-L1 inhibitor, Atezolizumab. Both patients with oesophageal adenocarcinoma were treated with Nivolumab (an anti-PD-L1). The patient with endometrial cancer received concurrent Lenvatinib (TKI) and the patient with metastatic TNBC received concurrent Nabpaclitaxel (see Table 4.3).

Table 4.3 Type of ICI, concomitant treatments (n (%)).

Treatment	n
ICI	20
Atezolizumab	4 (20%)
Nivolumab	2 (10%)
Pembrolizumab	14 (17%)
Concomitant Chemotherapy	20
No	5 (25%)
Yes	15 (75%)
Concomitant TKI	20
No	19 (95%)
Yes	1 (5%)

Clinical outcomes for each patient are reported in Table 4.4.. Third visit FBC was available for 13 patients, but eosinophils were only measurable in 8 of them. SII and NLR were calculated for all 13 (see Table 4.6).

Table *4.5* The median PFS and OS were 20.9 weeks and 34 weeks for the entire population and 20.1 weeks and 35.9 weeks for the NSCLC cohort (Figure 4.2). Four patients experienced Grade 3-4 irAE. Some patients with ongoing response had ICI held for 1 to 2 months for multiple Grade 2 toxicities and were rechallenged on disease progression.

Table 4.4 Patient Clinical Data and Outcomes. Key; PFS = Progression Free Survival, OS = Overall Survival, Durable Clinical Benefit = PFS of 180 days or greater. NSCLC = Non-Small Cell Lung Cancer, Squam = Squamous Cell, Adeno = Adenocarcinoma, SCLC = Small Cell Lung Cancer. DCB = Defined Clinical.

Patient Number	**Cancer Diagnosis**	**Immune Checkpoint Inhibitor**	**First Restaging CT (usually at 90 days)**	**PFS (weeks)**	**OS (weeks)**	**Durable Clinical Benefit (0 = no, 1 = yes)**
1	NSCLC Squam	Pembrolizumab	Stable Disease	11	11	0
2	NSCLC Squam	Pembrolizumab	Stable Disease	43	82	1
3	NSCLC Adeno	Pembrolizumab	Stable Disease	19	68	0
4	NSCLC Adeno	Pembrolizumab	Stable Disease	35	40	1
5	NSCLC Squam	Pembrolizumab	Partial Response	25	32	0
6	NSCLC Adeno	Pembrolizumab	Stable Disease	20	108	0
7	NSCLC Adeno	Pembrolizumab	Partial Response	47	107	1
8	Endometrial	Pembrolizumab	Stable Disease	29	36	1
9	NSCLC Adeno	Pembrolizumab	Stable Disease	12	25	0
10	NSCLC Adeno	Pembrolizumab	Stable Disease	21	56	0
11	NSCLC Squam	Pembrolizumab	Stable Disease	15	16	0
12	Melanoma	Pembrolizumab	Stable Disease	31	52	1
13	Oesophageal Adeno	Nivolumab	Progressive Disease	14	30	0
14	SCLC	Atezolizumab	Partial response	18	74	0

15	SCLC	Atezolizumab	Partial Response	23	23	0
16	NSCLC Squam	Pembrolizumab	Died	20	20	0
17	SCLC	Atezolizumab	Stable Disease	22	32	0
18	NSCLC Adeno	Pembrolizumab	Died	2	2	0
19	Breast Cancer	Atezolizumab	Died	8	8	0
20	Oesophageal Adeno	Nivolumab	Partial Response	56	56	1

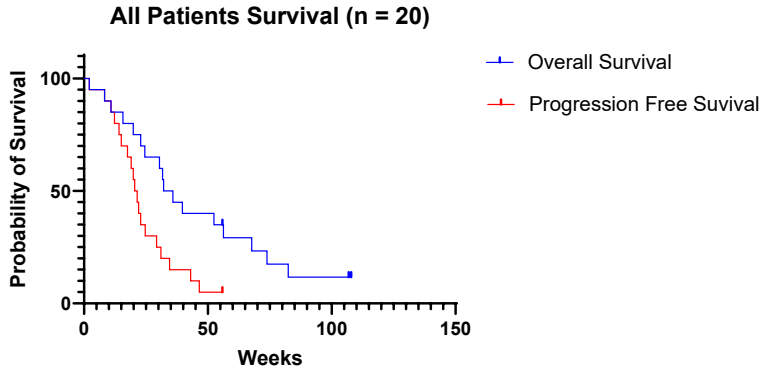

(a)

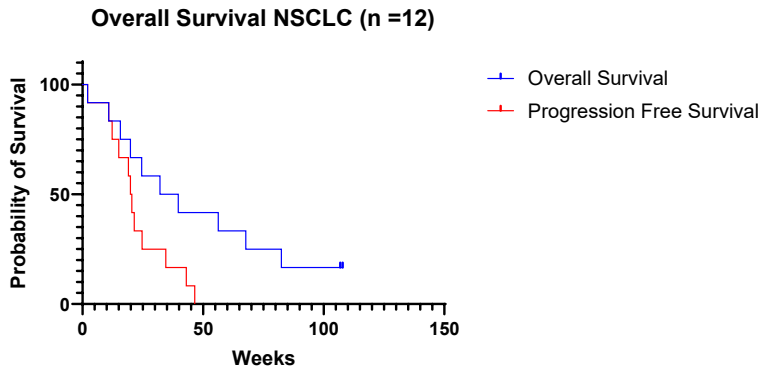

(b)

Figure 4.2 Kaplan-Meier Survival Curves for Overall Survival (measured in weeks): (a) all APC125 patients (n=20), and (b) Non-Small Cell Lung Cancer patients (n = 12).

The approved biomarker for ICI treatment in NSCLC PD-L1 TPS was analysed as a predictor of PFS and OS in the 12 patients with NSCLC. One patient (011) had insufficient tissue for PD-L1 testing and was excluded from the analysis. Four patients had high PD-L1

TPS as defined by a score ≥50% (actual values 80-100%). Seven patients had PD-L1 TPS of 0%. In these 11 patients, the Kaplan Meier survival curves for PFS and OS did not differ significantly by PD-L1 TPS status using the logrank (Mantel-Cox) test (see Figure 4.3). The median PFS was 25 weeks in the PD-L1 low group and 20 weeks in the PD-L1 high group (p = 0.083). The median OS was 32 weeks in the PD-L1 low group and 44 weeks in the PD-L1 high group (p=0.66).

Where possible all NSCLC samples especially adenocarcinoma subtype were sent to St James's Hospital Dublin or Cork University Hospital for standard of care Lung Panel testing. One patient (007) had Guardant 360 NGS of peripheral blood which detected HER2 amplification. This was confirmed by retesting tissue for HER2 IHC and ISH. This patient had a prolonged response to chemo/Pembo and subsequently to Trastuzumab deruxtecan, sadly recently succumbing to her illness 4 years post enrolling on study. Patient 016 (OS = 20 weeks) had a KRAS G12C mutation and Patient 018 (OS = 2 weeks) had a KRAS G12V mutation detected in their tumour specimens.

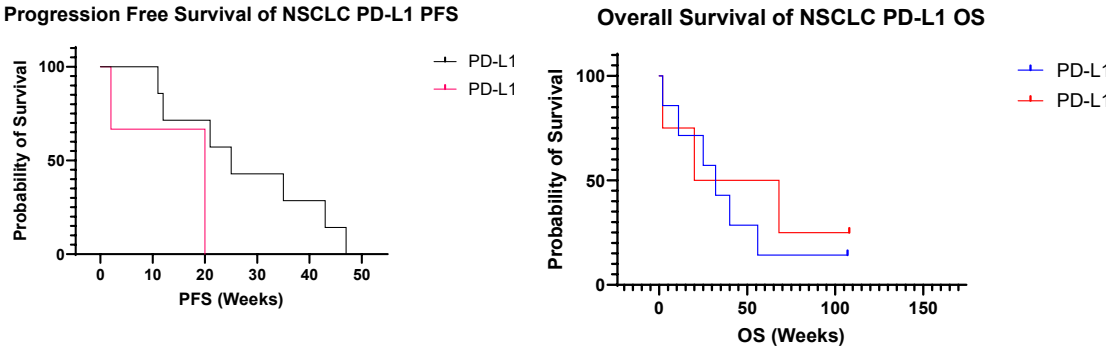

(a) (b)

Figure 4.3 Kaplan-Meier Survival Curves for Progression Free Survival (PFS) (a) and Overall Survival (OS) (measured in weeks) (b) of Non-Small Cell Lung Cancer (NSCLC) patients with known PD-L1 Tumour Proportion Score (TPS) (n= 11).

4.1.2 Baseline Markers of Inflammation

Seventeen patients had a baseline ESR measured. The mean ESR was 55 mm/hr (Standard Deviation 35), Median 56 [IQR 23, 88] (Range 5 to 114). All twenty patients had baseline Albumin (g/dL) measured. The mean Albumin was 34 g/dL (SD 4.6), Median 35 [IQR 31, 39] (Range 25 to 41). C Reactive Protein was measured in 18 patients, mean 33 mg/dL (SD 53), Median 14 [IQR 2.1, 54] (Range 0.3 to 219). Given the non-linear frequency distribution, the natural log frequency distribution was calculated. Lactate Dehydrogenase was measured in 17 patients, mean 302 U/L (SD 192), Median 246 [IQR 209, 294] (Range 136 to 799). The frequency distribution of the natural log was calculated for variables with a skewed distribution (Figure 4.4).

4.1.2.1 Neutrophil to Lymphocyte and Eosinophil Ratio

NLR was calculated for 20 patients. The NLR Mean 8.1 (SD 8.7), Median 4.7 [IQR 3.1, 8.8] (Range 1.1 to 31). Baseline Neutrophil to Eosinophil Ratio was calculated for 16 patients with detectable Eosinophils. The NER Mean was 133 (SD 266), Median 49 [IQR 23, 130] (Range 7.7 to 1099).

4.1.2.2 Systemic Inflammatory Index

Systemic Inflammatory Index (Platelets x Neutrophils/Lymphocytes) was available for all 20 patients (see Figure 4.5).

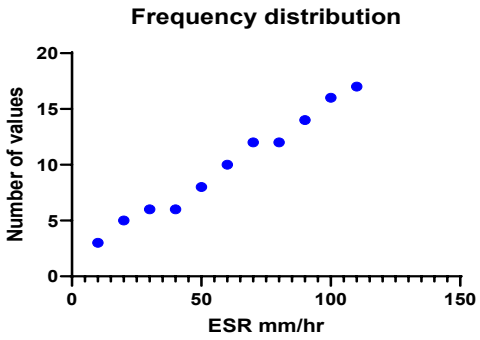

(a) ESR Baseline Values

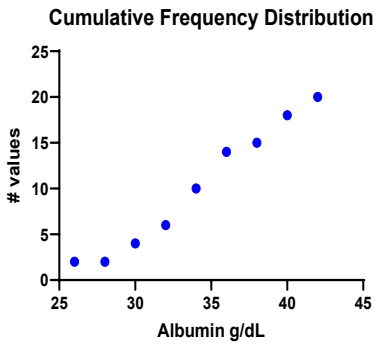

(b) Albumin Baseline Values

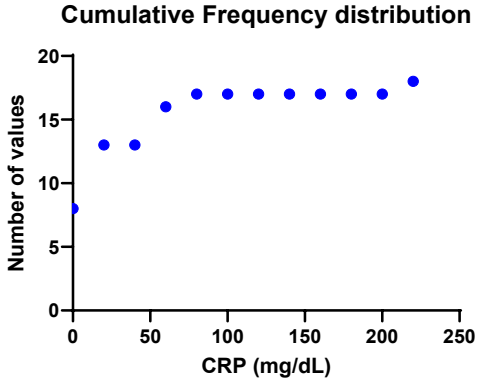

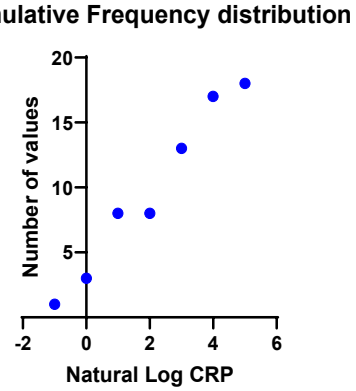

(c) Graphical Representation of CRP Baseline Values

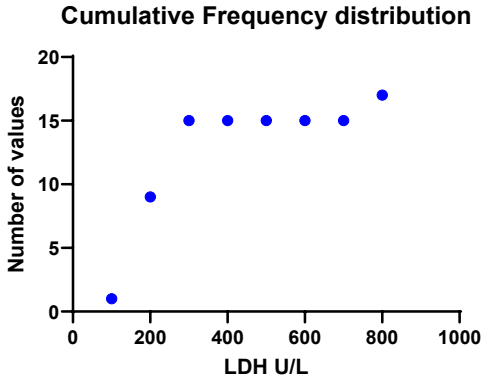

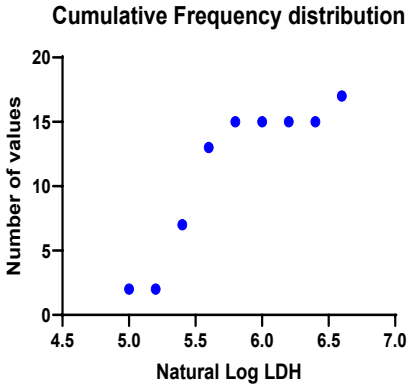

(d) Graphical Representation of LDH baseline values

Figure 4.4 Frequency Distribution of Baseline Routine Blood Test Values and Selected natural Log Frequency Distributions. Erythrocyte Sedimentation Rate mm/hr (ESR), C-Reactive Protein mg/dL (CRP), Lactate Dehydrogenase U/L (LDH).

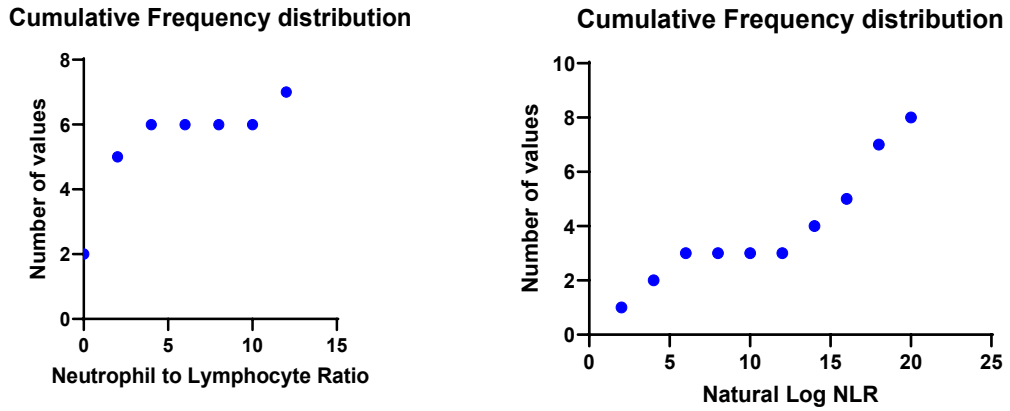

(a) Baseline and Log Transform NLR Values

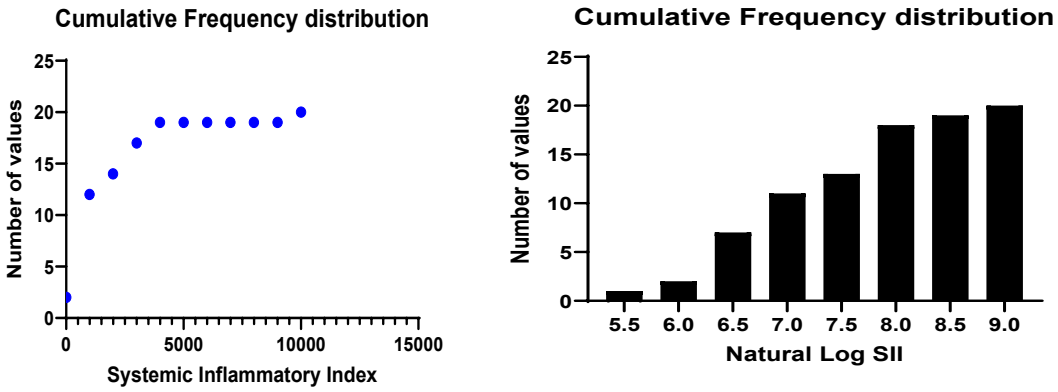

(b) Baseline and Log Transform SII Values

Figure 4.5 Cumulative Frequency Distribution and Natural Log Cumulative Frequency Distribution of Neutrophil to Lymphocyte Ratio (NLR) and Systemic Inflammatory Index (SII).

4.2 Longitudinal Inflammatory Markers and Changes Therein

The second visit FBC was analysed in 19 patients (1 had deceased). Eosinophils were not detected in five patients so NER could only be calculated in 14 samples. Second visit SII was calculated for all 19 patients (see Table 4.5). Third visit FBC was available for 13 patients, but eosinophils were only measurable in 8 of them. SII and NLR were calculated for all 13 (see Table 4.6).

Table 4.5 Descriptive Statistics of Second Visit Blood Draw.

	V2 NLR	V2 NER	V2 SII
Number of values	*19*	*14*	*19*
Minimum	1.1	3.4	114
25% Percentile	2.3	15	520
Median	3.6	34	686
75% Percentile	7.1	88	1917
Maximum	27	127	5971
Range	26	124	5856
95% CI of median			
Actual confidence level	98%	99%	98%
Lower confidence limit	2.3	11	520
Upper confidence limit	7.1	93	1917
Mean	5.8	48	1209
Std. Deviation	6.5	40	1359
Std. Error of Mean	1.5	11	312
Lower 95% CI of mean	2.6	25	555
Upper 95% CI of mean	8.9	71	1864
Coefficient of variation	112%	83%	112%
Geometric mean	3.8	31	778
Geometric SD factor	2.4	2.9	2.6
Lower 95% CI of geo. mean	2.5	17	489
Upper 95% CI of geo. mean	5.8	58	1240
Skewness	2.5	0.76	2.6
Kurtosis	6.9	-0.67	8.4

Table 4.6 Descriptive Statistics of third visit blood draw.

	V3 NLR	V3 NER	V3 SII
Number of values	*13*	*8*	*13*
Minimum	0.75	13	128
25% Percentile	1.4	18	216
Median	2.3	48	313
75% Percentile	4.8	125	817
Maximum	7.5	150	1473
Range	6.8	137	1345
95% CI of median			
Actual confidence level	98%	99%	98%
Lower confidence limit	1.4	13	202
Upper confidence limit	5.1	150	884
Mean	3.1	64	544
Std. Deviation	2.1	55	406
Std. Error of Mean	0.57	19	113
Lower 95% CI of mean	1.8	18	299
Upper 95% CI of mean	4.3	110	790
Coefficient of variation	67%	86%	75%
Geometric mean	2.5	45	415
Geometric SD factor	2.1	2.5	2.2
Lower 95% CI of geo. mean	1.6	21	258
Upper 95% CI of geo. mean	3.8	97	667
Skewness	0.87	1.0	1.0
Kurtosis	-0.0050	-0.49	0.58

4.3 Serial Measurements of Serum Immune Metabolites

L-Tryptophan ((T) and its metabolites, L-Kynurenine (K) and Kynurenic Acid (KA) were measured at baseline, second and third treatment visits (Visit 1, 2 and 3) (see Table 4.7) There was some drop out due to death or withdrawal from the study. On initial ANOVA there were no significant differences between these metabolites or their ratios comparing serial

V1, V2 and V3 values when the Bonferroni correction was applied. When one outlier (patient 008, endometrial cancer, treated with Pembrolizumab and Lenvatinib) was removed using Grub's test with an alpha of 0.05, a significant rise in the L-Kyn/L-Tryp ratio between V1 and V2 was observed (p = 0.0267), followed by a significant fall between V2 and V3 (p – 0.0170) (see Figure 4.6 and Figure 4.7).

Table 4.7 Immune Metabolites at Baseline, Second and Third Study Visits. *Average Concentrations (ng/mL) of L-Kynurenine, L-Tryptophan and Kynurenic Acid at each visit with Kynurenine/Tryptophan) (K/T) Ratio and Kynurenic Acid/Kynurenine (KA/K Ratio). The Standard Error of the Mean (SEM) is shown below each value.*

Visit Number		L-Kynurenine	L-Tryptophan	Kynurenic Acid	L-Kyn/L-Tryp	KA/L-Kyn
V1 (n =20)	**Mean** (ng/ml)	1053	15981	46	0.082	0.064
	SEM	186	1065	16	0.025	0.033
	Range	376 to 3954	6528 to 21655	0.02 to 299	0.02 to 0.542	0 to 0.677
V2 (n = 18)	**Mean** (ng/ml)	1116	16570	32	0.07	0.034
	SEM	125	1261	7	0.007	0.009
	Range	509 to 2067	6496 to 29774	0 to 111	0.026 to 0.127	0 to 0.124
V3 (n = 15)	**Mean** (ng/ml)	1054	16814	66	0.071	0.093
	SEM	99	1381	28	0.012	0.047
	Range	571 to 1971	9010 to 25900	4.43 to 344.88	0.03 to 0.22	0.005 to 0.54

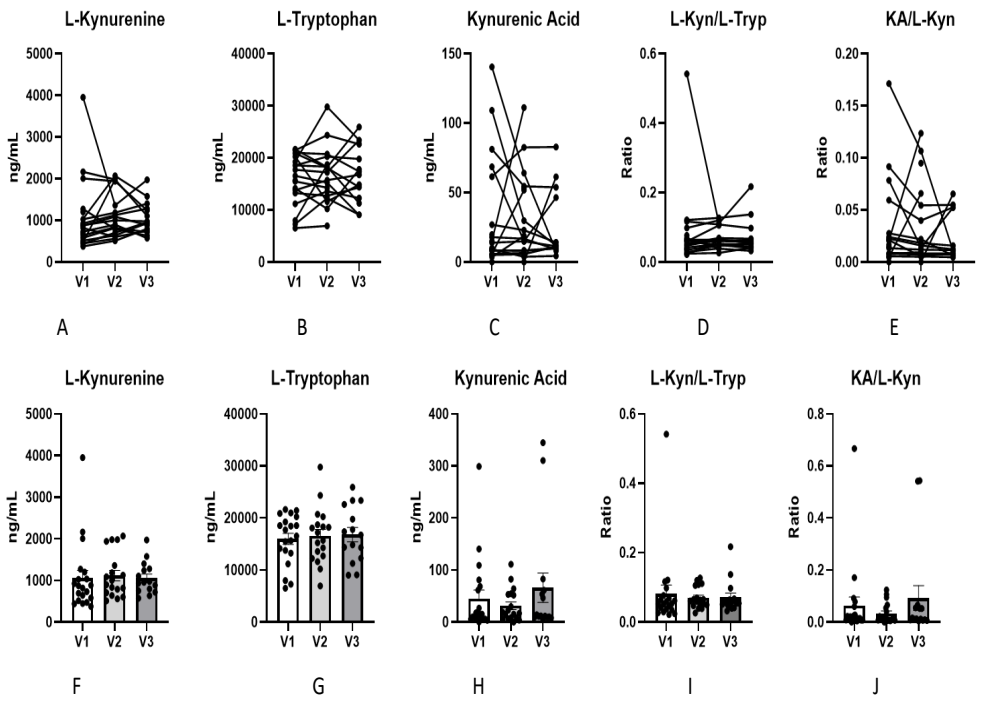

Figure 4.6 Serial Measurements of Immune Metabolites. Panels A-E show the immune metabolites for each patient, in Panels F-J, data are shown as mean ± SEM. One-way ANOVA repeated measures followed by Bon Ferroni's post hoc.

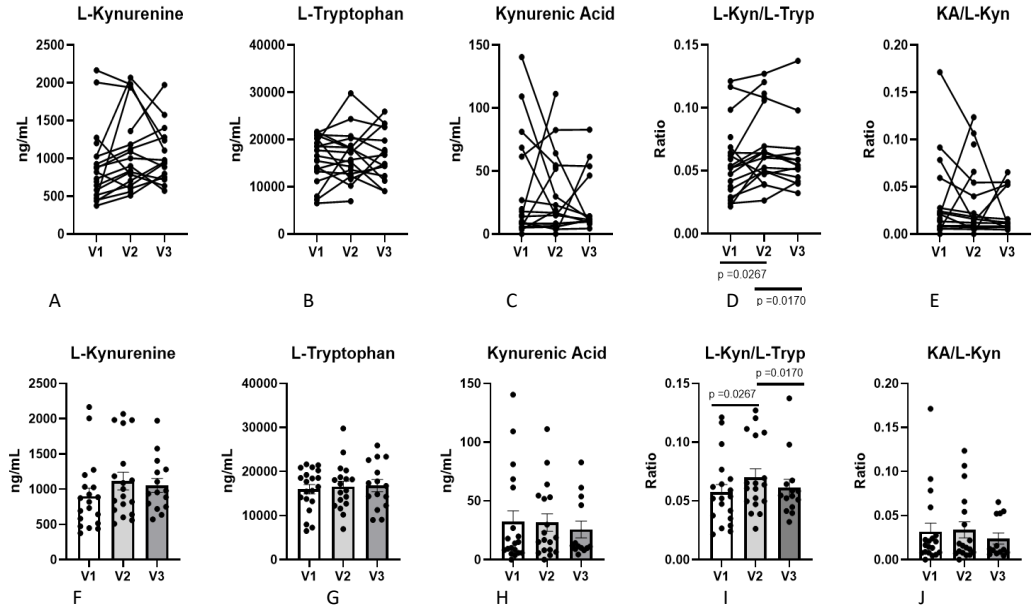

Figure 4.7 With outlier removed. Upper row (A-E) X/Y plot of individual values at each visit, Lower Row (F-J) Bar Chart of mean concentration at each visit, confidence interval. Statistically significant p-values reported. Data are mean ± SEM one-way ANOVA repeated measures followed by Bon Ferroni's post hoc.

An exploratory ANOVA analysis was carried out in the largest cancer population (NSCLC, n = 12, all treated with Pembrolizumab). An initial significant fall in K/T ratio between V2 and V3 was observed (p= 0.047). However, when the Bon Ferroni correction was applied this was no longer significant (p = 0.057). Grub's test for outliers with an alpha of 0.05 was applied to the 12 patients with NSCLC. This revealed multiple outliers (n =8) at multiple timepoints in different immune metabolites (See Table 4.8). Once the outliers were removed there were no significant changes in K, T, KA, K/T Ratio or KA/K ratio between visits (see Table 4.8 and Figure 4.8).

Table 4.8 Outlier Values of Immune Metabolites in 12 NSCLC patients identified using Grub's test, alpha = 0.05 (L-KYN = L-Kynurenine, KA = Kynurenic Acid, K/T Ratio = Tryptophan/Kynurenine Ratio).

Patient ID	Visit Number	L-KYN	KA	K/T Ratio	KA/KYN
002	V1	2165			
002	V3			0.098	
009	V2		111.2		
009	V3		310.4		0.544
010	V1		140.5		0.171

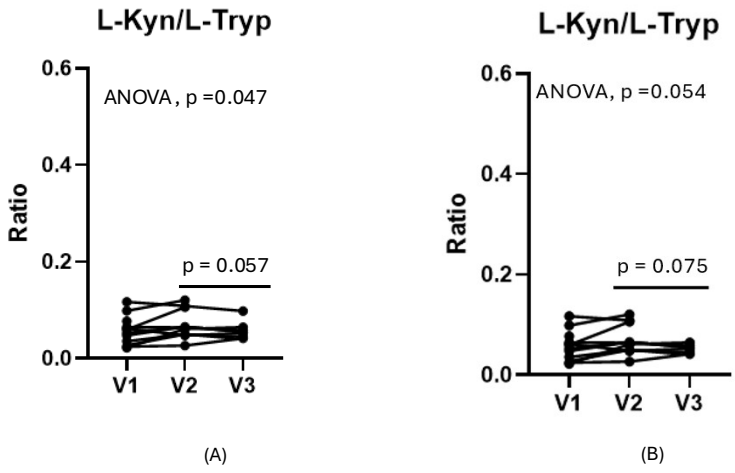

Figure 4.8 (A) Serial Analysis of K/T Ratio in all NSCLC patients (n =12). Initial ANOVA shows a significant decline in K/T Ratio between V2 and V3 which is no longer significant post Bon Ferroni correction. (B) Analysis of K/T ratio once outliers removed (n = 11). There is no significant change between visits.

4.4 Proteomic Analysis

A total of 19 patients had evaluable V1 Olink T96 proteomic blood samples of which five failed internal Quality Control, leaving 14 samples suitable for analysis. There were 17 V2 samples and 14 passed QC. All but one of the 14 V3 samples passed QC leaving 13 for analysis.

4.5 Faecal Microbiome Analysis

Fourteen first visit stool samples were provided. Fifteen second visit stool samples were also provided. There were 11 matched pairs from the same patient at visit 1 (T1) and visit 2. (T2) There were 574 unique species (Operational Taxonomic Units (OTU) in the pooled T1 samples and 704 unique species in the pooled T2 samples, with 1019 in common (see Figure 4.9). The relative abundance of the top 10 bacteria (using mixed microbial taxonomic ranks) in the pooled T1 and pooled T2 populations are shown in Figure 4.10 and the relative abundance of the top 30 groups from the same pooled samples are shown in Figure 4.11. An exploratory analysis of the relative top 20 bacterial genera in individual samples split by tumour type is shown in Figure 4.12.

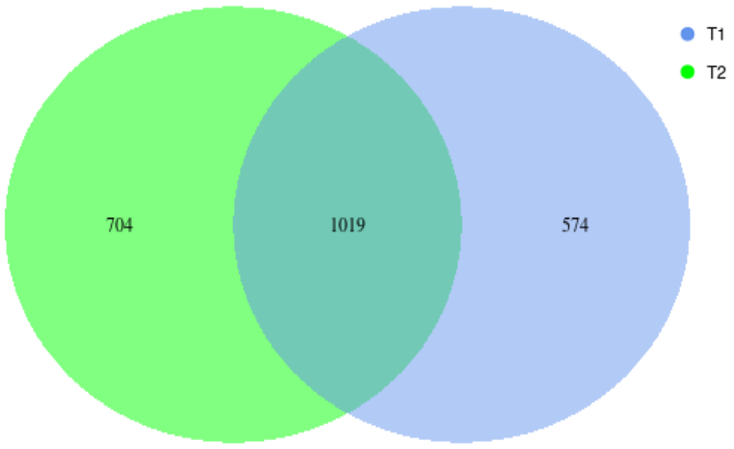

Figure 4.9 Venn Diagram of number of OTUs in Common between pre-treatment T1 (Blue) and second study visit T2 (Green). T1 represents Timepoint 1 i.e. pre-ICI treatment sample and T2 second faecal sample at second study visit 3-6 weeks later.

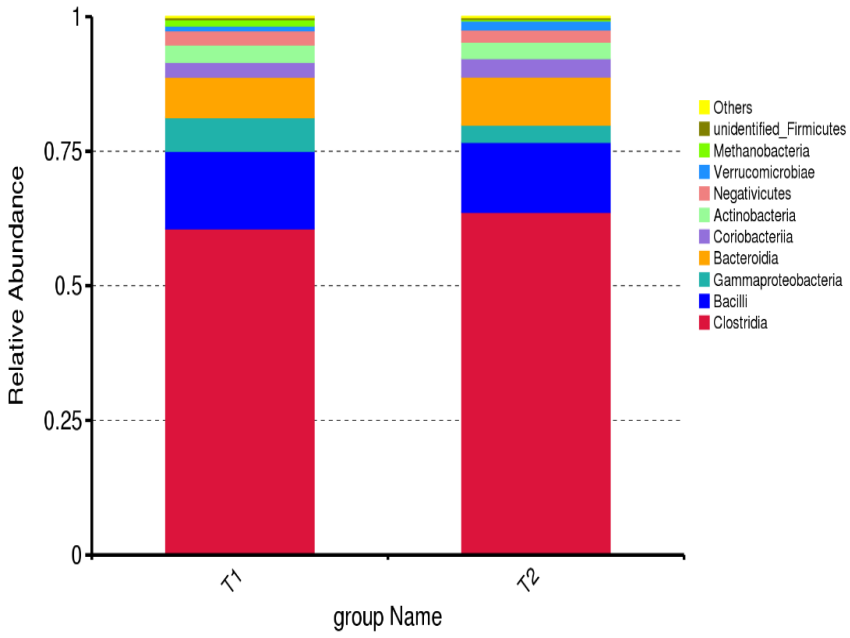

Figure 4.10 The relative abundance of the top 10 microbial taxa (mixed microbial ranks) of bacteria in the pooled analysis of T1 (first visit pre-ICI) and T2 (second visit, post one cycle of ICI) are shown. It is shown that *Clostridia* and *Bacteroidia* become more abundant on treatment whereas the relative abundance of Bacilli declines slightly.

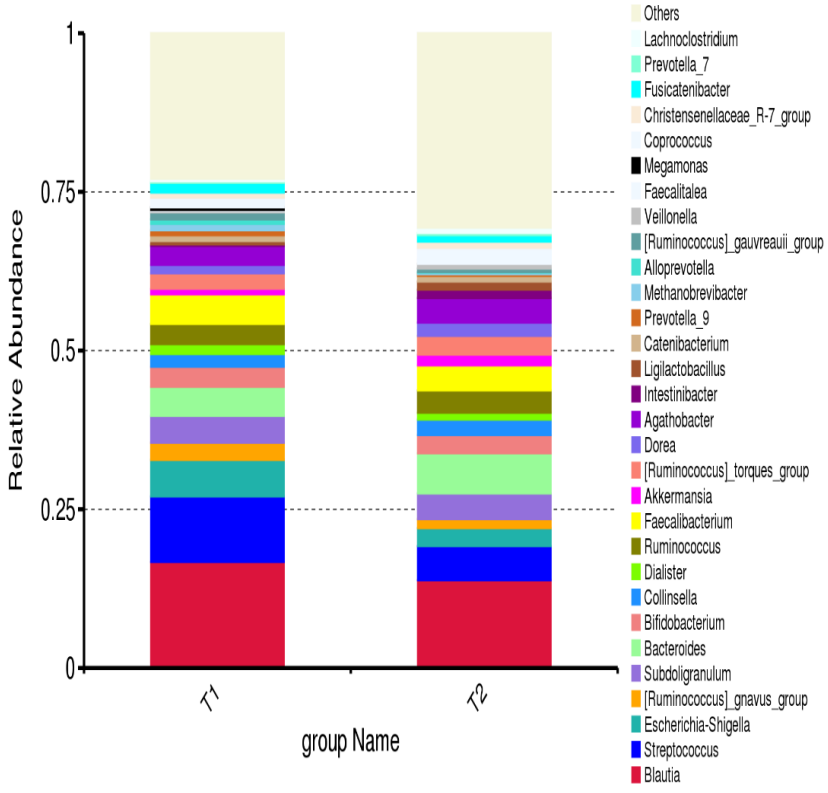

Figure 4.11 Relative Abundance of top 30 genera found in pooled T1 and T2 samples. The relative abundance of minor 'other' genera increases, with declines in the most abundant genera, *Blautia*, *Streptococcus* and *Escherichia Shigella*.

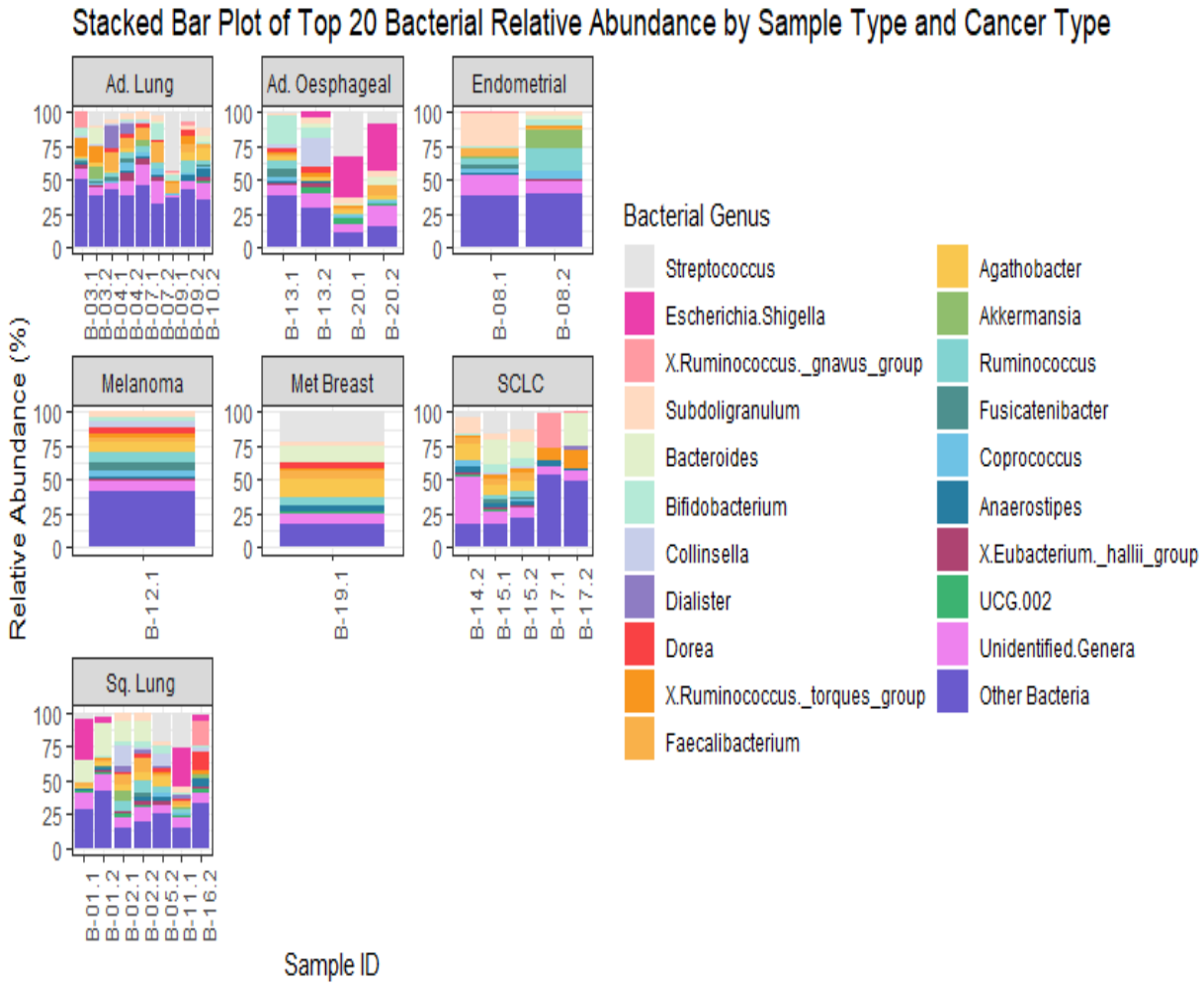

Figure 4.12 Relative Abundance of Bacterial Genera in Each Faecal Microbiome. Samples grouped by Cancer Type; Adenocarcinoma of Lung (Ad Lung) (n = 5), Adenocarcinoma Oesophagus (Ad Oesophageal), (n = 2), Metastatic Breast Cancer (Met Breast), (n = 1), Small Cell Lung Cancer (SCLC), n = 2 and then by first or second visit for that patient. E.g. B-01 1 is the first visit stool sample for patient 001 and B-01 2 is the second visit stool sample for patient 001. Patients who provided a single baseline sample (e.g. Patient 012 (Melanoma) and patient 019 (Metastatic Breast Cancer)) have only one Bar Plot.

Two-way ANOVA showed no significant difference in chao1 over time (Figure 4.13) but there was significant variation between individual patients (row factor p-value = 0.0081). Conversely Simpson and Shannon alpha diversity indices showed significant differences over time (see table below) but not between patients. Pielou's Evenness index increased significantly between visits. Student's paired t test was calculated for all three measures of alpha diversity for the 11 paired samples. Chao1 did not vary significantly between pre-treatment and post-treatment (p = 0.684). but other metrics of alpha diversity did ((Shannon (p = 0.05) and Pielou did (p = 0.019)) (shown below in Table 4.9 and in Figure 4.14).

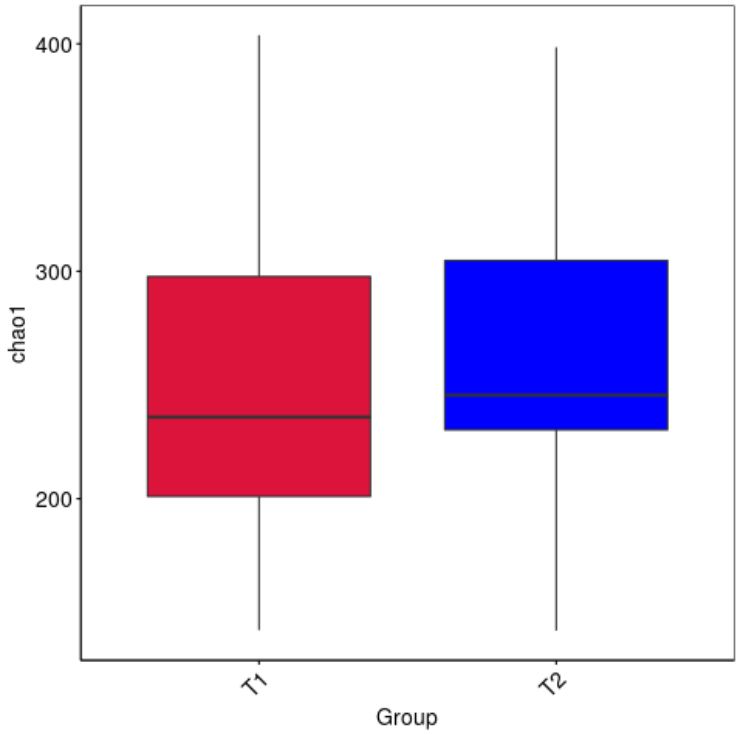

Figure 4.13 The alpha diversity of the pooled samples as measured by chao1 score increased between visits (T1 = pre-ICI treatment, T2 = pre second ICI treatment) but the 95% confidence intervals overlap indicating no significant change. (p = 0.684).

Table 4.9 Two-way ANOVA of different alpha diversity metrics. Pooled stool samples T1 – pre-treatment, T2 – pooled population ANOVA, Alpha (p value) was set at 0.05 *= significant.

	Chao1 (mean)	**Simpson (mean)**	**Shannon (mean)**	**Pielou-e Evenness Index (mean)**
T1 (n = 14)	256	0.922	5.23	0.66
T2 (n = 15)	267	0.959	5.79	0.72
T1 vs. T2 p-value of column factor (2way ANOVA)	0.155	0.023*	0.005*	0.0187*
T1 *vs.* T2 p-value of row factor	0.008*	0.495	0.068	0.488

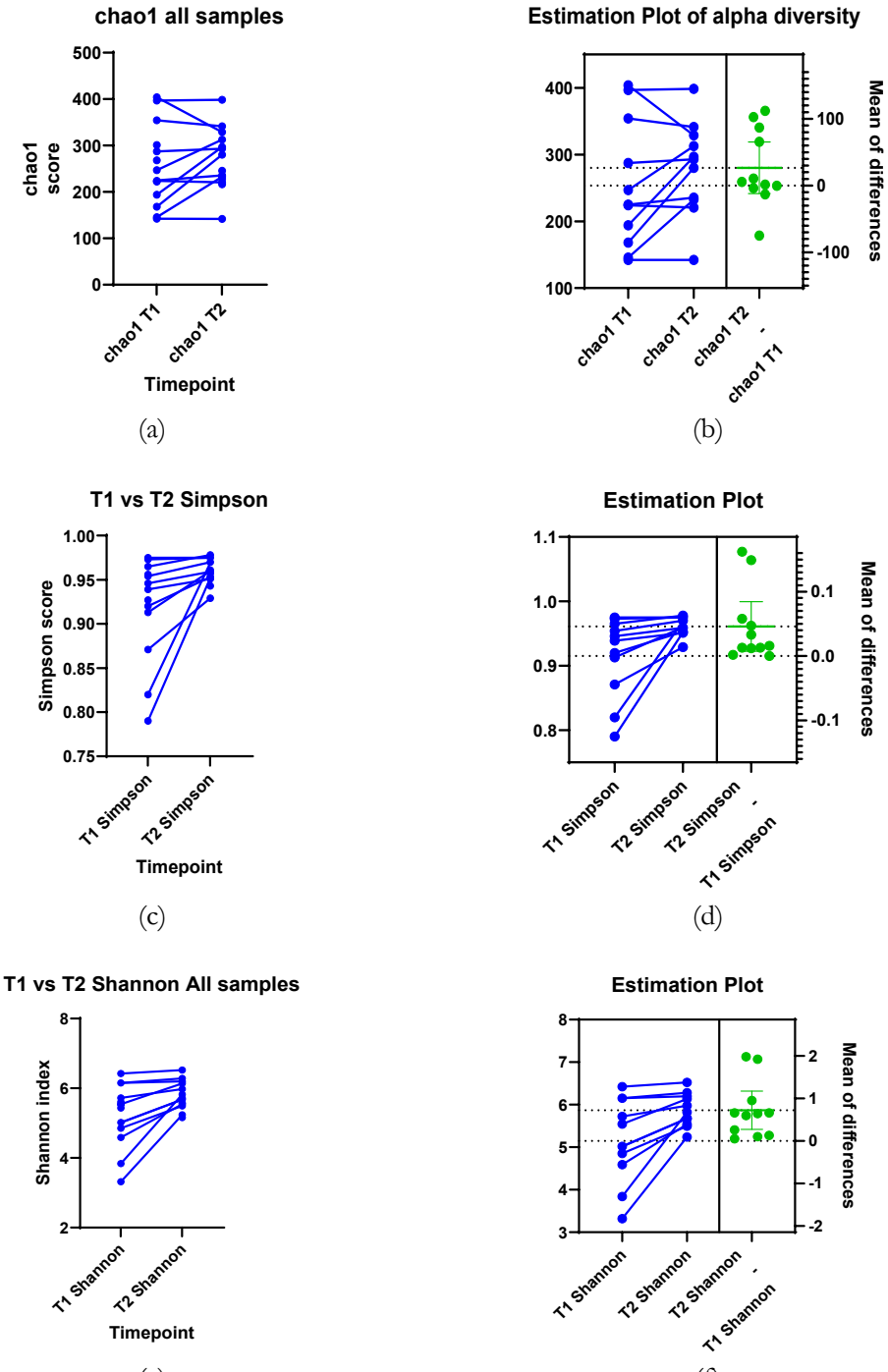

Figure 4.14 (a) Chao1 alpha diversity score for all samples with lines linking paired samples. Unpaired samples are represented by a dot and no line; (b) Estimation plot of the differences in chao1 between paired samples (unpaired samples not included.). The 95% confidence interval crosses 0 indicating no significant difference in sample means; (c) and (d) Changes in Simpson alpha diversity index over time and estimation plot; (e). and (f) Changes in Shannon alpha diversity index over time and estimation plot.

Pielou's evenness index increased between T1 and T2 from a mean of 0.66 (95% CI 0.61 to 0.71) to .72 (95% CI 0.71 to 0.74). Two-way ANOVA showed this to be significant (p = 0.019). Student's t-test of the paired samples (n =11) also showed significance (p = 0.019) (see Figure 4.15).

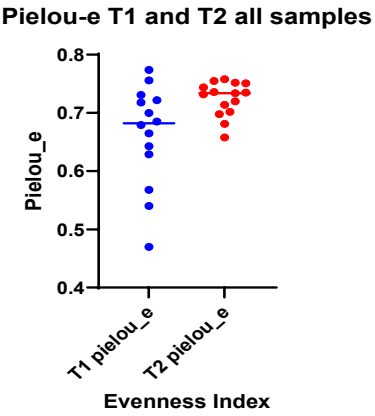

Figure 4.15 Pielou's evenness index in Faecal Microbiome Samples from Pre-treatment (T1) and prior to second ICI treatment (T2).

Beta diversity, assessed using UniFrac distance metrics, was summarised as the mean pairwise distance between samples at each timepoint. The mean UniFrac distance was lower at T2 compared to T1, indicating that samples were more similar (i.e. showed tighter clustering) at the later timepoint. This pattern was observed for both unweighted and weighted UniFrac distances, with a statistically significant reduction observed for weighted UniFrac. Ordination using Principal Coordinates Analysis suggested increased clustering of samples at T2, consistent with reduced dispersion in beta diversity space (see Table 4.10, Figures 4.16 and 4.17).

Table 4.10 Beta diversity between pooled T 1 and T2 faecal microbiome samples.

Beta diversity	T1-T2	p value
Unweighted Unifrac	0.408	0.005665
Weighted Unifrac	0.076	1.54E-11

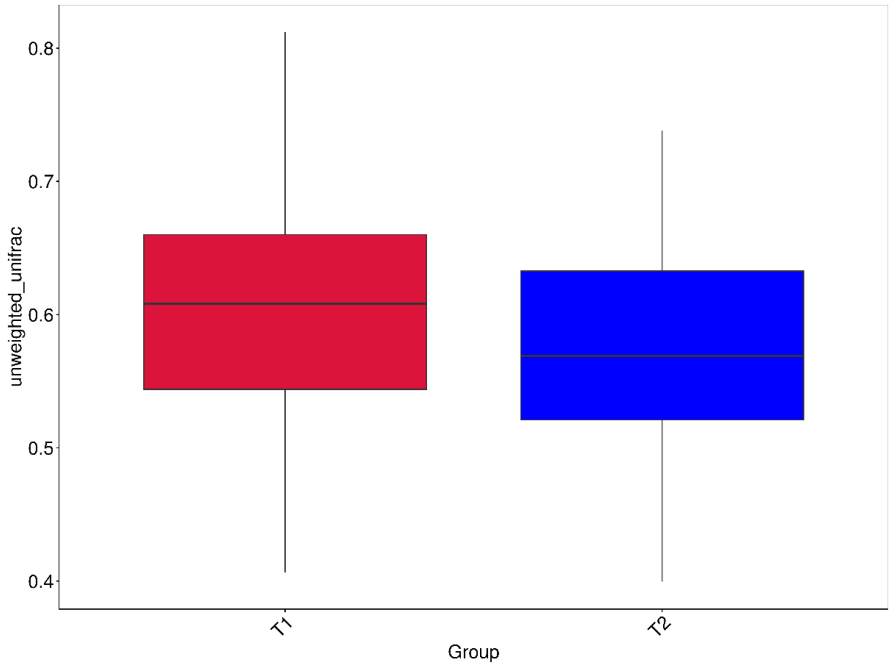

(a) Beta Diversity measured by Unweighted Unifrac (p = 0.00057 not significant)

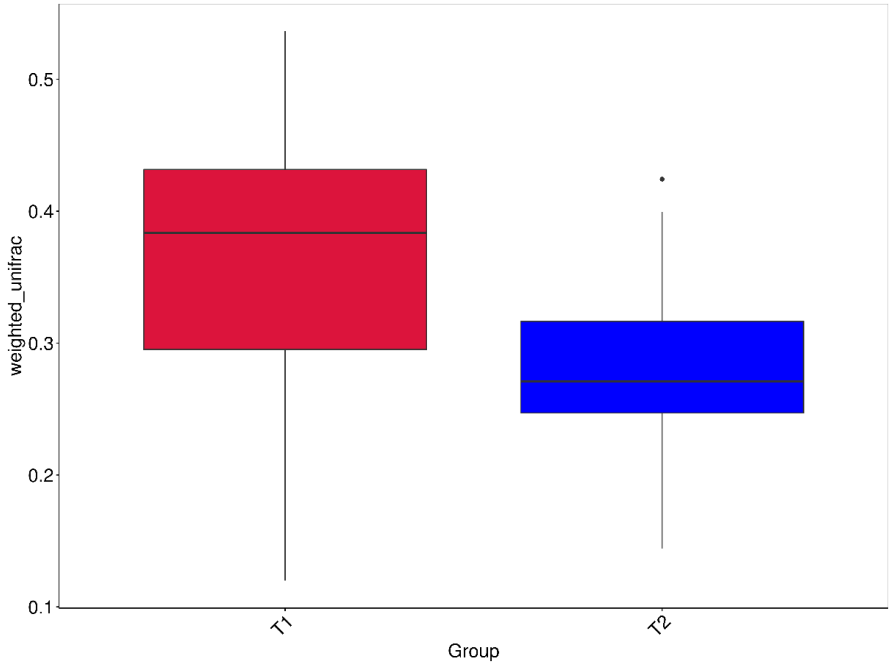

(b) Beta Diversity measured by Weighted Unifrac showing a statistically significant decline (p = 1.54E-11)

Figure 4.16 Beta Diversity changes between T1 and T2 populations measured by (A) Unweighted, and (B) Weighted Unifrac.

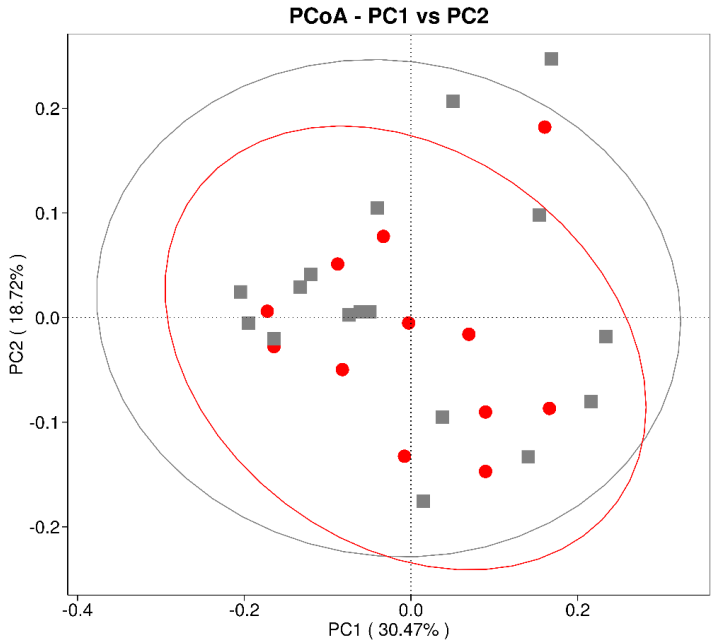

Figure 4.17 Principal Component Analysis of individual sample beta diversity. Gray Squares = T1 samples, Red Circles = T2 samples.

Volcano plots of log2 changes (x-axis) and -log 10 p-value (y-axis) were calculated at the genus taxonomic level for paired samples to show changes in abundance between Visit 1 and Visit 2. P-values which appear above the dashed horizontal line are significant (-log10 of 0.05 = 1.3) (see Figure 4.18 and Figure 4.19 for examples).

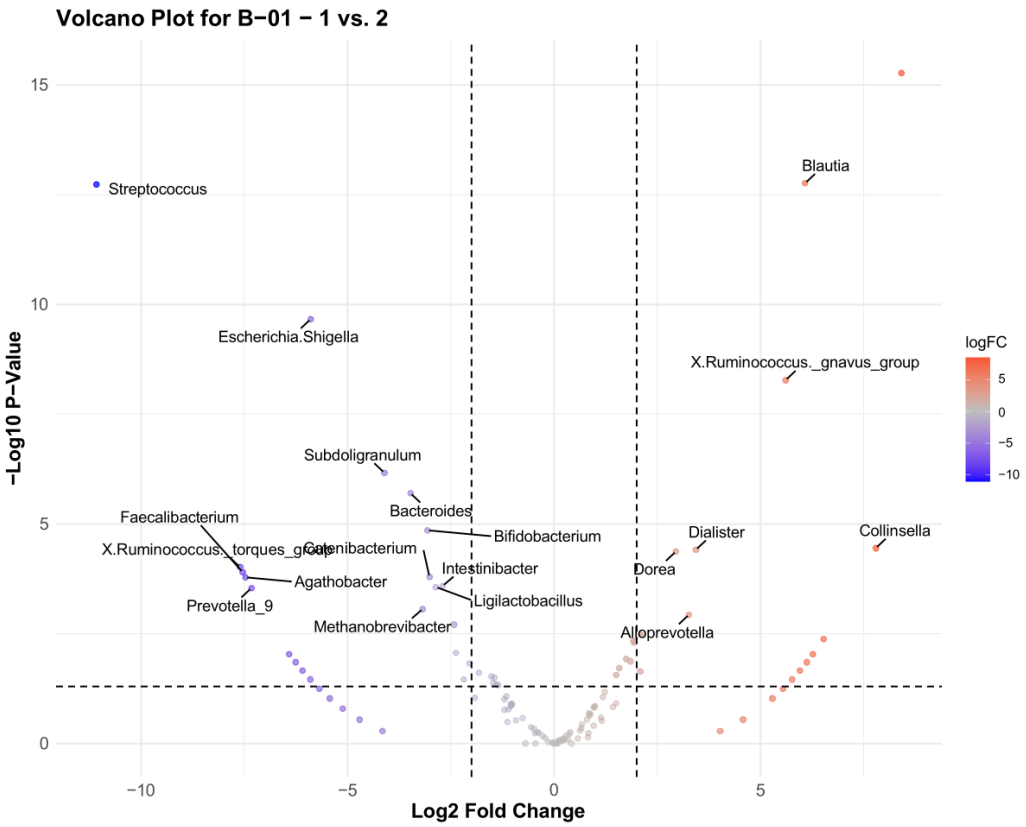

Figure 4.18 Volcano Plot of changes in log abundance between Visit 1 and Visit 2 for patient 1 (NSCLC Squam, non-responder). Declines in Streptococcus, Escherichia Shigella and *Subduoligranulum* are shown. *Blautia*, *Ruminococcus gnavus* and *Collinsella* all increased.

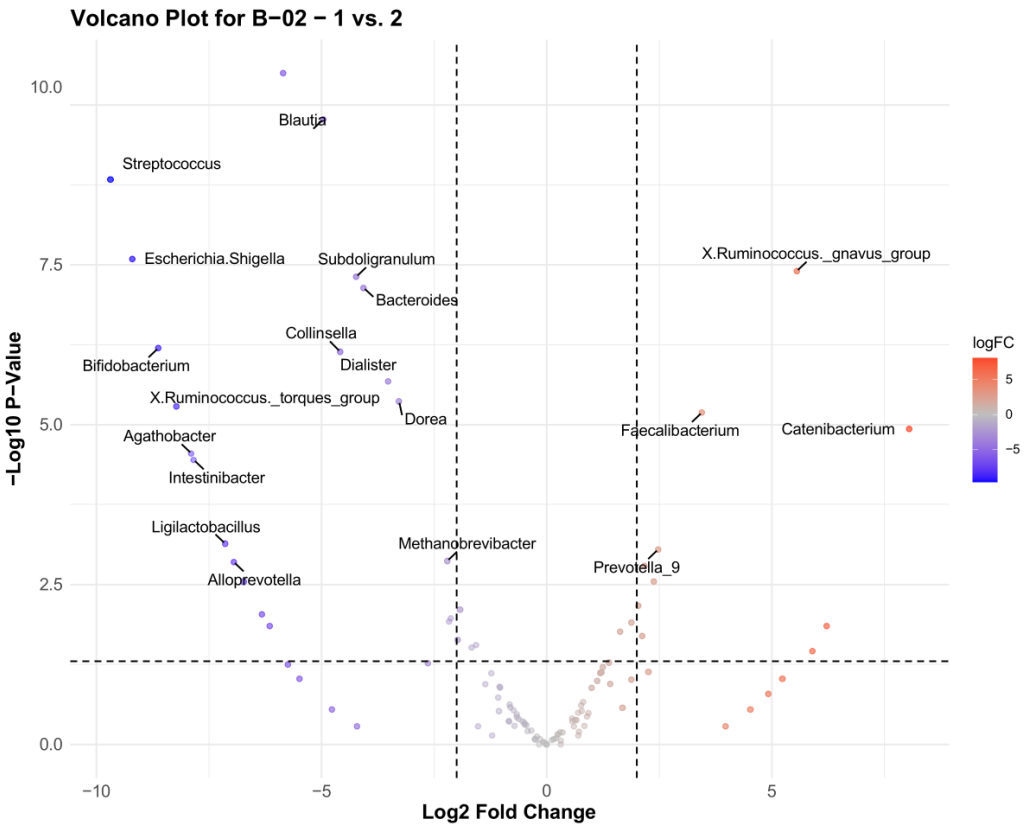

Figure 4.19 Volcano Plot of changes in log abundance between Visit 1 and Visit 2 for patient 2 (NSCLC Squam, responder). Declines of *Blautia, Streptococcus, Escherichia Shigella and Subduoligranulum* shown. *Ruminococcus gnavus Faecalibacterium Catenibacterium and Prevotella* all increased.

4.6 mRNA Analysis

There were 20 baseline (T1 or Visit 1) PAXgene® mRNA blood tubes taken and 18 matched T2 samples. There were 12 treatment-naïve cancer biopsy Formalin-Fixed Paraffin-Embedded Samples (FFPE) with sufficient tissue for mRNA Gene Expression Profiling (GEP). In one sample only there was sufficient normal (non-cancer) tissue in the sample from patient 12 (melanoma) to generate a comparative GEP of normal tissue, giving a total of 13 tissue samples. The tissue samples were of good quality with percentage of reads mapping to each reference varying from 45% to 76%. The average percentage of mRNA alignments was 55.6%. QC was worse in mRNA blood samples than in the tissue samples (see Table 4.11). The blood samples in PAXgene® tubes were diluted into aliquots prior to shipping to GenXPro which may have led to sample degradation and insufficient quantities of mRNA to analyse.

Quality Control: After raw data processing the average sequencing depth per sample (both tissue and blood) was 2,140,817 reads. On average, 67.46% of reads mapped to ENSEMBL_dna. Sample quality was much higher in tissue than in peripheral blood with higher numbers of genes counted and reads mapped.

Table 4.11 Mean values of mRNA Quality Control Metrics Comparing Tissue to Peripheral Blood.

	# Genes counted	% Genes counted	# Reads after UMI deduplication	% PCR duplicates	Reads mapped
Tissue (n = 13)	13769	22	4197824	44	2258097
Blood (n = 38)	6973	11	3711545	48	1212424

The FastQC summary heatmap (Figure 4.20) shows each sample as a row and different QC metrics in columns. Green is a pass, Yellow a warning and Red a fail. The Basic Statistics of basic metadata, read length and GC content were acceptable. There was poor Per Base and Per Tile Sequence Quality indicating poor quality at 3' ends and uneven sequencing. The Per Base Sequence Content and Per Sequence GC Content failed frequently which is not uncommon in mRNA Seq (K. D. Hansen et al. 2010). There were high fail rates in Sequence Duplication Levels and Overrepresented Sequences caused by non-performance of rRNA depletion.

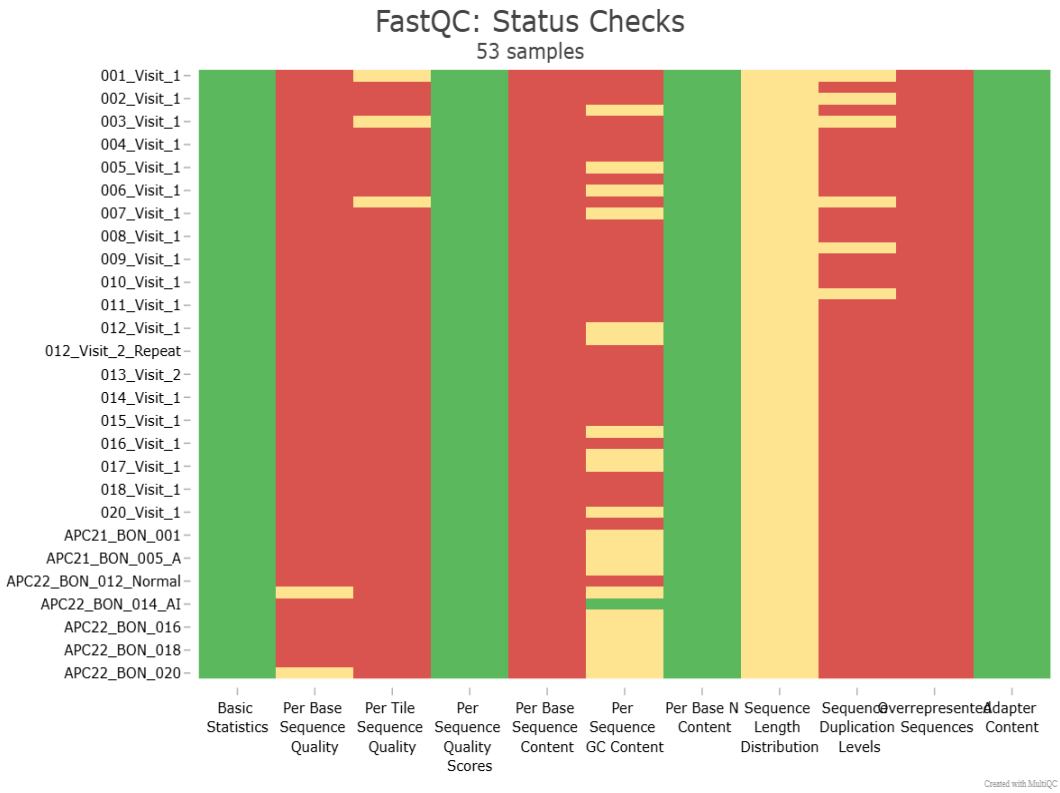

Figure 4.20 FASTQC Summary Data for blood and tissue samples.

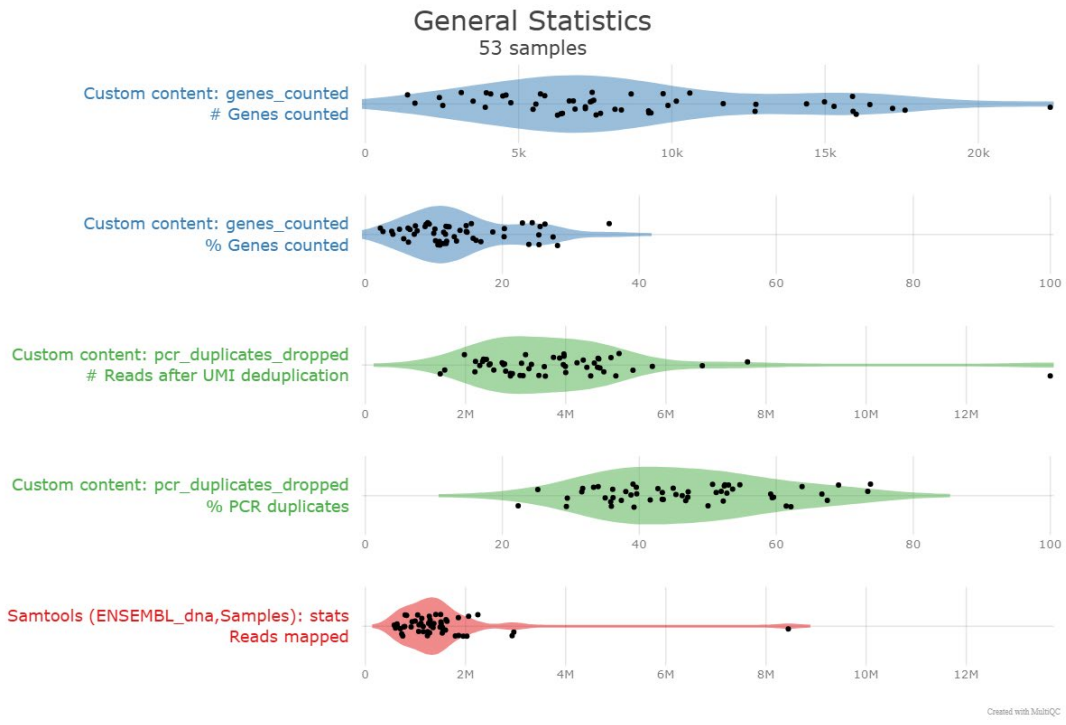

Figure 4.21 Summary of mRNA Quality Control Statistics

Tissue Results: Principal Component Analysis showed that most of the tissue samples clustered closely together. The three outliers were the non-tumour containing sections of the sample from Patient 012, Patient 005 NSCLC Squam and Patient 018 NSCLC Adeno (see Figure 4.22).

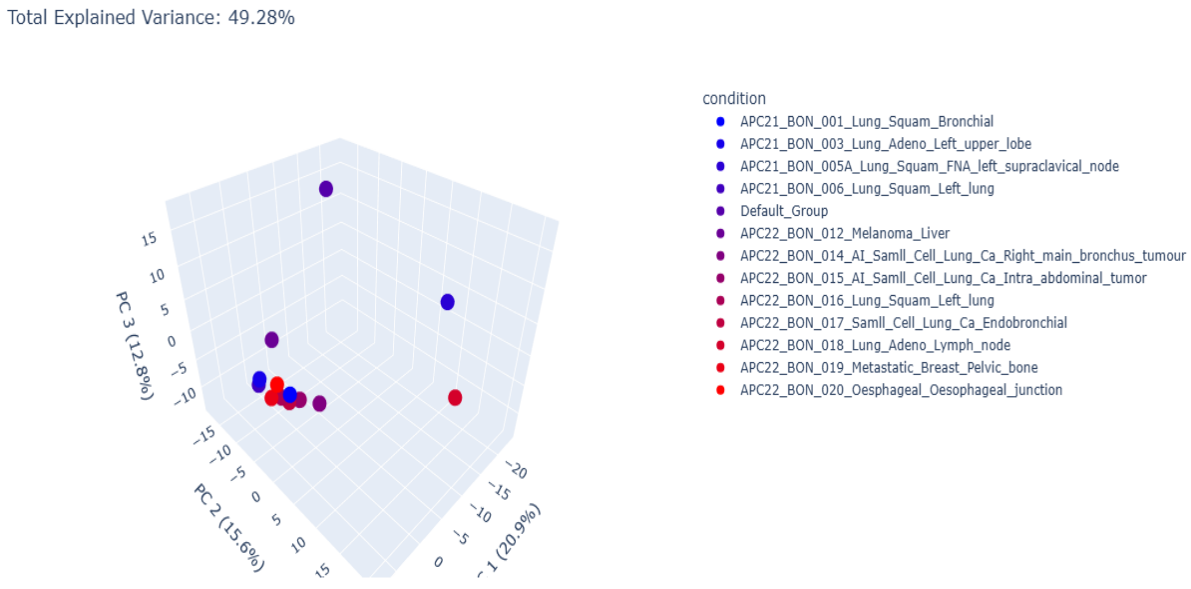

Figure 4.22 Cluster Analysis of Tissue Samples shows 3 outlier specimens; 012 non-cancer tissue and 005 (NSCLC Squam) and 018 (NSCLC Adeno).

mRNA Blood Sample Analysis: Paired blood samples from Visit 1 (pre-treatment, Timepoint 1) and Visit 2 (post first ICI treatment, Timepoint 2) were analysed to assess differential gene expression and generate gene set enrichment scores. Using standard filtering criteria ($p \leq 0.05$ and adjusted p-value ≤ 0.05), no genes met the threshold for statistically significant differential expression between Timepoint 1 and Timepoint 2 (see Figure 4.23 and Table 4.12). The lowest adjusted p-value observed was 0.052, which did not meet the predefined significance threshold.

A number of genes showed nominal evidence of differential expression (unadjusted $p \leq 0.05$), with 86 genes showing higher expression at Timepoint 1 and 69 at Timepoint 2. Of these, 24 were uniquely higher at Timepoint 1 and 7 uniquely higher at Timepoint 2, while 62 genes showed similar directional changes at both timepoints. Table 4.12 presents a subset of these genes (n = 9) ranked by nominal p-value. None of these genes remained significant after correction for multiple testing and should therefore be interpreted as exploratory

findings. As samples were pooled by timepoint and analysed without a paired statistical model or reference expression, these results are descriptive and may underestimate inter-individual variability. Furthermore, the magnitude of observed fold changes was minimal, indicating limited biological differences in gene expression between the two timepoints.

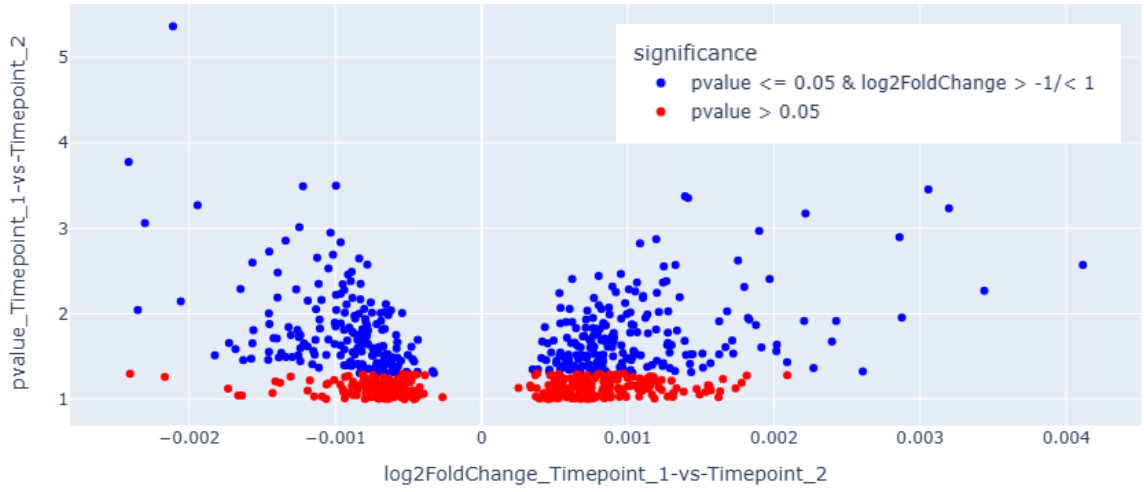

Figure 4.23 Volcano plot of differential gene expression between pooled blood samples at Timepoint 1 and Timepoint 2. Points are coloured by nominal p-value (blue: $p \leq 0.05$; red: $p > 0.05$). Log2 fold changes are minimal across all genes. No genes remained significant after multiple testing correction.

Table 4.12 Differential Gene Expression ranked by unadjusted p-value in Baseline Blood Sample (Timepoint 1) compared to Post Treatment Blood Sample (Timepoint 2). No gene showed significant differential abundance when corrections for multiple comparisons were made.

Gene	log2FoldChange (T1 *vs.* T2)	logfold change in Standard Error (T1 *vs.* T2)	p value (T1 vs T2)	nominal p value (T1 vs T2)
BCL2L1	-0.002110842	0.016291081	4.33E-09	0.052
MS4A3	-0.000995699	0.016295217	0.0003	0.761
PRDX2	-0.001221512	0.016294022	0.0003	0.761
CD300LF	0.001391872	0.016292781	0.0004	0.761
DENND10	0.001412962	0.016292594	0.0004	0.761
YIPF2	-0.002413948	0.016284918	0.0002	0.761
CXCR1	0.003057379	0.016275052	0.0003	0.761
ANAPC16	-0.001942372	0.016287894	0.0005	0.7793
KIAA0319L	0.003197533	0.01627093	0.0006	0.7793

Based on gene expression, we identified 6 up-regulated and 0 down-regulated terms from GO Biological Process using Gene Set Enrichment Analysis (GSEA) ("Gene Ontology Resource" 2025). The most significantly up-regulated terms were ureteric bud development (NES: 2.2724), mesonephros development (NES: 2.2684), mesonephric epithelium development (NES: 2.2519) (see Table 4.13).

Table 4.13 Top 6 enriched terms from GO Biological Process in Blood Samples from Timepoint_1 compared to Timepoint_2. Based on GSEA.

ID	Term	NES	Adj. P-Value	Genes
GO:0001657	ureteric bud development	2.27	0.00	LHX1, FOXC2, FOXC1, PKD2, GZF1, WNT2B, RARA, DLG1, CTNNBIP1, GLI3, BCL2, HS3ST3B1, GATA3, FGFR2, HOXB7, SPRY1, GDF11, SMAD2, MAGED1
GO:0001823	mesonephros development	2.27	0.00	LHX1, FOXC2, FOXC1, PKD2, GZF1, WNT2B, RARA, DLG1, CTNNBIP1, GLI3, BCL2, HS3ST3B1, GATA3, FGFR2, HOXB7, SPRY1, GDF11, SMAD2, MAGED1
GO:0072163	mesonephric epithelium development	2.25	0.00	LHX1, FOXC2, FOXC1, PKD2, GZF1, WNT2B, RARA, DLG1, CTNNBIP1, GLI3, BCL2, HS3ST3B1, GATA3, FGFR2, HOXB7, SPRY1, GDF11, SMAD2, MAGED1
GO:0072164	mesonephric tubule development	2.25	0.00	LHX1, FOXC2, FOXC1, PKD2, GZF1, WNT2B, RARA, DLG1, CTNNBIP1, GLI3, BCL2, HS3ST3B1, GATA3, FGFR2, HOXB7, SPRY1, GDF11, SMAD2, MAGED1
GO:0072073	kidney epithelium development	2.18	0.01	LHX1, FOXC2, PTPRO, FOXC1, PKD2, GZF1, WNT2B, MTSS1, RARA, DLG1, CTNNBIP1, GLI3, BCL2, HS3ST3B1, GATA3, FGFR2, HOXB7, IRX2, SPRY1, GDF11, KANK2, SLC22A6, SMAD2, MAGED1, ASXL1
GO:0048754	branching morphogenesis of an epithelial tube	2.09	0.01	LHX1, FOXC2, FKBPL, ESRP2, PKD2, GZF1, TNC, WNT2B, DLG1, CTNNBIP1, GLI3, BCL2, HS3ST3B1, MKS1, PML, FGFR2, HOXB7, NOTCH4, SPRY1, PKHD1, ABL1

4.7 Quality of Life Survey Results

The FACT-ICM Quality of Life Survey was optional. Seventeen patients completed it at V1 and only 10 at V3 enabling paired analysis of only 10 samples.

The baseline mean score was 165 (SD 21), Median 167 [IQR 147, 185] (Range 135 to 199). The V3 Subsequent Visit mean score was 168 (SD 24), Median 178 [IQR 143, 186] (Range

134 to 202). Two-way ANOVA with an alpha of 0.05 revealed no statistically significant difference between the two timepoints (see Figure 4.24 and Figure 4.25).

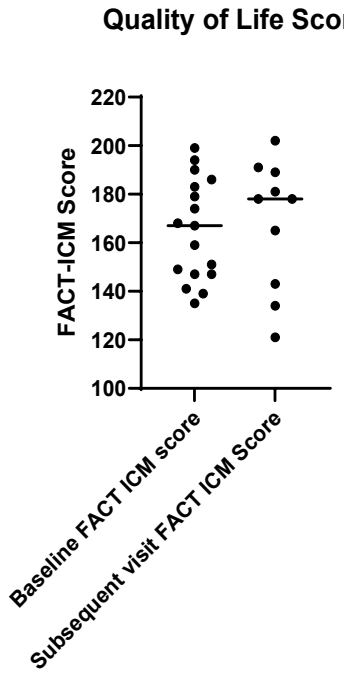

Figure 4.24 Baseline (n =17) and Subsequent (n =10) FACT-ICM Scores Note foreshortened Y-axis.

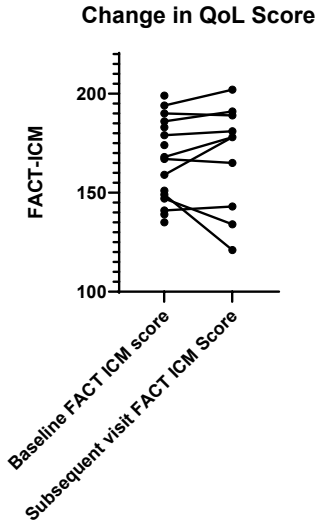

Figure 4.25 Change in FACT-ICM Score over time for individual patients (paired data, n =10) Note foreshortened Y-axis.

4.7.1 Subscale FACT-G and ICM Analysis

There were no significant changes in mean FACT-G subscale scores in any domain. The ICM Score which measures immune related side effects (irAE) based on patient reported symptoms was measured at V1 and V3. A higher score means fewer side effects. Although not statistically significant it was documented that there were some lower individual scores on V3 after 3 months (see Figure 4.26 and Figure 4.27).

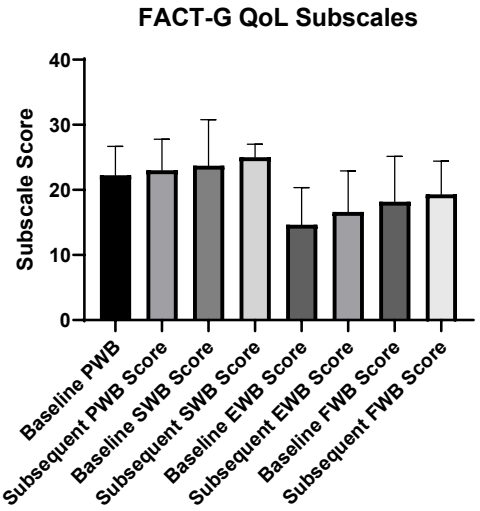

Figure 4.26 Each of the 4 subscales of the FACT-G questionnaire are shown at baseline and at Visit 3 (Subsequent Visit).

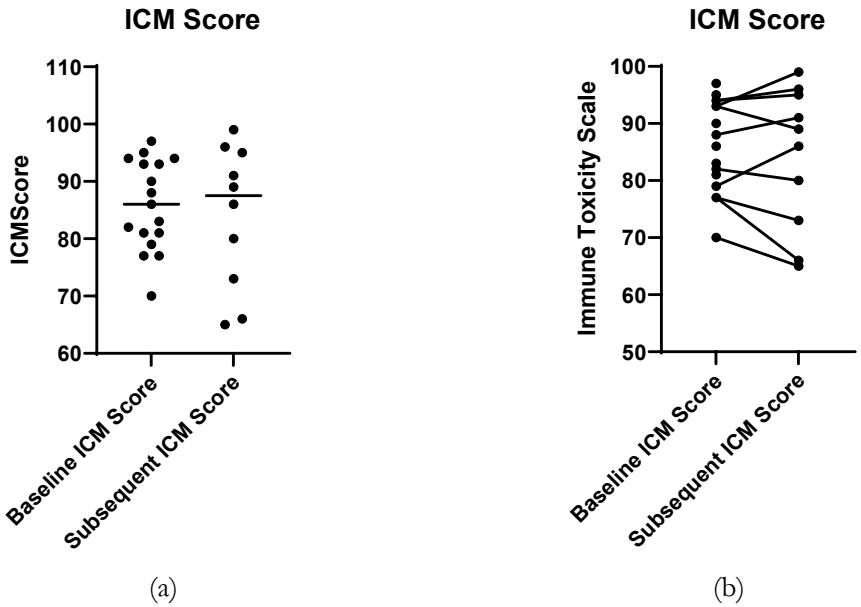

Figure 4.27 Baseline (a) and subsequent (b) ICM. Note foreshortened Y-axes.

4.8 CANTAB Psychomotor Testing Results

Patients and site staff found completing the CANTAB testing quite demanding and time intensive and with pandemic restrictions an inadequate number of paired samples were collected (n = 8)

From the various tasks performed with the patients the following observations can be made from the data.

In sum, the **Motor screening task** (MOT) showed improvement (non-significant), best improvement in MOTML (p=0.41)

Reaction time showed a non-significant improvement in the following parameters:

RTI Simple Mean Movement Time (RTISMMT) The mean time taken for a subject to release the response button and select the target stimulus after it flashed. (p=0.06).

Five-choice reaction time test (RTIFMMT) The mean time taken for a subject to release the "standby" button and select the target button, ms). (p=0.10);

Median Five-Choice Movement Time (RTIFMDMT) (p=0.12).

The mean time movement time taken for a subject to select the target stimulus after releasing the response button in the simple choice (RTISMMT (p=0.06)) and the Five-Choice were shorter (i.e. quicker) RTIFMMT (p=0.10), along with a non-significant shorter time in the median Five-Choice Movement Time (RTIFMDMT (p=0.12)).

Rapid visual processing showed significant improvement in RVPML response times (mean) & RVPMDL (median) (RVPML: p=0.04 & RVPMDL: p=0.02) A number of parameters showed a tendency for improvement in the **Spatial working memory task** (SWMTE 468 (p=0.22); SWMBE 468 (p=0.22); SWMWE468 (p=0.099); SWMDE468 (p=0.128))

These show a reduction in the tendency to revisit a box that was shown to be empty, within the same box error or within the same box error twice. This can be interpreted as n improvement in short term spatial working memory.

Match to sample visual search (MTS) showed a tendency for the mean (MTSRF) and median response to be quicker (non-significant), otherwise no other meaningful differences were apparent.

Paired associates learning (PAL) task showed no meaningful difference in PAL performance overall (pre *vs* post).

4.9 Correlation

4.9.1 Correlation of Baseline Height and Weight Measurements with Clinical Outcomes

Exploratory analyses were performed to assess associations between baseline BMI and BSA and survival outcomes. Neither BMI nor BSA showed evidence of association with progression-free survival (PFS) or overall survival (OS) when assessed using Spearman's rank correlation (Table 4.14). As PFS and OS represent time-to-event outcomes subject to censoring, these correlation analyses do not account for censoring and should therefore be interpreted cautiously. Kaplan–Meier and Cox regression analyses (presented below) provide a more appropriate assessment of survival outcomes. (Table 4.14).

Table 4.14 Spearman's Correlation Between PFS, OS and BMI and BSA.

		r	p value	95 % C.I. of rs
BMI	PFS	0.16	0.512	-0.321 to 0.569
	OS	0.35	0.135	-0.128 to 0.691
BSA	PFS	0.11	0.643	-0.361 to 0.537
	OS	0.31	0.180	-0.167 to 0.670

4.9.2 Correlation of Baseline Inflammatory Markers with PFS and OS

Exploratory analyses were performed to assess associations between baseline inflammatory markers and survival outcomes using Spearman's rank correlation. Higher ESR, CRP, and SII values showed negative associations with PFS and OS; however, only CRP ($p = 0.01$) and SII ($p = 0.020$) showed nominal associations with PFS (Table 4.15). These analyses do not account for censoring and should therefore be interpreted as exploratory. More robust assessment of survival outcomes was undertaken using Kaplan–Meier and Cox proportional hazards models.

Table 4.15 Spearman's Correlation (r) Between PFS, OS and each baseline inflammatory marker as a single variable; * = statistically significant p value (< 0.05).

			r	p value	95 % C.I. of r values
ESR		PFS	-0.462	0.06	-0.778 to 0.04
		OS	-0.311	0.224	-0.67 to 0.215
Albumin		PFS	-0.31	0.187	-0.668 to 0.170
		OS	-0.41	0.07	-.723 to 0.055
CRP		PFS	-0.59	0.01*	-.833 to -.156
		OS	-0.45	0.061	-0.764 to 0.036
LDH		PFS	0.173	0.504	-0.349 to 0.613
		OS	0.08	0.752	-0.428 to 0.552
NLR		PFS	-0.37	0.105	-0.707 to 0.097
		OS	-0.43	0.057	-0.741 to 0.027
NER		PFS	-0.38	0.152	-0.742 to 0.164
		OS	-0.12	0.650	-0.593 to 0.411
SII		PFS	-0.52	0.020*	-0.786 to -0.082
		OS	-0.339	0.143	-0.687 to 0.135

To more appropriately assess time-to-event outcomes, patients were stratified by biomarker levels and analysed using Kaplan–Meier survival curves and log-rank testing.

The median baseline ESR of 56 mm/hr was used to divide patients into ESR low (n =8) and high (n=9) groups and Kaplan Meier curves for PFS and OS for each group were calculated for the patients in each group. The median PFS in the ESR low group was 23.5 weeks and in the ESR high group 19 weeks (p= 0.056, n.s. Log-rank test). The median OS in the ESR low group was 42.0 weeks and in the ESR high group 32.1 weeks (p = 0.89, n.s. Log-rank test). Comparisons were also made between the top (n =4 ESR ≥88) and bottom (n = 4, ESR ≤23) ESR quartiles. The median PFS was 26.5 weeks in the lowest ESR quartile and 12.9 weeks in the highest (p = 0.100, n.s. Log-rank test). Median OS was 42.1 weeks in the lowest ESR quartile and 13.3 weeks in the highest (p = 0.461, n.s. Log-rank test) (see Figure 4.28).

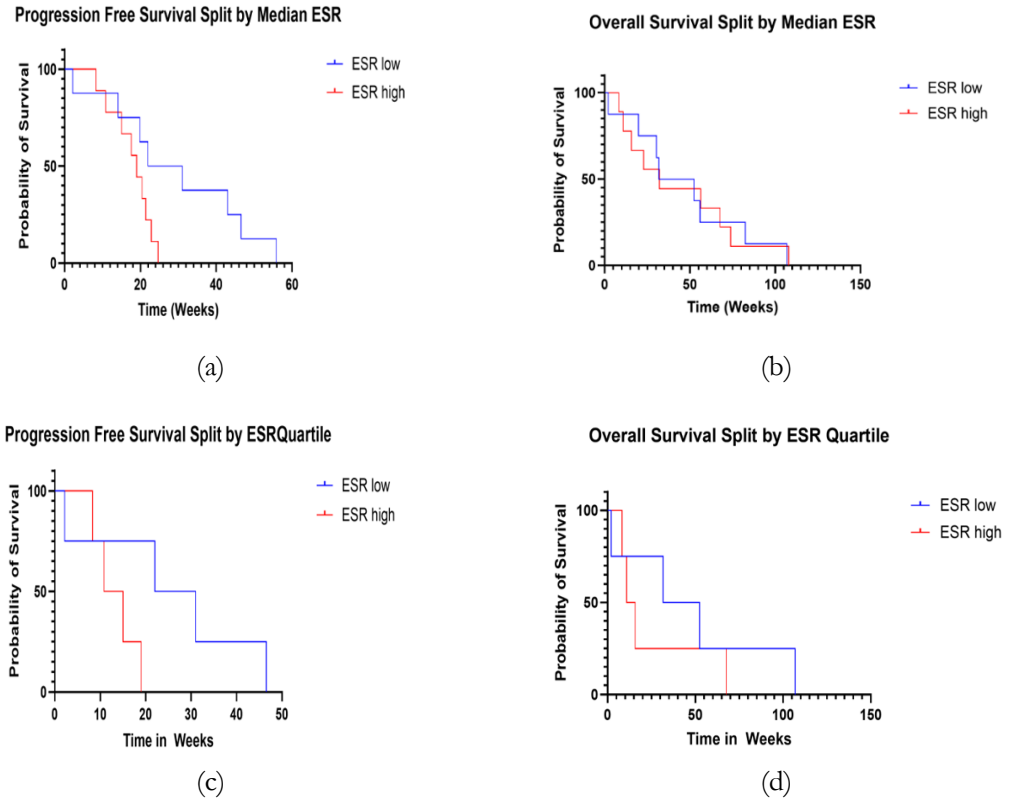

Figure 4.28 (a) PFS and (b) OS split by Median ESR 56 mm/he (n = 17 patients); (c) PFS and (d) OS spilt by lowest Quartile (n = 4, <23mm/hr) and highest Quartile (n = 4, >88mm/hr) ESR.

The median baseline CRP of 14 mg/L was used to divide patients into CRP low (n =9) and high (n=9) groups and Kaplan Meier curves for PFS and OS for each group were calculated for the patients in each group. The median PFS in the CRP low group was 22 weeks and, in the CRP, high group 20.4 weeks (p= 0.567, n.s. Log-rank test). The median OS in the CRP low group was 52.0 weeks and, in the CRP, high group 22.9 weeks (p = 0.417, n.s. Log-rank test). Comparisons were also made between the top (n =5 CRP ≥54) and bottom (n = 5, ESR ≤2.1) CRP quartiles. The median PFS was 31 weeks in the lowest CRP quartile and 10.9 weeks in the highest (p = 0.492, n.s. Log-rank test). Median OS was 39.7 weeks in the lowest CRP quartile and 10.6 weeks in the highest (p = 0.156, n.s. Log-rank test) (see Figure 4.29).

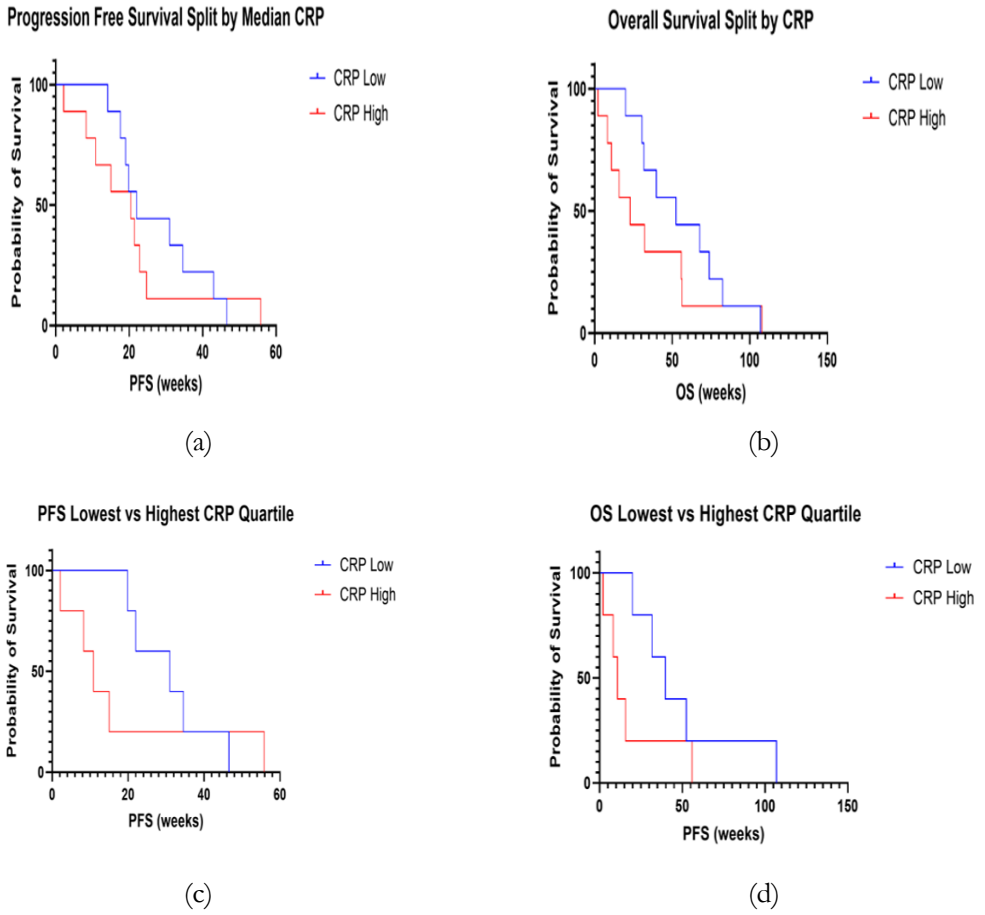

Figure 4.29 (a) PFS and (b) OS split by Median Pre-treatment CRP = 14 mg/L and (c) PFS and (d) OS Split by Lowest vs Highest Pre-treatment CRP Quartile (Lowest <2.1 mg/L, highest > 54 mg/L).

Cox proportional hazards regression was used to evaluate baseline inflammatory markers as predictors of survival while accounting for censoring. In multivariate analysis for PFS, higher LDH was associated with a lower hazard (HR 0.976, 95% CI 0.950–0.995), while ESR and CRP were associated with increased hazard (Table 4.16). These findings should be interpreted with caution given the small sample size and multiple comparisons.

Table 4.16 Cox Regression analysis of Baseline Inflammatory Variables as predictors of PFS.

Variable	Hazard Ratio	95% CI (profile likelihood)
Albumin	1.219	0.9560 to 1.629
ESR (mm/hr)	1.061	1.011 to 1.130
CRP	1.056	1.009 to 1.123
LDH	0.9761	0.9502 to 0.9945
Neut/Lymph Ratio	1.396	0.9433 to 2.241
Neut/Eosin Ratio	0.9853	0.9654 to 1.000
SII =P x N/L	0.9974	0.9943 to 0.9997

Multivariate Analysis of Baseline Inflammatory Variables and OS (Cox Regression) of baseline inflammatory markers were compared as predictors of overall survival using the Cox proportional hazards technique and only NLR was significant (shown in Table 4.17).

Table 4.17 Multivariate comparison of Baseline Inflammatory Markers as predictors of Overall Survival (* = CI does not include 1).

Variable	Hazard Ratio	95% CI
Albumin	1.345	0.8970 to 2.309
ESR	1.017	0.9649 to 1.078
CRP	1.094	0.9960 to 1.324
LDH	0.9874	0.9613 to 1.012
NLR	1.686	1.051 to 3.211*
NER	0.9968	0.9780 to 1.014
SII	0.9977	0.9928 to 1.000

The median baseline NLR of 4.7 was used to divide patients into NLR low (<4.7) and high (≥4.7) groups and Kaplan Meier curves for PFS and OS for each group were calculated for the 10 patients in each group. The median PFS in the NLR low group was 25.6 weeks and in the NLR high group 20.1 weeks (p= 0.289, n.s.). The median OS in the NLR low group was 46.1 weeks and in the NLR high group 23.7 weeks (p = 0.126, n.s.). Comparisons were also made between the top (≥8.8) and bottom (≤3.1) NLR quartiles. The median PFS was 34.6 weeks in the lowest NLR quartile and 12.3 weeks in the highest (p = 0.07, n.s.). The

median OS was 67.7 weeks in the lowest NLR quartile and 22.9 weeks in the highest ($p = 0.10$, n.s.) (see Figure 4.30).

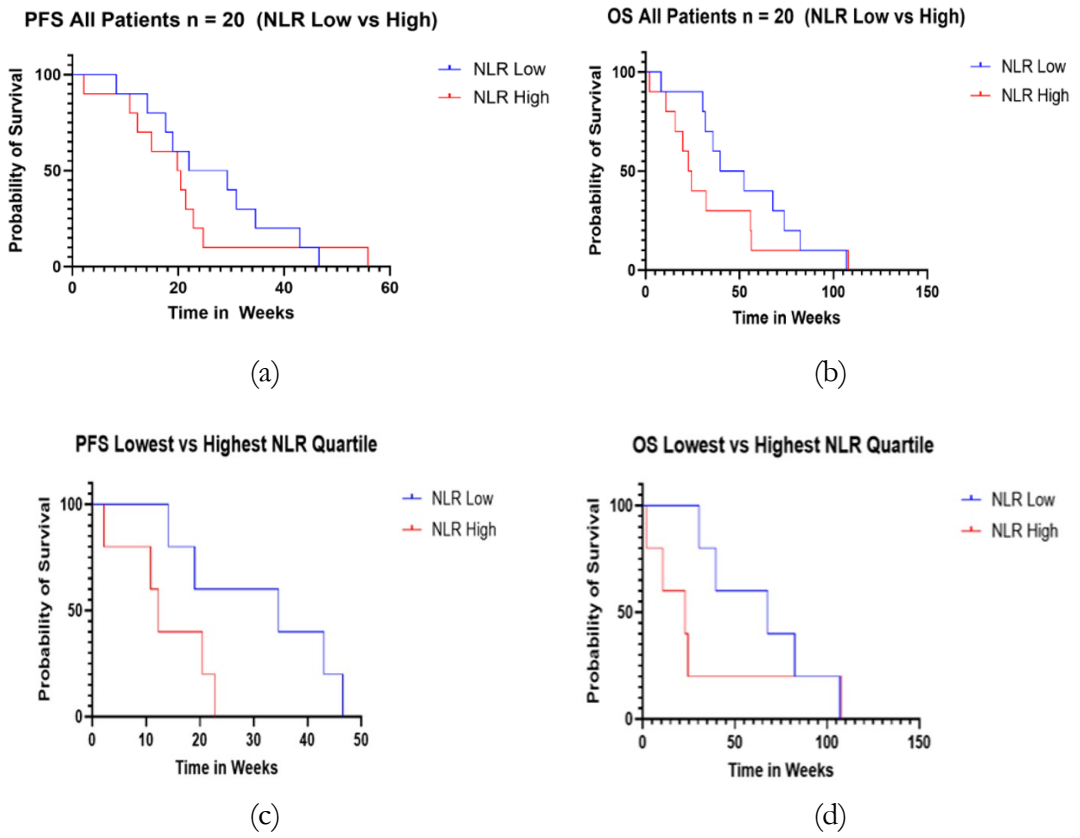

Figure 4.30 Kaplan-Meier Curves of (a) PFS and (b) OS (weeks) for all patients split by median NLR low (<4.7) in blue and high (≥4.7) in red; (c) PFS and (d) OS (weeks) for highest and lowest NLR quartile (n = 5 in each group) low (in blue and high in red).

4.9.3 Correlation of Natural Logs of Skewed Distributions of Baseline Inflammatory Markers with PFS and OS

When the Skew of baseline markers distribution was greater than 2 the natural log was calculated and mapped then checked as a univariate and multivariate predictor of survival. None of the log transformations predicted either PFS or OS.

Table 4.18 Natural Log Transforms as predictors of OS.

Variable	Estimate	95% CI
CRP	1.438	0.6499 to 3.459
LDH	1.068	0.07433 to 16.72
Neut/Lymph Ratio	5.394	0.5099 to 85.52
Neut/Eosin Ratio	1.785	0.9302 to 3.869
SII = P x N/L	0.3146	0.007553 to 6.632

4.9.4 Correlation of Clinical Outcomes with Second and Third Visit NLR, NER, SII and serial changes

Exploratory analyses were carried out to determine whether post-treatment blood inflammatory indices taken at second and third study visits correlated with clinical outcomes. Similar analyses were undertaken to determine if serial changes in individual patient inflammatory indices correlated with clinical outcomes. The V2 SII correlated negatively with PFS. r= -.49 p = 0.03 (Table 4.19) but not with OS r = -0.29 p = 0.22). None of the other inflammatory indices taken at the second study visit (V2) correlated with OS or PFS. None of the third visit inflammatory indices correlated significantly with PFS or OS. Serial changes in NLR were calculated and compared with PFS and OS. There were no significant predictors of PFS or OS found. (Table 4.20) Serial changes in NLR between visits did not correlate with either PFS or OS. (Table 4.21)

.

Table 4.19 Spearman Correlation of Second Visit Inflammatory Markers with Progression Free and Overall Survival.

	PFS	V2 NLR	V2 NER	V2 SII	PFS p-value	PFS CI
PFS	1.00	-0.16	-0.17	-0.49		
V2 NLR	-0.16	1.00	0.35	0.78	0.52	-0.5815 to 0.3313
V2 NER	-0.17	0.35	1.00	0.62	0.55	-0.6537 to 0.4096
V2 SII	-0.49	0.78	0.62	1.00	0.03	-0.7802 to -0.03695

	OS	V2 NLR	V2 NER	V2 SII	OS p-value	OS CI
OS	1.00	-0.14	-0.24	-0.29		
V2 NLR	-0.14	1.00	0.35	0.78	0.55	-0.5719 to 0.3440
V2 NER	-0.24	0.35	1.00	0.62	0.40	-0.6939 to 0.3465
V2 SII	-0.29	0.78	0.62	1.00	0.22	-0.6682 to 0.1987

Table 4.20 Spearman Correlation of Third Visit Inflammatory Markers with Progression Free and Overall Survival.

	PFS	V3 NLR	V3 NER	V3 SII	PFS p-value	CI of r for PFS
PFS	1.00	-0.19	-0.48	-0.32		
V3 NLR	-0.19	1.00	0.94	0.80	0.53	-0.68 to 0.42
V3 NER	-0.48	0.94	1.00	0.94	0.24	
V3 SII	-0.32	0.80	0.94	1.00	0.28	-0.75 to 0.29

	OS	V3 NLR	V3 NER	V3 SII	OS p-value	CI of r for OS
OS	1.00	-0.11	-0.38	-0.26		
V3 NLR	-0.11	1.00	0.94	0.80	0.72	-0.63 to 0.48
V3 NER	-0.38	0.94	1.00	0.94	0.36	
V3 SII	-0.26	0.80	0.94	1.00	0.38	-0.72 to 0.35

Table 4.21 Spearman Coefficients of changes in NLR between visits correlated with Progression Free Survival and Overall Survival

	PFS	V2 - V1 NLR	V3 - V1 NLR	V3 - V2 NLR	PFS p value
PFS	1.00	0.01	0.31	-0.19	
V2 - V1 NLR	0.01	1.00	0.59	-0.68	0.96
V3 - V1 NLR	0.31	0.59	1.00	-0.07	0.23
V3 - V2 NLR	-0.19	-0.68	-0.07	1.00	0.54

	OS	V2 - V1 NLR	V3 - V1 NLR	V3 - V2 NLR	OS p value
OS	1.00	-0.02	0.24	-0.31	
V2 - V1 NLR	-0.02	1.00	0.59	-0.68	0.92
V3 - V1 NLR	0.24	0.59	1.00	-0.07	0.34

V3 - V2 NLR	-0.31	-0.68	-0.07	1.00	0.30

4.9.5 Correlation of Immune Metabolites with Clinical Outcomes and Quality of Life FACT-ICM Questionnaire

When measurements of or serial changes in K/T ratio were correlated with the clinical outcomes of OS and PFS there were no significant associations (Table 4.22) (Patient 008 was excluded as an outlier). This analysis was repeated for the 12 patients with NSCLC and again there were no significant correlations. (Table 4.23) The K/T ratio measured over 3 trial visits (V1, V2 and V3) and its changes were examined as a correlate of FACT-ICM subsection scores. There were some significant correlations between pre-treatment K/T ratio and first visit Emotional Well Being (EWB0) (r= 0.514, 2-tailed p = 0.042) and first visit Functional Well Being (FWB0) (r = 0.606 (2-tailed p = 0.013) scores. The FACT-ICM questionnaire was re-administered on the 3rd study visit at 3 months. The repeat Physical Well Being score at three months (PWB1) correlated negatively with second (r = -0.799, 2-tailed p = 0.006) and third study (r = -0.663, 2-tailed p = 0.037) visit K/T ratios (Table 4.24). After adjusting for multiple comparisons using the Bonferroni correction only V2 K/T ratio correlated significantly with the repeated PWB score at 3 months (r = -0.799, adjusted p = 0.018).

Table 4.22 Spearman Coefficients of changes in K/T Ratio (n = 19) between visits correlated with Progression Free Survival and Overall Survival.

Correlations

			V1	V2	V3	V2V1	V3V2	V3V1	PFS	OS
Spearman's rho	V1	Correlation Coefficient	1.000	.595*	.420	-.369	-.113	-.646*	-.079	-.164
		Sig. (2-tailed)	.	.012	.135	.120	.701	.012	.748	.502
		N	19	17	14	19	14	14	19	19
	V2	Correlation Coefficient	.595*	1.000	.872**	.329	-.246	.030	.025	-.172
		Sig. (2-tailed)	.012	.	<.001	.197	.397	.920	.922	.496
		N	17	18	14	17	14	14	18	18
	V3	Correlation Coefficient	.420	.872**	1.000	.103	.137	.150	.226	.015
		Sig. (2-tailed)	.135	<.001	.	.725	.641	.610	.436	.958
		N	14	14	14	14	14	14	14	14
	V2V1	Correlation Coefficient	-.369	.329	.103	1.000	-.159	.713**	.096	.184
		Sig. (2-tailed)	.120	.197	.725	.	.587	.004	.694	.450
		N	19	17	14	19	14	14	19	19
	V3V2	Correlation Coefficient	-.113	-.246	.137	-.159	1.000	.506	.327	.042
		Sig. (2-tailed)	.701	.397	.641	.587	.	.065	.254	.887
		N	14	14	14	14	14	14	14	14
	V3V1	Correlation Coefficient	-.646*	.030	.150	.713**	.506	1.000	.312	.169
		Sig. (2-tailed)	.012	.920	.610	.004	.065	.	.277	.563
		N	14	14	14	14	14	14	14	14
	PFS	Correlation Coefficient	-.079	.025	.226	.096	.327	.312	1.000	.641**
		Sig. (2-tailed)	.748	.922	.436	.694	.254	.277	.	.002
		N	19	18	14	19	14	14	20	20
	OS	Correlation Coefficient	-.164	-.172	.015	.184	.042	.169	.641**	1.000
		Sig. (2-tailed)	.502	.496	.958	.450	.887	.563	.002	.
		N	19	18	14	19	14	14	20	20

*. Correlation is significant at the 0.05 level (2-tailed).

**. Correlation is significant at the 0.01 level (2-tailed).

Table 4.23 Spearman's Correlation of K/T ratio changes with PFS and OS in 12 patients with NSCLC.

Correlations

			V1	V2	V3	V2V1	V3V2	V3V1	PFS	OS
Spearman's rho	V1	Correlation Coefficient	1.000	.648*	.433	-.497	-.363	-.950**	-.217	-.476
		Sig. (2-tailed)	.	.031	.244	.101	.337	<.001	.499	.118
		N	12	11	9	12	9	9	12	12
	V2	Correlation Coefficient	.648*	1.000	.748*	.251	-.791*	-.361	-.233	-.279
		Sig. (2-tailed)	.031	.	.020	.456	.011	.339	.491	.407
		N	11	11	9	11	9	9	11	11
	V3	Correlation Coefficient	.433	.748*	1.000	-.117	-.211	-.300	.100	.317
		Sig. (2-tailed)	.244	.020	.	.765	.586	.433	.798	.406
		N	9	9	9	9	9	9	9	9
	V2V1	Correlation Coefficient	-.497	.251	-.117	1.000	-.194	.883**	-.007	.224
		Sig. (2-tailed)	.101	.456	.765	.	.617	.002	.983	.484
		N	12	11	9	12	9	9	12	12
	V3V2	Correlation Coefficient	-.363	-.791*	-.211	-.194	1.000	.228	.194	.143
		Sig. (2-tailed)	.337	.011	.586	.617	.	.555	.617	.713
		N	9	9	9	9	9	9	9	9
	V3V1	Correlation Coefficient	-.950**	-.361	-.300	.883**	.228	1.000	.050	.433
		Sig. (2-tailed)	<.001	.339	.433	.002	.555	.	.898	.244
		N	9	9	9	9	9	9	9	9
	PFS	Correlation Coefficient	-.217	-.233	.100	-.007	.194	.050	1.000	.755**
		Sig. (2-tailed)	.499	.491	.798	.983	.617	.898	.	.005
		N	12	11	9	12	9	9	12	12
	OS	Correlation Coefficient	-.476	-.279	.317	.224	.143	.433	.755**	1.000
		Sig. (2-tailed)	.118	.407	.406	.484	.713	.244	.005	.
		N	12	11	9	12	9	9	12	12

*. Correlation is significant at the 0.05 level (2-tailed).

**. Correlation is significant at the 0.01 level (2-tailed).

Table 4.24 Pearsons's Correlation of K/T ratio with FACT-ICM QoL Scores, unadjusted for multiple comparisons.

Correlations

			V1	V2	V3	V2V1	V3V2	V3V1
Spearman's rho	V1	Correlation Coefficient	1.000	.595*	.420	-.369	-.113	-.646*
		Sig. (2-tailed)	.	.012	.135	.120	.701	.012
		N	19	17	14	19	14	14
	V2	Correlation Coefficient	.595*	1.000	.872**	.329	-.018	-.124
		Sig. (2-tailed)	.012	.	<.001	.197	.949	.659
		N	17	18	14	17	15	15
	V3	Correlation Coefficient	.420	.872**	1.000	.103	.137	.150
		Sig. (2-tailed)	.135	<.001	.	.725	.641	.610
		N	14	14	14	14	14	14
	V2V1	Correlation Coefficient	-.369	.329	.103	1.000	-.159	.713**
		Sig. (2-tailed)	.120	.197	.725	.	.587	.004
		N	19	17	14	19	14	14
	V3V2	Correlation Coefficient	-.113	-.018	.137	-.159	1.000	.222
		Sig. (2-tailed)	.701	.949	.641	.587	.	.426
		N	14	15	14	14	15	15
	V3V1	Correlation Coefficient	-.646*	-.124	.150	.713**	.222	1.000
		Sig. (2-tailed)	.012	.659	.610	.004	.426	.
		N	14	15	14	14	15	15
	PWB0	Correlation Coefficient	-.174	-.295	-.145	-.177	-.121	.419
		Sig. (2-tailed)	.520	.268	.653	.513	.693	.154
		N	16	16	12	16	13	13
	SWB0	Correlation Coefficient	.224	-.154	.139	-.120	-.472	-.110
		Sig. (2-tailed)	.403	.569	.667	.657	.103	.720
		N	16	16	12	16	13	13
	EWB0	Correlation Coefficient	.514*	.329	.123	.057	-.090	-.051
		Sig. (2-tailed)	.042	.214	.704	.833	.770	.868
		N	16	16	12	16	13	13
	FWB0	Correlation Coefficient	.606	.326	.374	.043	-.196	.119
		Sig. (2-tailed)	.013	.218	.231	.875	.520	.698
		N	16	16	12	16	13	13
	ICM0	Correlation Coefficient	.082	.125	-.004	-.196	.356	.286
		Sig. (2-tailed)	.763	.645	.991	.467	.232	.344
		N	16	16	12	16	13	13
	BASELINEFACTICM	Correlation Coefficient	.349	.050	.098	.001	-.113	.217
		Sig. (2-tailed)	.185	.854	.762	.996	.713	.476
		N	16	16	12	16	13	13
	PWB1	Correlation Coefficient	-.535	-.799**	-.663*	.073	.153	.201
		Sig. (2-tailed)	.111	.006	.037	.841	.672	.578
		N	10	10	10	10	10	10
	SWB1	Correlation Coefficient	.359	.095	.170	-.296	.146	.120
		Sig. (2-tailed)	.309	.795	.639	.407	.687	.742
		N	10	10	10	10	10	10
	EWB1	Correlation Coefficient	.134	-.070	-.043	.012	.563	.116
		Sig. (2-tailed)	.712	.847	.907	.973	.090	.750
		N	10	10	10	10	10	10
	FWB1	Correlation Coefficient	.098	-.193	-.098	-.031	.460	.330
		Sig. (2-tailed)	.788	.593	.788	.933	.181	.351
		N	10	10	10	10	10	10
	ICM1	Correlation Coefficient	.091	-.249	-.176	-.103	.489	.164
		Sig. (2-tailed)	.803	.487	.627	.777	.151	.651
		N	10	10	10	10	10	10
	SUBSFACTICM	Correlation Coefficient	-.091	-.403	-.243	-.164	.463	.188
		Sig. (2-tailed)	.789	.219	.498	.629	.178	.602
		N	11	11	10	11	10	10

*. Correlation is significant at the 0.05 level (2-tailed).

**. Correlation is significant at the 0.01 level (2-tailed).

4.9.6 Correlation of Proteomic Data with Clinical Outcomes

Cox regression analysis of the Olink V1 data did not show any significant correlation with OS. Principal Component Regression (PCA) using OS as a dependant variable did not reveal any significant proteomic variable, however the estimates of variance that were less than minus one (adverse effect on overall survival) and greater than 1 are shown below in Table 4.25 (Samples that passed QC only). PCA of the 14 V2 and the 13 V3 samples passing QC did not show any estimates of variance outside the range -1 to 1.

Table 4.25 Principal Component Analysis of Pre-Treatment Proteomic markers and Overall Survival. Soluble cytokines and proteins with Principal Component Analysis Estimates of Variance less than minus one or greater than one from the 14 V1 blood samples passing Quality Control.

Protein Assay	Estimate of Variance for Overall Survival
PDGF subunit B	-2.024
VEGFR-2	-1.981
TIE2	-1.464
LAP TGF-beta-1	-1.379
ANGPT2	-1.24
IL15	-1.211
CSF-1	-1.181
TNFSF14	-1.138
ARG1	-1.125
FGF2	-1.119
TRAIL	1.193
ICOSLG	1.512

When PDGF subunit B V1 values were ranked from lowest to highest there was no obvious trend in what type of cancer was associated with a high or lower value (Table 4.26).

Table 4.26 Correlation of V1 Olink PDGF BB values with Cancer Subtype.

PDGF Subunit B Value	Type of Cancer
8.692	Endometrial
8.957	Ad Lung
9.204	Sq Lung
9.239	Sq Lung
9.262	Ad Lung
9.271	SCLC
9.275	Sq Lung
9.276	Melanoma
9.281	Ad Oesphageal
9.338	SCLC
9.360	Sq Lung
9.400	Ad Lung
9.360	Ad Oesphageal
9.400	SCLC
9.407	Sq Lung
9.420	Ad Lung

Patients with baseline V1 high PDGF (Subunit B) values in the Olink assay had shorter median PFS (20 vs 29 weeks, HR 1.45, 95 % CI 0.49 to 4.31, p = 0.69) than PDGF low when split into 2 groups of 7. Similarly, the median OS for PDGF high was 32 versus 40 weeks for PDGF low (HR 1.25, 95% CI 0.32 to 4.1, p = 0.84). These differences were not statically significant (Figure 4.31).

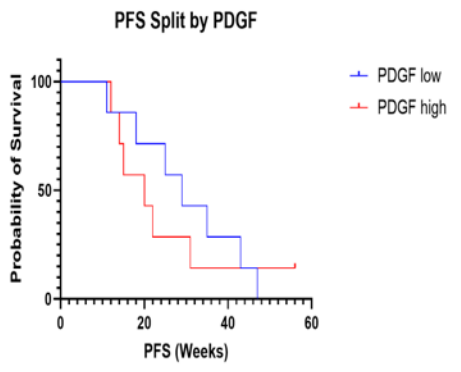

(a)

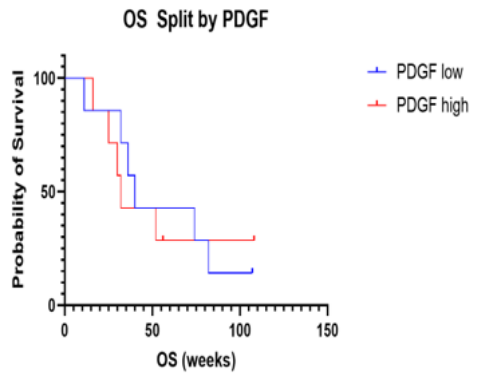

(b)

Figure 4.31 Kaplan Meir Curves of PFS (a) and OS (b) for V1 PDGF BB high (upper half of values, n=7) and low (n =7).

4.9.7 Correlation of mRNA data with the clinical outcome of Favourable vs. Unfavourable first restaging CT scan response

Untargeted gene expression was analysed in all samples, Tissue, Blood Timepoint 1 (First Visit) and Timepoint 2 (2nd visit 3-6 weeks later) according to initial CT Scan response assessment by iRECIST with patients being divided into Favourable (Partial Response or Stable Disease) *vs.* Progressive Disease or Died). The Normalised Enrichment Score (NES) was used to compare gene expression between these two groups. We identified **67** highly significantly over-expressed genes and **91** highly significantly under-expressed genes. Most notably **TAPBP** (Log2FC: -1.004), **AC004687.1** (Log2FC: -1.046), **MTCO2P12** (Log2FC: 1.667). Based on differential gene expression, we were **unable to cluster** the samples (Figure 4.32).

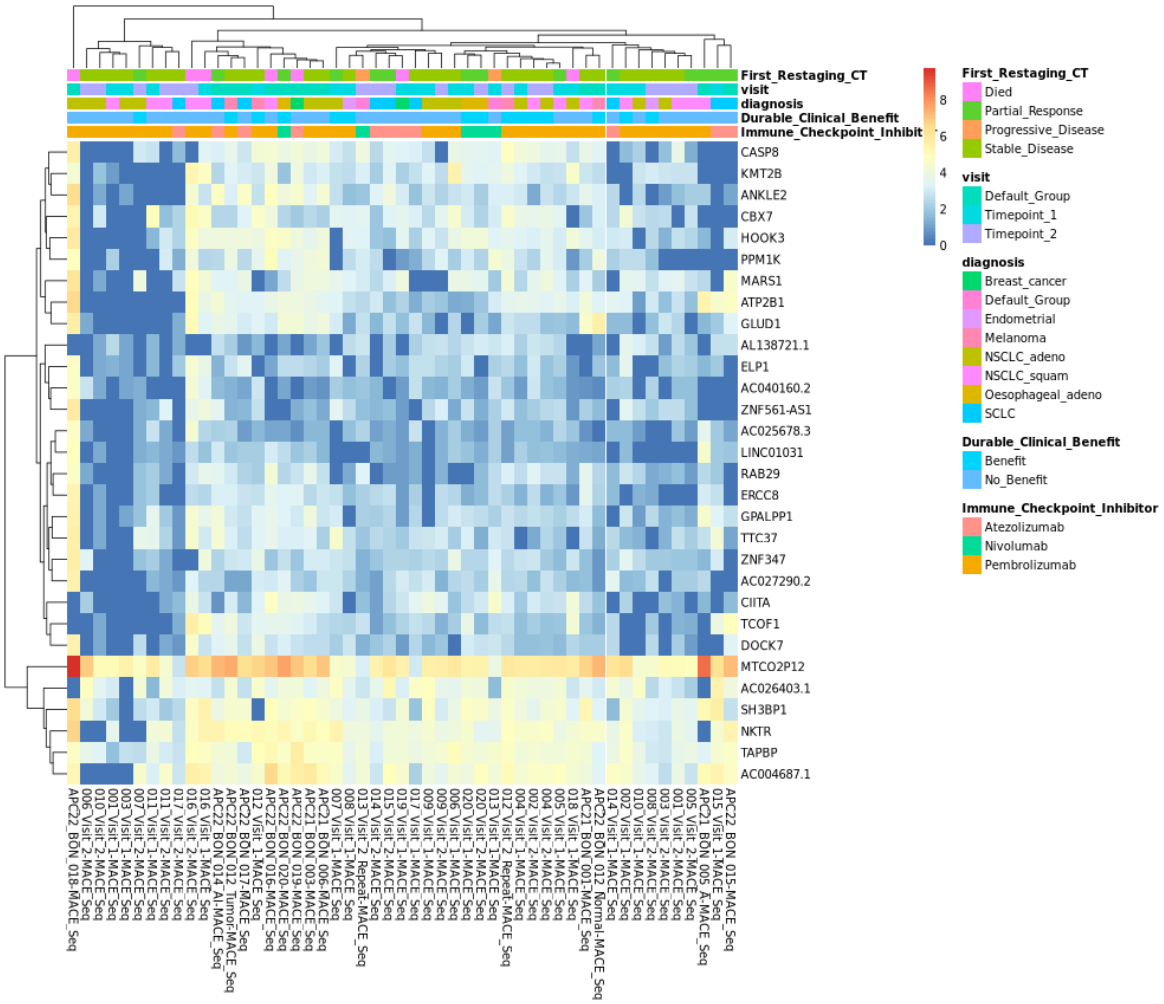

Figure 4.32 Heatmap showing the log-TPM (Transcripts Per Million) expression of the genes with the lowest log2 fold change standard error (lfcSE) from the list of significantly differentially expressed genes.

Differentially expressed genes were strictly filtered by mean, log2 fold change and standard error to further increase specificity of downstream analyses. P-values and FDR-values are based on 1000 permutations, and a cut-off p-value of 0.05 was used. The most significantly differentially expressed genes in blood and tissue samples between favourable early CT response vs unfavourable response (includes patients who had died prior to 3-month restaging CT) were **TAPBP, AC004687.1, MT-CO2P12, AC026403.1, SH3BP1, NKTR, HOOK3, CIITA, GPALPP1** and **TCOF1** (Table 4.27).

Table 4.27 Top 20 differentially expressed genes in Favourable (Partial Response, Stable Disease) compared to Unfavourable (Progressive Disease, Died) based on log2 fold change in mRNA expression.

Gene	Description	Mean	Log2 Fold Change	Standard Error	P-Value	Adj. P-Value
TAPBP	TAP binding protein [Source:HGNC Symbol;Acc:HGNC:11566]	31.84	-1.00	0.11	0.00	0.00
AC004687.1	novel transcript, MIR142 host	42.06	-1.05	0.17	0.00	0.01
MTCO2P12	MT-CO2 pseudogene 12 [Source:HGNC Symbol;Acc:HGNC:52028]	213.41	1.67	0.18	0.00	0.01
AC026403.1	60S acidic ribosomal protein (RPLP0) pseudogene	24.86	1.75	0.20	0.00	0.02
SH3BP1	SH3 domain binding protein 1 [Source:HGNC Symbol;Acc:HGNC:10824]	44.45	-1.42	0.22	0.00	0.00
NKTR	natural killer cell triggering receptor [Source:HGNC Symbol;Acc:HGNC:7833]	54.14	-1.12	0.22	0.00	0.01
HOOK3	hook microtubule tethering protein 3 [Source:HGNC Symbol;Acc:HGNC:23576]	21.05	-2.01	0.23	0.00	0.00
CIITA	class II major histocompatibility complex transactivator [Source:HGNC Symbol;Acc:HGNC:7067]	6.67	-2.38	0.24	0.00	0.00
GPALPP1	GPALPP motifs containing 1 [Source:HGNC Symbol;Acc:HGNC:20298]	13.54	-1.26	0.25	0.00	0.00
TCOF1	treacle ribosome biogenesis factor 1 [Source:HGNC Symbol;Acc:HGNC:11654]	8.19	-1.66	0.25	0.00	0.01
KMT2B	lysine methyltransferase 2B [Source:HGNC Symbol;Acc:HGNC:15840]	12.99	-1.95	0.26	0.00	0.01

Gene	Description	Mean	Log2 Fold Change	Standard Error	P-Value	Adj. P-Value
RAB29	RAB29, member RAS oncogene family [Source:HGNC Symbol;Acc:HGNC:9789]	7.17	-2.30	0.26	0.00	0.00
ZNF347	zinc finger protein 347 [Source:HGNC Symbol;Acc:HGNC:16447]	13.33	-2.21	0.26	0.00	0.00
AC027290.2	novel transcript	10.99	-2.70	0.27	0.00	0.00
DOCK7	dedicator of cytokinesis 7 [Source:HGNC Symbol;Acc:HGNC:19190]	11.27	-2.08	0.28	0.00	0.00
ERCC8	ERCC excision repair 8, CSA ubiquitin ligase complex subunit [Source:HGNC Symbol;Acc:HGNC:3439]	9.25	-2.14	0.28	0.00	0.00
TTC37	tetratricopeptide repeat domain 37 [Source:HGNC Symbol;Acc:HGNC:23639]	14.97	-1.40	0.28	0.00	0.01
CASP8	caspase 8 [Source:HGNC Symbol;Acc:HGNC:1509]	17.39	-2.09	0.28	0.00	0.02
AL138721.1	ribosomal protein S12 (RPS12) pseudogene	4.01	1.15	0.28	0.00	0.00
ATP2B1	ATPase plasma membrane Ca2+ transporting 1 [Source:HGNC Symbol; Acc:HGNC:814]	30.34	-1.90	0.28	0.00	0.00

These genes were analysed using GSEA in 6 different databases namely *WikiPathways, Reactome, Disease Gene Network, GO Molecular Functions, GO Biological Processes* and *GO Cellular Component*. GSEA findings from each database are listed as well as cnet plots. The GSEA findings for all databases queried are summarized in the Master GSEA Table (Table 4.28) below. *WikiPathways* GSEA findings are summarized in Table 4.29. The Dotplot and Cnet plots for the GSEA carried out using the WikiPathways database are shown in Figure 4.33 and Figure 4.34 below (the GSEA results for the other five databases queried are detailed in Appendix K).

Database	Up-regulated Pathways	Down-regulated Pathways
Wikipathways	miRNA targets in ECM and membrane receptors	Type II interferon signaling
	Burn wound healing	Immune response to tuberculosis
	Fatty acid omega-oxidation	Genes associated with the developn rheumatoid arthritis
Reactome	Degradation of the ECM	Interferon gamma signaling
	Regulation of Insulin-like Growth Factor (IGF) transport anduptake by Insulin-like Growth Factor Binding Proteins (IGF-BPs	Interferonalpha/beta signaling,
	ECM organization	Interleukin-2 family signaling
Disease **Gene Network**	Pleural Effusion, Malignant,	Autoimmune Primary Adrenal Insu
	Benign Neoplasm	Addison's disease due to autoimmu
	Intervertebral Disc Degeneration	Increased megakaryocyte count
GO Molecular Functions	extracellular matrix structural constituent	MHC protein binding
	growth factor binding	MHC protein complex binding
	fibronectin binding	MHC class I protein complexbindir
GO **Biological Processes**	ethanol metabolic process	alpha-beta T cellactivation,
	retinol metabolic process	alpha-beta T cell differentiation
	extracellular matrix organization	positive regulation of alpha-beta T
GO Cellular Component	collagen-containing extracellular matrix	immunologicalsynapse
	external encapsulating structure,	MHC class II protein complex,
	extracellular matrix	MHC protein com-plex

***WikiPathways* GSEA Analysis;** Based on gene expression, we identified **25 up-regulated** and **5 down-regulated** terms from *WikiPathways* using GSEA (Agrawal et al. 2024). The most significantly up-regulated terms in the Favourable group were **miRNA targets in ECM and membrane receptors** (NES: 2.29), **Burn wound healing** (NES: 2.0389), and **Fatty acid omega-oxidation** (NES: 2.1945). The most significantly down-regulated terms were **Type II interferon signalling** (NES: -2.7723), **Immune response to tuberculosis** (NES: -2.2946), and **Genes associated with the development of rheumatoid arthritis** (NES: -2.1292). These are listed in Table 4.29 and are shown graphically in Figure 4.33 and Figure 4.34, respectively.

Table 4.28 Top 15 enriched terms from WikiPathways in Favourable (Partial Response, Stable Disease) compared to Unfavourable (Progressive Disease, Died) based on gene expression.

ID	Term	NES	Adj. P-Value	Genes
WP619	Type II interferon signaling	-2.77	0.00	CYBB, IRF9, STAT1, EIF2AK2, IRF1, TAP1, OAS1, GBP1, IRF2, STAT2, IFIT2, IL1B, CXCL9, IFI6, IRF8, REG1A, SOCS1, ICAM1, ISG15, JAK2, CIITA
WP2911	miRNA targets in ECM and membrane receptors	2.29	0.00	LAMC1, COL4A2, COL1A2, COL6A2, COL6A1, COL5A1, COL6A3, COL3A1, COL5A2, COL4A1, FN1
WP5055	Burn wound healing	2.04	0.00	AMBP, SERPINH1, COL1A2, FBN1, CCL2, MMP2, COL1A1, VEGFA, XIST, CD248
WP206	Fatty acid omega-oxidation	2.19	0.00	ADH1B, ADH1A, ADH1C, ADH4
WP4239	Epithelial to mesenchymal transition in colorectal cancer	1.84	0.00	CLDN1, CDH1, CLDN4, COL4A2, MMP2, ID1, CLDN12, GDF15, CLDN7, LRP5, WNT5B, KRAS, HRAS, NOTCH3, VTN, COL4A1, EZH2, EED, FN1, JUP, STRAP, SMAD4, FOXQ1, CLDN3, COL4A5, ...
WP3996	Ethanol effects on histone modifications	2.14	0.00	ADH1B, ADH1A, ADH1C, ALDH1A3, TYMS, CYP2E1, AHCY
WP4197	Immune response to tuberculosis	-2.29	0.00	IFNAR2, PSMB8, IRF9, STAT1, IRF1, TAP1, OAS1, IFI35, MX1, STAT2, SOCS1, IFIT3, JAK2
WP2813	Mammary gland development: embryonic development - stage 1 of 4	2.14	0.00	CDH1, CLDN4
WP176	Folate metabolism	1.99	0.01	SOD3, APOB, SAA1, CCL2, SHMT2, APOA1, ALB, FGA, MPO, SERPINE1,

ID	Term	NES	Adj. P-Value	Genes
				AHCY, GPX3, SCARB1, SHMT1, TNF, HBA1, MTRR, PLG, NFKB1, ABCA1, RFK
WP2005	miR-targeted genes in muscle cell	1.59	0.01	CLDN1, LAMC1, SH3BP4, COL1A2, COL1A1, RFT1, E2F1, WDFY1, CDKAL1, PXDN, GPD2, GFPT1, FNDC3B, CCN1, COL3A1, LAMC2, GNPNAT1, FSTL1, TYMS, LAMTOR3, KRAS, NAPG, ACAA2, LMNB2, RDH10, ...
WP1533	Vitamin B12 metabolism	2.03	0.01	APOE, SOD3, APOB, SAA1, CCL2, SHMT2, APOA1, ALB, FGA, MPO, SERPINE1, SCARB1, MMUT, LRP2, TNF, HBA1, MTRR, PLG
WP2004	miR-targeted genes in lymphocytes	1.50	0.01	CLDN1, LAMC1, SH3BP4, COL4A2, RFT1, AURKB, E2F1, WDFY1, FADS1, CDKAL1, PXDN, GPD2, GFPT1, FNDC3B, CCN1, LAMC2, GNPNAT1, TYMS, LAMTOR3, KRAS, NAPG, ACAA2, LMNB2, RDH10, LY6K, ...
WP5033	Genes associated with the development of rheumatoid arthritis	-2.13	0.02	IRF5, CD244, CD40, SLC22A4, CTLA4, CIITA, HLA-DRB1, STAT4
WP716	Vitamin A and carotenoid metabolism	1.99	0.02	ADH1A, RBP4, ADH4, DHRS3, ALDH1A3, RDH5, RBP1, RDH10
WP4754	IL18 signaling	1.57	0.02	CLDN1, CLDN4, COL1A2, CCL2, MMP2, MMP14, TIMP3, COL1A1, CLDN12, BMP2, VEGFA, DES, PARP1, ARG1, IL17RC, SDC4, COL3A1, HSPB1, NFATC4, CCNB2, APBA2, LMNB2, PTMS, NCAPH2, ZNF219, ...

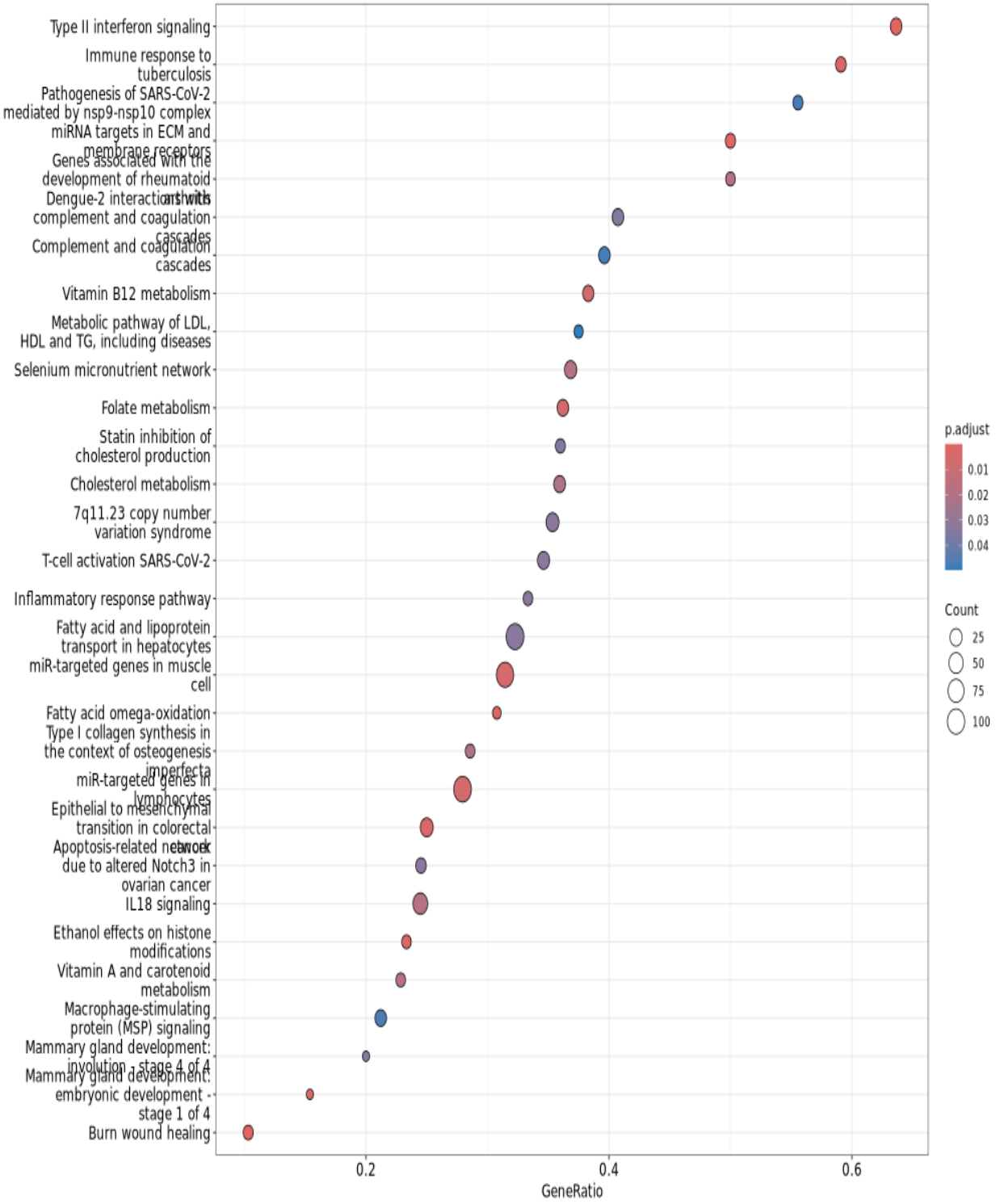

Figure 4.33 Favourable (Partial Response, Stable Disease) compared to Unfavourable (Progressive Disease, Died) Dotplot of enriched pathways from WikiPathways. Dots represent

enriched pathways, with size indicating gene count and colour showing significance (e.g., adjusted p-value).

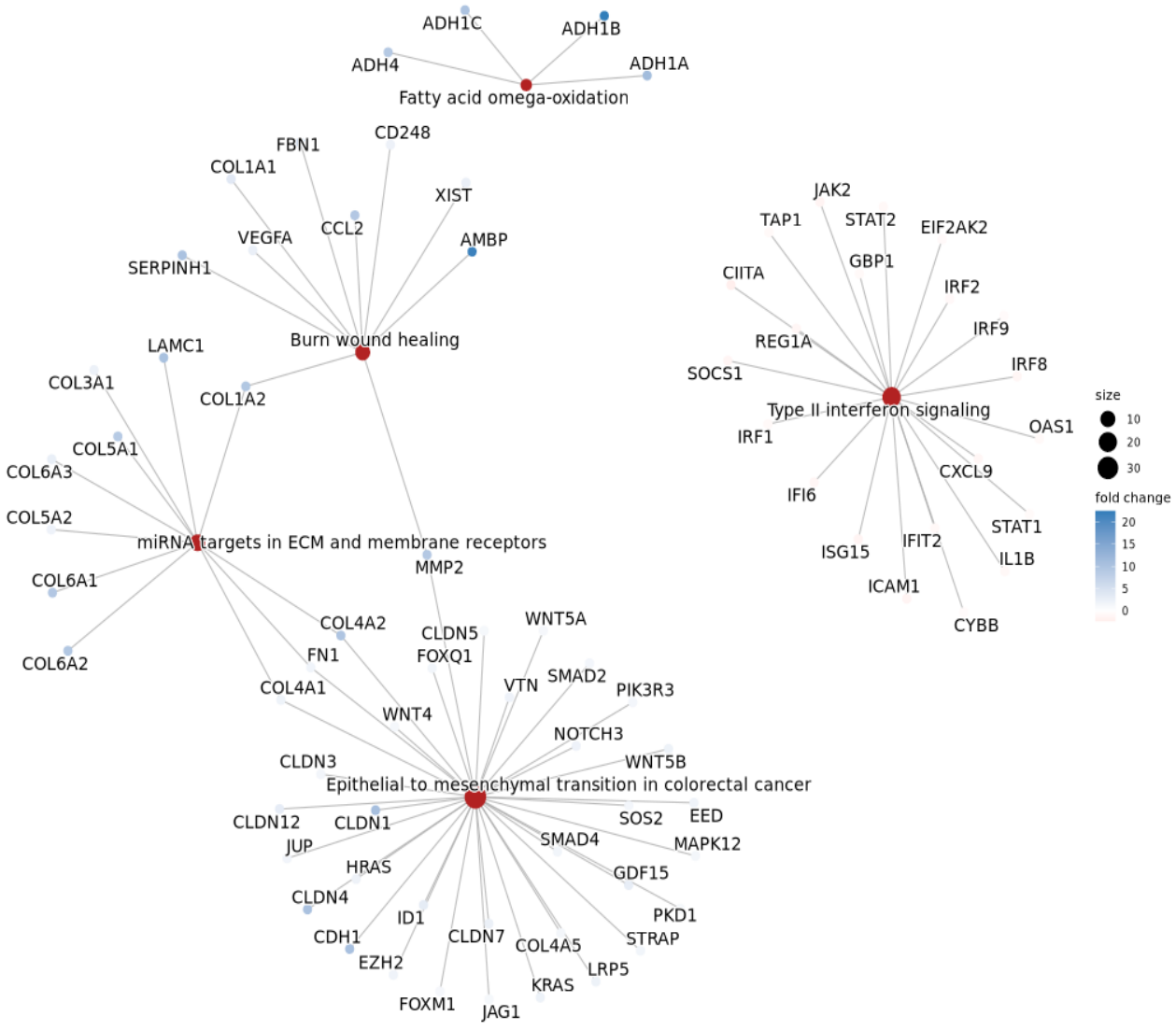

Figure 4.34 Favourable (Partial Response, Stable Disease) compared to Unfavourable (Progressive Disease, Died) Cnet (Category-network) plot of gene-pathway relationships from *WikiPathways*. Pathways and their associated genes are connected, with node size and edge thickness indicating enrichment and shared genes.

4.9.8 Correlation of FACT-ICM QoL Questionnaire with Clinical Outcomes

While a higher Baseline FACT-ICM did correlate weakly with better outcomes in terms of OS (Spearman r = .374) this was not statistically significant (p = .139). Similarly higher baseline FACT-ICM score was associated with better PFS but not statistically significant (r = .299, p = .242).

There were no significant changes over time in any of the 5 subscales of the FACT-ICM Questionnaire. Two of the 10 patients who opted to complete the second Quality of Life questionnaire had Grade 3 to 4 autoimmune toxicity but their scores did not fall significantly. The questions used to assess for autoimmune toxicity may overlap with toxicity of cytotoxic treatment and cancer burden.

4.9.9 Correlation of Faecal Microbiome Data with Clinical Outcomes

Due to low sample size, it was not possible to correlate faecal microbiome diversity or other metrics such as species abundance or presence with clinical outcomes. For example, when the 14 patients who provided visit 1 (T1) samples had OS (weeks) analysed using Cox regression (survival times from 6 missing patient samples excluded) against chao1 there was no significant correlation. (Table 4.30 and Figure 4.35) The Hazard Ratio was 0.993 with a 95% CI of 0.983 to 1.001, beta1 = -0.0074, SE 0.0046, 95% CI (-0.0176 to 0.0006). Baseline (T1) Simpson and Shannon diversity did not correlate with OS either. None of the alpha metrics of diversity at either timepoint correlated with development of autoimmune toxicity (Figure 4.36).

Table 4.29 Cox regression of T1 alpha diversity indices (n=14) as predictors of Overall Survival.

Alpha Diversity Index	Hazard Ratio Estimate	95% Confidence Interval	P-value
Chao1	0.9907	0.9734 to 1.008	ns
Simpson	0.4816	4.774e-025 to 4.321e+023	ns
Shannon	1.340	0.01359 to 112.7	ns

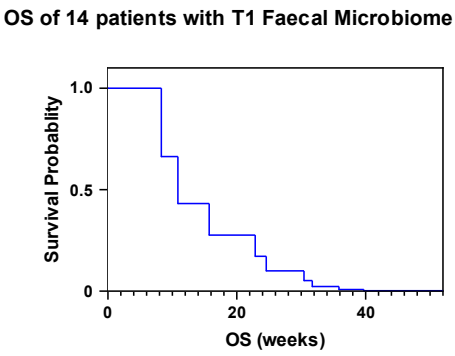

Figure 4.35 OS (weeks) for the 14 patients with T1 faecal microbiome samples

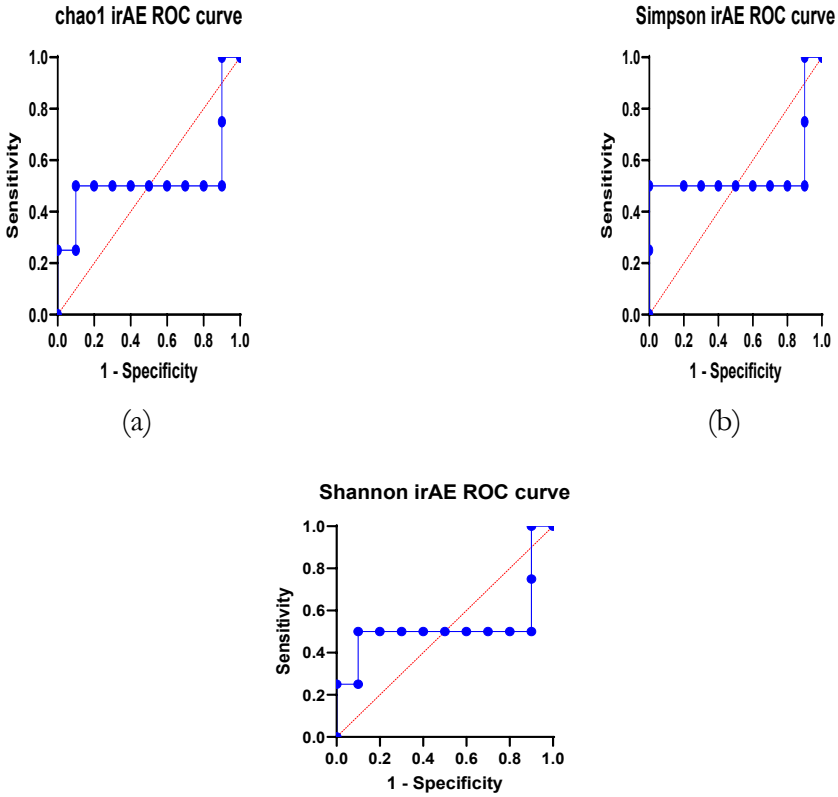

Figure 4.36 Alpha diversity indices as a predictor of autoimmune toxicity, reporter operating curves.

When the Volcano Plots generated in EdgeR were assessed there was no way to determine if changes in individual taxa correlated with clinical outcomes. With regards to changes grouped by CT response (Partial Response vs Other) or Durable clinical benefit (Present *vs.* Absent) there were not enough sample numbers to perform any principal component analysis (PCA) (Figure 4.37).

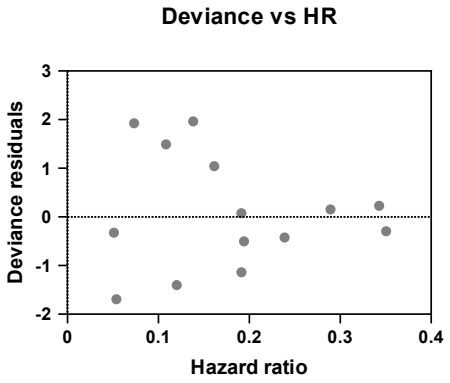

Figure 4.37 Graph of Deviance residuals against Hazard Ratio. Cox regression of chao1 alpha diversity.

5 Discussion

5.1 Introduction

This study aimed to explore investigational biomarkers in predicting benefit and toxicity from ICI in solid malignancies. Proteomics, Faecal Microbiome Next Generation Sequencing and mRNA analysis of blood and tissue were carried out in an attempt to detect biomarkers worthy of future research. It is frustrating for clinicians to have to wait until the 2- or 3-month restaging CT scan to decide whether ICI have helped the patient. Clinicians are particularly interested in dynamic biomarkers where early changes in circulating blood cells, proteins and messenger RNA (mRNA) can help predict outcome and perhaps inform change of treatment.

5.2 Inflammatory Markers and Immune Metabolites as Biomarkers

In this small study elevated pre-treatment levels of known baseline inflammatory markers such as ESR, CRP, NLR and SII performed as previously described in the literature and were associated with worse clinical outcomes. After correction for multiple comparisons elevated NLR was the best predictor of poor OS with a Hazard Ratio of 1.051 to 3.211 (95% Confidence Interval). It is unclear whether NLR or SII is a better predictor of response to ICI therapy for NSCLC (Y. Li et al. 2025; Fu et al. 2019). Examining the Kaplan-Meier curves for median split and highest vs. lowest quartiles a clear trend was seen towards worse outcomes with higher baseline NLR. Elevated baseline NLR is not specific enough to allow the clinician to choose dual immunotherapy combining anti CTLA4 with anti PD-L1 ICI but perhaps could be used to identify patients who would benefit from clinical trials of novel agents. such as antibodies to LAG-3 or bispecific antibodies targeting VEGF and PD-L1 (T. Li et al. 2024). Recent studies have shown that both low baseline and falling serial NLR are associated with better outcomes to ICI treatment in MSI high and low metastatic colorectal cancer (H. Ouyang et al. 2023). Ouyang *et al* then combined changes in NLR with TMB, and dramatic differences were seen in

OS between the most favourable group (Reduction in NLR and TMB >10 mut/Mb) vs the least favourable group (Rise in NLR and TMB < 10 mut/Mb). In the most favourable group Ouyang *et al* found median OS was not reached but in the least favourable group median OS was 13.63 months. A large retrospective cohort study of 1714 ICI patients with 16 different tumour types combined both baseline NLR with TMB and found that patients with the highest quintile (top 20%) NLR in 14 types of cancer had unfavourable outcomes compared with the lowest 80% (Valero et al. 2021). When TMB was combined with NLR the best outcomes were seen in NLR low/TMB high patients across a wide variety of solid tumour types. This literature and the results of APC 125 point to simple inflammatory indices such as NLR having a role to play in treatment selection and clinical trials of ICI.

It is challenging to identify a normal healthy subject plasma range and a range in cancer patients for Tryptophan and its metabolites. Both small numbers and differences in techniques and units used across studies contribute to confusion (Badawy and Guillemin 2019; Aarsland et al. 2022; Metri et al. 2023) . Previous studies were summarized in a review article (Y. Chen and Guillemin 2009) which mostly used micromolar (μM) concentrations. Patients with resectable lung cancer had pre-operative Tryptophan values of 10.9 ± 5.2 μM (Cascino et al. 1991) compared to 4.7 ± 0.7 μM in control subjects. Patients with haematologic malignancies had higher Tryptophan concentrations e.g. Hodgkin Lymphoma 56.4 ± 13.1 μM (Denz et al. 1993) as did the healthy controls ≤65 μM. The Hodgkin patients' Kynurenine values were 2.3 ± 1.1 μM compared to ≤3.5 μM in controls giving a K/T ratio of 0.04. In APC 125 the pre-treatment (V1) mean Tryptophan value was 15981 ng/mL equivalent to 78.2 μM with a Kynurenine value of 1053 ng/mL equivalent to 5.1 μM. This yielded a mean APC 125 pre-treatment K/T ratio of 0.07, higher than but similar to the previously reported baseline (pre-treatment) lymphoma values.

An initial rise in K/T ratio following exposure to ICI was also reported in a large study of melanoma and renal cell cancer (RCC) patients. (Haoxin Li et al. 2019a). This analysis combined two phase 1 trials, the 91-patient RCC CA209-009 study, with various doses of Nivolumab, and the Nivolumab arm of the 78-patirnt metastatic melanoma phase 1b CA209-038 study as a training set (Ribas et al. 2017; Choueiri et al. 2016) . Li et al used as a validation set a large phase 3 RCC study (Checkmate-025) which randomised RCC patients to Nivolumab or to the mTOR inhibitor Everolimus (Motzer et al. 2015). In the RCC CheckMate 025 study, the baseline mean Kynurenine was 6.34 μM (SDV ± 1.33, Range 8.95), baseline mean Tryptophan was 44.5 μM (±

10.22, Range 81.8). The mean baseline K/T ratio was 0.143 ((± 0.04, Range 0.32). The baseline Kynurenine values in the APC125 study were similar to this published RCC cohort but the mean tryptophan value was almost twice as high. We observed a significant rise in K/T ratio between V1 and V2 and a fall from V2 to V3 when one outlier was excluded using Grubb's test. This outlier, Patient 8 (endometrial cancer), had a pre-treatment serum Kynurenine concentration of 3954 ng/mL or 18.99 μM which is outside reported ranges. In the Li *et al* study the highest pre-treatment Kynurenine concentration was 12.32 μM. This melanoma patient had a pre-treatment K/T ratio of 0.54 which was much higher than the reported highest value (0.38) in the CheckMate 025 study.

In their cohort K/T ratio stabilized at 4-8 weeks whereas we observed a significant fall from V2 to V3 at 3 months. In Li's population melanoma patients with an initial ≥50% rise in K/T ratio had a much shorter median OS than those with a lesser increase (17.7 months vs > 38 months ($p = 6.0 \times 10^{-5}$, log-rank test)). We did not observe any linkage between changes in K/T ratio and PFS and OS which may again be due to our much smaller sample size, differences in tumour type and the fact that most of our patients received cytotoxic chemotherapy with ICI whereas the Li et al cohort only received ICI. The initial rise in K/T ratio between pre-treatment and second treatment visit may be a way to identify patients who would benefit from addition of IDO inhibitors to ICI treatment but requires prospective validation in a larger more homogenous cohort.

Numerous studies have shown that increased IDO activity as evidenced by higher K/T ratios are associated with depression and decreased Quality of Life(QoL) (Lanser et al. 2020; Holthuijsen, et al. 2024). This led us to correlate a range of tryptophan metabolites with the FACT-ICM score. There were some unexpected findings in APC125 where higher K/T ratio correlated positively with first visit Emotional and Functional Well Being Scores (EWB0 and FWB0 (Table 4.24). The unexpected first visit finding may be explained by small sample size. Alternatively, some authors have suggested that kynurenine has a neuro-protective role (Abujrais et al. 2025; Savitz et al. 2015). As was expected the repeat scores (EWB1 and FWB1) at the 3-month visit correlated negatively with 2nd and 3rd visit K/T ratios.

Multiple clinical trials of IDO1 inhibitors in combination with ICI have failed most noticeably in metastatic melanoma where the IDO1 inhibitor combined with pembrolizumab was not

superior to pembrolizumab alone (Long et al. 2019). This has led to discontinuation of clinical trials using the Bristol Myers Squibb drugs BMS-986205 (Rose 2018). It is apparent that IDO1 has complex non-enzymatic immune signalling roles and that IDO2 and Tryptophan 2,3-Dioxygenase (TDO2) which metabolizes Tryptophan down the Kynurenine pathway play an important role in evading IDO1 blockade (X. Wang et al. 2026). If the field is to move forward both drugs modifying the activity of all 3 enzymes and biomarker driven patient selection using early dynamic changes in K/T ratio may help.

5.3 Proteomic Analysis of Serum Cytokines and Soluble Receptors

Proteomic Analysis using the Olink platform suggests that initial high levels of circulating Platelet Derived Growth Factor Subunit Beta (PDGF BB, Vascular Endothelial Growth Factor Receptor 2 (VEGFR-2), tyrosine kinase with immunoglobin and EGF homology domains 2 (TIE2) and others may have an adverse effect on survival whereas initial high levels of Tumour Necrosis Factor-related apoptosis-inducing ligand (TRAIL) and Inducible T cell co-stimulator ligand (ICOSLG) may have favourable effects.

It is interesting to note that the three potential adverse markers are all associated with angiogenesis and thrombosis. There are many Tyrosine Kinase Inhibitors (TKI) which target PDGF, VEGF and TIE2 receptor signalling and some have been licenced combined with ICI in hepatocellular carcinoma (HCC) and renal cell carcinoma (RCC) (Y. Song et al. 2020; Hu et al. 2022; Zhou et al. 2024; Modi and Kulkarni 2019). The monoclonal antibody Bevacizumab which targets circulating VEGF has been successfully combined with ICI in HCC leading to FDA and EMA approval. The phase III trial IMBRACE151 found that the addition of bevacizumab to chemotherapy and the ICI Atezolizumab was only of benefit in patients with high levels of VEGF A mRNA. One second line phase II NSCLC trial compared the combination of the anti VEGF Receptor 2 monoclonal antibody Ramucirumab with Pembrolizumab in patients previously treated with chemotherapy to physician's choice (most patients in the control arm received Docetaxel and Ramucirumab) and found encouraging results (Reckamp et al. 2022). A small (n = 24) Japanese phase 2 neoadjuvant NSCLC trial combined 2 cycles of Pembrolizumab and ramucirumab and demonstrated promising activity (6

patients achieved pCR) with increase in the CD8+ T cells in the TME (Aokage et al. 2024). VEGF-R2 plays a crucial role in tumour neo angiogenesis and is also found on the surface of circulating tumour cells (Kallergi et al. 2009) . It has been suggested that neo angiogenesis plays a role in generating an immunosuppressive tumour microenvironment and that vascular normalization permits ICI efficacy (Tu et al. 2023) PDGF BB also activates STAT3 and is associated with adverse outcomes in urothelial cancer patients receiving ICI (Ando et al. 2023).

In our proteomic data baseline elevated serum TRAIL levels were the strongest potential favourable biomarker. TRAIL induces tumour cell apoptosis and upregulates PD-L1 expression (Pimentel et al. 2023). TRAIL is associated with activation of the IFN-γ pathway. We did not identify serum IFN-γ levels as a predicative biomarker in APC125. It is believed that one mechanism of ICI anti-tumour activity is loss of IFN-γ signalling (Wong et al. 2023). In sum our proteomic findings suggest that circulating pro-angiogenic factors portend poor ICI response and that there may be markers of a favourable ICI response such as TRAIL.

5.4 Messenger RNA Analysis

Initial analysis of blood mRNA samples did not yield any meaningful results in terms of correlation with any clinical outcome. The one gene which approached significance when abundance of expression was compared between blood samples pre and post initial ICI samples was *BCL2L1*. It has been suggested that the protein product of this gene Bcl-xl may maintain tumour cell viability and be a potential target for novel agents which would act synergistically with ICI (Newman et al. 2026).

GSEA and Pathway Analysis of Changes in Serial Blood Samples

There were no significant differences in genes differentially expressed between Timepoint 1 and Timepoint 2. The table of differentially expressed genes between blood samples taken at baseline and at second study visit in section 4.8 shows very small absolute differences (measured in log2fold change). The gene in which the largest change in expression was seen **BCL2 like 1**, codes through alternate splicing for pro and anti-apoptotic proteins. (Boise et al. 1993) While GSEA can point to activation of biological pathways when standard mRNA expression fails to distinguish between groups it is likely that our data set is too small for this to be a meaningful result. There were remarkably few pathways upregulated or downregulated across our paired

mRNA blood samples. The most significantly up-regulated terms were found in the *GO Biological Process* database and included ureteric bud development (NES: 2.2724), mesonephros development (NES: 2.2684), and mesonephric epithelium development (NES: 2.2519). These are all pathways involved in the development of the embryological kidney and reproductive organs but have no known linkage to cancer beyond rare malignancies arising from embryological remnants (Santana Gonzalez et al. 2021; Wu et al. 2014). Given the small differences in gene expression between the pooled pre-treatment and subsequent visit mRNA samples the apparent change in gene expression and associated GSEA results are likely not significant (Subramanian et al. 2005).

It was decided to analyse all blood and tissue samples together to see if there were any candidate genes or pathways that correlated with clinical outcomes. When all samples were combined (Tissue, Visit 1 Blood and Visit 2 Blood) it was possible to see differences between patients who had an initial restaging CT scan as Favourable (Partial Response, Stable Disease) vs Unfavourable (Progressive Disease or Died) outcome at 12 weeks post initiation of treatment. The clinical groups split by 1st CT Response are unbalanced in size with the Favourable (PR, SD) n= 16 outnumbering the Unfavourable (PD, Died) n = 4. The heatmap of DGA (Fig 4.32) does not show clustering by clinical groups (1st CT Scan Response or Defined Clinical Benefit) but shows tissue samples clustering together. This makes it less likely that the results discussed below are biologically meaningful. Apparent GSEA pathway differences in the APC 125 population between clinical groups may be caused by heterogenous tumour types, variations in treatment and small sample size. A larger patient sample size might have made it possible to explore the relative contributions of each sample type and to explore whether there is an mRNA signature that can be derived from any single or longitudinal test (e.g. baseline tissue and blood mRNA or tissue and Visit 2 blood mRNA to predict outcome at 3-6 weeks post treatment. Such a test would enable clinicians to change treatment earlier than the standard restaging CT scan at 3 months allows.

Differential Gene Expression between First CT Scan Groups

When comparing first CT scan response (Favourable *vs.* Unfavourable) the most significantly differentially expressed gene *Transporter Associated with Antigen Protein Binding Protein (TAPBP)* was under-expressed in the Favourable group. TAPBP or Tapasin is part of the Immunoglobulin Super Family (ISF) and peptide loading complex (PLC) (Darley et al. 2025). Tapasin is important in how CD8+ T cells recognize tumour antigens via MHC I. Tapasin helps load tumour antigens onto MHC I in tumour cells prior to its transport to and expression on the extra cellular membrane. Autoantibodies which develop to TAPBP on-treatment have been shown to correlate with favourable response in NSCLC to ICI (Dai et al. 2024). Higher *TAPBP* mRNA levels in tumour tissue in gastric cancer samples correlate with improved PFS in patients treated with ICI (K. Wang et al. 2022). In keeping with our finding of decreased Tapasin correlating with better ICI outcomes recent *in vitro* and mouse model work suggest that loss of Tapasin can counter-intuitively enhance ICI effectiveness (Moniwa et al. 2025). *AC004687.1* was under-expressed in the Favourable group in our study. AC004687.1 is one of the genes whose overexpression was used in an immune score for Oral Squamous Cell Carcinoma Prognosis (Huang et al. 2020). It has been described as a long non coding RNA transcript and that higher levels of its expression is associated with favourable outcomes in HCC (Ye et al. 2020). Two genes over-expressed in the Favourable group were MT-*CO2P12* and *AC026403.1. MT-CO2P12* is a mitochondrial pseudo gene which influences cytochrome c activity ("MTCO2P12 MT-CO2 Pseudogene 12 [Homo Sapiens (Human)] - Gene - NCBI" 2025). It is thought that disturbances in oxidative phosphorylation may influence response to ICI (Tian et al. 2024). Cytochrome c plays a key role in generating and metabolizing ROS and is itself a pro-apoptotic protein when released into the cytoplasm (Alshehri 2024). *AC026403.1* is a pseudogene related to the 60S acidic Ribosomal Protein (RPLP0). It has not previously been identified as predicting ICI response. It is unknown whether *AC026403.1* transcription has any influence on RPLP0 expression or function.

Pathway Analysis based on Gene Sene Set Enrichment Analysis (GSEA)

Observing the summary of Pathways Up and Down-Regulated by database certain commonalities emerge (Table 4.28). In the Favourable group, pathways associated with ECM (Extra Cellular Matrix) organization and remodelling are upregulated in 5 of the 6 databases queried i.e. every database except *Disease Gene Network* (See Appendix K, Table K.2 and Fig K.3 and K.4). This is not in keeping with the body of work in the field which suggests that ECM

remodelling is an adverse prognostic feature and leads to ICI resistance (Fejza et al. 2023). Two GSEA Databases (*Reactome* and *GO Molecular Function*) demonstrate upregulation of growth factor binding or regulation. (Detailed in Appendix K Results of Gene Sequencing Enrichment Analysis, Tables K.1 and K.3 Figs K1, K2, K.5, K.6)). A variety of metabolic process pathways were upregulated including fatty acid omega-oxidation, ethanol and retinol metabolic processes. Somewhat surprisingly pathways associated with immune cell activation including IFN-γ (also termed Type II IFN) and MHC protein complex are downregulated in the Favourable group in every database queried except *Disease Gene Network*. It may have been more informative to perform peripheral blood mRNA screening of known transcripts known to affect prognosis such as PD-1 and CTLA-4 (W. Wang et al. 2017). This approach has been combined with mRNA sequencing of peripheral blood leucocytes which may be possible in future on our stored PMBC specimens (Jiang et al. 2021). Our findings are at best hypothesis generating and need validation in a larger more homogenous patient and treatment population. It is possible that the apparent linkage of ECM remodelling upregulation and IFN-γ pathway downregulation with favourable response to ICI found in APC 125 is artefactual and will not be borne out in future work.

The ECM has emerged as a critical component of the TME which influences cancer cell growth, immune cell activation and tumour tolerance as well as affecting drug and immune cell influx to the TME(Mai et al. 2024). ECM stiffness makes it more difficult for cytotoxic T cells to enter the TME(Fejza et al. 2023). Remodelling the ECM is a complex process driven by tumour cell signalling which encourages stromal cells to become Cancer Associated Fibroblasts (CAF). ECM remodelling is essential for local invasion of cancer cells into host tissue and for circulating tumour cells to enter the capillary network (Winkler et al. 2020). Other work has shown that higher baseline levels of circulating ECM components, such as collagens and their degradation products such as PRO-C3 are associated with worse outcomes in melanoma patients treated with ICI (Jensen et al. 2018). An increase in serum levels of the ECM remodelling proteins Citrullinated and Matrix Metalloproteinase (MMP) Degraded Vimentin (VICM), which is a marker of M1 macrophage activity, between baseline and 6 weeks was associated with better outcomes in melanoma patients treated with PD-1 inhibitors (Hurkmans et al. 2020). This could mean that the GSEA increase in ECM remodelling in patients with favourable initial restaging CT scans observed in APC 125 has a biological rationale. The burn wound healing pathway

which is activated in mammals post burn injuries is a pro-inflammatory state also seen in tumourigenic TME with high levels of VEGF and TGF-beta (Walter et al. 2023; MacCarthy-Morrogh and Martin 2020). Wound healing involves remodelling of the ECM(Walter et al. 2023). It is possible that a TME high in proliferative cytokines (Burn wound response) might be inflamed or "hot" containing T cells that can be activated by ICI. Potentially treatment with ICIs could reset this inflamed milieu leading to better outcomes.

Upregulation of genes associated with control of Insulin-like growth factor (IGF) in the APC 125 Favourable group is not concordant with the existing concept that IGF is pro tumour growth and mediates ICI resistance in Triple Negative Breast Cancer. (Choi et al. 2025; D. Song et al. 2024).

WikiPathways terms which were downregulated in the Favourable first CT Scan response group and over-expressed in the Unfavourable group were "Type II interferon signalling", "Immune response to tuberculosis" and "Genes associated with the development of rheumatoid arthritis". Type II Interferon (IFN) signalling is mediated uniquely by IFN-γ (gamma). (Brea-Iglesias et al. 2025). IFN-γ pathway mediator mRNA expression is associated with favourable outcomes in patients treated with ICI(Ayers et al. 2017). It is associated with an initial favourable response to ICI through the activation of cytotoxic CD8+ T cells and sensitizing tumour cells to apoptosis(Litchfield et al. 2021). However chronic IFN-γ exposure leads to the emergence of ICI resistance (C. Liu and Gao 2019). The pathway associated with human response to TB is a mixture of Type I and Type II IFN signalling(Cliff et al. 2015). There are some similarities in how cancer and TB escape immune surveillance but this pathway has not been associated with differential response to ICI before (Waagmeester et al. 2025). The "Genes associated with the development of rheumatoid arthritis" pathway contains genes important in B and T cell signalling, cytokines and CTLA4 (Willighagen et al. 2024). It has not previously been implicated as a marker of ICI response.

5.5 Faecal Microbiome Analysis

It is important to be conservative in interpreting these results given the huge amount of genomic data generated for each sample and the low number of samples. The observation that chao1 varied significantly ($p=0.08$) between patients but not between baseline and post first treatment samples whereas the converse was true for Simpson and Shannon indices may mean that

treatment including supportive steroids and antibiotics led to an increase in evenness (i.e. decline in dominance) but not richness. The increase in evenness as measured by the Pielou index suggests that treatment leads to greater diversity in the faecal microbiome but whether this is caused by immunotherapy, cytotoxic chemotherapy or supportive medicines such as steroids and antibiotics cannot be established from this data.

In APC 125 alpha diversity measured by chao1, Simpson and Shannon indices at baseline did not correlate with overall survival. This may be due to low patient numbers. This is in contrast to a small NSCLC study (n = 5) where there were distinct changes in the abundance of certain genera which differed between responders and non-responders to ICI with or without chemotherapy (Sarkar et al. 2023). In their work responders showed decreased abundance of *Odoribacter*, *Gordonibacter*, *Candidatus Stoquefichus*, *Escherichia-Shigella*, and *Collinsella*, and increase in abundance of *Clostridium sensu stricto 1*. Non-responders showed an increase in *Prevotella*, *Porphyromonas*, *Streptococcus*, and *Escherichia-Shigella*, and decrease in abundance of *Akkermansia*. A larger international study of ICI in patients with melanoma treated with either single agent Pembrolizumab or combined Ipilimumab/Nivolumab examined serial faecal samples in 175 patients and found that longitudinal changes in Sub-Genus Bins (SGB) was associated with longer or shorter PFS (Björk et al. 2024). In patients with PFS > 12 months producers of Short Chain Fatty Acids (SCFA) remained highly abundant and increased as expected but surprisingly some taxa associated with increased inflammation such as *Prevotella merdae* were also increased. Patients who had an SGB profile similar to that found in Inflammatory Bowel Disease (IBD) had a higher likelihood of developing colitis if treated with combined ICI rather than single agent Pembrolizumab.

In APC 125 *Clostridia* and *Bacteroidia* become more abundant on treatment whereas the relative abundance of *Bacilli* declined slightly. An increase in *Clostridia* and *Bacteroides* in serial faecal samples was reported in 29 NSCLC patients who experienced secondary ICI resistance and irAE (Zeng et al. 2023). *Bacilli* such as *Lachnoclostridium* are associated with favourable ICI response (Yousefi et al. 2024).

5.6 FACT-ICM Quality of Life Score

We did not observe any significant changes in FACT-ICM between pre-treatment visit and repeat administration at 3 months (visit 3). This is likely due to the fact that patients who

experienced disease progression and toxicity not to mention died or came off treatment either declined to or could not complete the QoL survey at 3 months.

5.7 CANTAB Psychomotor Testing

Generally, the data appears underpowered with an N of eight persons with repeat visits. 2-4 persons would make the results more robust and certainly point toward improvement in some cognitive domains. However, it is interesting that there is a trend towards improvement in several domains including the Motor Screening Task and Paired Visual Learning. It may be that patients who were benefitting from treatment had a decreased burden of disease and felt well enough to undertake the second CANTAB assessment. Patients found completing the CANTAB assessment fatiguing and several declined to repeat it at Visit 3. This investigator found the CANTAB tasks fatiguing as did study nurses (who performed better!). Patients did not enjoy participating in the testing even when coached remotely by a psychologist on another tablet device. Study personell found that the time spent coaching patients to fulfil the task in person was onerous and detracted from other duties. Many patients declined to repeat the test at 3 months. It is possible that a better measure of fatigue would have been an alternate rapid mobile phone-based set of tasks with more frequent sampling. This approach has been pioneered in Alzheimer's Dementia (Hassenstab et al. 2020). More recently similar approaches using a 15 minute mobile phone based test called BrainCheck have been used to assess cognitive function in patients with haematological malignancies (Franco-Rocha et al. 2023).

5.8 Future Research Directions

Future work will examine reanalysing frozen faecal microbiome aliquots from this study in conjunction with another ongoing UCC project in a similar population. This will focus on exploring if there are consistent changes in faecal microbiome composition NSCLC patients in patients who respond to ICI compared to non-responders. Pre-treatment use of antibiotics and steroids will be analysed. It would be interesting to validate circulating baseline VEGF R2 as a marker of adverse outcomes in a larger homogenous population and ideally to perform a biomarker directed clinical trial of adding anti-angiogenic agents to ICI therapies.

5.9 Additional Research on Stored Samples and Existing Data

The following are suggestions for additional research using stored samples and existing data:

- To explore flow cytometry of stored Peripheral Blood Mononuclear Cells especially T helper and T suppressor cells and changes from baseline during treatment as well as correlation with clinical outcomes
- It may be possible to carry out single cell sequencing of DNA and RNA from these stored PMBC.
- To explore novel markers of the Tumour Microenvironment in stored biopsy samples via IHC
- To carry out bioinformatic (PCA) analysis of serial changes between study visit samples in serum proteomic data especially the candidate biomarkers Platelet Derived Growth Factor Subunit Beta (PDGF BB) and Vascular Endothelial Growth Factor Receptor 2 (VEGF R2).
- To explore if NLR and other inflammatory markers correlate with FACT-ICM QoL scores and CANTAB test results
- To analyse the impact of pre-treatment steroid and antibiotic use on the faecal microbiome.

6 Conclusions and Limitations

6.1 Findings And Future Directions

This small study shows that it is possible to gather blood, stool and tissue samples from Irish patients undergoing standard of care ICI therapy. While baseline NLR may play a role in assigning patients receiving ICI to groups with a predicted poor outcome NLR alone is not sensitive enough to base treatment decisions on.

The changes in serum K/T ratio evident in this study cohort mirror those seen in larger studies, with a rise between Pre-treatment and subsequent on-treatment visits. We did not have sufficient patient numbers to demonstrate that an increase in tryptophan metabolites correlates with adverse outcomes. If drugs targeting IDO function or accelerating its degradation become available, then it may be important to monitor K/T ratio and tissue IDO expression (Tang et al. 2021).

Proteomic analysis identified candidate serum biomarkers (PDGF BB, VEGF-R2) of adverse prognosis which correlates with previously published larger patient data sets. It may be possible to use these biomarkers to inform future therapeutic interventions, especially co-targeting angiogenesis and the PD1/PDL1 pathway (Duran et al. 2021). This is an approach which has been successful in hepatocellular carcinoma but of mixed efficacy in lung cancer (Joerg et al. 2023; Padda and Reckamp 2021). High serum levels of TNF-related apoptosis-inducing ligand (TRAIL) and Inducible T cell co-stimulator ligand (ICOSLG) may be markers of favourable prognosis where patients can safely be treated with existing regimens.

Tapasin a gene involved in the MHC protein loading complex was downregulated in patients with a favourable response assessed by first CT scan and is emerging as a candidate biomarker. mRNA expression analysis in our study seems to point to the expression of ECM remodelling genes as a favourable biomarker and somewhat surprisingly immune activation as unfavourable.

This unexpected finding may be artefactual and disproven by future work. The different findings from our proteomic and mRNA targets may be explained in that the proteomic assay was targeted against proteins known to be relevant to immune oncology whereas the mRNA analysis was untargeted and aimed to discover novel differential gene expression between groups.

This study has led to a larger similar study in collaboration with Cancer Research within UCC focusing on the effects of the faecal microbiome on efficacy and side effects of ICI. It is planned to re-analyse frozen aliquots of microbial DNA from the APC125 study in UCC to expand numbers of NSCLC patients.

It may be more sensible to focus on a single malignancy treated with more homogenous therapies such as stage IV adenocarcinoma of lung in future Irish collaborative multicentre studies to maximize statistical power and to identify robust biomarkers. Future research should include novel techniques such as single cell RNA analysis and measurement of ctDNA which may be more powerful biomarkers than bulk mRNA expression (Pang et al. 2022; Bratman et al. 2020). Ideally clinical trials incorporating dynamic biomarkers to escalate and deescalate therapy or guide initial choice of single vs dual ICI treatment should open in Ireland. This is an exciting time for cancer patients as well scientists and clinicians seeking to optimize choice of existing and novel ICI. Ongoing collaboration between all three groups will enable us to choose treatments with a higher chance of response and less toxicity.

REFERENCES

Aarsland, Tore Ivar Malmei, Johanne Telnes Instanes, Maj-Britt Rocio Posserud, Arve Ulvik, Ute Kessler, and Jan Haavik. 2022. "Changes in Tryptophan-Kynurenine Metabolism in Patients with Depression Undergoing ECT-A Systematic Review." *Pharmaceuticals (Basel, Switzerland)* 15 (11): 1439. https://doi.org/10.3390/ph15111439.

Abdul-Rahman, Toufik, Shankhaneel Ghosh, Sarah M. Badar, et al. 2024. "The Paradoxical Role of Cytokines and Chemokines at the Tumor Microenvironment: A Comprehensive Review." *European Journal of Medical Research* 29 (1): 124. https://doi.org/10.1186/s40001-024-01711-z.

Abujrais, Sandy, Anne Simeit, Mara Link, et al. 2025. "Potential Region-Specific Neuroprotective Effects of Kynurenine Administration in Healthy Rodents Using High-Resolution Mass Spectrometry." *ACS Chemical Neuroscience* 16 (19): 3682–93. https://doi.org/10.1021/acschemneuro.4c00586.

Agrawal, Ayushi, Hasan Balcı, Kristina Hanspers, et al. 2024. "WikiPathways 2024: Next Generation Pathway Database." *Nucleic Acids Research* 52 (D1): D679–89. https://doi.org/10.1093/nar/gkad960.

Alshehri, Bader. 2024. "Cytochrome c and Cancer Cell Metabolism: A New Perspective." *Saudi Pharmaceutical Journal : SPJ* 32 (12): 102194. https://doi.org/10.1016/j.jsps.2024.102194.

Altman, Douglas G., Lisa M. McShane, Willi Sauerbrei, and Sheila E. Taube. 2012. "Reporting Recommendations for Tumor Marker Prognostic Studies (REMARK): Explanation and Elaboration." *BMC Medicine* 10 (May): 51. https://doi.org/10.1186/1741-7015-10-51.

Alvarez, Maite, Itziar Otano, Luna Minute, et al. 2019. "Impact of Prophylactic TNF Blockade in the Dual PD-1 and CTLA-4 Immunotherapy Efficacy and Toxicity." *Cell Stress* 3 (7): 236–39. https://doi.org/10.15698/cst2019.07.193.

Anders, Simon, Paul Theodor Pyl, and Wolfgang Huber. 2015. "HTSeq—a Python Framework to Work with High-Throughput Sequencing Data." *Bioinformatics* 31 (2): 166–69. https://doi.org/10.1093/bioinformatics/btu638.

Ando, Kiyohiro, Ryo Kurashina, Noriko Motoi, et al. 2023. "Positive Regulatory Loop of Platelet-Derived Growth Factor DD-Induced STAT3 Activation Is Associated with Poor Prognosis in Advanced Urothelial Carcinoma." *Biochemical and Biophysical Research Communications* 676 (October): 165–70. https://doi.org/10.1016/j.bbrc.2023.07.054.

Aokage, Keiju, Shohei Koyama, Shogo Kumagai, et al. 2024. "Efficacy, Safety, and Influence on Tumor Microenvironment of Neoadjuvant Pembrolizumab plus Ramucirumab for PD-L1 Positive NSCLC: A Phase 2 Trial (EAST ENERGY)." *Clinical Cancer Research*, ahead of print, October 25. https://doi.org/10.1158/1078-0432.CCR-24-1561.

Ashburner, Michael, Catherine A. Ball, Judith A. Blake, et al. 2000. "Gene Ontology: Tool for the Unification of Biology." *Nature Genetics* 25 (1): 25–29. https://doi.org/10.1038/75556.

Assarsson, Erika, Martin Lundberg, Göran Holmquist, et al. 2014. "Homogenous 96-Plex PEA Immunoassay Exhibiting High Sensitivity, Specificity, and Excellent Scalability." *PLOS ONE* 9 (4): e95192. https://doi.org/10.1371/journal.pone.0095192.

Ayers, Mark, Jared Lunceford, Michael Nebozhyn, et al. 2017. "IFN-γ–Related mRNA Profile Predicts Clinical Response to PD-1 Blockade." *The Journal of Clinical Investigation* 127 (8): 2930–40. https://doi.org/10.1172/JCI91190.

"Babraham Bioinformatics - FastQC A Quality Control Tool for High Throughput Sequence Data." 2025. https://www.bioinformatics.babraham.ac.uk/projects/fastqc/.

Badawy, Abdulla A. B., and Gilles Guillemin. 2019. "The Plasma [Kynurenine]/[Tryptophan] Ratio and Indoleamine 2,3-Dioxygenase: Time for Appraisal." *International Journal of Tryptophan Research: IJTR* 12: 1178646919868978. https://doi.org/10.1177/1178646919868978.

Bagchi, Sreya, Robert Yuan, and Edgar G. Engleman. 2021. "Immune Checkpoint Inhibitors for the Treatment of Cancer: Clinical Impact and Mechanisms of Response and Resistance." *Annual Review of Pathology* 16 (January): 223–49. https://doi.org/10.1146/annurev-pathol-042020-042741.

Bailly, Christian, Xavier Thuru, Laurence Goossens, and Jean-François Goossens. 2023. "Soluble TIM-3 as a Biomarker of Progression and Therapeutic Response in Cancers and Other of Human Diseases." *Biochemical Pharmacology* 209 (March): 115445. https://doi.org/10.1016/j.bcp.2023.115445.

Björk, Johannes R., Laura A. Bolte, Andrew Maltez Thomas, et al. 2024. "Longitudinal Gut Microbiome Changes in Immune Checkpoint Blockade-Treated Advanced Melanoma." *Nature Medicine* 30 (3): 785–96. https://doi.org/10.1038/s41591-024-02803-3.

Blackwell, Andrew D., Barbara J. Sahakian, Robyn Vesey, James M. Semple, Trevor W. Robbins, and John R. Hodges. 2003. "Detecting Dementia: Novel Neuropsychological Markers of Preclinical Alzheimer's Disease." *Dementia and Geriatric Cognitive Disorders* 17 (1–2): 42–48. https://doi.org/10.1159/000074081.

Boise, Lawrence H., Maribel González-García, Christina E. Postema, et al. 1993. "Bcl-x, a Bcl-2-Related Gene That Functions as a Dominant Regulator of Apoptotic Cell Death." *Cell* 74 (4): 597–608. https://doi.org/10.1016/0092-8674(93)90508-N.

Boneva, Stefaniya, Anja Schlecht, Daniel Böhringer, et al. 2020. "3' MACE RNA-Sequencing Allows for Transcriptome Profiling in Human Tissue Samples after Long-Term Storage." *Laboratory Investigation* 100 (10): 1345–55. https://doi.org/10.1038/s41374-020-0446-z.

Bonneville, Russell, Melanie A. Krook, Hui-Zi Chen, et al. 2020. "Detection of Microsatellite Instability Biomarkers via Next-Generation Sequencing." *Methods in Molecular Biology (Clifton, N.J.)* 2055: 119–32. https://doi.org/10.1007/978-1-4939-9773-2_5.

Boutsikou, Efimia, Kalliopi Domvri, Georgia Hardavella, Dora Tsiouda, Konstantinos Zarogoulidis, and Theodoros Kontakiotis. 2018. "Tumour Necrosis Factor, Interferon-Gamma and Interleukins as Predictive Markers of Antiprogrammed Cell-Death Protein-1 Treatment in Advanced Non-Small Cell Lung Cancer: A Pragmatic Approach in Clinical Practice." *Therapeutic Advances in Medical Oncology* 10: 1758835918768238. https://doi.org/10.1177/1758835918768238.

Bratman, Scott V., S. Y. Cindy Yang, Marco A. J. Iafolla, et al. 2020. "Personalized Circulating Tumor DNA Analysis as a Predictive Biomarker in Solid Tumor Patients Treated with Pembrolizumab." *Nature Cancer* 1 (9): 9. https://doi.org/10.1038/s43018-020-0096-5.

Braune, Jan, Laura Keller, Florian Schiller, et al. 2020. "Circulating Tumor DNA Allows Early Treatment Monitoring in BRAF- and NRAS-Mutant Malignant Melanoma." *JCO Precision Oncology* 4 (November): 20–31. https://doi.org/10.1200/PO.19.00174.

Brea-Iglesias, Jenifer, María Gallardo-Gómez, Ana Oitabén, et al. 2025. "Genomics Guiding Personalized First-Line Immunotherapy Response in Lung and Bladder Tumors." *Journal of Translational Medicine* 23 (1): 404. https://doi.org/10.1186/s12967-025-06323-7.

Bridge, Jennifer A., James C. Lee, Adil Daud, James W. Wells, and Jeffrey A. Bluestone. 2018. "Cytokines, Chemokines, and Other Biomarkers of Response for Checkpoint Inhibitor Therapy in Skin Cancer." *Frontiers in Medicine* 5 (December). https://doi.org/10.3389/fmed.2018.00351.

Brueckl, Natalie F., Ralph M. Wirtz, Fabian P. M. Reich, et al. 2021. "Predictive Value of mRNA Expression and Dynamic Changes from Immune Related Biomarkers in Liquid Biopsies before and after Start of Pembrolizumab in Stage IV Non-Small Cell Lung Cancer (NSCLC)." *Translational Lung Cancer Research* 10 (11). https://doi.org/10.21037/tlcr-21-587.

Buchbinder, Elizabeth I., and Anupam Desai. 2016. "CTLA-4 and PD-1 Pathways." *American Journal of Clinical Oncology* 39 (1): 98–106. https://doi.org/10.1097/COC.0000000000000239.

Capone, Mariaelena, Diana Giannarelli, Domenico Mallardo, et al. 2018. "Baseline Neutrophil-to-Lymphocyte Ratio (NLR) and Derived NLR Could Predict Overall Survival in Patients with Advanced Melanoma Treated with Nivolumab." *Journal for Immunotherapy of Cancer* 6 (July). https://doi.org/10.1186/s40425-018-0383-1.

Casadevall, David, Sergi Clavé, Álvaro Taus, et al. 2017. "Heterogeneity of Tumor and Immune Cell PD-L1 Expression and Lymphocyte Counts in Surgical NSCLC Samples." *Clinical Lung Cancer* 18 (6): 682-691.e5. https://doi.org/10.1016/j.cllc.2017.04.014.

Cascino, A., C. Cangiano, F. Ceci, et al. 1991. "Increased Plasma Free Tryptophan Levels in Human Cancer: A Tumor Related Effect?" *Anticancer Research* 11 (3): 1313–16.

Chalmers, Zachary R., Caitlin F. Connelly, David Fabrizio, et al. 2017. "Analysis of 100,000 Human Cancer Genomes Reveals the Landscape of Tumor Mutational Burden." *Genome Medicine* 9 (1): 34. https://doi.org/10.1186/s13073-017-0424-2.

Chao, A. 1987. "Estimating the Population Size for Capture-Recapture Data with Unequal Catchability." *Biometrics* 43 (4): 783–91.

Chaput, N., P. Lepage, C. Coutzac, et al. 2017. "Baseline Gut Microbiota Predicts Clinical Response and Colitis in Metastatic Melanoma Patients Treated with Ipilimumab." *Annals of Oncology: Official Journal of the European Society for Medical Oncology* 28 (6): 1368–79. https://doi.org/10.1093/annonc/mdx108.

Chatterjee, Samit, Wojciech G. Lesniak, Michelle S. Miller, et al. 2017. "Rapid PD-L1 Detection in Tumors with PET Using a Highly Specific Peptide." *Biochemical and Biophysical Research Communications* 483 (1): 258–63. https://doi.org/10.1016/j.bbrc.2016.12.156.

Chauvin, Joe-Marc, and Hassane M. Zarour. 2020. "TIGIT in Cancer Immunotherapy." Review. *Journal for ImmunoTherapy of Cancer* 8 (2): e000957. https://doi.org/10.1136/jitc-2020-000957.

Chen, Xiao-Jiang, Shu-Qiang Yuan, Jin-Ling Duan, et al. 2020. "The Value of PD-L1 Expression in Predicting the Efficacy of Anti-PD-1 or Anti-PD-L1 Therapy in Patients with Cancer: A Systematic Review and Meta-Analysis." *Disease Markers* 2020 (1): 6717912. https://doi.org/10.1155/2020/6717912.

Chen, Yiquan, and Gilles J. Guillemin. 2009. "Kynurenine Pathway Metabolites in Humans: Disease and Healthy States." *International Journal of Tryptophan Research : IJTR* 2 (January): 1–19. https://www.ncbi.nlm.nih.gov/pmc/articles/PMC3195227/.

Chhabra, Neeraj, and Joseph Kennedy. 2021. "A Review of Cancer Immunotherapy Toxicity: Immune Checkpoint Inhibitors." *Journal of Medical Toxicology* 17 (4): 411–24. https://doi.org/10.1007/s13181-021-00833-8.

Choi, Eunhee, Cunming Duan, and Xiao-chen Bai. 2025. "Regulation and Function of Insulin and Insulin-like Growth Factor Receptor Signalling." *Nature Reviews Molecular Cell Biology*, February 10, 1–23. https://doi.org/10.1038/s41580-025-00826-3.

Choueiri, Toni K., Mayer N. Fishman, Bernard Escudier, et al. 2016. "Immunomodulatory Activity of Nivolumab in Metastatic Renal Cell Carcinoma." *Clinical Cancer Research: An Official Journal of the American Association for Cancer Research* 22 (22): 5461–71. https://doi.org/10.1158/1078-0432.CCR-15-2839.

Clarke, Gerard, Peter Fitzgerald, John F. Cryan, Eugene M. Cassidy, Eamonn M. Quigley, and Timothy G. Dinan. 2009. "Tryptophan Degradation in Irritable Bowel Syndrome: Evidence of Indoleamine 2,3-Dioxygenase Activation in a Male Cohort." *BMC Gastroenterology* 9 (January): 6. https://doi.org/10.1186/1471-230X-9-6.

Clarke, Gerard, Paul J. Kennedy, John A. Groeger, et al. 2020. "Impaired Cognitive Function in Crohn's Disease: Relationship to Disease Activity." *Brain, Behavior, & Immunity - Health* 5 (May): 100093. https://doi.org/10.1016/j.bbih.2020.100093.

Cliff, Jacqueline M., Stefan H. E. Kaufmann, Helen McShane, Paul van Helden, and Anne O'Garra. 2015. "The Human Immune Response to Tuberculosis and Its Treatment: A View from the Blood." *Immunological Reviews* 264 (1): 88–102. https://doi.org/10.1111/imr.12269.

Cortes, Javier, David W. Cescon, Hope S. Rugo, et al. 2020. "Pembrolizumab plus Chemotherapy versus Placebo plus Chemotherapy for Previously Untreated Locally Recurrent Inoperable or

Metastatic Triple-Negative Breast Cancer (KEYNOTE-355): A Randomised, Placebo-Controlled, Double-Blind, Phase 3 Clinical Trial." *The Lancet* 396 (10265): 1817–28. https://doi.org/10.1016/S0140-6736(20)32531-9.

Cossarizza, Andrea, Hyun-Dong Chang, Andreas Radbruch, et al. 2019. "Guidelines for the Use of Flow Cytometry and Cell Sorting in Immunological Studies (Second Edition)." *European Journal of Immunology* 49 (10): 1457–973. https://doi.org/10.1002/eji.201970107.

Costantini, Adrien, Catherine Julie, Coraline Dumenil, et al. 2018. "Predictive Role of Plasmatic Biomarkers in Advanced Non-Small Cell Lung Cancer Treated by Nivolumab." *Oncoimmunology* 7 (8): e1452581. https://doi.org/10.1080/2162402X.2018.1452581.

Coull, J. T., C. D. Frith, R. S. J. Frackowiak, and P. M. Grasby. 1996. "A Fronto-Parietal Network for Rapid Visual Information Processing: A PET Study of Sustained Attention and Working Memory." *Neuropsychologia* 34 (11): 1085–95. https://doi.org/10.1016/0028-3932(96)00029-2.

Cresswell, George D., Daniel Nichol, Inmaculada Spiteri, et al. 2020. "Mapping the Breast Cancer Metastatic Cascade onto ctDNA Using Genetic and Epigenetic Clonal Tracking." *Nature Communications* 11 (1): 1. https://doi.org/10.1038/s41467-020-15047-9.

Criscitiello, Carmen, Antonio Marra, Stefania Morganti, et al. 2020. "Pre-Treatment Blood Parameters Predict Efficacy from Immunotherapy Agents in Early Phase Clinical Trials." *The Oncologist* n/a (n/a). https://doi.org/10.1634/theoncologist.2020-0518.

Cristescu, Razvan, Michael Nebozhyn, Chunsheng Zhang, et al. 2022. "Transcriptomic Determinants of Response to Pembrolizumab Monotherapy across Solid Tumor Types." *Clinical Cancer Research* 28 (8): 1680–89. https://doi.org/10.1158/1078-0432.CCR-21-3329.

Cristiano, Stephen, Alessandro Leal, Jillian Phallen, et al. 2019. "Genome-Wide Cell-Free DNA Fragmentation in Patients with Cancer." *Nature* 570 (7761): 385–89. https://doi.org/10.1038/s41586-019-1272-6.

Dai, Liyuan, Qiaoyun Tan, Lin Li, et al. 2024. "High-Throughput Antigen Microarray Identifies Longitudinal Prognostic Autoantibody for Chemoimmunotherapy in Advanced Non-Small Cell Lung Cancer." *Molecular & Cellular Proteomics* 23 (5). https://doi.org/10.1016/j.mcpro.2024.100749.

Darley, Rachel, Patricia T. Illing, Patrick Duriez, et al. 2025. "Evidence of Focusing the MHC Class I Immunopeptidome by Tapasin." *Frontiers in Immunology* 16 (April). https://doi.org/10.3389/fimmu.2025.1563789.

Davar, Diwakar, Ana Carrizosa Anderson, and Ivan Diaz-Padilla. 2025. "Therapeutic Potential of Targeting LAG-3 in Cancer." *Journal for Immunotherapy of Cancer* 13 (7): e011652. https://doi.org/10.1136/jitc-2025-011652.

Denz, H., B. Orth, G. Weiss, et al. 1993. "Weight Loss in Patients with Hematological Neoplasias Is Associated with Immune System Stimulation." *The Clinical Investigator* 71 (1): 37–41. https://doi.org/10.1007/BF00210961.

"DISGENET: Genomics Platform for Precision Medicine." 2025. https://www.disgenet.com.

Duchemann, Boris, Jordi Remon, Marie Naigeon, et al. 2020. "Integrating Circulating Biomarkers in the Immune Checkpoint Inhibitor Treatment in Lung Cancer." *Cancers* 12 (12): 3625. https://doi.org/10.3390/cancers12123625.

Duran, Camille L., Lucia Borriello, George S. Karagiannis, David Entenberg, Maja H. Oktay, and John S. Condeelis. 2021. "Targeting Tie2 in the Tumor Microenvironment: From Angiogenesis to Dissemination." *Cancers* 13 (22): 5730. https://doi.org/10.3390/cancers13225730.

Echle, Amelie, Niklas Timon Rindtorff, Titus Josef Brinker, Tom Luedde, Alexander Thomas Pearson, and Jakob Nikolas Kather. 2021. "Deep Learning in Cancer Pathology: A New Generation of Clinical Biomarkers." *British Journal of Cancer* 124 (4): 4. https://doi.org/10.1038/s41416-020-01122-x.

Elliott, R., and R. J. Dolan. 1999. "Differential Neural Responses during Performance of Matching and Nonmatching to Sample Tasks at Two Delay Intervals." *The Journal of Neuroscience: The Official Journal of the Society for Neuroscience* 19 (12): 5066–73. https://doi.org/10.1523/JNEUROSCI.19-12-05066.1999.

Evelo, Chris, WikiPathways Maintenance Bot, Michiel Adriaens, et al. 2025. *Fatty Acid Omega-Oxidation*. March 4. https://www.wikipathways.org/instance/WP206.
Ewels, Philip, Måns Magnusson, Sverker Lundin, and Max Käller. 2016. "MultiQC: Summarize Analysis Results for Multiple Tools and Samples in a Single Report." *Bioinformatics* 32 (19): 3047–48. https://doi.org/10.1093/bioinformatics/btw354.
Fejza, Albina, Greta Carobolante, Evelina Poletto, et al. 2023. "The Entanglement of Extracellular Matrix Molecules and Immune Checkpoint Inhibitors in Cancer: A Systematic Review of the Literature." *Frontiers in Immunology* 14 (October): 1270981. https://doi.org/10.3389/fimmu.2023.1270981.
Franco-Rocha, Oscar Y., Misty L. Mahaffey, William Matsui, and Shelli R. Kesler. 2023. "Remote Assessment of Cognitive Dysfunction in Hematologic Malignancies Using Web-Based Neuropsychological Testing." *Cancer Medicine* 12 (5): 6068–76. https://doi.org/10.1002/cam4.5331.
Fray, P. J., and T. W. Robbins. 1996. "CANTAB Battery: Proposed Utility in Neurotoxicology." *Neurotoxicology and Teratology*, Symposium on Computerized Behavioral Testing of Humans in Neurotoxicology Research, vol. 18 (4): 499–504. https://doi.org/10.1016/0892-0362(96)00027-X.
Fu, Xiaobin, Tingting Li, Yaqing Dai, and Jiancheng Li. 2019. "Preoperative Systemic Inflammation Score (SIS) Is Superior to Neutrophil to Lymphocyte Ratio (NLR) as a Predicting Indicator in Patients with Esophageal Squamous Cell Carcinoma." *BMC Cancer* 19 (1): 721. https://doi.org/10.1186/s12885-019-5940-6.
Gadgeel, Shirish, Delvys Rodríguez-Abreu, Giovanna Speranza, et al. 2020. "Updated Analysis From KEYNOTE-189: Pembrolizumab or Placebo Plus Pemetrexed and Platinum for Previously Untreated Metastatic Nonsquamous Non–Small-Cell Lung Cancer." *Journal of Clinical Oncology*, ahead of print, March 9. World. https://doi.org/10.1200/JCO.19.03136.
Gandhi, Leena, Delvys Rodríguez-Abreu, Shirish Gadgeel, et al. 2018. "Pembrolizumab plus Chemotherapy in Metastatic Non–Small-Cell Lung Cancer." *New England Journal of Medicine* 378 (22): 2078–92. https://doi.org/10.1056/NEJMoa1801005.
Ganesan, Shridar, and Janice Mehnert. 2020. "Biomarkers for Response to Immune Checkpoint Blockade." *Annual Review of Cancer Biology* 4 (1): 331–51. https://doi.org/10.1146/annurev-cancerbio-030419-033604.
Gao, Yanmei, Chunhe Yang, Ning He, Guodong Zhao, Jianfei Wang, and Yadong Yang. 2020. "Integration of the Tumor Mutational Burden and Tumor Heterogeneity Identify an Immunological Subtype of Melanoma With Favorable Survival." *Frontiers in Oncology* 10 (October). https://doi.org/10.3389/fonc.2020.571545.
Garon, Edward B., Naiyer A. Rizvi, Rina Hui, et al. 2015. "Pembrolizumab for the Treatment of Non–Small-Cell Lung Cancer." *New England Journal of Medicine* 372 (21): 2018–28. https://doi.org/10.1056/NEJMoa1501824.
Gene Ontology Resource. 2025. "Gene Ontology Resource." http://geneontology.org/.
Goodman, Aaron M., Andrea Castro, Rachel Marty Pyke, et al. 2020. "MHC-I Genotype and Tumor Mutational Burden Predict Response to Immunotherapy." *Genome Medicine* 12 (1): 45. https://doi.org/10.1186/s13073-020-00743-4.
"GSEA User Guide." 2025. https://www.gsea-msigdb.org/gsea/doc/GSEAUserGuideFrame.html.
Haddad, Robert I., Tanguy Y. Seiwert, Laura Q. M. Chow, et al. 2022. "Influence of Tumor Mutational Burden, Inflammatory Gene Expression Profile, and PD-L1 Expression on Response to Pembrolizumab in Head and Neck Squamous Cell Carcinoma." *Journal for Immunotherapy of Cancer* 10 (2): e003026. https://doi.org/10.1136/jitc-2021-003026.
Hansen, Aaron R., Kari Ala-Leppilampi, Chris McKillop, et al. 2020. "Development of the Functional Assessment of Cancer Therapy-Immune Checkpoint Modulator (FACT-ICM): A Toxicity Subscale to Measure Quality of Life in Patients with Cancer Who Are Treated with ICMs." *Cancer* 126 (7): 1550–58. https://doi.org/10.1002/cncr.32692.

Hansen, Kasper D., Steven E. Brenner, and Sandrine Dudoit. 2010. "Biases in Illumina Transcriptome Sequencing Caused by Random Hexamer Priming." *Nucleic Acids Research* 38 (12): e131. https://doi.org/10.1093/nar/gkq224.

Hanspers, Kristina, Friederike Ehrhart, WikiPathways Maintenance Bot, et al. 2025. *miRNA Targets in ECM and Membrane Receptors*. March 8. https://www.wikipathways.org/instance/WP2911.

Haslam, Alyson, Jennifer Gill, and Vinay Prasad. 2020. "Estimation of the Percentage of US Patients With Cancer Who Are Eligible for Immune Checkpoint Inhibitor Drugs." *JAMA Network Open* 3 (3): e200423. https://doi.org/10.1001/jamanetworkopen.2020.0423.

Hassenstab, Jason, Andrew J. Aschenbrenner, David A. Balota, et al. 2020. "Remote Cognitive Assessment Approaches in the Dominantly Inherited Alzheimer Network (DIAN)." *Alzheimer's & Dementia* 16 (S6): e038144. https://doi.org/10.1002/alz.038144.

Hellmann, Matthew D., Tudor-Eliade Ciuleanu, Adam Pluzanski, et al. 2018. "Nivolumab plus Ipilimumab in Lung Cancer with a High Tumor Mutational Burden." *New England Journal of Medicine* 378 (22): 2093–104. https://doi.org/10.1056/NEJMoa1801946.

Holthuijsen, Daniëlle D. B., Eline H. van Roekel, Martijn J. L. Bours, Per M. Ueland, Stéphanie O. Breukink, Maryska L. G. Janssen-Heijnen, Eric T. P. Keulen, Biljana Gigic, et al. 2024. "Longitudinal Associations of Plasma Kynurenines and Ratios with Anxiety and Depression Scores in Colorectal Cancer Survivors up to 12 Months Post-Treatment." *Psychoneuroendocrinology* 163 (May): 106981. https://doi.org/10.1016/j.psyneuen.2024.106981.

Holthuijsen, Daniëlle D. B., Eline H. van Roekel, Martijn J. L. Bours, Per M. Ueland, Stéphanie O. Breukink, Maryska L. G. Janssen-Heijnen, Eric T. P. Keulen, Stefanie Brezina, et al. 2024. "Longitudinal Associations of Plasma Kynurenines and Ratios with Fatigue and Quality of Life in Colorectal Cancer Survivors up to 12 Months Post-Treatment." *International Journal of Cancer* 155 (7): 1172–90. https://doi.org/10.1002/ijc.34992.

Horn, Leora, Aaron S. Mansfield, Aleksandra Szczęsna, et al. 2018. "First-Line Atezolizumab plus Chemotherapy in Extensive-Stage Small-Cell Lung Cancer." *The New England Journal of Medicine* 379 (23): 2220–29. https://doi.org/10.1056/NEJMoa1809064.

Hu, Haoyue, Yue Chen, Songtao Tan, et al. 2022. "The Research Progress of Antiangiogenic Therapy, Immune Therapy and Tumor Microenvironment." *Frontiers in Immunology* 13 (February). https://doi.org/10.3389/fimmu.2022.802846.

Huang, Su-Ning, Guo-Sheng Li, Xian-Guo Zhou, et al. 2020. "Identification of an Immune Score-Based Gene Panel with Prognostic Power for Oral Squamous Cell Carcinoma." *Medical Science Monitor : International Medical Journal of Experimental and Clinical Research* 26 (June): e922854-1-e922854-14. https://doi.org/10.12659/MSM.922854.

Hurkmans, Daan P., Christina Jensen, Stijn L. W. Koolen, et al. 2020. "Blood-Based Extracellular Matrix Biomarkers Are Correlated with Clinical Outcome after PD-1 Inhibition in Patients with Metastatic Melanoma." *Journal for Immunotherapy of Cancer* 8 (2): e001193. https://doi.org/10.1136/jitc-2020-001193.

Hwang, Michael, Jenna Vanliere Canzoniero, Samuel Rosner, et al. 2022. "Peripheral Blood Immune Cell Dynamics Reflect Antitumor Immune Responses and Predict Clinical Response to Immunotherapy." *Journal for ImmunoTherapy of Cancer* 10 (6): e004688. https://doi.org/10.1136/jitc-2022-004688.

Jardim, Denis L., Aaron Goodman, Debora de Melo Gagliato, and Razelle Kurzrock. 2021. "The Challenges of Tumor Mutational Burden as an Immunotherapy Biomarker." *Cancer Cell* 39 (2): 154–73. https://doi.org/10.1016/j.ccell.2020.10.001.

Jenkins, Liam, Ute Jungwirth, Alexandra Avgustinova, et al. 2022. "Cancer-Associated Fibroblasts Suppress CD8+ T-Cell Infiltration and Confer Resistance to Immune-Checkpoint Blockade." *Cancer Research* 82 (16): 2904–17. https://doi.org/10.1158/0008-5472.CAN-21-4141.

Jensen, Christina, Daniel Hargbøl Madsen, Morten Hansen, et al. 2018. "Non-Invasive Biomarkers Derived from the Extracellular Matrix Associate with Response to Immune Checkpoint Blockade (Anti-CTLA-4) in Metastatic Melanoma Patients." *Journal for Immunotherapy of Cancer* 6 (December): 152. https://doi.org/10.1186/s40425-018-0474-z.

Ji, Shoujian, Huan Chen, Keyan Yang, et al. 2020. "Peripheral Cytokine Levels as Predictive Biomarkers of Benefit from Immune Checkpoint Inhibitors in Cancer Therapy." *Biomedicine & Pharmacotherapy = Biomedecine & Pharmacotherapie* 129 (September): 110457. https://doi.org/10.1016/j.biopha.2020.110457.

Jiang, Yi-Quan, Zi-Xian Wang, Ming Zhong, et al. 2021. "Investigating Mechanisms of Response or Resistance to Immune Checkpoint Inhibitors by Analyzing Cell-Cell Communications in Tumors Before and After Programmed Cell Death-1 (PD-1) Targeted Therapy: An Integrative Analysis Using Single-Cell RNA and Bulk-RNA Sequencing Data." *Oncoimmunology* 10 (1): 1908010. https://doi.org/10.1080/2162402X.2021.1908010.

Jin, Yueping, Hui Dong, Liliang Xia, et al. 2019. "The Diversity of Gut Microbiome Is Associated With Favorable Responses to Anti-Programmed Death 1 Immunotherapy in Chinese Patients With NSCLC." *Journal of Thoracic Oncology: Official Publication of the International Association for the Study of Lung Cancer* 14 (8): 1378–89. https://doi.org/10.1016/j.jtho.2019.04.007.

Jo, Yunju, Hyung-seung Jin, and Yoon Park. 2024. "No More LAGging behind PD-1: Uncovering the Unique Role of LAG-3 in T-Cell Exhaustion." *Cellular & Molecular Immunology* 21 (12): 1351–53. https://doi.org/10.1038/s41423-024-01227-w.

Joerg, Vincent, Bernhard Scheiner, Antonio D´Alessio, et al. 2023. "Efficacy and Safety of Atezolizumab/Bevacizumab in Patients with HCC after Prior Systemic Therapy: A Global, Observational Study." *Hepatology Communications* 7 (11): e0302. https://doi.org/10.1097/HC9.0000000000000302.

Jørgensen, Jan Trøst. 2020. "PD-L1 Expression and Efficacy of Pembrolizumab as Monotherapy in NSCLC." *Chinese Clinical Oncology* 9 (4): 4. https://doi.org/10.21037/cco.2020.01.03.

Joseph, Richard W., Jeroen Elassaiss-Schaap, Richard Kefford, et al. 2018. "Baseline Tumor Size Is an Independent Prognostic Factor for Overall Survival in Patients With Melanoma Treated With Pembrolizumab." *Clinical Cancer Research : An Official Journal of the American Association for Cancer Research* 24 (20): 4960–67. https://doi.org/10.1158/1078-0432.CCR-17-2386.

Kallergi, G., S. Agelaki, V. Gannoukaraki, et al. 2009. "VEGF, VEGFR2 and HIF-1α Expression in Circulating Tumor Cells (CTCs) of Breast Cancer Patients." *Cancer Research* 69 (2_Supplement): 1028. https://doi.org/10.1158/0008-5472.SABCS-1028.

Kaltenmeier, Christof, Richard L. Simmons, Samer Tohme, and Hamza O. Yazdani. 2021. "Neutrophil Extracellular Traps (NETs) in Cancer Metastasis." *Cancers* 13 (23): 6131. https://doi.org/10.3390/cancers13236131.

Kennedy, Paul J., Andrew P. Allen, Ann O'Neill, et al. 2015. "Acute Tryptophan Depletion Reduces Kynurenine Levels: Implications for Treatment of Impaired Visuospatial Memory Performance in Irritable Bowel Syndrome." *Psychopharmacology* 232 (8): 1357–71. https://doi.org/10.1007/s00213-014-3767-z.

Kim, Bo-Ra, Jiwon Shin, Robin Guevarra, et al. 2017. "Deciphering Diversity Indices for a Better Understanding of Microbial Communities." *Journal of Microbiology and Biotechnology* 27 (12): 2089–93. https://doi.org/10.4014/jmb.1709.09027.

Klindworth, Anna, Elmar Pruesse, Timmy Schweer, et al. 2013. "Evaluation of General 16S Ribosomal RNA Gene PCR Primers for Classical and Next-Generation Sequencing-Based Diversity Studies." *Nucleic Acids Research* 41 (1): e1. https://doi.org/10.1093/nar/gks808.

Kojima, Takashi, Manish A. Shah, Kei Muro, et al. 2020. "Randomized Phase III KEYNOTE-181 Study of Pembrolizumab Versus Chemotherapy in Advanced Esophageal Cancer." *Journal of Clinical Oncology*, October 7, JCO.20.01888. https://doi.org/10.1200/JCO.20.01888.

Langmead, Ben, and Steven L. Salzberg. 2012. "Fast Gapped-Read Alignment with Bowtie 2." *Nature Methods* 9 (4): 357–59. https://doi.org/10.1038/nmeth.1923.

Lanser, Lukas, Patricia Kink, Eva Maria Egger, et al. 2020. "Inflammation-Induced Tryptophan Breakdown Is Related With Anemia, Fatigue, and Depression in Cancer." *Frontiers in Immunology* 11: 249. https://doi.org/10.3389/fimmu.2020.00249.

Le, Dung T., Jennifer N. Uram, Hao Wang, et al. 2015. "PD-1 Blockade in Tumors with Mismatch-Repair Deficiency." *New England Journal of Medicine* 372 (26): 2509–20. https://doi.org/10.1056/NEJMoa1500596.

Li, Haoxin, Kevin Bullock, Carino Gurjao, et al. 2019a. "Metabolomic Adaptations and Correlates of Survival to Immune Checkpoint Blockade." *Nature Communications* 10 (1): 4346. https://doi.org/10.1038/s41467-019-12361-9.

Li, Haoxin, Kevin Bullock, Carino Gurjao, et al. 2019b. "Metabolomic Adaptations and Correlates of Survival to Immune Checkpoint Blockade." *Nature Communications* 10 (September). https://doi.org/10.1038/s41467-019-12361-9.

Li, Hongjin, Mark B. Lockwood, Judith M. Schlaeger, Tingting Liu, Oana C. Danciu, and Ardith Z. Doorenbos. 2023. "Tryptophan and Kynurenine Pathway Metabolites and Psychoneurological Symptoms Among Breast Cancer Survivors." *Pain Management Nursing : Official Journal of the American Society of Pain Management Nurses* 24 (1): 52–59. https://doi.org/10.1016/j.pmn.2022.09.002.

Li, Tianye, Mengke Niu, Jianwei Zhou, Kongming Wu, and Ming Yi. 2024. "The Enhanced Antitumor Activity of Bispecific Antibody Targeting PD-1/PD-L1 Signaling." *Cell Communication and Signaling* 22 (1): 179. https://doi.org/10.1186/s12964-024-01562-5.

Li, Yaqing, Jianping Xu, Lijuan Zhang, and Zhigang Cai. 2025. "The Association of Immune-Inflammation Indices at Multiple Time Points with Treatment Response and Survival in Advanced Non-Small Cell Lung Cancer Patients Receiving Immune Checkpoint Inhibitors." *World Journal of Surgical Oncology* 23 (1): 195. https://doi.org/10.1186/s12957-025-03833-y.

Lim, Su Yin, Ines Pires da Silva, Nurudeen A. Adegoke, et al. 2024. "Size Matters: Integrating Tumour Volume and Immune Activation Signatures Predicts Immunotherapy Response." *Molecular Cancer* 23 (October): 228. https://doi.org/10.1186/s12943-024-02146-0.

Lipson, Evan J., F. Stephen Hodi, Hussein Tawbi, et al. 2025. "Nivolumab plus Relatlimab in Advanced Melanoma: RELATIVITY-047 4-Year Update." *European Journal of Cancer* 225 (July). https://doi.org/10.1016/j.ejca.2025.115547.

Litchfield, Kevin, James L. Reading, Clare Puttick, et al. 2021. "Meta-Analysis of Tumor- and T Cell-Intrinsic Mechanisms of Sensitization to Checkpoint Inhibition." *Cell* 184 (3): 596-614.e14. https://doi.org/10.1016/j.cell.2021.01.002.

Liu, Chengfei, and Allen C. Gao. 2019. "IFNγ, a Double-Edged Sword in Cancer Immunity and Metastasis." *Cancer Research* 79 (6): 1032–33. https://doi.org/10.1158/0008-5472.CAN-19-0083.

Liu, Jingjing, Shuang Li, Shuang Zhang, et al. 2019. "Systemic Immune-inflammation Index, Neutrophil-to-lymphocyte Ratio, Platelet-to-lymphocyte Ratio Can Predict Clinical Outcomes in Patients with Metastatic Non-small-cell Lung Cancer Treated with Nivolumab." *Journal of Clinical Laboratory Analysis* 33 (8). https://doi.org/10.1002/jcla.22964.

Lo, Y. M. Dennis, Diana S. C. Han, Peiyong Jiang, and Rossa W. K. Chiu. 2021. "Epigenetics, Fragmentomics, and Topology of Cell-Free DNA in Liquid Biopsies." *Science* 372 (6538): eaaw3616. https://doi.org/10.1126/science.aaw3616.

Long, Georgina V., Reinhard Dummer, Omid Hamid, et al. 2019. "Epacadostat plus Pembrolizumab versus Placebo plus Pembrolizumab in Patients with Unresectable or Metastatic Melanoma (ECHO-301/KEYNOTE-252): A Phase 3, Randomised, Double-Blind Study." *The Lancet Oncology* 20 (8): 1083–97. https://doi.org/10.1016/S1470-2045(19)30274-8.

Love, Michael I., Wolfgang Huber, and Simon Anders. 2014. "Moderated Estimation of Fold Change and Dispersion for RNA-Seq Data with DESeq2." *Genome Biology* 15 (12): 550. https://doi.org/10.1186/s13059-014-0550-8.

Lozupone, Catherine, and Rob Knight. 2005. "UniFrac: A New Phylogenetic Method for Comparing Microbial Communities." *Applied and Environmental Microbiology* 71 (12): 8228–35. https://doi.org/10.1128/AEM.71.12.8228-8235.2005.

Lutz, Kevin C., Shuang Jiang, Michael L. Neugent, Nicole J. De Nisco, Xiaowei Zhan, and Qiwei Li. 2022. "A Survey of Statistical Methods for Microbiome Data Analysis." *Frontiers in Applied Mathematics and Statistics* 8 (June). https://doi.org/10.3389/fams.2022.884810.

Ma, Weijie, Sixi Wei, Siqi Long, et al. 2023. "Dynamic Evaluation of Blood Immune Cells Predictive of Response to Immune Checkpoint Inhibitors in NSCLC by Multicolor Spectrum Flow Cytometry." *Frontiers in Immunology* 14: 1206631. https://doi.org/10.3389/fimmu.2023.1206631.

MacCarthy-Morrogh, Lucy, and Paul Martin. 2020. "The Hallmarks of Cancer Are Also the Hallmarks of Wound Healing." *Science Signaling* 13 (648): eaay8690. https://doi.org/10.1126/scisignal.aay8690.

Mai, Zizhao, Yunfan Lin, Pei Lin, Xinyuan Zhao, and Li Cui. 2024. "Modulating Extracellular Matrix Stiffness: A Strategic Approach to Boost Cancer Immunotherapy." *Cell Death & Disease* 15 (5): 1–16. https://doi.org/10.1038/s41419-024-06697-4.

Marabelle, Aurélien, Marwan Fakih, Juanita Lopez, et al. 2020. "Association of Tumour Mutational Burden with Outcomes in Patients with Advanced Solid Tumours Treated with Pembrolizumab: Prospective Biomarker Analysis of the Multicohort, Open-Label, Phase 2 KEYNOTE-158 Study." *The Lancet Oncology* 21 (10): 1353–65. https://doi.org/10.1016/S1470-2045(20)30445-9.

Martin, Marcel. 2011. "Cutadapt Removes Adapter Sequences from High-Throughput Sequencing Reads." *EMBnet.Journal* 17 (1): 1. https://doi.org/10.14806/ej.17.1.200.

Mc Neil, Valencia, and Seung Won Lee. 2025. "Advancing Cancer Treatment: A Review of Immune Checkpoint Inhibitors and Combination Strategies." *Cancers* 17 (9): 9. https://doi.org/10.3390/cancers17091408.

Meng, Xiangjiao, Zhaoqin Huang, Feifei Teng, Ligang Xing, and Jinming Yu. 2015. "Predictive Biomarkers in PD-1/PD-L1 Checkpoint Blockade Immunotherapy." *Cancer Treatment Reviews* 41 (10): 868–76. https://doi.org/10.1016/j.ctrv.2015.11.001.

Metri, Najwa-Joelle, Ali S. Butt, Ava Murali, Genevieve Z. Steiner-Lim, and Chai K. Lim. 2023. "Normative Data on Serum and Plasma Tryptophan and Kynurenine Concentrations from 8089 Individuals Across 120 Studies: A Systematic Review and Meta-Analysis." *International Journal of Tryptophan Research: IJTR* 16: 11786469231211184. https://doi.org/10.1177/11786469231211184.

Milacic, Marija, Deidre Beavers, Patrick Conley, et al. 2024. "The Reactome Pathway Knowledgebase 2024." *Nucleic Acids Research* 52 (D1): D672–78. https://doi.org/10.1093/nar/gkad1025.

Mildner, Finn, Sieghart Sopper, Arno Amann, et al. 2020. "Systematic Review: Soluble Immunological Biomarkers in Advanced Non-Small-Cell Lung Cancer (NSCLC)." *Critical Reviews in Oncology/Hematology* 153 (September): 102948. https://doi.org/10.1016/j.critrevonc.2020.102948.

Modi, Siddharth J., and Vithal M. Kulkarni. 2019. "Vascular Endothelial Growth Factor Receptor (VEGFR-2)/KDR Inhibitors: Medicinal Chemistry Perspective." *Medicine in Drug Discovery* 2 (June): 100009. https://doi.org/10.1016/j.medidd.2019.100009.

Mok, Tony S. K., Yi-Long Wu, Iveta Kudaba, et al. 2019. "Pembrolizumab versus Chemotherapy for Previously Untreated, PD-L1-Expressing, Locally Advanced or Metastatic Non-Small-Cell Lung Cancer (KEYNOTE-042): A Randomised, Open-Label, Controlled, Phase 3 Trial." *The Lancet* 393 (10183): 1819–30. https://doi.org/10.1016/S0140-6736(18)32409-7.

Moniwa, Keigo, Serina Tokita, Toshiyuki Sumi, et al. 2025. "Loss of Tapasin in Tumors Potentiates T-Cell Recognition and Anti-Tumor Effects of Immune Checkpoint Blockade." *Cancer Science* n/a (n/a). https://doi.org/10.1111/cas.70027.

Morita, Mitsunori, Motohiro Tamiya, Daichi Fujimoto, et al. 2020. "Prediction of Patients with a Tumor Proportion Score > 50% Who Do Not Respond to First-Line Monotherapy with Pembrolizumab." *BMC Cancer* 20 (1): 93. https://doi.org/10.1186/s12885-020-6582-4.

Motzer, Robert J., Bernard Escudier, David F. McDermott, et al. 2015. "Nivolumab versus Everolimus in Advanced Renal-Cell Carcinoma." *New England Journal of Medicine* 373 (19): 1803–13. https://doi.org/10.1056/NEJMoa1510665.
"MTCO2P12 MT-CO2 Pseudogene 12 [Homo Sapiens (Human)] - Gene - NCBI." 2025. https://www.ncbi.nlm.nih.gov/gene?Db=gene&Cmd=DetailsSearch&Term=107075310.
Munari, Enrico, Giuseppe Zamboni, Gianluigi Lunardi, et al. 2018. "PD-L1 Expression Heterogeneity in Non–Small Cell Lung Cancer: Defining Criteria for Harmonization between Biopsy Specimens and Whole Sections." *Journal of Thoracic Oncology* 13 (8): 1113–20. https://doi.org/10.1016/j.jtho.2018.04.017.
Nejman, Deborah, Ilana Livyatan, Garold Fuks, et al. 2020. "The Human Tumor Microbiome Is Composed of Tumor Type-Specific Intracellular Bacteria." *Science (New York, N.Y.)* 368 (6494): 973–80. https://doi.org/10.1126/science.aay9189.
Newman, Dane M., Courtney L. Andersen, Leonie A. Cluse, et al. 2026. "Dual Bcl-2/Bcl-Xl Inhibition via AZD0466 Combines with Immune Checkpoint Blockade to Enhance Anti-Tumour Activity." *Cell Death & Disease* 17 (1): 177. https://doi.org/10.1038/s41419-025-08354-w.
Ng, Kevin W., Jan Attig, George R. Young, et al. 2019. "Soluble PD-L1 Generated by Endogenous Retroelement Exaptation Is a Receptor Antagonist." *eLife* 8. https://doi.org/10.7554/eLife.50256.
Nguyen, Van Thien Chi, Trong Hieu Nguyen, Nhu Nhat Tan Doan, et al. 2023. "Multimodal Analysis of Methylomics and Fragmentomics in Plasma Cell-Free DNA for Multi-Cancer Early Detection and Localization." *eLife* 12: RP89083. https://doi.org/10.7554/eLife.89083.
Okuma, Yusuke, Wakui H, Utsumi H, et al. 2018. "Soluble Programmed Cell Death Ligand 1 as a Novel Biomarker for Nivolumab Therapy for Non-Small-Cell Lung Cancer." Clinical Lung Cancer, Clin Lung Cancer, September. https://doi.org/10.1016/j.cllc.2018.04.014.
"Olink Proteomics - Protein Screening for Biomarker Discovery." 2020. March 24. 165. https://bioxpedia.com/olink-proteomics/.
Ouyang, Hui, Bijing Xiao, Yan Huang, and Zhiqiang Wang. 2023. "Baseline and Early Changes in the Neutrophil–Lymphocyte Ratio (NLR) Predict Survival Outcomes in Advanced Colorectal Cancer Patients Treated with Immunotherapy." *International Immunopharmacology* 123 (October): 110703. https://doi.org/10.1016/j.intimp.2023.110703.
Ouyang, Peng, Lijuan Wang, Jianlong Wu, et al. 2024. "Overcoming Cold Tumors: A Combination Strategy of Immune Checkpoint Inhibitors." *Frontiers in Immunology* 15 (March). https://doi.org/10.3389/fimmu.2024.1344272.
Owen, A. M., J. J. Downes, B. J. Sahakian, C. E. Polkey, and T. W. Robbins. 1990. "Planning and Spatial Working Memory Following Frontal Lobe Lesions in Man." *Neuropsychologia* 28 (10): 1021–34. https://doi.org/10.1016/0028-3932(90)90137-d.
Ozel, Irem, Inga Duerig, Maksim Domnich, Stephan Lang, Ekaterina Pylaeva, and Jadwiga Jablonska. 2022. "The Good, the Bad, and the Ugly: Neutrophils, Angiogenesis, and Cancer." *Cancers* 14 (3): 536. https://doi.org/10.3390/cancers14030536.
Padda, Sukhmani K., and Karen L. Reckamp. 2021. "Combination of Immunotherapy and Antiangiogenic Therapy in Cancer—a Rational Approach." *Journal of Thoracic Oncology* 16 (2): 178–82. https://doi.org/10.1016/j.jtho.2020.11.007.
Pang, Jianyu, Qian Yu, Yongzhi Chen, Hongjun Yuan, Miaomiao Sheng, and Wenru Tang. 2022. "Integrating Single-Cell RNA-Seq to Construct a Neutrophil Prognostic Model for Predicting Immune Responses in Non-Small Cell Lung Cancer." *Journal of Translational Medicine* 20 (1): 531. https://doi.org/10.1186/s12967-022-03723-x.
Park, Juwon, Robert W. Wysocki, Zohreh Amoozgar, et al. 2016. "Cancer Cells Induce Metastasis-Supporting Neutrophil Extracellular DNA Traps." *Science Translational Medicine* 8 (361): 361ra138. https://doi.org/10.1126/scitranslmed.aag1711.
Paz-Ares, Luis, Alexander Luft, David Vicente, et al. 2018. "Pembrolizumab plus Chemotherapy for Squamous Non–Small-Cell Lung Cancer." *New England Journal of Medicine* 379 (21): 2040–51. https://doi.org/10.1056/NEJMoa1810865.

Peng, Weiyi, Chengwen Liu, Chunyu Xu, et al. 2012. "PD-1 Blockade Enhances T-Cell Migration to Tumors by Elevating IFN-γ Inducible Chemokines." Microenvironment and Immunology. *Cancer Research* 72 (20): 5209–18. https://doi.org/10.1158/0008-5472.CAN-12-1187.

Perez-Ruiz, Elisabeth, Luna Minute, Itziar Otano, et al. 2019. "Prophylactic TNF Blockade Uncouples Efficacy and Toxicity in Dual CTLA-4 and PD-1 Immunotherapy." *Nature* 569 (7756): 7756. https://doi.org/10.1038/s41586-019-1162-y.

Pillai, Rathi N., Suresh S. Ramalingam, Meena Thayu, et al. 2021. "Daratumumab Plus Atezolizumab in Previously Treated Advanced or Metastatic NSCLC: Brief Report on a Randomized, Open-Label, Phase 1b/2 Study (LUC2001 JNJ-54767414)." *JTO Clinical and Research Reports* 2 (2): 100104. https://doi.org/10.1016/j.jtocrr.2020.100104.

Pimentel, Julio M., Jun-Ying Zhou, and Gen Sheng Wu. 2023. "The Role of TRAIL in Apoptosis and Immunosurveillance in Cancer." *Cancers* 15 (10): 2752. https://doi.org/10.3390/cancers15102752.

Pistillo, Maria Pia, Vincenzo Fontana, Anna Morabito, et al. 2019. "Soluble CTLA-4 as a Favorable Predictive Biomarker in Metastatic Melanoma Patients Treated with Ipilimumab: An Italian Melanoma Intergroup Study." *Cancer Immunology, Immunotherapy: CII* 68 (1): 97–107. https://doi.org/10.1007/s00262-018-2258-1.

Prasad, Vinay, Alyson Haslam, and Timothee Olivier. 2024. "Updated Estimates of Eligibility and Response: Immune Checkpoint Inhibitors." *Journal of Clinical Oncology* 42 (16_suppl): e14613–e14613. https://doi.org/10.1200/JCO.2024.42.16_suppl.e14613.

Puhr, Hannah Christina, and Aysegül Ilhan-Mutlu. 2019. "New Emerging Targets in Cancer Immunotherapy: The Role of LAG3." Review. *ESMO Open* 4 (2): e000482. https://doi.org/10.1136/esmoopen-2018-000482.

Ramos-Paradas, Javier, Susana Hernández-Prieto, David Lora, et al. 2021. "Tumor Mutational Burden Assessment in Non-Small-Cell Lung Cancer Samples: Results from the TMB2 Harmonization Project Comparing Three NGS Panels." Immunotherapy Biomarkers. *Journal for ImmunoTherapy of Cancer* 9 (5): e001904. https://doi.org/10.1136/jitc-2020-001904.

Ratsika, Anna, Martin G. Codagnone, Thomaz F. S. Bastiaanssen, et al. 2024. "Maternal High-Fat Diet-Induced Microbiota Changes Are Associated with Alterations in Embryonic Brain Metabolites and Adolescent Behaviour." *Brain, Behavior, and Immunity*, ahead of print, July 18. https://doi.org/10.1016/j.bbi.2024.07.020.

Reck, Martin, Delvys Rodríguez-Abreu, Andrew G. Robinson, et al. 2016. "Pembrolizumab versus Chemotherapy for PD-L1–Positive Non–Small-Cell Lung Cancer." *New England Journal of Medicine* 375 (19): 1823–33. https://doi.org/10.1056/NEJMoa1606774.

Reckamp, Karen L., Mary W. Redman, Konstantin H. Dragnev, et al. 2022. "Phase II Randomized Study of Ramucirumab and Pembrolizumab Versus Standard of Care in Advanced Non–Small-Cell Lung Cancer Previously Treated With Immunotherapy—Lung-MAP S1800A." *Journal of Clinical Oncology* 40 (21): 2295–307. https://doi.org/10.1200/JCO.22.00912.

Reese, Aspen T., and Robert R. Dunn. 2018. "Drivers of Microbiome Biodiversity: A Review of General Rules, Feces, and Ignorance." *mBio* 9 (4): 10.1128/mbio.01294-18. https://doi.org/10.1128/mbio.01294-18.

Ribas, Antoni, Salvador Martín-Algarra, Shailender Bhatia, et al. 2017. "Abstract CT073: Immunomodulatory Effects of Nivolumab and Ipilimumab in Combination or Nivolumab Monotherapy in Advanced Melanoma Patients: CheckMate 038." *Cancer Research* 77 (13_Supplement): CT073. https://doi.org/10.1158/1538-7445.AM2017-CT073.

Rivas-Fuentes, Selma, Alfonso Salgado-Aguayo, Silvana Pertuz Belloso, Patricia Gorocica Rosete, Noé Alvarado-Vásquez, and Guillermo Aquino-Jarquin. 2015. "Role of Chemokines in Non-Small Cell Lung Cancer: Angiogenesis and Inflammation." *Journal of Cancer* 6 (10): 938–52. https://doi.org/10.7150/jca.12286.

Robinson, Mark D., Davis J. McCarthy, and Gordon K. Smyth. 2010. "edgeR: A Bioconductor Package for Differential Expression Analysis of Digital Gene Expression Data." *Bioinformatics* 26 (1): 139–40. https://doi.org/10.1093/bioinformatics/btp616.

Rose, Suzanne. 2018. "Companies Scaling Back IDO1 Inhibitor Trials." *Cancer Discovery* 8 (7): OF5. https://doi.org/10.1158/2159-8290.CD-ND2018-007.

Routy, Jean-Pierre, Bertrand Routy, Gina M. Graziani, and Vikram Mehraj. 2016. "The Kynurenine Pathway Is a Double-Edged Sword in Immune-Privileged Sites and in Cancer: Implications for Immunotherapy." *International Journal of Tryptophan Research* 9 (January): IJTR.S38355. https://doi.org/10.4137/IJTR.S38355.

Rusdi, Numlil Khaira, and Jeanne Adiwinata Pawitan. 2019. "Cancer Immunotherapy and Flow Cytometry in Immunotherapy Monitoring." *Biomedical and Pharmacology Journal* 12 (3): 1587–93. https://biomedpharmajournal.org/vol12no3/cancer-immunotherapy-and-flow-cytometry-in-immunotherapy-monitoring/.

Sahakian, B. J., and A. M. Owen. 1992. "Computerized Assessment in Neuropsychiatry Using CANTAB: Discussion Paper." *Journal of the Royal Society of Medicine* 85 (7): 399–402. https://www.ncbi.nlm.nih.gov/pmc/articles/PMC1293547/.

Saller, Maximilian, Egon Willighagen, and Eric Weitz. 2024. *Burn Wound Healing*. July 22. https://www.wikipathways.org/instance/WP5056.

Samstein, Robert M., Chung-Han Lee, Alexander N. Shoushtari, et al. 2019. "Tumor Mutational Load Predicts Survival after Immunotherapy across Multiple Cancer Types." *Nature Genetics* 51 (2): 202–6. https://doi.org/10.1038/s41588-018-0312-8.

Santana Gonzalez, Laura, Ioanna A. Rota, Mara Artibani, et al. 2021. "Mechanistic Drivers of Müllerian Duct Development and Differentiation Into the Oviduct." *Frontiers in Cell and Developmental Biology* 9 (March). https://doi.org/10.3389/fcell.2021.605301.

Sarkar, Joy, Eduardo Cortes Gomez, Takaaki Oba, et al. 2023. "Fluctuations in Gut Microbiome Composition During Immune Checkpoint Inhibitor Therapy." *World Journal of Oncology* 14 (3): 178–87. https://doi.org/10.14740/wjon1587.

Savitz, Jonathan, Wayne C. Drevets, Chelsey M. Smith, et al. 2015. "Putative Neuroprotective and Neurotoxic Kynurenine Pathway Metabolites Are Associated with Hippocampal and Amygdalar Volumes in Subjects with Major Depressive Disorder." *Neuropsychopharmacology* 40 (2): 463–71. https://doi.org/10.1038/npp.2014.194.

Scagliotti, Giorgio Vittorio, Purvish Parikh, Joachim von Pawel, et al. 2008. "Phase III Study Comparing Cisplatin plus Gemcitabine with Cisplatin plus Pemetrexed in Chemotherapy-Naive Patients with Advanced-Stage Non-Small-Cell Lung Cancer." *Journal of Clinical Oncology: Official Journal of the American Society of Clinical Oncology* 26 (21): 3543–51. https://doi.org/10.1200/JCO.2007.15.0375.

Schiller, Joan H., David Harrington, Chandra P. Belani, et al. 2002. "Comparison of Four Chemotherapy Regimens for Advanced Non-Small-Cell Lung Cancer." *The New England Journal of Medicine* 346 (2): 92–98. https://doi.org/10.1056/NEJMoa011954.

Sforzini, Luca, Maria Antonietta Nettis, Valeria Mondelli, and Carmine Maria Pariante. 2019. "Inflammation in Cancer and Depression: A Starring Role for the Kynurenine Pathway." *Psychopharmacology* 236 (10): 2997–3011. https://doi.org/10.1007/s00213-019-05200-8.

Shankar, Bairavi, Jiajia Zhang, Abdul Rafeh Naqash, et al. 2020. "Multisystem Immune-Related Adverse Events Associated With Immune Checkpoint Inhibitors for Treatment of Non–Small Cell Lung Cancer." *JAMA Oncology*, ahead of print, October 29. https://doi.org/10.1001/jamaoncol.2020.5012.

Sharma, Padmanee, Siwen Hu-Lieskovan, Jennifer A. Wargo, and Antoni Ribas. 2017. "Primary, Adaptive, and Acquired Resistance to Cancer Immunotherapy." *Cell* 168 (4): 707–23. https://doi.org/10.1016/j.cell.2017.01.017.

Simpson, Rebecca C., Erin R. Shanahan, Marcel Batten, et al. 2022. "Diet-Driven Microbial Ecology Underpins Associations between Cancer Immunotherapy Outcomes and the Gut Microbiome." *Nature Medicine*, ahead of print, September 22. https://doi.org/10.1038/s41591-022-01965-2.

Smyth, Elizabeth C., Andrew Wotherspoon, Clare Peckitt, et al. 2017. "Mismatch Repair Deficiency, Microsatellite Instability, and Survival." *JAMA Oncology* 3 (9). https://doi.org/10.1001/jamaoncol.2016.6762.

Snyder, Alexandra, Vladimir Makarov, Taha Merghoub, et al. 2014. "Genetic Basis for Clinical Response to CTLA-4 Blockade in Melanoma." Research-article. Https://Doi.Org/10.1056/NEJMoa1406498, Massachusetts Medical Society, December 3. World. https://doi.org/10.1056/NEJMoa1406498.

Socinski, M., V. Velcheti, T. Mekhail, et al. 2019. "Final Efficacy Results from B-F1RST, a Prospective Phase II Trial Evaluating Blood-Based Tumour Mutational Burden (bTMB) as a Predictive Biomarker for Atezolizumab (Atezo) in 1L Non-Small Cell Lung Cancer (NSCLC)." *Annals of Oncology* 30 (October): v919–20. https://doi.org/10.1093/annonc/mdz394.081.

Song, Daqiang, Yushen Wu, Jie Li, et al. 2024. "Insulin-like Growth Factor 2 Drives Fibroblast-Mediated Tumor Immunoevasion and Confers Resistance to Immunotherapy." *The Journal of Clinical Investigation* 134 (22): e183366. https://doi.org/10.1172/JCI183366.

Song, Yuxiao, Yang Fu, Qi Xie, Bo Zhu, Jun Wang, and Bicheng Zhang. 2020. "Anti-Angiogenic Agents in Combination With Immune Checkpoint Inhibitors: A Promising Strategy for Cancer Treatment." *Frontiers in Immunology* 11 (August). https://doi.org/10.3389/fimmu.2020.01956.

Stelloo, E., A. M. L. Jansen, E. M. Osse, et al. 2017. "Practical Guidance for Mismatch Repair-Deficiency Testing in Endometrial Cancer." *Annals of Oncology*, 3rd ESO-ESMO International Consensus Guidelines for advanced breast cancer (ABC 3), vol. 28 (1): 96–102. https://doi.org/10.1093/annonc/mdw542.

Stephens, Matthew. 2017. "False Discovery Rates: A New Deal." *Biostatistics* 18 (2): 275–94. https://doi.org/10.1093/biostatistics/kxw041.

Strickler, John H., Brent A. Hanks, and Mustafa Khasraw. 2021. "Tumor Mutational Burden as a Predictor of Immunotherapy Response: Is More Always Better?" Perspectives. *Clinical Cancer Research* 27 (5): 1236–41. https://doi.org/10.1158/1078-0432.CCR-20-3054.

Subramanian, Aravind, Pablo Tamayo, Vamsi K. Mootha, et al. 2005. "Gene Set Enrichment Analysis: A Knowledge-Based Approach for Interpreting Genome-Wide Expression Profiles." *Proceedings of the National Academy of Sciences of the United States of America* 102 (43): 15545–50. https://doi.org/10.1073/pnas.0506580102.

Tawbi, Hussein A., Dirk Schadendorf, Evan J. Lipson, et al. 2022. "Relatlimab and Nivolumab versus Nivolumab in Untreated Advanced Melanoma." *New England Journal of Medicine* 386 (1): 24–34. https://doi.org/10.1056/NEJMoa2109970.

Tian, Jihua, Jing Luo, Xing Zeng, et al. 2024. "Targeting Oxidative Phosphorylation to Increase the Efficacy of Immune-Combination Therapy in Renal Cell Carcinoma." Immunotherapy Biomarkers. *Journal for ImmunoTherapy of Cancer* 12 (2): e008226. https://doi.org/10.1136/jitc-2023-008226.

Tieng, Francis Yew Fu, Nadiah Abu, Learn-Han Lee, and Nurul-Syakima Ab Mutalib. 2021. "Microsatellite Instability in Colorectal Cancer Liquid Biopsy—Current Updates on Its Potential in Non-Invasive Detection, Prognosis and as a Predictive Marker." *Diagnostics* 11 (3): 3. https://doi.org/10.3390/diagnostics11030544.

Torlakovic, Emina, Hyun J. Lim, Julien Adam, et al. 2020. "'Interchangeability' of PD-L1 Immunohistochemistry Assays: A Meta-Analysis of Diagnostic Accuracy." *Modern Pathology* 33 (1): 4–17. https://doi.org/10.1038/s41379-019-0327-4.

Tougeron, D., J. F. Emile, A. Bodere, et al. 2024. "502O Pembrolizumab in Combination with CAPOX and Bevacizumab in Patients with Microsatellite Stable Metastatic Colorectal Cancer and a High Immune Infiltrate: Preliminary Results of FFCD 1703 POCHI Trial." *Annals of Oncology* 35 (September): S428. https://doi.org/10.1016/j.annonc.2024.08.571.

Troncone, Giancarlo, and Cesare Gridelli. 2017. "The Reproducibility of PD-L1 Scoring in Lung Cancer: Can the Pathologists Do Better?" *Translational Lung Cancer Research* 6 (Suppl 1): S74–77. https://doi.org/10.21037/tlcr.2017.10.05.

Tu, Jingyao, Hang Liang, Chunya Li, et al. 2023. "The Application and Research Progress of Anti-Angiogenesis Therapy in Tumor Immunotherapy." *Frontiers in Immunology* 14 (June). https://doi.org/10.3389/fimmu.2023.1198972.

Turajlic, Samra, Kevin Litchfield, Hang Xu, et al. 2017. "Insertion-and-Deletion-Derived Tumour-Specific Neoantigens and the Immunogenic Phenotype: A Pan-Cancer Analysis." *The Lancet Oncology* 18 (8): 1009–21. https://doi.org/10.1016/S1470-2045(17)30516-8.

Valero, Cristina, Mark Lee, Douglas Hoen, et al. 2021. "Pretreatment Neutrophil-to-Lymphocyte Ratio and Mutational Burden as Biomarkers of Tumor Response to Immune Checkpoint Inhibitors." *Nature Communications* 12 (1): 1. https://doi.org/10.1038/s41467-021-20935-9.

Valkenburg, Kenneth C., Amber E. de Groot, and Kenneth J. Pienta. 2018. "Targeting the Tumour Stroma to Improve Cancer Therapy." *Nature Reviews. Clinical Oncology* 15 (6): 366–81. https://doi.org/10.1038/s41571-018-0007-1.

Waagmeester, Andra, Egon Willighagen, Kristina Hanspers, and Eric Weitz. 2025. *Immune Response to Tuberculosis*. March 4. https://www.wikipathways.org/instance/WP4197.

Walter, Annika S., Elias Volkmer, Gerd Gauglitz, Wolfgang Böcker, and Maximilian M. Saller. 2023. "Systematic Review of Molecular Pathways in Burn Wound Healing." *Burns: Journal of the International Society for Burn Injuries* 49 (7): 1525–33. https://doi.org/10.1016/j.burns.2023.03.006.

Wang, Chiyun, Elan Hahn, Elzbieta Slodkowska, et al. 2018. "Reproducibility of PD-L1 Immunohistochemistry Interpretation across Various Types of Genitourinary and Head/Neck Carcinomas, Antibody Clones, and Tissue Types." *Human Pathology* 82 (December): 131–39. https://doi.org/10.1016/j.humpath.2018.07.024.

Wang, Ke-wei, Mei-dan Wang, Zi-xi Li, et al. 2022. "An Antigen Processing and Presentation Signature for Prognostic Evaluation and Immunotherapy Selection in Advanced Gastric Cancer." *Frontiers in Immunology* 13 (October). https://doi.org/10.3389/fimmu.2022.992060.

Wang, Wei, Ge Shen, Shikai Wu, et al. 2017. "PD-1 mRNA Expression in Peripheral Blood Cells and Its Modulation Characteristics in Cancer Patients." *Oncotarget* 8 (31): 50782–91. https://doi.org/10.18632/oncotarget.15006.

Wang, Xijie, Zhe Chen, Linxi Chen, and Chengfeng Qiu. 2026. "IDO Family: The Metabolic Crossroads Connecting Immunity, Nerves and Tumors." *Journal of Translational Medicine* 24 (1): 289. https://doi.org/10.1186/s12967-026-07758-2.

Wang, Yida, Hanxiao Chen, Tianzhuo Zhang, et al. 2021. "Plasma Cytokines Interleukin-18 and C-X-C Motif Chemokine Ligand 10 Are Indicative of the Anti-Programmed Cell Death Protein-1 Treatment Response in Lung Cancer Patients." *Annals of Translational Medicine* 9 (1): 33. https://doi.org/10.21037/atm-20-1513.

Wang, Zhijie, Jianchun Duan, Shangli Cai, et al. 2019. "Assessment of Blood Tumor Mutational Burden as a Potential Biomarker for Immunotherapy in Patients With Non–Small Cell Lung Cancer With Use of a Next-Generation Sequencing Cancer Gene Panel." *JAMA Oncology* 5 (5): 696–702. https://doi.org/10.1001/jamaoncol.2018.7098.

Wei, Chen, Mengyu Wang, Quanli Gao, et al. 2022. "Dynamic Peripheral Blood Immune Cell Markers for Predicting the Response of Patients with Metastatic Cancer to Immune Checkpoint Inhibitors." *Cancer Immunology, Immunotherapy : CII* 72 (1): 23–37. https://doi.org/10.1007/s00262-022-03221-5.

Wei, Feifei, Koichi Azuma, Yoshiro Nakahara, et al. 2023. "Machine Learning for Prediction of Immunotherapeutic Outcome in Non-Small-Cell Lung Cancer Based on Circulating Cytokine Signatures." Immunotherapy Biomarkers. *Journal for ImmunoTherapy of Cancer* 11 (7): e006788. https://doi.org/10.1136/jitc-2023-006788.

Willighagen, Egon, Marvin Martens, Finterly Hu, and Eric Weitz. 2024. *Genes Associated with the Development of Rheumatoid Arthritis*. July 23. https://www.wikipathways.org/instance/WP5033.

Winkler, Juliane, Abisola Abisoye-Ogunniyan, Kevin J. Metcalf, and Zena Werb. 2020. "Concepts of Extracellular Matrix Remodelling in Tumour Progression and Metastasis." *Nature Communications* 11 (1): 5120. https://doi.org/10.1038/s41467-020-18794-x.

Wong, Chun Wai, Yang Yu Huang, and Adam Hurlstone. 2023. "The Role of IFN-γ-Signalling in Response to Immune Checkpoint Blockade Therapy." *Essays in Biochemistry* 67 (6): 991–1002. https://doi.org/10.1042/EBC20230001.

Wu, Haixia, Lin Zhang, Wenfeng Cao, Yuanjing Hu, and Yixin Liu. 2014. "Mesonephric Adenocarcinoma of the Uterine Corpus." *International Journal of Clinical and Experimental Pathology* 7 (10): 7012–19. https://www.ncbi.nlm.nih.gov/pmc/articles/PMC4230074/.

Xu, Shuangbin, Erqiang Hu, Yantong Cai, et al. 2024. "Using clusterProfiler to Characterize Multiomics Data." *Nature Protocols* 19 (11): 3292–320. https://doi.org/10.1038/s41596-024-01020-z.

Yamaguchi, Hirohito, Jung-Mao Hsu, Linlin Sun, Shao-Chun Wang, and Mien-Chie Hung. 2024. "Advances and Prospects of Biomarkers for Immune Checkpoint Inhibitors." *Cell Reports Medicine* 5 (7): 101621. https://doi.org/10.1016/j.xcrm.2024.101621.

Yamamoto, Hiroyuki, and Kohzoh Imai. 2019. "An Updated Review of Microsatellite Instability in the Era of Next-Generation Sequencing and Precision Medicine." *Seminars in Oncology* 46 (3): 261–70. https://doi.org/10.1053/j.seminoncol.2019.08.003.

Ye, Jiaxiang, Siyao Wu, Shan Pan, Junqi Huang, and Lianying Ge. 2020. "Risk Scoring Based on Expression of Long Non-Coding RNAs Can Effectively Predict Survival in Hepatocellular Carcinoma Patients with or without Fibrosis." *Oncology Reports* 43 (5): 1451–66. https://doi.org/10.3892/or.2020.7528.

Yousefi, Yeganeh, Kelly J. Baines, and Saman Maleki Vareki. 2024. "Microbiome Bacterial Influencers of Host Immunity and Response to Immunotherapy." *Cell Reports Medicine* 5 (4): 101487. https://doi.org/10.1016/j.xcrm.2024.101487.

Yu, Yao, Jingjiao Ma, Jie Chen, et al. 2020. "T-Cell Inflamed Gene Expression to Predict Prognosis and Response to Immune Checkpoint Inhibitors." *Journal of Clinical Oncology* 38 (15_suppl): e15264–e15264. https://doi.org/10.1200/JCO.2020.38.15_suppl.e15264.

Yuan, Xiangliang, Yi Xiao, and Dihua Yu. 2025. "Turn Cold Tumors Hot by Reprogramming the Tumor Microenvironment." *Nature Biotechnology* 43 (4): 466–70. https://doi.org/10.1038/s41587-025-02597-w.

Zeng, Yanlin, Qingya Shi, Xinyu Liu, et al. 2023. "Dynamic Gut Microbiota Changes in Patients with Advanced Malignancies Experiencing Secondary Resistance to Immune Checkpoint Inhibitors and Immune-Related Adverse Events." *Frontiers in Oncology* 13 (April): 1144534. https://doi.org/10.3389/fonc.2023.1144534.

Zhang, Binbin, Yi Liu, Sijing Zhou, Huihui Jiang, Ke Zhu, and Ran Wang. 2020. "Predictive Effect of PD-L1 Expression for Immune Checkpoint Inhibitor (PD-1/PD-L1 Inhibitors) Treatment for Non-Small Cell Lung Cancer: A Meta-Analysis." *International Immunopharmacology* 80 (March): 106214. https://doi.org/10.1016/j.intimp.2020.106214.

Zheng, Danping, Timur Liwinski, and Eran Elinav. 2020. "Interaction between Microbiota and Immunity in Health and Disease." *Cell Research* 30 (6): 492–506. https://doi.org/10.1038/s41422-020-0332-7.

Zhou, Yue, Lei Tao, Jiahao Qiu, et al. 2024. "Tumor Biomarkers for Diagnosis, Prognosis and Targeted Therapy." *Signal Transduction and Targeted Therapy* 9 (1): 1–86. https://doi.org/10.1038/s41392-024-01823-2.

Zou, Wei, Stephanie J. Yaung, Frederike Fuhlbrück, et al. 2021. "ctDNA Predicts Overall Survival in Patients With NSCLC Treated With PD-L1 Blockade or With Chemotherapy." *JCO Precision Oncology*, no. 5 (May): 827–38. https://doi.org/10.1200/PO.21.00057.

APPENDIX A

Patient Information Leaflet

Study title: Biomarker Prediction of Response to Immune Checkpoint Inhibitors

Chief Investigator:	Dr Brian Bird (Bons)
Chief Investigators Title: (Bons Cork)	Consultant Medical Oncologist
Telephone number of Chief Investigator:	+353 21 434 3703
Consultant co-investigator's name: Cork	Dr Conleth Murphy, Bon Secours
Consultant co-investigator's name: Cork	Dr Deirdre O'Mahony, Bon Secours

All investigators listed above are Consultant Medical Oncologists

Clinical Data Controller's Identity:	Dr Brian Bird, Bon Secours Cork
Clinical Data Controller's contact details:	+ 353 21 434 3703
Bons Data Protection Officer's Identity:	Dr Clive Stainton
Bons Data Protection Officer's Contact Details:	DPO@bonsecours.ie

You are being invited to take part in a research study to be carried out at Bon Secours Hospital Cork by Dr Brian Bird, in collaboration with, Dr Conleth Murphy, Dr Deirdre O'Mahony, Dr Dearbhaile Collins (CUH) and the senior scientists Dr Ken Nally & Prof Paul O'Toole UCC and Dr Stephen Finn Consultant Histopathologist, St James' Hospital Dublin 8. There is an additional part to this study where you can choose to complete a questionnaire which measures your quality of life. This questionnaire is part of a Final Year Medical Student Project being carried out by Mr James Boyle UCC.

Before you decide whether you wish to take part, you should read the information provided below carefully and, if you wish, discuss it with your family, friends or GP (doctor). Take time to ask questions – do not feel rushed and don't feel under pressure to make a quick decision.

You should clearly understand the risks and benefits of taking part in this study so that you can make a decision that is right for you. This process is known as 'Informed Consent'.

You do not have to take part in this study. If you decide not to take part, it will not affect your future medical care.

You can change your mind about taking part in the study any time you like. Even if the study has started, you can still opt out. You do not have to give us a reason. If you do opt out, rest assured it will not affect the quality of treatment you get in the future.

Why is this study being done?

The immune system helps detect and kill cancer cells. When cancer cells hide from the immune system or send immune cells to sleep the cancer can spread and grow. New cancer immunotherapy drugs called Immune Checkpoint Inhibitors (ICI) can unmask the cancer to the immune system. This helps the immune system attack cancer cells. While these drugs are very helpful for some patients, other patients may have no benefit from them or only have side effects. Our team of doctors and scientists want to better understand how the immune system can defeat the cancer. We want to use blood tests to look at what the immune system is doing before and after 1 to 4 doses of immunotherapy. We will measure changes in immune cells and hormones called cytokines in patients' blood samples. We want to look at stored tumour samples and see which tumours are able to escape from the immune system even when we try and use immunotherapy to help the immune system recognize cancer cells.

We also want to look at stool samples as little is known about immunotherapy treatment and serial changes in the faecal microbiome (collection of bacteria, fungi and viruses). In addition, because little is known about the effect of immunotherapy on brain function, cognition and quality of life we would like to use the CANTAB test to see if there are any changes in how you process and remember information. The CANTAB test is carried out by you on a smart tablet screen, supervised by a UCC scientist. It takes a little less than one hour to complete. It involves moving shapes and solving puzzles.

The optional questionnaire is called the Functional Assessment of Cancer Therapy – Immune Checkpoint Modulator (FACT-ICM). We would like you to fill in the optional Quality of Life questionnaire to see how your treatment is affecting your enjoyment of life and if it is causing fatigue. We do know that quality of life is generally better with immune treatment than with chemotherapy.

This research study will try to see if we can predict which patients will benefit most from immunotherapy and which patients may need additional or alternative treatment. It will not affect how you are treated or the drugs you receive. It may help future patients.

Who is organising and funding this study?

This research is being conducted by Dr Brian Bird, Bon Secours Hospital Cork, working with doctors and nurses in the Bon Secours Hospital Cork, and Cork University Hospital. Blood and stool samples will be analysed in The Nally Lab and O'Toole lab respectively in APC Microbiome Ireland, University College Cork. Samples of tumour that are already stored in the hospital pathology laboratory will be sent to Dr Stephen Finn, Dept of Histopathology, St James' Hospital, Dublin 8 for his lab to analyse.

This research is funded by a grant to Dr Bird from Roche Ireland and a philanthropic patient donation to Trinity College Dublin. This research will contribute to Dr Bird writing an MD thesis. Dr Bird is not being paid to conduct this study or to recruit patients. Roche will not have access to patient data or benefit from the study.

Why am I being asked to take part?

You are being asked to take part because you are about to start anti-cancer treatment with a type of anti-cancer immunotherapy drug called an Immune Checkpoint Inhibitor. Some patients on this study may receive chemotherapy as well as immunotherapy. We would like your permission to study some extra blood samples and your previously stored tumour tissue to see if we can predict how your immune system and cancer respond to immunotherapy treatment.

How will the study be carried out?

When will this study take place? This study will take place between January 2021 and December 2022.

Where will this study take place? This study will be carried out in the chemotherapy day ward of your hospital if you are being treated as a day case and in the inpatient cancer ward if you are being treated as an inpatient.

How many people will be taking part in this study? Up to 75 people will take part in this study. This may be expanded in future if funding and ethics committee approval is obtained.

What can people taking part expect to happen for example, giving blood samples and so on? If you agree to take part in this study, we will take a blood sample before you receive your first dose of immunotherapy. We will take our second sample when you attend for treatment 3-6 weeks later. If for some reason you have to permanently discontinue (stop) immunotherapy treatment before the 3-6 week appointment we will take the second sample at that time. We

also want to take a single blood tube to look at immune chemicals in the blood when you attend for treatment around the 3 month mark.

We would also like you to provide two stool samples. The first stool sample will be taken at baseline before you receive your first dose of immunotherapy treatment. The second stool sample will be taken when you attend for treatment 3-6 weeks later.

Tumour samples

If there is tissue from your tumour still stored in the hospital lab we will send a sample to St James' Hospital Dublin (SJH) for testing. If your tumour has already been tested in SJH as part of your usual care we will use that data and any stored data in SJH. No extra samples of your tumour will be taken from you as part of this research.

The Cambridge Neuropsychological Test Automated Battery (CANTAB) test will also be performed before your first treatment of immunotherapy and again 3 months later. The CANTAB test is carried out by you on a smart tablet screen, supervised by a UCC scientist. It takes a little less than one hour to complete. It involves moving shapes and solving puzzles. There is an optional questionnaire that measures Quality of Life in patients on immunotherapy, called the Functional Assessment of Cancer Therapy – Immune Checkpoint Modulator (FACT-ICM) to see how your treatment is affecting your enjoyment of life and if it is causing fatigue. This will be offered to you before your first treatment of immunotherapy and again 3 months later.

What will happen to me if I agree to take part?

What will happen to me (in particular)? Before you receive your first dose of immunotherapy we will take extra blood samples. These will be no more than 39 millilitres or 4 tablespoons in volume. We will repeat this at 3-6 weeks later when you attend for your second treatment or sooner if you have to stop immunotherapy. If there is tissue from your tumour still stored in the hospital lab we will send a sample to St James' Hospital Dublin (SJH) for testing. If your tumour has already been tested in SJH as part of your usual care we will use that data and any stored data in SJH.

You will be asked to provide a stool sample in a container which we will provide before you receive your first dose of immunotherapy treatment and again 3-6 weeks later. You will be provided with instructions for producing the sample. The sample will be collected when you attend for your first and second immunotherapy treatment.

The Cambridge Neuropsychological Test Automated Battery (CANTAB) test will also be performed before your first treatment of immunotherapy and again 3 months later. This test will be performed in your treating hospital by one of the researchers from APC Microbiome Ireland UCC. We are interested in whether the immunotherapy you are receiving changes

how quickly you process information presented on a smart screen. The CANTAB test will take around one hour and will measure processing speed and attention. A single blood tube for immune chemicals will be taken at the 3 month visit also.

Do I need to attend the hospital for an extra visit? We will try and take these blood samples early in the morning on the day of your scheduled treatment visit. If you are also receiving chemotherapy with your immunotherapy and are taking steroid the day before you receive chemotherapy, we may ask you to attend for an extra visit and have your blood taken before you take any steroid pre-medication.

Do I need to give an extra blood sample? Extra blood sample will be taken 3-6 weeks apart. Each tube contains 5-10 ml of blood. The total extra blood volume taken on each occasion for this research study will not exceed 40 ml. Taking this extra amount of blood should not cause extra weakness or tiredness. There is a 3rd blood sample of 5 millilitres around 3 months to look at changes in immune chemicals called immune metabolites.

Do I need to fill in a questionnaire? You will be asked to complete the CANTAB test as mentioned above. If you develop side effects of immunotherapy treatment these will be documented by your regular doctors and nurses and recorded for study purposes. There is an optional questionnaire that measures Quality of Life in patients on immunotherapy, called the FACT-ICM. We ask that you to fill in this questionnaire before you start immunotherapy and around 3 months later when you attend for treatment. This data will be used in this study to see if changes in the immune system affect how you think about things and remember them. If you consent, your data can be added to another ethically approved study relating to ICI biomarker treatment conducted by one of our study investigators, Mr James Boyle, as part of his Final Year Medical Student Project in UCC.

How long will the study take? We will follow your progress using whatever CT scans or other imaging tests you would normally get for at least 3 months. At the end of the 3 month period if you are continuing immunotherapy treatment we will continue to record data from your scans until you finish immunotherapy treatment. Results from these scans will be used in the study.

Where will I be going? You will attend the Chemotherapy Day ward in your usual hospital.

Who will I be talking to? You will be talking to the Research Nurses and Doctors. A UCC scientist will administer the CANTAB test at baseline and 3 months. If you choose to complete the quality of life FACT-ICM questionnaire a UCC Medical Student may help you complete it.

Will researchers be looking at my medical records? Researchers will look at your medical records to record your age, height and weight, cancer diagnosis and other details (including X-rays, survival details, tumour data).

Will my medical records be private? Your medical records will not leave the hospital where you are treated. Blood and X-ray results will be identified by a study number not by your name or date of birth. The key for this number will be kept in your treating hospital.

Video/and or Audio recordings?

There are no video or audio recordings in this study

What other treatments are available to me?

If you decide not to take part, you will receive exactly the same treatment that you and your consultant have decided on. This study seeks to learn from your care to help future patients, not to change it now.

What are the benefits?

You will not benefit personally from this study. It is hoped that by increasing our understanding of who immunotherapy helps that we will be able to help future patients. We may be able to decide who will do well with immunotherapy alone and who needs additional or different treatment.

What are the risks?

We will try to take the extra research blood samples at the same time as your routine pre-treatment blood tests to reduce the number of times your skin is pricked with a needle. It is possible that you will experience pain or bruising at the point in your skin where a needle is inserted to draw blood. Some known risks, although rare, are associated with placing a needle into a vein or under the skin. Patients may feel faint, or experience mild pain, bruising, irritation or redness at the site of puncture. In rare cases, inflammation of the vein or infection may occur. Care will be taken to avoid these complications. There are no risks with providing a stool sample but you may find it unpleasant. The CANTAB test takes an hour and it may take 30 minutes to complete the optional Quality of Life FACT-ICM questionnaire.

This is an observational study and all research tests and analyses will be used for research purposes only and will not impact the clinical care you receive.

For more information about risks and side effects, ask your study doctor.

This study is trying to see whether experimental testing of your blood and tumour tissue can predict how you and your tumour respond to immunotherapy treatment. The scientists in

UCC will never know your name or date of birth (DOB) just your age, type of cancer, treatment details and scan response to immunotherapy. The doctors and scientists in SJH will know your name and DOB if they have already tested your tumour as part of your routine care. If your tumour sample is sent to St. James's Hospital only as part of this study it will be identified by a study number and your name and DOB will not be shared with SJH. Every effort will be made to protect the confidentiality of your health care data.

It is possible that somebody might be able to identify you from the information that leaves the hospital or from a future publication in a medical or scientific journal.

What if something goes wrong when I'm taking part in this study?

If you find participating in the study upsetting we welcome you to discuss these feelings with your doctors and the research nurses. You can withdraw from the study at any time and your care will not be affected.

We strongly urge you to call your Oncology Liaison Nurse during business hours and St Bernadette's Ward (021 480 1676) if you become unwell or develop side effects of ICI (and/or chemotherapy) treatment. This study does not alter your medical care or change the decisions your doctors make.

If you wish to make a complaint please contact Dr Brian Bird's office on 021 434 3703. If the complaint cannot be resolved then you can contact the Quality & Safety Department of Bon Secours Cork on 021 480 1600.

Will it cost me anything to take part?

There are no payments for taking part in this study. If we ask you to attend for an extra visit which you only need because of the study such as taking a blood sample your car parking expenses will be covered.

Is the study confidential?

Will you be contacting my GP or any other healthcare provider? Your GP will be informed that you are taking part in this study

Will you be looking at my medical records? The study team of doctors and nurses will be looking at your medical records.

Who else will be looking at my medical records? Cancer research clerical staff employed by the hospital called Data Managers will look at your medical records. If the study is audited

(inspected) by regulatory bodies such as the Health Products Regulatory Agency, then they can look at your medical records.

Will the information about me be kept private and confidential? Information about you will be kept in a secure password protected database in the hospital. When your samples leave the hospital, they will be identified by a code called a study number. Your age, gender, cancer diagnosis, response to treatment and side effects of treatment will be shared with the laboratory scientists and doctors but no other data.

Will information kept about me identify me? The information kept about you will identify you only within the hospital.

How long will you be keep the information about me? This information will be kept for 10 years from the completion of the study.

Where will you be sending information about me? Your information (without name, or address, or date of birth) will be shared with our scientific partners. If work from this study is accepted for publication, you might be described for example as Male, age 60-64, with lung cancer or Female, age 45-49 with melanoma in a journal article.

Who will be able to see the information about me? The scientists in UCC and SJH Dublin will be able to see your coded information.

What will happen to any voice recordings, video recordings or photographs you take? Where will you be sending the voice recordings, video recordings or photographs? Who will have access to them? How long will you be keeping them? There are no voice or video recordings as part of this research study. If you have a visible condition of scientific or medical interest such as a cancer on your skin, a large lump, or a rash you can decide if your doctor can photograph it or not. Sometimes this is done to help with your medical care and observe what happens to it with treatment and time. If you are willing for such photos to be used as part of this study and future publications you can give consent for this. Such photos would never show your face or if essential to show your face would have a black bar covering your eyes to preserve your privacy. Only a minority of patients will have findings that need photography. These photos will be stored in your hospital electronic record if used for clinical purposes only. If you consent to them being recorded as part of the trial they will be kept electronically in a password protected database identified by your study number and the date taken. They will only be accessed by study doctors and nurses. They will be deleted 10 years after completion of study.

Samples

What will happen to any samples you collect from me? Blood samples will be labelled with your study number only and sent to the Nally Lab APC Microbiome Ireland UCC. There they will be tested to see how active your immune system is and for markers of how the cancer is trying to fool the immune system or send it to sleep. The scientists in this laboratory will have access

to your samples. Stool samples will be labelled with your study number only and sent to the O'Toole Lab at APC Microbiome Ireland, UCC. All samples will be stored in secure freezers.

Where will you be sending the samples? If your tumour tissue is already stored in the hospital laboratory a sample will be sent to Dr Stephen Finn, SJH, for testing. This sample will be labelled with your study number. If your tumour has already been tested in SJH as part of your routine care then Dr Finn will be informed and will access stored data on your previously tested sample as well as the study sample sent to SJH. Dr Finn and his lab scientists will have access to these samples.

Will any genetic or DNA research be done on the samples? Genetic analysis of your cancer and immune cells in blood and tissue to see which genes are switched on or off will take place. If funding permits, we may look at tiny fragments of your tumour's genetic material circulating in your blood called circulating tumour DNA (ctDNA) and messenger RNA (mRNA).

Results

Will I get any results from this research study? Your doctor and nurses will explain how your cancer is responding to treatment separately from this study. Research findings from this study will not be shared directly with you. You are welcome to ask your study doctors and nurses if any scientific publications have resulted from this study but these may happen in several years' time.

Will my GP/consultant/other healthcare provider get the results? Your consultant will be informed of the results of this study.

Will you be publishing the results of this study in medical journals? It is hoped to publish the results of this study in medical journals and present it at medical and scientific conferences.

Will any information capable of identifying me appear in any publications or presentations? If work from this study is accepted for publication you might be described for example as "Male, age 60-64, with lung cancer" or "Female, age 45-49 with melanoma in a journal article."

Future Research Studies

Will you be keeping any information or samples for use in future research studies? If you give permission samples may be stored and data retained for future cancer research.

Data Protection

You have the right to withdraw consent to your personal data being used in this research project. You will be able to do this by contacting Dr Brian Bird at 021 434 3703.

We will be using your personal information in our research to help us study whether we can predict how cancer responds to treatment with Immune Checkpoint Inhibitors. Your data is being processed for scientific research purposes.

The legal basis for this health research are:

Article 6(1)(f) Legitimate Interests of the General Data Protection Regulation 2016 & Article 9(2)(j) Scientific Research purposes of the General Data Protection Regulation 2016

None of your personal information such as your name or date of birth leaves the Bon Secours Hospital. The key linking your study code to your personal information will be kept securely under password-protected software and no personal patient information will be shared except with Dr Finn in SJH if your tumour has already been tested there as part of your routine care.

Pseudo-Anonymized data from your medical records solely pertaining to your cancer and immunotherapy risk factors and the features of your cancer reported in the pathology report may be shared with our scientific collaborators. Like your tissue samples, this data will be labelled with the code created for you, and the link between the code and your personal details will remain with your investigators in the Bon Secours Hospital Cork in a secure password-protected file.

This data will be retained for 10 years post completion of study i.e. from when the last patient sample is taken. It is possible that a data breach during data processing might lead to your identity being inadvertently shared with our scientific collaborators. You have a right to withdraw from the study at any time by contacting Dr Brian Bird (021 434 3703) or speaking with your Research Nurse or Consultant. You have a right to lodge a complaint with the Data Protection Commissioner if you believe your data has been mishandled. You have a right to request access to your clinical data stored on site in hospital but not to individual research results. You may request that inaccurate information is revised or deleted. You may request that your personal data is deleted unless it would interfere with a pending publication. You may request your data which is held in Bon Secours Cork in a portable electronic format. No automatic processing of your data or profiling will take place.

If you choose to withdraw from the study then no further blood or stool samples or clinical data will be gathered on you. Any samples that have not been tested will be destroyed. Where your samples have been analysed and included in an anonymised database for publication it is not possible to destroy this data.

If you give consent for your data to be used for future cancer research then it will be processed only for these reasons once approved by a Clinical Ethics Committee. Your data will not be processed for any other reason.

Your anonymized data will not be processed outside of the European Union or a "data haven" which agrees to apply EU standards of Data Protection.

Consent to Future Uses

You have given your consent for the purposes outlined in this study only. Now we want to see if you are willing for us to use your clinical data stored as part of this study and any stored samples in future research. You are free to reject involvement in any future research. Future research would be carried out by our scientific collaborators in UCC and SJH and their research partners who may include commercial companies. Any such research would have to be approved by an Irish Clinical Research Ethics Committee.

You will not benefit from future research but it may help other patients in future. You will not have rights to income from any discoveries or treatments resulting from this research.

If new scientific information on cancer and the immune system becomes available, we may wish to access your stored clinical data (age, sex, type of cancer, response to treatment) to see if it applies to participants in this study. Blood samples will be stored in the Nally Lab at APC Microbiome Ireland, UCC; stool samples will be stored in the O'Toole Lab at APC Microbiome Ireland, UCC and tissue samples in SJH Dublin 8. You can decide if you permit us to keep your blood, stool and tissue for future research on cancer and the immune system or if you wish to have your samples destroyed at the end of the study. This would usually happen 2 years after the last sample is collected and all of the research you have consented to is completed.

You may choose if you wish for your samples to be used for research into other areas of science and medicine in future or not. One example might be autoimmune disease research.

If you change your mind and wish to withdraw from future research after giving consent your stored specimens will be destroyed where possible. If it has already been analysed as part of a new research project it will not be possible to destroy this data.

If you have died your next of kin cannot withdraw consent for processing of your stored samples. They can decide if they wish to be informed of any important clinical findings especially if these may be hereditary.

Where can I get further information?

If you have any further questions about the study or if you want to opt out of the study, you can rest assured it will not affect the quality of treatment you get in the future.

If you need any further information now or at any time in the future, please contact:

Name: Dr Brian Bird

Address: Bon Secours Cork

Phone No (Office Hours Only): 021 434 3703

APPENDIX B

Informed Consent Form

INFORMED CONSENT FORM

Study Title: Biomarker Prediction of Response to Immune Checkpoint Inhibitors

Study Doctor Name: Dr Brian Bird, Dr Conleth Murphy, Dr Deirdre O' Mahony

Hospital Name: Bon Secours Hospital, Cork

Please Initial box.

1.	I confirm that I have been given a copy of the Patient Information Leaflet and Consent Form, Bon Secours Hospital Cork, Version 1.0, December 2020. I have read the patient information leaflet and consent form or it has been read to me. This information was explained to me and my questions were answered.	☐
2.	I understand that my participation is voluntary and that I am free to withdraw at any time without giving any reason and without my medical care or legal rights being affected.	☐
3.	I understand that relevant parts of my medical records may be seen by the research team at Bon Secours Hospital Cork provided they agree not to disclose my name.	☐
4.	I understand that data related to me collected during this study will be processed and analysed as is required by this research study and in accordance with the General Data Protection Regulation.	☐
5.	I understand that my samples (blood, stool and tissue) may be used for research as described in the Patient Information Leaflet.	☐

6. I agree to take part in the above study. ☐

Name of Patient (Print)	Signature of Patient	Date (dd/mm/yyyy)
Name of Investigator (Print)	Signature of Investigator	Date (dd/mm/yyyy)
Name of Research Nurse Print (IF APPLICABLE)	Signature of Research Nurse	Date (dd/mm/yyyy)

FUTURE USE OF DATA AND SAMPLES IN RESEARCH STUDIES

FUTURE CONTACT [please choose one or more as you see fit]		
OPTION 1: I consent to be re-contacted by researchers about possible future research **related** to the current study for which I may be eligible.	**Yes** ☐	**No** ☐
OPTION 2: I consent to be re-contacted by researchers about possible future research **unrelated** to the current study for which I may be eligible.	**Yes** ☐	**No** ☐

STORAGE AND FUTURE USE OF INFORMATION		
RETENTION OF RESEARCH MATERIAL IN THE FUTURE [please choose on or more as you see fit]		
Future Related Research		
OPTION 1: I give permission for data to be stored for *possible future research* ***related*** to the current study ***only if consent is obtained*** at the time of the future research but only if the research is approved by a Research Ethics Committee.	**Yes** ☐	**No** ☐
OPTION 2: I give permission for material/data to be stored for *possible future research* ***related*** to the current study ***without further***	**Yes** ☐	**No** ☐

consent being required but only if the research is approved by a Research Ethics Committee.		
Future Unrelated Research		
OPTION 3: I give permission for data to be stored for *possible future research* ***unrelated*** to the current study ***only if consent is obtained*** at the time of the future research but only if the research is approved by a Research Ethics Committee.	**Yes** ☐	**No** ☐
OPTION 4: I give permission for data to be stored for *possible future research* ***unrelated*** to the current study ***without further consent*** being required but only if the research is approved by a Research Ethics Committee.	**Yes** ☐	**No** ☐
Commercial/Pharmaceutical Research		
OPTION 5: I agree that some future research projects may be carried out by researchers working for **commercial/pharmaceutical companies.**	**Yes** ☐	**No** ☐
OPTION 6: I understand **I will not be entitled to a share of any profits** that may arise from the future use of my material/data or products derived from it.	**Yes** ☐	**No** ☐

_____ _____ _____

Patient Name (Block Capitals) Patient Signature Date

To be completed by the Principal Investigator or nominee

I, the undersigned, have taken the time to fully explain to the above patient the nature and purpose of this study in a way that they could understand. I have explained the risks involved as well as the possible benefits. I have invited them to ask questions on any aspect of the study that concerned them.

Name (Block Capitals)	Qualifications	Signature	Date

APPENDIX C

Genetics Informed Consent Form

GENETICS INFORMED CONSENT FORM

Study Title: Biomarker Prediction of Response to Immune Checkpoint Inhibitors

Chief Investigator: Dr Brian Bird (Bons)

Clinical Lead at CUH: Dr Dearbhaile Collins

Hospital Names: Bon Secours Hospital, Cork & Cork University Hospital

Note: This section asks for your permission for us to store your blood and tumour samples for genetic purposes. It would allow us to see which genes are switched on and off or changed (mutated) in your immune and cancer cells.

I have read and understood the **Information Leaflet** about this research project. The information has been fully explained to me and I have been able to ask questions, all of which have been answered to my satisfaction.	**Yes** ☐	**No** ☐
I understand that I don't have to take part in this study and that I can opt out at any time. I understand that I don't have to give a reason for opting out and I understand that opting out won't affect my future medical care.	**Yes** ☐	**No** ☐
I understand that I can withdraw my biological material before it has been analysed at any time without any negative repercussions.	**Yes** ☐	**No** ☐
I understand that my biological material will be disposed of in a lawful and respectful way.	**Yes** ☐	**No** ☐
I am aware of the potential risks, benefits and alternatives of this research study.	**Yes** ☐	**No** ☐
I give permission for researchers to look at my medical records to get information. I have been assured that information about me will be kept private and confidential.	**Yes** ☐	**No** ☐

I have been given a copy of the Information Leaflet and this completed consent form for my records.	**Yes** ☐	**No** ☐
I consent to take part in this research study involving genetic testing having been fully informed of the risks, benefits and alternatives.	**Yes** ☐	**No** ☐
I give informed explicit consent to have my data processed as part of this research study.	**Yes** ☐	**No** ☐
I consent to give blood samples for genetic testing prior to my first and second ICI treatments and allow access to my previously stored tumour tissue sample or samples for this research project. I understand that giving blood and tissue sample or samples for this research is my own decision.	**Yes** ☐	**No** ☐
I consent to be contacted by researchers as part of this research study.	**Yes** ☐	**No** ☐
I consent to the storage of my samples at Bons Secours Cork and/or Cork University Hospital for later use in genetic research pertaining to immunotherapy research.	**Yes** ☐	**No** ☐

_____	_____	_____
Name of Patient (Print)	Signature of Patient	Date dd/mmm/yyyy
_____	_____	_____
Name of Investigator (Print)	Signature of Investigator	Date dd/mmm/yyyy
_____	_____	_____
Name of Research Nurse (Print) (Print) (If APPLICABLE)	Signature of Research Nurse	Date dd/mmm/yyyy

APPENDIX D

Schedule of Trial Activities, Blood Sample Instructions

Table D.1. APC125 Trial Schedule of Activities

	Screening	Visit 1 (baseline)	Visit 2 (3-6 weeks post dose 1)	Visit 3 (3 months from visit 1)	Follow up at 6 months
Informed Consent	X				
Genetics ICF	X				
Blood		X	X	X	
Stool		X	X		
Archival Tissue		X			
CANTAB testing (+/- 2/52)		X		X	
FACT-ICM Questionnaire		X		X	
Adverse Events			X		
Con Meds	X		X		
Imaging	X			X	Date of Progression
Data collection	X	x		X	X Survival status

APC125 Bons Cork Immune Checkpoint Biomarker Study Protocol:

1st blood collection post signing informed consent, prior to first immune checkpoint inhibitor (ICI) treatment (Ideally prior to any steroid pre-meds)

1. Routine Fully Identifiable Standard of Care Bloods to Hospital Laboratory – FBC, Albumin, LDH, CRP, ESR – can be taken in the week prior to starting ICI if convenient

2. Coded Blood Samples (Keep at room temperature, UCC Staff to be contacted and collect in less than 2 hours)

    i. 3 x 10 ml LARGE EDTA BD tubes (PMBC for flow and plasma for cytokines and metabolites)

    ii. 1 Paxgene 2.5 ml tube (for mRNA)

    iii. Serum Z tube 4.5 ml (for kynurenine/tryptophan ratio)

2nd blood collection post signing informed consent, 3-6 weeks post 1st dose ICI prior to 2nd or 3rd dose of immune checkpoint inhibitor (ICI) treatment, also off study bloods if not already taken post 1st dose of ICI (Ideally prior to any steroid pre-meds or therapeutic steroids for side effects)

3. Coded Blood Samples (Keep at room temperature, UCC Staff to be contacted and collect in less than 2 hours)

    i. 3 x 10 ml LARGE EDTA tubes (PMBC for flow and plasma for cytokines and metabolites)
    ii. 1 Paxgene 2.5 ml tube (for mRNA)
    iii. Serum Z tube 4.5 ml (for kynurenine/tryptophan ratio)

3rd and Final blood collection approx. 3 months post initial ICI, prior next ICI treatment

4. Coded Blood Sample (Keep at room temperature, UCC Staff to be contacted and collect in less than 2 hours)

    i. Serum Z tube 4.5 ml (for kynurenine/tryptophan ratio)

Figure D.1. Instructions for Blood Sample Collection for APC125

APPENDIX E

SEPMATETM_50 Procedure to Isolate and Freeze PMBC for Flow Cytometry

PRODUCT INFORMATION SHEET

SepMate™

SepMate™-50

CATALOG #15450 20 TUBES/BAG
CATALOG #15460 5X20 TUBES/BAG

SepMate™-15

CATALOG #15415 20 TUBES/BAG
CATALOG #15420 5X20 TUBES/BAG

STEMCELL™

INTENDED USE

SepMate™ tubes are designed for the in vitro isolation of mononuclear cells (MNCs) from human whole peripheral blood and cord blood samples by density gradient centrifugation.

PRODUCT DESCRIPTION

Polypropylene tube with insert. Gamma-irradiated.

STORAGE

Store at room temperature (15 - 25°C).

DIRECTIONS FOR USE

Ensure that sample, phosphate-buffered saline with 2% fetal bovine serum (PBS + 2% FBS; Catalog #07905), density gradient medium (see Notes on reverse page), and centrifuge are all at room temperature (15 - 25°C).

1. Add density gradient medium to the SepMate™ tube by carefully pipetting it through the central hole of the SepMate™ insert. Refer to Table 1 for required volumes. The top of the density gradient medium will be above the insert.

   Note: Small bubbles may be present in the density gradient medium after pipetting. This will not affect performance.
2. Dilute sample with an equal volume of PBS + 2% FBS. Mix gently.

   For example, dilute 5 mL of sample with 5 mL of PBS + 2% FBS.
3. Keeping the SepMate™ tube vertical, add the diluted sample by pipetting it down the side of the tube. The sample will mix with the density gradient medium above the insert.

   Note: The sample can be poured down the side of the tube. Take care not to pour the diluted sample directly through the central hole.
4. Centrifuge at **1200 x *g*** (see Notes) for **10 minutes** at room temperature, with the **brake on**.

   Note: For samples older than 24 hours, a centrifugation time of 20 minutes is recommended.
5. Pour off the top layer, which contains the enriched MNCs, into a new tube. Do not hold the SepMate™ tube in the inverted position for longer than 2 seconds.

   Note: Some red blood cells (RBCs) may be present on the surface of the SepMate™ insert after centrifugation. This will not affect performance.
6. Wash enriched MNCs with PBS + 2% FBS. Repeat wash.

   Note: Centrifuging at 300 x g for 8 minutes at room temperature, with the brake on, is recommended.

SEPMATE™ PROCEDURE

Numbers in brackets refer to steps under Directions for Use.

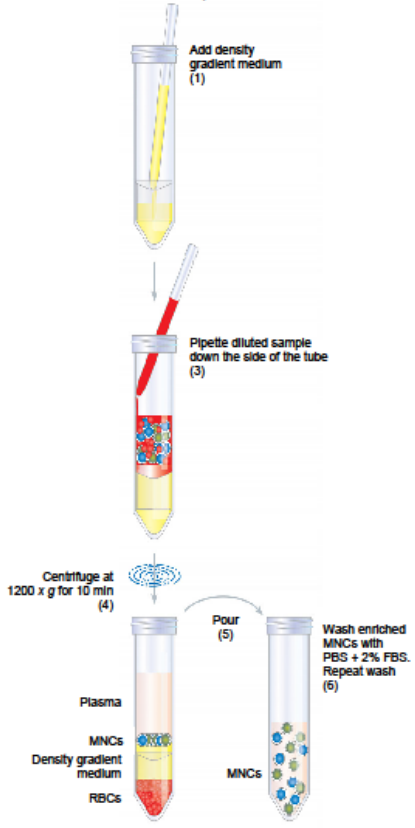

Table 1: Density Gradient Medium Volumes

SEPMATE™ TUBE	INITIAL BLOOD SAMPLE (mL)	DENSITY GRADIENT MEDIUM (mL)
15	0.5 - 4.0	4.5
15	> 4 - 5	3.5
50	4 - 17	15

FOR RESEARCH USE ONLY. NOT INTENDED FOR HUMAN OR ANIMAL DIAGNOSTIC OR THERAPEUTIC USES.

STEMCELL™

TOLL FREE PHONE 1 800 667 0322 • PHONE +1 604 877 0713
INFO@STEMCELL.COM • TECHSUPPORT@STEMCELL.COM • FOR GLOBAL CONTACT DETAILS VISIT WWW.STEMCELL.COM

VERSION 2.0.0
DOCUMENT #29251

CATALOG #15450	50 mL tubes, 20 tubes/bag
CATALOG #15460	50 mL tubes, 5 x 20 tubes/bag
CATALOG #15415	15 mL tubes, 20 tubes/bag
CATALOG #15420	15 mL tubes, 5 x 20 tubes/bag

SepMate™

PRODUCT INFORMATION SHEET

NOTES

Samples

SepMate™ can be used with human whole peripheral blood and cord blood samples. It has not been tested with samples older than 48 hours. For use of SepMate™ with samples other than human whole peripheral blood or cord blood please contact STEMCELL Technologies' Technical Support at techsupport@stemcell.com.

SepMate™-15

SepMate™-15 is designed to process 0.5 - 5 mL of initial sample.

A minimum packed RBC volume of 0.25 mL is required. For patient samples with low hematocrits, the minimum sample volume may therefore be greater than 0.5 mL.

There is a maximum packed RBC volume of 3 mL. For patient samples with very high hematocrits, the maximum sample volume may therefore be less than 5 mL.

SepMate™-50

SepMate™-50 is designed to process 4 - 17 mL of initial sample.

A minimum packed RBC volume of 2 mL is required. For patient samples with low hematocrits, the minimum sample volume may therefore be greater than 4 mL.

There is a maximum packed RBC volume of 12 mL. For patient samples with very high hematocrits, the maximum sample volume may therefore be less than 17 mL.

Density Gradient Medium

Density gradient medium refers to Lymphoprep™ (Catalog #07801), Ficoll-Paque™ PLUS or other similar density gradient media.

Recommended Medium

The recommended medium is phosphate-buffered saline with 2% fetal bovine serum (PBS + 2% FBS, Catalog #07905).

Conversion of *g* to RPM

To convert *g* to rpm, use the following formula:

$$RPM = \sqrt{\frac{RCF}{(1.118 \times 10^{-5}) \times (Radius)}}$$

Where: RPM = centrifuge speed in revolutions per minute
RCF = relative centrifugal force (*g*)
Radius = radius of centrifuge rotor in centimeters (cm)

Troubleshooting

If the density gradient medium above the SepMate™ insert appears red after centrifugation (i.e. some RBCs have not pelleted), the SepMate™ tube can be spun at 1200 x *g* for another 10 minutes with the brake on. This situation may occur with samples that are older than 24 hours.

Platelet Removal (optional)

Platelets present in the plasma layer may be removed from the enriched MNCs in one of the following ways:

- In step 5, pipette off the supernatant above the MNC layer before pouring
- In step 6, perform one of the washes at 120 x *g* for 10 minutes at room temperature, with the brake off

SUPPLEMENTARY PROCEDURE

Use of SepMate™ with RosetteSep™ Cocktails

SepMate™ tubes can be used with RosetteSep™ cell enrichment cocktails to isolate specific cell types from human whole blood. For available RosetteSep™ cocktails please refer to www.rosettesep.com.

To use SepMate™ with RosetteSep™ cocktails:

1. Add RosetteSep™ cocktail to the whole blood sample using volumes recommended in the RosetteSep™ cocktail Product Information Sheet.
2. Incubate for **10 minutes** at room temperature (15 - 25°C).
   Note: The 10-minute incubation time is specific to this procedure. It will have minimal effect on performance.
3. Follow the steps under SepMate™ Directions for Use, on reverse page.
   Note: Use density gradient medium recommended in the RosetteSep™ cocktail Product Information Sheet.

STEMCELL™ TECHNOLOGIES

TOLL FREE PHONE 1 800 667 0322 • PHONE +1 604 877 0713

INFO@STEMCELL.COM • TECHSUPPORT@STEMCELL.COM • FOR GLOBAL CONTACT DETAILS VISIT WWW.STEMCELL.COM

VERSION 2.0.0

DOCUMENT #29251

APPENDIX F

Analysis of Serum Samples for Immune Metabolites

Note – Serum Samples were centrifuged within one hour of collection and then the methods used below in plasma were followed.

"Tryptophan metabolites quantified included L-kynurenine (L-Kyn), 3-hydroxy-anthranilic acid (3-HANA) and were determined in plasma using HPLC with UV and fluorescence detector as previously described ((Clarke et al. 2009; Kennedy et al. 2015)). Briefly, the samples were spiked with internal standard (3-Nitro-L-Tyrosine) prior to being deproteinised by addition of 20 µL of 4 M perchloric acid to 200 µL of plasma. The samples were centrifuged at 21,000 g for 15 min at 4 °C on a Hettich Mikro 22R centrifuge (AGB, Dublin, Ireland), and 100 µL of supernatant was then transferred to a HPLC vial for analysis on the HPLC system (consisting of a CBM-20A system controller, a LC-20AD pump, a CTO-20AC column oven at 30 °C, a SIL-20AC HT autosampler, a Prominence DGU-20A5R degasser, Shimadzu SPD-10 VP UV–Vis detector and Prominence RF-20A fluorescence detector).

All samples were injected onto a reversed phase Luna 3 µm C18 (2) 150 × 2 mm column (Phenomenex), which was protected by Krudkatcher disposable pre-column filters (Phenomenex) and SecurityGuard cartridges (Phenomenex). The mobile phase consisted of 50 mM acetic acid, 100 mM zinc acetate with 3 % (v/v) acetonitrile and was filtered through Millipore 0.45 µm HV Durapore membrane filters (AGB) and vacuum degassed prior to use. Compounds were eluted isocratically over a 30-min runtime at a flow rate of 0.3 mL/min after a 20 µl injection. The column was maintained at a temperature of 30 °C and samples/standards were kept at 8 °C in the cooled autoinjector prior to injection. The fluorescent detector was set at an excitation wavelength of 254 nm and an emission wavelength of 404 nm. The UV detector was set to 330 nm. Tryptophan metabolites were identified by their characteristic retention times as determined by standard injections which were run at regular intervals during the sample analysis. Internal standard peak height ratios were measured and compared with standard

injections using the software LabSolutions (Shimadzu) and results were expressed as ng/ml of plasma."

APPENDIX G

"OLINK® Target 96 Immuno Oncology" 2025; "OLINK Proteomics Protein Screening for Biomarker Discovery" 2020

UniProt ID	**Gene**	**Protein** name
P10145	CXCL8	Interleukin-8
Q07011	TNFRSF9	Tumor necrosis factor receptor superfamily member 9
Q02763	TEK	Angiopoietin-1 receptor
P80098	CCL7	C-C motif chemokine 7
P29965	CD40LG	CD40 ligand
P01583	IL1A	Interleukin-1 alpha
Q9BZW8	CD244	Natural killer cell receptor 2B4
P01133	EGF	Pro-epiderma l growth factor
Q15389	ANGPT1	Angiopoietin-1
P13232	IL7	Interleukin-7
P49763	PGF	Placenta growth factor
P05231	IL6	Interleukin-6
Q9Y653	ADGRG1	Adhesion G-protein coupled receptor G1
P13500	CCL2	C-C motif chemokine 2
O95727	CRTAM	Cytotoxic and regulatory

		T-cell molecule
O14625	CXCL11	C-X-C motif chemokine 11
Q99616	CCL13	C-C motif chemokine 13
P50591	TNFSF10	Tumor necrosis factor ligand superfamily member 10
P09038	FGF2	Fibroblast growth factor 2
Q07325	CXCL9	C-X-C motif chemokine 9
P01732	CD8A	T-cell surface Glycoprotein CD8 alpha chain
Q16790	CA9	Carbonic anhydrase 9
Q8WXI7	MUC16	Mucin-16
P00813	ADA	Adenosine deaminase
P01730	CD4	T-cell surface glycoprotein CD4
P29474	NOS3	Nitric oxide synthase 3
P60568	IL2	Interleukin-2
O00182	LGALS9	Galectin-9
P35968	KDR	Vascular endothelial growth factor receptor 2
P25942	CD40	Tumor necrosis factor receptor superfamily member 5
Q14116	IL18	Interleukin-18
P20718	GZMH	Granzyme H
P43629	KIR3DL1	Killer cell immunoglobulin-like receptor 3DL1
P01137	TGFB1	Transforming growth factor beta-1 proprotein
P09341	CXCL1	Growth-regulated alpha protein
O43557	TNFSF14	Tumor necrosis factor ligand superfamily member 14
O95760	IL33	Interleukin-33
O43508	TNFSF12	Tumor necrosis factor ligand superfamily member 12
P01127	PDGFB	Platelet-derived growth factor subunit B
Q15116	PDCD1	Programmed cell death protein 1

P48023	FASLG	Tumor necrosis factor ligand superfamily member 6
P10747	CD28	T-cell-specific surface glycoprotein CD28
Q99731	CCL19	C-C motif chemokine 19
P80075	CCL8	C-C motif chemokine 8
P13236	CCL4	C-C motif chemokine 4
P40933	IL15	Interleukin-15
P09382	LGALS1	Galectin-1
Q9NZQ7	CD274	Programmed cell death 1 ligand 1
P26842	CD27	CD27 antigen
P42830	CXCL5	C-X-C motif chemokine 5
P05113	IL5	Interleukin-5
P14210	HGF	Hepatocyte growth factor
P12544	GZMA	Granzyme A
P09601	HMOX1	Heme oxygenase 1
P78423	CX3CL1	Fractalkine
P02778	CXCL10	C-X-C motif chemokine 10
P32970	CD70	CD70 antigen
P22301	IL10	Interleukin-10
Q9NP84	TNFRSF12A	Tumor necrosis factor receptor superfamily member 12A
P55773	CCL23	C-C motif chemokine 23
P06127	CD5	T-cell surface glycoprotein CD5
P10147	CCL3	C-C motif chemokine 3
P09237	MMP7	Matrilysin
P05089	ARG1	Arginase-1
O76036	NCR1	Natural cytotoxicity triggering receptor 1
P07585	DCN	Decorin
O75509	TNFRSF21	Tumor necrosis factor receptor superfamily member 21
P43489	TNFRSF4	Tumor necrosis factor receptor superfamily member 4
Q29980_Q29983	MICB_MICA	MHC class I polypeptide-related sequence A_MHC class I polypeptide-related sequence B
Q92583	CCL17	C-C motif chemokine 17

O15123	ANGPT2	Angiopoietin-2
P21246	PTN	Pleiotrophin
P48061	CXCL12	Stromal cell-derived factor 1
P01579	IFNG	Interferon gamma
Q9UQV4	LAMP3	Lysosome-associated membrane glycoprotein 3
Q14790	CASP8	Caspase-8
O75144	ICOSLG	ICOS ligand
P39900	MMP12	Macrophage metalloelastase
O43927	CXCL13	C-X-C motif chemokine 13
Q9BQ51	PDCD1LG2	Programmed cell death 1 ligand 2
P15692	VEGFA	Vascular endothelial growth factor A, long form
P05112	IL4	Interleukin-4
P18627	LAG3	Lymphocyte activation gene 3 protein
P42701	IL12RB1	Interleukin-12 receptor subunit beta-1
P35225	IL13	Interleukin-13
P78556	CCL20	C-C motif chemokine 20
P01375	TNF	Tumor necrosis factor
Q13241	KLRD1	Natural killer cells antigen CD94
P10144	GZMB	Granzyme B
Q01151	CD83	CD83 antigen
P29459_P29460	IL12A_IL12B	Interleukin-12
P09603	CSF1	Macrophage colony-stimulating factor 1

APPENDIX H

"OLINK® Assay Technical Details ("Olink Proteomics - Protein Screening for Biomarker Discovery" 2020)

Sample controls

There are six required and two recommended external controls that are added to separate wells on the plate.

- **Inter-plate controls**
  Inter-plate Control (IPC) is included in triplicate on each plate and these are run as normal samples. The IPC is a pool of 92 antibodies, each with one pair of unique DNA-tags positioned in fixed proximity and can be seen as a synthetic sample, expected to give a high signal for all assays. The median of the IPC triplicates is used to normalize each assay, to compensate for potential variation between runs and plates.
- **Negative controls**
  Negative Control is also included in triplicate on each plate and consists of buffer run as a normal sample. These are used to monitor any background noise generated when DNA-tags come in close proximity without prior binding to the appropriate protein. The negative controls set the background levels for each protein assay and are used to calculate the limit of detection.
- **Sample controls**
  It is highly recommended to include a pooled plasma sample, run in duplicate, on each plate. This sample control will be used to assess potential variation between and within plates through the calculation of inter- and intra-assay CV's.

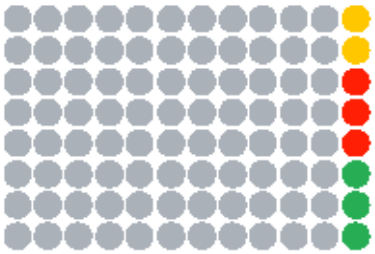

Fig 2. Recommended control setup for a PEA run.

Sample QC

Each of the internal controls is spiked into the samples at the same concentration. The signals for these are therefore expected to be the same over the plate. Sample QC is performed using the Detection Control and Incubation Control 2, on the initially calculated NPX values. Within each plate, the levels of these controls are monitored for each sample and compared against the median of all samples. If either of the controls differ by more than the acceptance criteria ±0.3 NPX, the sample is considered deviant and fails QC. Deviating values for the internal controls can be caused by factors such as errors in pipetting or pre-analytical variations in the samples that affect the performance, for example matrix effects.

TERMINOLOGY

Matrix effects are defined as changes in the analytical readout that can be caused by all other sample components except the specific analyte to be quantified.

Plate QC

The internal controls are also used in plate QC. This assesses the variation over the plate for each of Incubation Control 1 and 2 and the Detection Control. If the variation for one of the controls is too large, the entire plate is considered unreliable.

Normalization using inter-plate controls

Calculation of NPX

Olink uses an arbitrary, relative quantification unit called Normalized Protein Expression (NPX). In qPCR, the x-axis value of the point where the reaction curve intersects the threshold line is called the Ct, or "threshold cycle." This indicates the number of cycles needed for the signal to surpass the fluorescent signal threshold line. NPX is derived from the Ct values obtained from the qPCR using the following equations:

Extension Control:

$$Ct_{Analyte} - Ct_{Extension\ Control} = dCt_{Analyte}$$

Inter-plate Control:

$$dCt_{Analyte} - dCt_{Inter\text{-}plate\ Control} = ddCt_{Analyte}$$

Adjustment against a correction factor:

$$\text{Correction factor} - ddCt_{Analyte} = NPX_{Analyte}$$

TERMINOLOGY

The correction factor is calculated by Olink during the validation of the panels. The value is pre-determined, using Negative Control, and used to invert the scale so that a higher value corresponds to a higher signal. It is also used to ensure that background levels are approximately zero.

NPX is a relative quantification unit logarithmically related to protein concentration. Even if two different proteins have the same NPX values, their absolute concentrations may differ. NPX should be compared for each assay separately between samples within a run. NPX should not be compared between runs without proper inter-plate normalization due to the risk of falsely interpreting shifts in median between runs as a biological difference. However, relative differences in NPX can be compared more easily, often without additional normalization steps.

APPENDIX I

Extraction of Microbial DNA from Faecal Samples

DNA Extraction procedure for human faeces.

I. Cell Lysis

1. Transfer 0.25g of sample into a fresh, autoclaved 2ml screw cap tube containing one 3.5mm zirconia bead and one scoop of 0.1mm and 1mm beads respectively. Add 1ml of lysis buffer.
2. Homogenize for 60 seconds at a maximum speed on a Mini-BeadBeater.
3. Place on ice for 30-60 seconds to allow the tube to cool. Repeat steps 2 and 3 twice more.
4. Incubate at 70°C for 15 min.
5. Centrifuge at 4°C for 5 min at full speed. Transfer the supernatant to a fresh 2ml Eppendorf tube.
6. Add 300ul of fresh lysis buffer to the lysis tube and repeat the steps 2-5, and then pool the supernatant.

II. Precipitation of nucleic acids

7. Add 347ul of 7.5M (260ul of 10M) ammonium acetate to each lysate tube, mix well and incubate on ice for 5mins.
8. Centrifuge at 4°C for 10 min at full speed.
9. Transfer the supernatant to two 1.5ml Eppendorf tubes, add one volume of isopropanol (650ul) and mix well, and incubate on ice for 30 min (or ON).
10. Centrifuge at 4°C for 15 min at full speed, remove the supernatant using aspiration(decanting), wash the nucleic acids pellet with 300ul 70% ethanol, and dry the pellet for ~30mins, or until completely dry.
11. Dissolve the nucleic acid pellet in 100ul of TE (Tris-EDTA) buffer and pool the two aliquots.

III. Removal of RNA, protein and purification

12. Add 2ul of DNase-free RNase (10mg/ml) and incubate at 37°C for 15min.
13. Add 15ul of Proteinase K and 200ul of Buffer AL (from the QIAamp DNA Stool Mini Kit), mix well, and incubate at 70°C for 10 min.
14. Add 200ul of ethanol and mix well. Transfer to a QIAamp column and centrifuge at full speed for 1 min.
15. Discard the flow through. Add 500ul of Buffer AW1 (Qiagen) and centrifuge for 1 min at room temperature.
16. Discard the flow through. Add 500ul of Buffer AW2 (Qiagen) and centrifuge for 1 min at room temperature.
17. Discard the flow through. Place column in new collecting tube and dry it by centrifugation at room temperature for 1 min.
18. Place column in Eppendorf tube. Add 200ul (or 100ul) of Buffer AE (Qiagen) and incubate at room temperature for 2 min.
19. Centrifuge at room temperature for 1 min to elute the DNA. (can repeat elution step for higher efficiency)
20. Discard the column and store the labelled tube at -20°C.

(Can check quality of DNA by running on 0.8% gel)

(Measure DNA conc. with Nano Drop)

APPENDIX J

FACT – ICM Questionnaire

FACT – ICM QUESTIONNAIRE

BELOW IS A LIST OF STATEMENTS THAT OTHER PEOPLE WITH YOUR ILLNESS HAVE SAID ARE IMPORTANT. **PLEASE CIRCLE OR MARK ONE NUMBER PER LINE TO INDICATE YOUR RESPONSE AS IT APPLIES TO THE PAST 7 DAYS.**

PHYSICAL WELL-BEING		**Not at all**	**A little bit**	**Somewhat**	**Quite a bit**	**Very much**
GP1	I have a lack of energy	0	1	2	3	4
GP2	I have nausea.....	0	1	2	3	4
GP3	Because of my physical condition, I have trouble meeting the needs of my family	0	1	2	3	4
GP4	I have pain.....	0	1	2	3	4
GP5	I am bothered by side effects of treatment.....	0	1	2	3	4
GP6	I feel ill.....	0	1	2	3	4
GP7	I am forced to spend time in bed.....	0	1	2	3	4

SOCIAL/FAMILY WELL-BEING		**Not at all**	**A little bit**	**Somewhat**	**Quite a bit**	**Ve mu**
GS1	I feel close to my friends.....	0	1	2	3	
GS2	I get emotional support from my family	0	1	2	3	
GS3	I get support from my friends	0	1	2	3	
GS4	My family has accepted my illness	0	1	2	3	
GS5	I am satisfied with family communication about my illness	0	1	2	3	

GS6	I feel close to my partner (or the person who is my main support)	0	1	2	3		4
Q1	*Regardless of your current level of sexual activity, please answer the following question. If you prefer not to answer it, please mark this box and go to the next section.*	☐					
GS7	I am satisfied with my sex life……..	0	1	2	3		4

EMOTIONAL WELL-BEING		**Not at all**	**A little bit**	**Somewhat**	**Quite a bit**	**V m**
GE1	I feel sad	0	1	2	3	
GE2	I am satisfied with how I am coping with my illness.....	0	1	2	3	
GE3	I am losing hope in the fight against my illness..	0	1	2	3	
GE4	I feel nervous.....	0	1	2	3	
GE5	I worry about dying.....	0	1	2	3	
GE6	I worry that my condition will get worse	0	1	2	3	

FUNCTIONAL WELL-BEING		**Not at all**	**A little bit**	**Somewhat**	**Quite a bit**	**Very much**
GF1	I am able to work (include work at home)	0	1	2	3	4
GF2	My work (include work at home) is fulfilling.....	0	1	2	3	4
GF3	I am able to enjoy life.....	0	1	2	3	4
GF4	I have accepted my illness.....	0	1	2	3	4
GF5	I am sleeping well	0	1	2	3	4
GF6	I am enjoying the things I usually do for fun	0	1	2	3	4
GF7	I am content with the quality of my life right now……..	0	1	2	3	4

ADDITIONAL CONCERNS	**Not at all**	**A little bit**	**Somewhat**	**Quite a bit**	**V m**

AA1	My fatigue keeps me from doing the things I want to do…….	0	1	2	3		4
ICM1	I have been bothered by diarrhea	0	1	2	3		4
Hep8	I have discomfort or pain in my stomach area ...	0	1	2	3		4
Cx6	I am bothered by constipation	0	1	2	3		4
AA9	I am bothered by a skin rash	0	1	2	3		4
Lym1	I am bothered by itching	0	1	2	3		4
ICM2	I am bothered by dry skin.....	0	1	2	3		4
ICM3	I am bothered by vitiligo (white patches appearing on my skin) …….....	0	1	2	3		4
Br20	I have weakness in my arms or legs.....	0	1	2	3		4
ICM4	I feel pain, soreness or aches in some of my muscles.....	0	1	2	3		4
BRM1	I have pain in my joints.....	0	1	2	3		4
AA10	I am bothered by swelling in certain areas of my body …….	0	1	2	3		4
BMT13	I am bothered by a change in the way food tastes	0	1	2	3		4
Ga1	I have a loss of appetite.....	0	1	2	3		4
O2	I have been vomiting.....	0	1	2	3		4
B1	I have been short of breath	0	1	2	3		4
L2	I have been coughing	0	1	2	3		4
BRM3	I am bothered by fevers (episodes of high body temperature)	0	1	2	3		4
MS3	I am bothered by headaches	0	1	2	3		4
Lym2	I have trouble sleeping at night	0	1	2	3		4
BRM5	I am bothered by dry mouth	0	1	2	3		4
NP3	I am bothered by worsening eyesight.....	0	1	2	3		4
ICM6	I am bothered by short-term treatment reactions that I experience immediately after, or within 24 hours of, an infusion (such as chills, dizziness, hives, rashes lasting no more than 24 hours) ...	0	1	2	3		4

ICM7	I am troubled by not knowing when exactly my side effects will happen, how long they will last and how bad they will be	0	1	2	3		4
ICM5	I worry about negative impacts that my treatment may have upon my long-term health.....	0	1	2	3		4

APPENDIX K

Results Of Gene Sequencing Enrichment Analysis (GSEA)

Reactome GSEA Analysis

Using gene expression **62 up-regulated** and **8 down-regulated** terms from *Reactome* using GSEA (Milacic et al. 2024) were identified. The most significantly up-regulated terms in the Favourable group were **Degradation of the extracellular matrix** (NES: 2.4392), **Regulation of Insulin-like Growth Factor (IGF) transport and uptake by Insulin-like Growth Factor Binding Proteins (IGFBPs)** (NES: 2.3115), and **Extracellular matrix organization** (NES: 2.1393). The most significantly down-regulated terms were **Interferon gamma signalling** (NES: -2.3485), **Interferon alpha/beta signalling** (NES: -2.4013), **Interleukin-2 family signalling** (NES: -2.1072).

Table K.1. Top 15 enriched terms from *Reactome* in Favourable (Partial Response, Stable Disease) compared to Unfavourable (Progressive Disease, Died) based on gene expression.

ID	Term	NES	Adj. Value	Genes
R-HSA-1474228	Degradation of the extracellular matrix	2.44	0.00	CDH1, LAMC1, HSPG2, COL4A2, COL1A2, COL6A2, FBN1, COL6A1, MMP2, HTRA1, MMP14, COL5A1, COL1A1, LAMA5, COL6A3, A2M, COL3A1, LAMC2, COL15A1, LAMB3, COL5A2, COL17A1, COL4A1, BMP1, MMP17, ...
R-HSA-381426	Regulation of Insulin-like Growth Factor (IGF) transport and uptake by Insulin-like Growth Factor Binding Proteins (IGFBPs)	2.31	0.00	IGFBP2, LAMC1, IGFBP5, APOE, VWA1, IGFBP6, APOB, FBN1, MMP2, CP, C3, F5, IGFBP3, CCN1, FSTL1, APP, APOA1, ALB, FN1, MFGE8, APOA2, FGA
R-HSA-1474244	Extracellular matrix organization	2.14	0.00	FBLN1, CDH1, LAMC1, SERPINH1, HSPG2, COL4A2, BGN, COL1A2, COL6A2, FBN1, COL6A1, MMP2, HTRA1, MMP14, COL5A1, PTPRS, COL1A1, DDR1, COL27A1, LAMA5, SDC1, BMP2, COL6A3, PXDN, A2M, ...

ID	Term	NES	Adj. Value	Genes
R-HSA-3000178	ECM proteoglycans	2.35	0.00	LAMC1, HSPG2, COL4A2, BGN, COL1A2, COL6A2, COL6A1, COL5A1, PTPRS, COL1A1, LAMA5, COL6A3, COL3A1, APP, HAPLN1, VTN, COL5A2, COL4A1, FN1, SERPINE1, ITGA9, COL4A5, COL9A2, ITGA2, DCN, ...
R-HSA-8957275	Post-translational protein phosphorylation	2.23	0.00	LAMC1, IGFBP5, APOE, VWA1, APOB, FBN1, CP, C3, F5, IGFBP3, CCN1, FSTL1, APP, APOA1, ALB, FN1, MFGE8, APOA2, FGA, BMP4, WFS1, SPARCL1, AHSG, LAMB2, MSLN, ...
R-HSA-2173782	Binding and Uptake of Ligands by Scavenger Receptors	2.39	0.00	AMBP, APOE, COL4A2, APOB, COL1A2, SAA1, COL1A1, MSR1, COL3A1, APOA1, COL4A1, ALB
R-HSA-1650814	Collagen biosynthesis and modifying enzymes	2.34	0.00	SERPINH1, COL4A2, COL1A2, COL6A2, COL6A1, COL5A1, COL1A1, COL27A1, COL6A3, COL3A1, COL15A1, COL5A2, COL17A1, COL4A1, BMP1, COL14A1, COL4A5, COL9A2, PCOLCE2, P4HA1, COL16A1, P3H3, PLOD2
R-HSA-877300	Interferon gamma signaling	-2.35	0.00	HLA-F, RAF1, TRIM5, HLA-B, HLA-DPA1, CAMK2D, TRIM38, TRIM46, TRIM14, IRF9, IRF5, HLA-E, TRIM68, STAT1, MAPK1, TRIM22, IRF1, OAS1, GBP1, HLA-DRA, PTAFR, MAPK3, IRF2, IRF7, HLA-A, ...
R-HSA-2022090	Assembly of collagen fibrils and other multimeric structures	2.34	0.00	COL4A2, COL1A2, COL6A2, COL6A1, COL5A1, COL1A1, COL27A1, COL6A3, PXDN, COL3A1, LAMC2, COL15A1, LAMB3, COL5A2, COL17A1, COL4A1, BMP1, COL14A1
R-HSA-1442490	Collagen degradation	2.34	0.00	COL4A2, COL1A2, COL6A2, COL6A1, MMP2, MMP14, COL5A1, COL1A1, COL6A3, COL3A1, COL15A1, COL5A2, COL17A1, COL4A1
R-HSA-3000171	Non-integrin membrane-ECM interactions	2.32	0.00	LAMC1, HSPG2, COL4A2, COL1A2, COL5A1, COL1A1, DDR1, LAMA5, SDC1, SDC4,COL3A1, LAMC2, LAMB3, VTN, COL5A2, COL4A1, FN1, CASK, TRAPPC4, COL4A5, ITGA2, LAMC3, LAMB2, TNC
R-HSA-1474290	Collagen formation	2.22	0.00	SERPINH1, COL4A2, COL1A2, COL6A2, COL6A1, COL5A1, COL1A1, COL27A1, COL6A3, PXDN, COL3A1, LAMC2, COL15A1, LAMB3, COL5A2, COL17A1,

ID	Term	NES	Adj. Value	Genes
				COL4A1, BMP1, COL14A1, COL4A5, COL9A2, PCOLCE2, P4HA1, COL16A1, P3H3, ...
R-HSA-909733	Interferon alpha/beta signaling	-2.40	0.00	BST2, GBP2, USP18, HLA-F, HLA-B, IFNAR2, PSMB8, IFIT5, IRF9, IRF5, ADAR, HLA-E, STAT1, EIF2AK2, IRF1, IFITM3, OAS1, IFI35, IRF2, MX1, IRF7, HLA-A, STAT2, IFIT2, SAMHD1, ...
R-HSA-8948216	Collagen chain trimerization	2.37	0.00	COL4A2, COL1A2, COL6A2, COL6A1, COL5A1, COL1A1, COL27A1, COL6A3, COL3A1, COL15A1, COL5A2, COL17A1, COL4A1
R-HSA-8874081	MET activates PTK2 signaling	2.25	0.00	LAMC1, COL1A2, COL5A1, COL1A1, COL27A1, LAMA5, PTK2, COL3A1, LAMC2, LAMB3, COL5A2, FN1

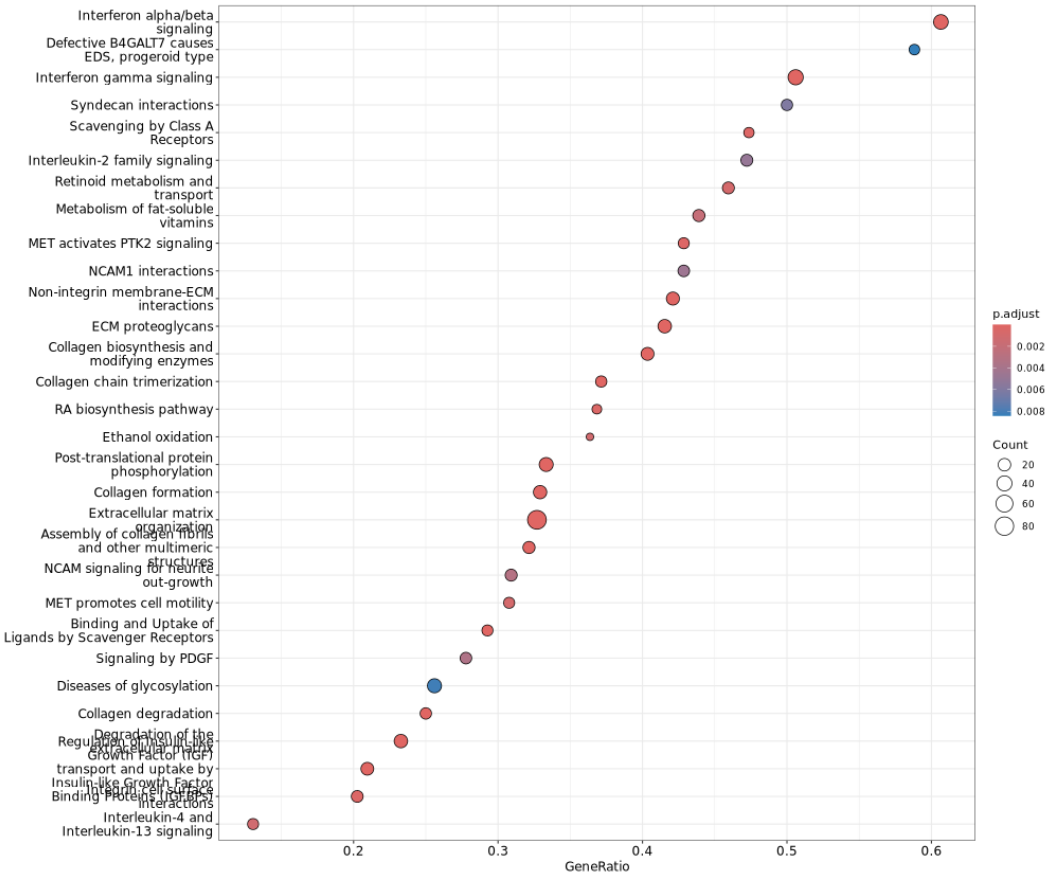

Figure K.1. Dotplot of enriched pathways in Favourable (Partial Response, Stable Disease) compared to Unfavourable (Progressive Disease, Died) from *Reactome*. Dots represent enriched pathways, with size indicating gene count and colour showing significance (e.g., adjusted p-value)

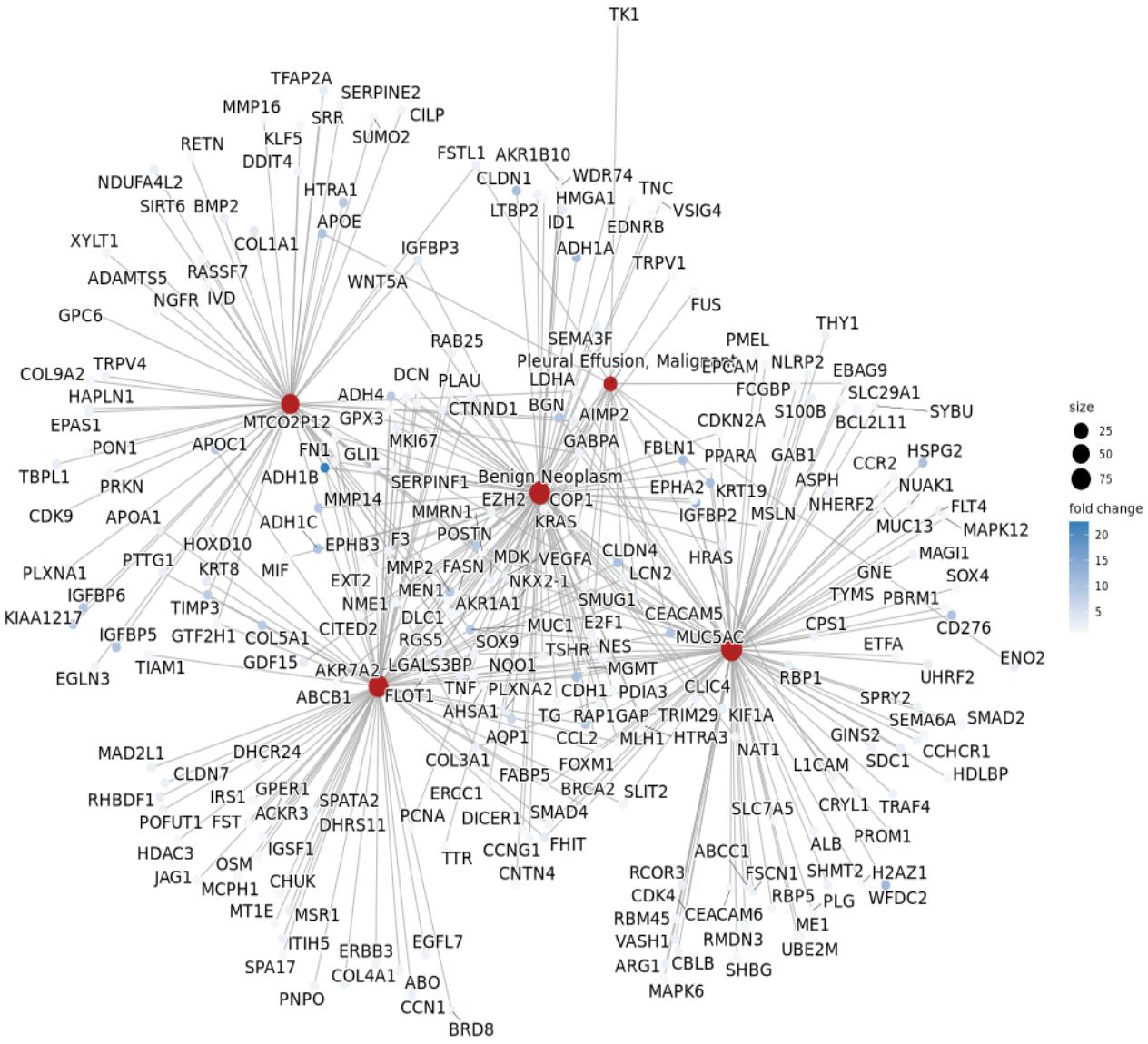

Figure K.2. Favourable (Partial Response, Stable Disease) compared to Unfavourable (Progressive Disease, Died) Cnetplot of gene-pathway relationships from *Reactome*. Pathways and their associated genes are connected, with node size and edge thickness indicating enrichment and shared genes.

Disease Gene Network GSEA

Based on gene expression, we identified **1092 up-regulated** and **39 down-regulated** terms from *Disease Gene Network* using GSEA to compare Favourable (Partial Response, Stable Disease) compared to Unfavourable (Progressive Disease, Died) ("DISGENET" 2025). The most significantly up-regulated terms were **Pleural Effusion, Malignant** (NES: 2.3673), **Benign Neoplasm** (NES: 2.0629), **Intervertebral Disc Degeneration** (NES: 1.9876). The most significantly down-regulated terms were **Autoimmune Primary Adrenal Insufficiency** (NES: -2.1149), **Addison's disease due to autoimmunity** (NES: -2.0027), and **Increased megakaryocyte count** (NES: -1.9958).

Table K.2. Top 15 enriched terms from *Disease Gene Network* in Favourable (Partial Response, Stable Disease) compared to Unfavourable (Progressive Disease, Died). Based on gene expression.

ID	Term	NES	Adj. P-Value	Genes
C0080032	Pleural Effusion, Malignant	2.37	0.00	WFDC2, KRT19, CDH1, APOE, MUC5AC, CCL2, MUC1, POSTN, ENO2, CEACAM5, VEGFA, LCN2, NKX2-1, MDK, FSTL1, KRAS, TK1, EBAG9
C0086692	Benign Neoplasm	2.06	0.00	ADH1B, IGFBP2, ADH1A, CLDN1, KRT19, FBLN1, CDH1, CLDN4, ADH1C, CCL2, ADH4, MMP14, AQP1, IGFBP3, ID1, CEACAM5, E2F1, GDF15, RGS5, VEGFA, SEMA3F, PLXNA2, LCN2, MKI67, KIF1A, ...
C0158266	Intervertebral Disc Degeneration	1.99	0.00	ADH1B, IGFBP5, APOE, IGFBP6, BGN, KIAA1217, MMP2, HTRA1, MMP14, MUC1, POSTN, TIMP3, COL1A1, IGFBP3, KRT8, TBPL1, CDK9, TFAP2A, BMP2, AIMP2, VEGFA, NDUFA4L2, COL3A1, TRPV4, FSTL1, ...
C1134719	Invasive Ductal Breast Carcinoma	1.86	0.00	ADH1B, CDH1, CLDN4, MUC5AC, APOC1, CCL2, MMP2, ADH4, MMP14, COL5A1, MUC1, POSTN, TIMP3, RHBDF1, CEACAM5, FHIT, KRT8, VEGFA, PTTG1, LCN2, MKI67, CLDN7, MSR1, MAD2L1, CCN1, ...
C0345905	Intrahepatic Cholangiocarcinoma	1.79	0.00	KRT19, FBLN1, CDH1, CLDN4, CD276, HSPG2, MUC5AC, BGN, CCL2, MMP2, MUC1, POSTN, CDK4, CEACAM5, FHIT, RCOR3, SDC1, UHRF2, AIMP2,

ID	Term	NES	Adj. P-Value	Genes
				VEGFA, LCN2, ASPH, PROM1, VASH1, ARG1, ...
C0033999	Pterygium	2.04	0.00	IGFBP2, CDH1, CLDN4, COL1A2, FBN1, MMP2, MMP14, POSTN, IGFBP3, LAPTM4B, AIMP2, VEGFA, PLXNA2, S100B, COL3A1, PRDX2, TRPV4, EFEMP1, GABPA, ANGPTL4, XRCC6, NHP2, FKBP10, COL4A1, SPRR3, ...
C4284013	Primary cholangiocarcinoma of intrahepatic biliary tract	1.94	0.00	KRT19, FBLN1, CDH1, CD276, HSPG2, MUC5AC, MMP2, MUC1, POSTN, CDK4, CEACAM5, SDC1, UHRF2, VEGFA, ASPH, PROM1, SHMT2, THY1, COL3A1, CCHCR1, FLT4, RBP1, CPS1, TYMS, TRAF4, ...
C0007124	Noninfiltrating Intraductal Carcinoma	1.73	0.00	ADH1B, CLDN1, KRT19, CDH1, CD276, ADH1C, MMP2, ADH4, MUC1, POSTN, SCGB3A1, COL1A1, DDR1, IGFBP3, PCBP4, SOX2, FHIT, TBPL1, SDC1, KRT18, TFAP2A, BMP2, VEGFA, ELF3, PARP1, ...
C0029434	Osteogenesis Imperfecta	2.22	0.00	SERPINH1, BGN, COL1A2, COL5A1, COL1A1, COL3A1, LAMC2, LRP5, FKBP10, SLC6A2, MBTPS2, RNASE1, BMP1, PLS3, FN1, SMAD4, SERPINF1, MTCO2P12, TSHR, ACVR2B, FGFR3, GPR180, DCN, TNC, PLOD2, ...
C0023896	Alcoholic Liver Diseases	1.98	0.00	ADH1B, ADH1A, HSPG2, ADH1C, SAA1, CCL2, RBP4, ADH4, CEACAM5, KRT8, KRT18, CERS6, EGR1, APOA1, GABPA, GSTA4, HAMP, EIF2S1, XPR1, CYP2E1, PSMD14, NXN, ELANE, MIF, AKR1A1, ...
C0026267	Mitral Valve Prolapse Syndrome	2.12	0.00	COL1A2, FBN1, MMP2, MMP14, COL5A1, COL1A1, TTN, PCGF2, COL3A1, SCD, KRAS, HRAS, HSPD1, COL5A2, SLC6A2, ABO, VPS13B, BAZ1B, XYLT1, BMP4, PLAU, TAB2, TPM2, AEBP1, TSHR, ...
C0085136	Central Nervous System Neoplasms	2.02	0.00	AMBP, IGFBP2, CDH1, CD276, APOE, CCL2, AQP1, DDR1, RHBDF1, CDK4, VEGFA, DES, PARP1, PROM1, PHLDB1, NKX2-1, LAMC2, PRAME, BRCA2, ALB, PAWR, NES, ERCC1, MTCO2P12, PLAU, ...
C0028259	Nodule	1.90	0.00	KRT19, CDH1, PLAAT3, BGN, MMP2, HTRA1, SFTPA1, AQP1, COL1A1,

ID	Term	NES	Adj. P-Value	Genes
				MVD, IGFBP3, CEACAM5, BMP2, VEGFA, CHGA, PLXNA2, DES, PROM1, MAD2L1, S100B, ADCY6, ITIH5, SFN, PRDX2, KRAS, ...
C1368683	Epithelioma	1.83	0.00	KRT19, FBLN1, CDH1, MMP2, MMP14, MUC1, TTN, SOX2, CEACAM5, FHIT, SDC1, ST14, VEGFA, ELF3, PTK2, PROM1, S100B, POU2F1, MDK, SCD, HSPB1, TYMS, KRAS, HRAS, NOTCH3, ...
C1260959	Drusen	2.29	0.00	APOE, APOB, CFI, HTRA1, TIMP3, VEGFA, PLXNA2, APP, EFEMP1, VTN, GABPA, ALB, CRYAB, XYLT1, CFB

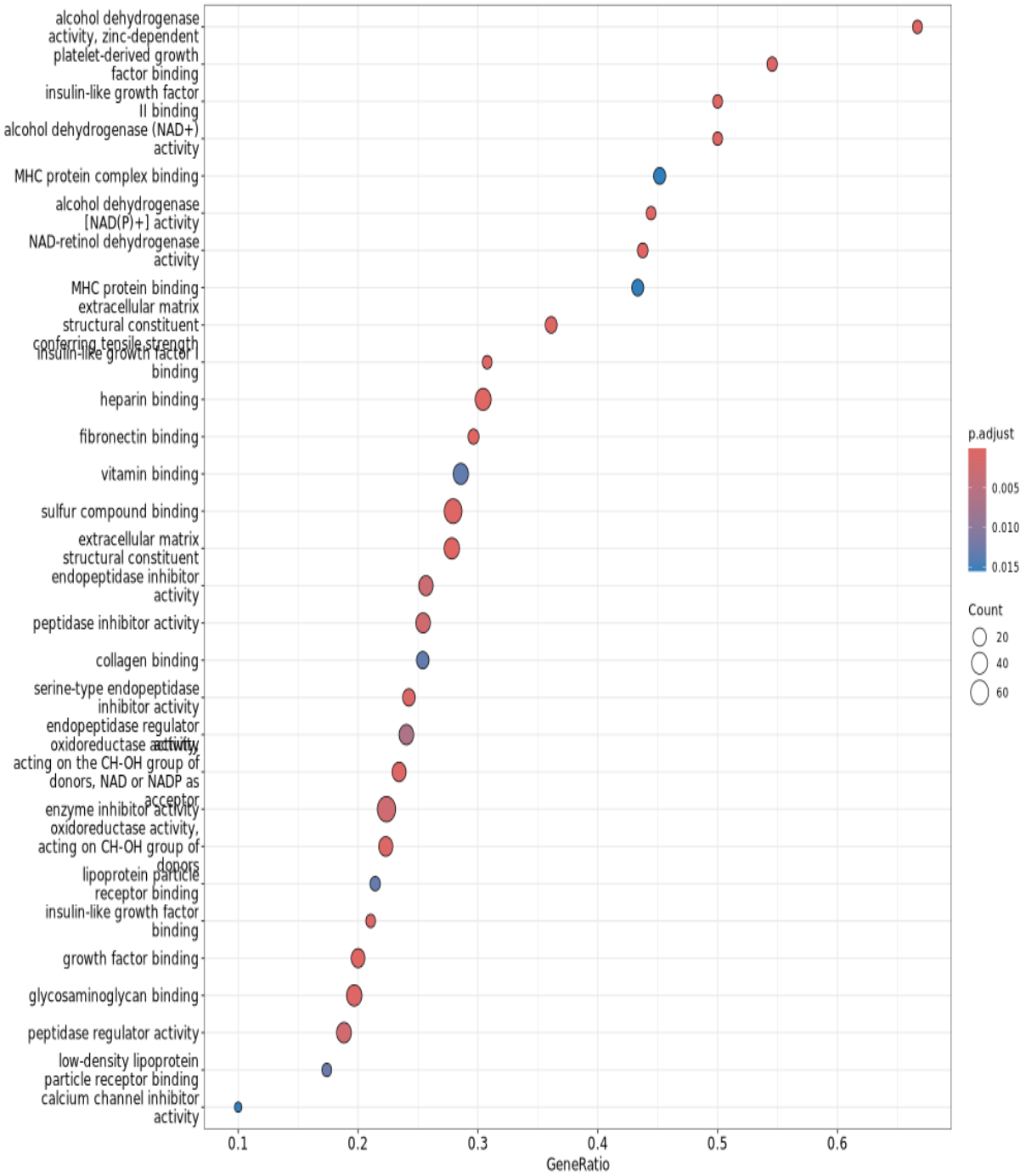

Figure K.3. Dotplot of enriched pathways from *Disease Gene Network* in Favourable (Partial Response, Stable Disease) compared to Unfavourable (Progressive Disease, Died).. Dots represent enriched pathways, with size indicating gene count and colour showing significance (e.g., adjusted p-value).

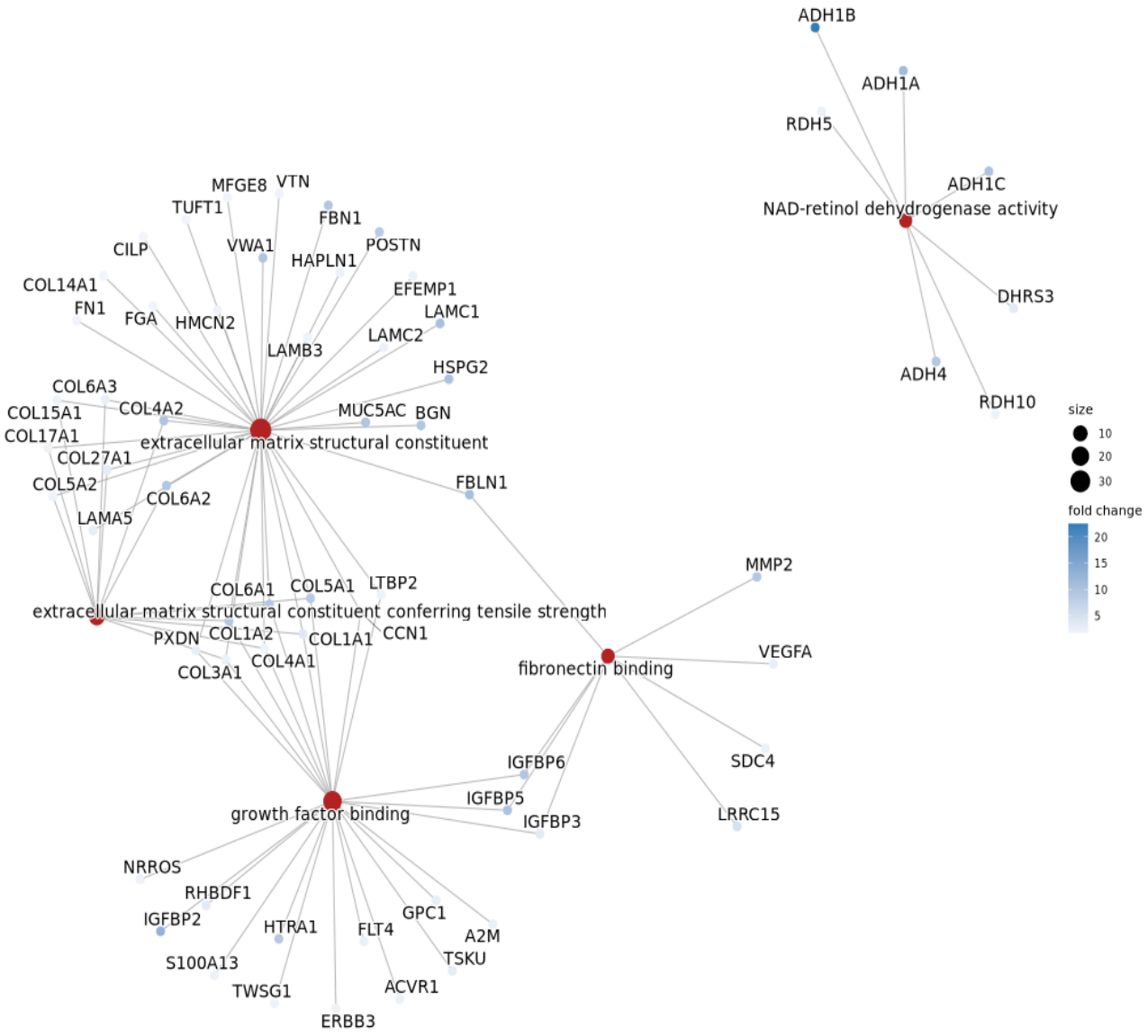

Figure K.4. Cnetplot of gene-pathway relationships from *Disease Gene Network*. Pathways and their associated genes are connected, with node size and edge thickness indicating enrichment and shared genes.

GO Molecular Function GSEA:

Based on gene expression, we identified **30 up-regulated** and **3 down-regulated** terms from *GO Molecular Function* using GSEA (Ashburner et al. 2000; Gene Ontol. Resour. 2025). The most significantly up-regulated terms were **extracellular matrix structural constituent** (NES:

2.419), **growth factor binding** (NES: 2.2577), **fibronectin binding** (NES: 2.3856). The most significantly down-regulated terms were **MHC protein binding** (NES: -2.0467), **MHC protein complex binding** (NES: -2.0399), and **MHC class I protein complex binding** (NES: -2.0617).

Table K.3. Top 15 enriched terms from GO Molecular Function in Partial Response, Stable Disease compared to Progressive Disease, Died. Based on gene expression

ID	Term	NES	Adj. P-Value	Genes
GO:0005201	extracellular matrix structural constituent	2.42	0.00	FBLN1, LAMC1, HSPG2, COL4A2, VWA1, MUC5AC, BGN, COL1A2, COL6A2, FBN1, COL6A1, COL5A1, POSTN, COL1A1, COL27A1, LAMA5, COL6A3, PXDN, CCN1, COL3A1, LAMC2, COL15A1, EFEMP1, HAPLN1, LTBP2, ...
GO:0019838	growth factor binding	2.26	0.00	IGFBP2, IGFBP5, IGFBP6, COL1A2, COL6A1, HTRA1, COL5A1, COL1A1, IGFBP3, RHBDF1, TSKU, GPC1, PXDN, A2M, CCN1, COL3A1, ACVR1, FLT4, NRROS, S100A13, LTBP2, TWSG1, COL4A1, ERBB3
GO:0001968	fibronectin binding	2.39	0.00	FBLN1, IGFBP5, IGFBP6, MMP2, LRRC15, IGFBP3, VEGFA, SDC4
GO:0030020	extracellular matrix structural constituent conferring tensile strength	2.36	0.00	COL4A2, COL1A2, COL6A2, COL6A1, COL5A1, COL1A1, COL27A1, COL6A3, COL3A1, COL15A1, COL5A2, COL17A1, COL4A1
GO:0004745	NAD-retinol dehydrogenase activity	2.23	0.00	ADH1B, ADH1A, ADH1C, ADH4, DHRS3, RDH5, RDH10
GO:0018455	alcohol dehydrogenase [NAD(P)+] activity	2.08	0.00	ADH1B, ADH1A, ADH1C, ADH4
GO:0031995	insulin-like growth factor II binding	2.06	0.00	IGFBP2, IGFBP5, IGFBP6, IGFBP3
GO:0008201	heparin binding	1.96	0.00	APOE, SOD3, APOB, FBN1, SAA1, COL5A1, POSTN, PTPRS, NAV2, VEGFA, CCN1, LAMC2, MDK, FSTL1, APP, LTBP2, VTN, TWSG1, COL17A1, PRSS57, FN1, SLIT2, MPO, FGF9, BMP4, ...

ID	Term	NES	Adj. P-Value	Genes
GO:0016616	oxidoreductase activity, acting on the CH-OH group of donors, NAD or NADP as acceptor	2.02	0.00	ADH1B, ADH1A, ADH1C, ADH4, DHRS3, KDSR, CBR1, RDH5, CRYL1, AKR1B10, PRXL2B, RDH10, ALDH3A1, AKR1C2, IDH3B, NSDHL, ADHFE1, LDHA, ME1, HSD3B7, CBR3, RDH11, DHRS11, SDR42E1, IDH3A, ...
GO:0048407	platelet-derived growth factor binding	2.14	0.00	COL1A2, COL6A1, COL5A1, COL1A1, COL3A1, COL4A1
GO:0016614	oxidoreductase activity, acting on CH-OH group of donors	1.99	0.00	ADH1B, ADH1A, ADH1C, ADH4, DHRS3, KDSR, GPD2, CBR1, RDH5, CRYL1, AKR1B10, PRXL2B, RDH10, ALDH3A1, AKR1C2, IDH3B, NSDHL, ADHFE1, LDHA, ME1, HSD3B7, CBR3, RDH11, DHRS11, SDR42E1, ...
GO:0004024	alcohol dehydrogenase activity, zinc-dependent	1.94	0.00	ADH1B, ADH1A, ADH1C, ADH4
GO:1901681	sulfur compound binding	1.82	0.00	APOE, SOD3, APOB, FBN1, SAA1, COL5A1, POSTN, PTPRS, NAA80, NAV2, VEGFA, HLCS, MOCS1, CCN1, SUMF1, LAMC2, MDK, FSTL1, APP, LTBP2, VTN, TWSG1, KMT5C, COL17A1, BMT2, ...
GO:0004022	alcohol dehydrogenase (NAD+) activity	2.03	0.00	ADH1B, ADH1A, ADH1C, ADH4
GO:0005539	glycosaminoglycan binding	1.82	0.00	APOE, SOD3, APOB, BGN, FBN1, SAA1, COL5A1, POSTN, PTPRS, NAV2, VEGFA, CCN1, LAMC2, MDK, FSTL1, APP, HAPLN1, LTBP2, VTN, TWSG1, COL17A1, PRSS57, PODXL2, FN1, SEMA5A, ...

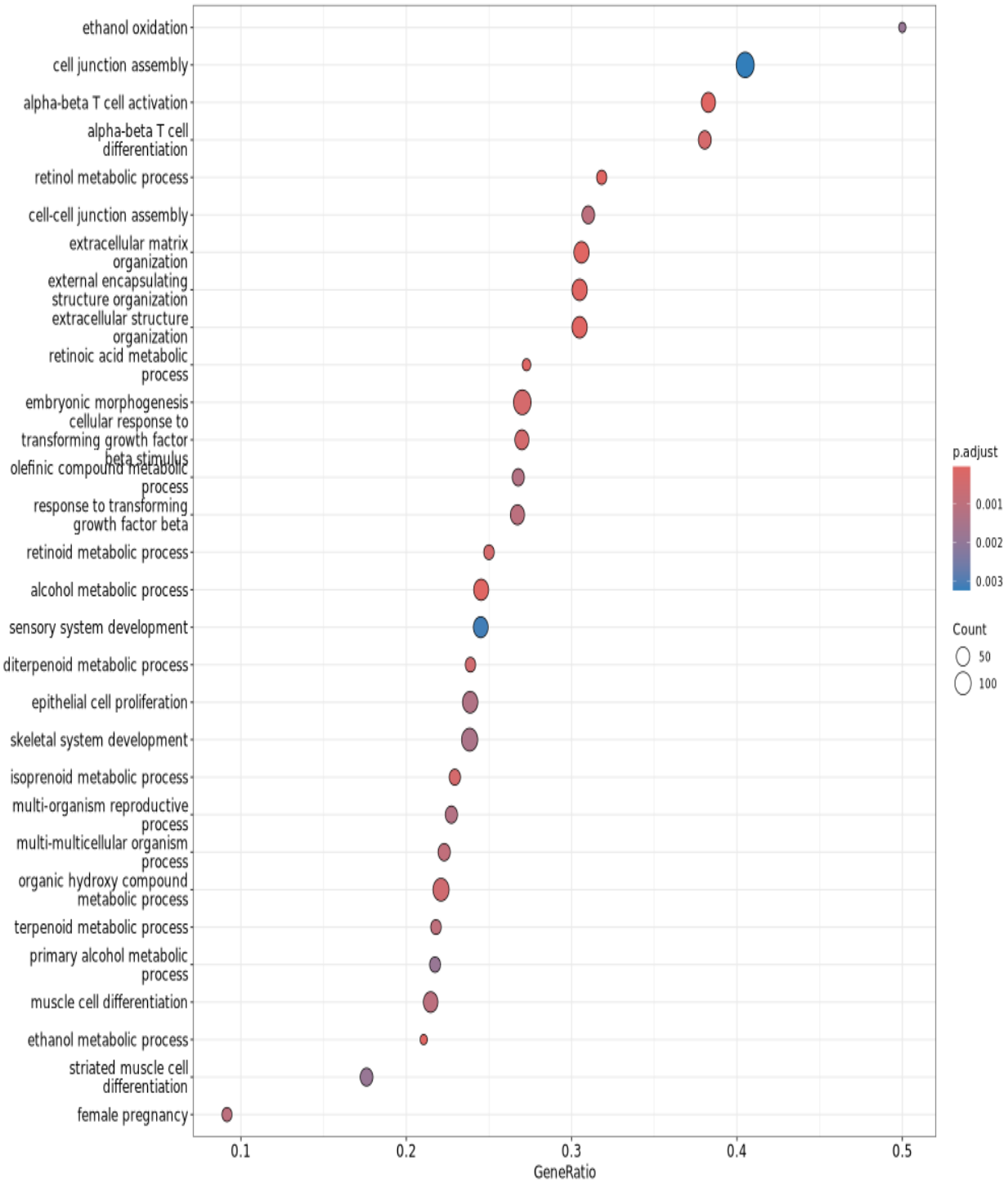

Figure K.5. Dotplot of *GO Molecular Function* enriched pathways. Dots represent enriched pathways, with size indicating gene count and colour showing significance (e.g., red = low, blue = higher adjusted p-value).

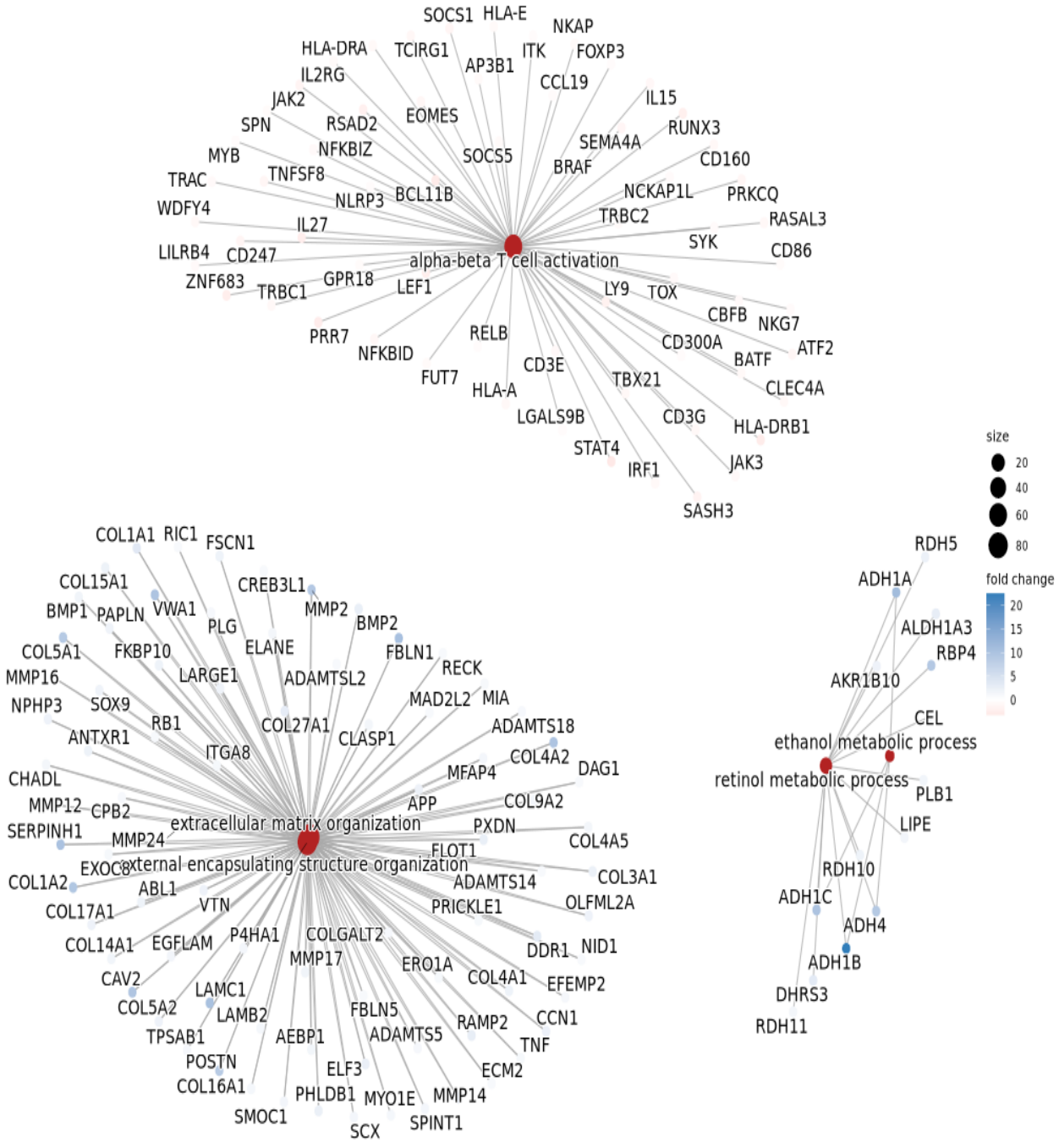

Figure K.6. Cnetplot of *GO Molecular Function* gene-pathway relationships. Pathways and their associated genes are connected, with node size and edge thickness indicating enrichment and shared genes.

GO Biological Processes GSEA

We identified **140 up-regulated** and **14 down-regulated** terms from GO Biological Process in group "Partial Response, Stable Disease" compared to group "Progressive Disease, Died" (). The most significantly up-regulated terms were **ethanol metabolic process, retinol metabolic process, extracellular matrix organization**. The most significantly down-regulated terms were **alpha-beta T cell activation, alpha-beta T cell differentiation, positive regulation of alpha-beta T cell activation**.

Table K.4. Top 15 enriched terms from GO Biological Process in Partial Response, Stable Disease compared to Progressive Disease, Died. based on gene expression.

ID	Term	NES	Adj. P-Value	Genes
GO:0006067	ethanol metabolic process	2.36	0.00	ADH1B, ADH1A, ADH1C, ADH4
GO:0042572	retinol metabolic process	2.34	0.00	ADH1B, ADH1A, ADH1C, RBP4, ADH4, DHRS3, ALDH1A3, RDH5, AKR1B10, RDH10, PLB1, LIPE, CEL, RDH11
GO:0046631	alpha-beta T cell activation	-2.00	0.00	CD300A, CCL19, FOXP3, NLRP3, MYB, ITK, RELB, LGALS9B, SPN, CD86, GPR18, NCKAP1L, NKG7, SYK, TRBC2, IL2RG, SOCS5, HLA-E, AP3B1, NKAP, FUT7, TRAC, LILRB4, TOX, CBFB, ...
GO:0030198	extracellular matrix organization	1.89	0.00	FBLN1, LAMC1, SERPINH1, COL4A2, VWA1, CAV2, COL1A2, MMP2, MMP14, COL5A1, POSTN, COL1A1, DDR1, COL27A1, RAMP2, BMP2, PXDN, ELF3, PHLDB1, CCN1, COL3A1, APP, COL15A1, ANTXR1, NPHP3, ...
GO:0045229	external encapsulating structure organization	1.89	0.00	FBLN1, LAMC1, SERPINH1, COL4A2, VWA1, CAV2, COL1A2, MMP2, MMP14, COL5A1, POSTN, COL1A1, DDR1, COL27A1, RAMP2, BMP2, PXDN, ELF3, PHLDB1, CCN1, COL3A1, APP, COL15A1, ANTXR1, NPHP3, ...
GO:0043062	extracellular structure organization	1.88	0.00	FBLN1, LAMC1, SERPINH1, COL4A2, VWA1, CAV2, COL1A2, MMP2, MMP14, COL5A1, POSTN, COL1A1, DDR1, COL27A1, RAMP2, BMP2, PXDN, ELF3, PHLDB1, CCN1, COL3A1, APP, COL15A1, ANTXR1, NPHP3, ...
GO:0006066	alcohol metabolic process	1.81	0.00	ADH1B, ADH1A, APOE, ADH1C, APOB, APOC1, RBP4, ADH4, MVD, DHRS3, RFT1, TSKU, ALDH1A3, BMP2, GPD2, ISYNA1, PPIP5K1, RDH5, APP, PLPP2, SPTSSA, LRP5, DEGS2, DHCR7, APOA1, ...

ID	Term	NES	Adj. P-Value	Genes
GO:0042573	retinoic acid metabolic process	2.31	0.00	ADH1B, ADH1A, ADH1C, ALDH1A3, RBP1, RDH10
GO:0048598	embryonic morphogenesis	1.61	0.00	COL4A2, FBN1, COL6A1, MMP2, RBP4, HOXB5, MMP14, COL5A1, GRHL2, SOX2, LAMA5, ALDH1A3, TRIM28, TFAP2A, SIX4, CDON, ST14, PCGF2, WLS, TBX2, IFT122, PHLDB1, SLC39A1, CCN1, SDC4, ...
GO:0001523	retinoid metabolic process	2.20	0.00	ADH1B, ADH1A, ADH1C, RBP4, ADH4, DHRS3, ALDH1A3, RDH5, RBP1, AKR1B10, RDH10, RARRES2, PLB1, LIPE, CEL, RDH11
GO:0046632	alpha-beta T cell differentiation	-2.03	0.00	CCL19, FOXP3, NLRP3, MYB, ITK, RELB, SPN, CD86, GPR18, NCKAP1L, SYK, IL2RG, SOCS5, AP3B1, NKAP, FUT7, LILRB4, TOX, CBFB, NFKBIZ, BRAF, IRF1, BATF, HLA-DRA, JAK3, ...
GO:0006720	isoprenoid metabolic process	2.03	0.00	ADH1B, ADH1A, ADH1C, RBP4, ADH4, MVD, DHRS3, RFT1, ALDH1A3, RDH5, RBP1, AKR1B10, RDH10, DOLPP1, ALG13, ALG3, DPAGT1, DPM3, CYP2E1, RARRES2, PLB1, LIPE, ALG2, CEL, RDH11
GO:0071560	cellular response to transforming growth factor beta stimulus	1.81	0.00	CLDN1, COL4A2, CAV2, COL1A2, FBN1, HTRA1, POSTN, COL1A1, BAMBI, ID1, GDF15, BMP2, PTK2, PARP1, NKX2-1, COL3A1, ACVR1, SPRY1, NRROS, SAP130, CRKL, SPRY2, LTBP2, SMURF1, TWSG1, ...
GO:0016101	diterpenoid metabolic process	2.16	0.00	ADH1B, ADH1A, ADH1C, RBP4, ADH4, DHRS3, ALDH1A3, RDH5, RBP1, AKR1B10, RDH10, RARRES2, PLB1, LIPE, CEL, RDH11
GO:1901615	organic hydroxy compound metabolic process	1.62	0.00	ADH1B, ADH1A, APOE, ADH1C, APOB, APOC1, RBP4, ADH4, MVD, DHRS3, RFT1, TSKU, ALDH1A3, BMP2, GPD2, ISYNA1, PPIP5K1, RDH5, ACOT8, NQO1, APP, PLPP2, SPTSSA, LRP5, DEGS2, ...

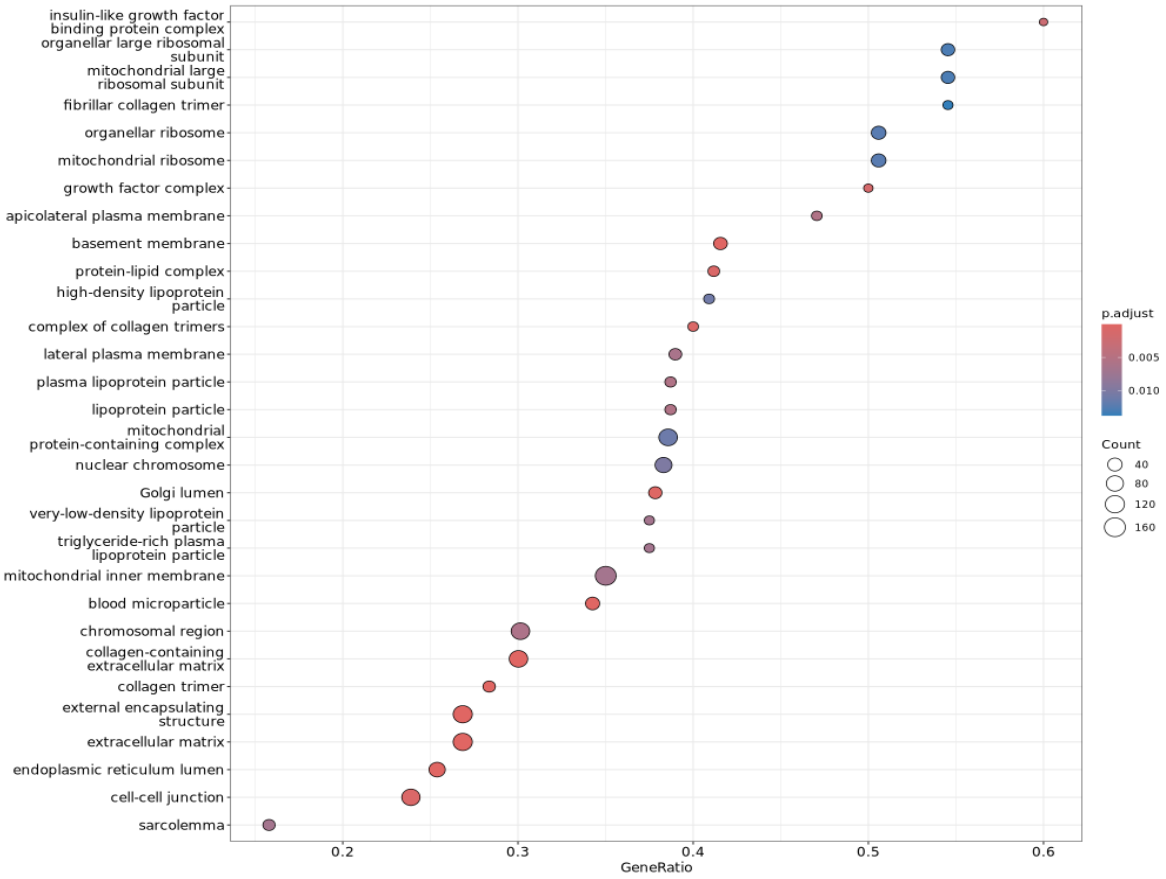

Figure K.7. Dotplot of *GO Biological Process* enriched pathways. Dots represent enriched pathways, with size indicating gene count and colour showing significance (e.g., red = lower and blue = higher adjusted p-value).

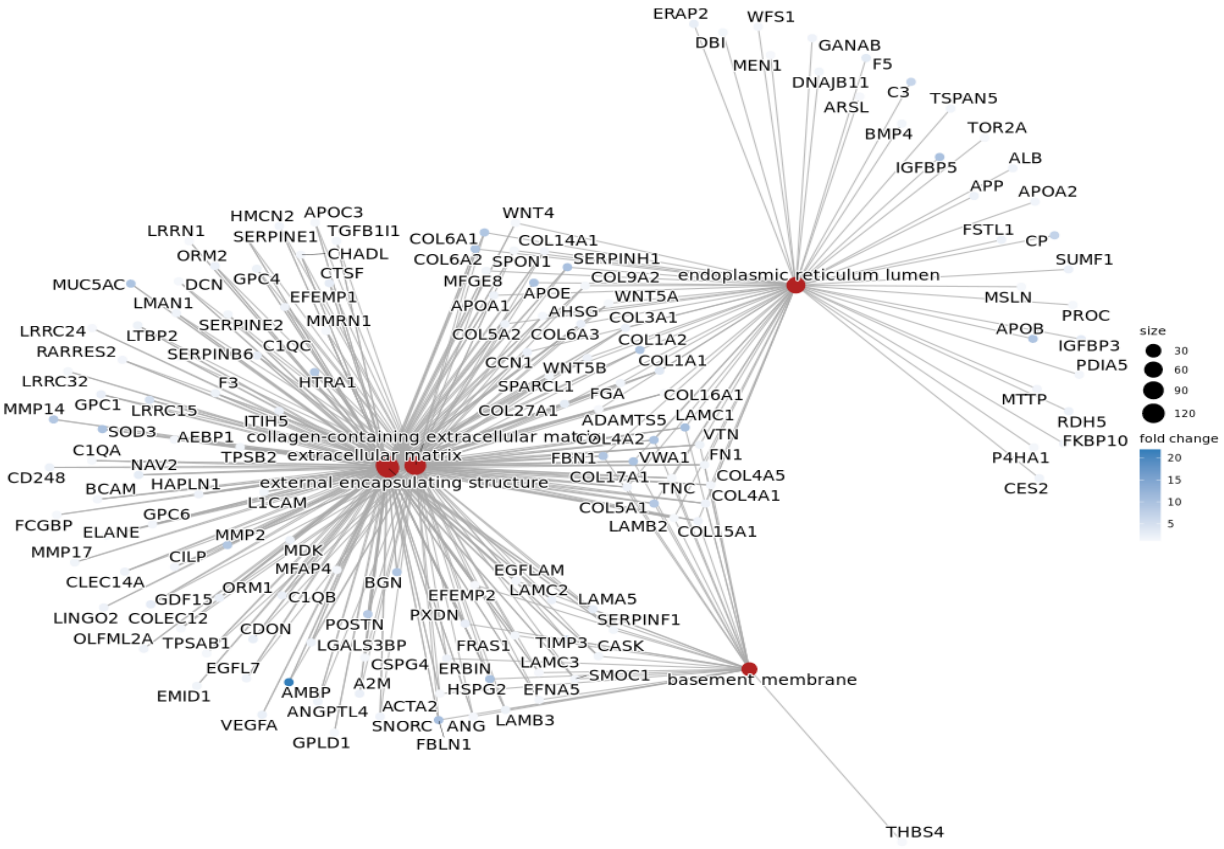

Figure K.8. Cnetplot of *GO Biological Process* gene-pathway relationships. Pathways and their associated genes are connected, with node size and edge thickness indicating enrichment and shared genes.

GO Cellular Component GSEA:

We identified **41 up-regulated** and **4 down-regulated** terms from GO Cellular Component in group "Partial Response, Stable Disease" compared to group "Progressive Disease, Died". The most significantly up-regulated terms were **collagen-containing extracellular matrix, external encapsulating structure, a**nd **extracellular matrix**. The most significantly down-regulated terms were **immunological synapse, MHC class II protein complex,** and MHC **protein complex**.

Table K.5. Top 15 enriched terms from *GO Cellular Component* in Partial Response, Stable Disease compared to Progressive Disease, Died. based on gene expression.

ID	Term	NES	Adj. P-Value	Genes
GO:0062023	collagen-containing extracellular matrix	2.25	0.00	AMBP, FBLN1, LAMC1, SERPINH1, HSPG2, APOE, SOD3, COL4A2, VWA1, BGN, COL1A2, COL6A2, FBN1, COL6A1, MMP2, HTRA1, COL5A1, POSTN, TIMP3, LRRC15, COL1A1, CTSF, COL27A1, NAV2, GDF15, ...
GO:0030312	external encapsulating structure	2.12	0.00	AMBP, FBLN1, LAMC1, SERPINH1, HSPG2, APOE, SOD3, COL4A2, VWA1, MUC5AC, BGN, COL1A2, COL6A2, FBN1, COL6A1, MMP2, HTRA1, MMP14, COL5A1, POSTN, TIMP3, LRRC15, COL1A1, CTSF, COL27A1, ...
GO:0031012	extracellular matrix	2.12	0.00	AMBP, FBLN1, LAMC1, SERPINH1, HSPG2, APOE, SOD3, COL4A2, VWA1, MUC5AC, BGN, COL1A2, COL6A2, FBN1, COL6A1, MMP2, HTRA1, MMP14, COL5A1, POSTN, TIMP3, LRRC15, COL1A1, CTSF, COL27A1, ...
GO:0005788	endoplasmic reticulum lumen	2.05	0.00	LAMC1, SERPINH1, IGFBP5, APOE, COL4A2, VWA1, APOB, COL1A2, COL6A2, FBN1, COL6A1, COL5A1, CP, C3, COL1A1, F5, IGFBP3, COL27A1, ERAP2, COL6A3, CCN1, SUMF1, COL3A1, RDH5, FSTL1, ...
GO:0005604	basement membrane	2.24	0.00	FBLN1, LAMC1, HSPG2, COL4A2, VWA1, FBN1, COL5A1, TIMP3, LAMA5, PXDN, LAMC2, ERBIN, COL15A1, LAMB3, VTN, COL17A1, COL4A1, FN1, CASK, SERPINF1, SMOC1, FRAS1, EGFLAM, EFNA5, COL4A5, ...
GO:0005581	collagen trimer	2.27	0.00	COL4A2, COL1A2, COL6A2, COL6A1, COL5A1, SFTPA1, COL1A1, COL27A1, C1QC, COL6A3, C1QB, MSR1, COL3A1, COL15A1, COL5A2, COL17A1, COL4A1, EMID1, COL14A1
GO:0072562	blood microparticle	2.09	0.00	AMBP, APOE, CP, C3, IGHG4, HBG2, C1QC, HSPA1B, IGHG3, C1QB, A2M, ORM1, ORM2, LGALS3BP, APOA1, VTN, ANGPTL4, ALB, FN1, APOA2, FGA, CFB, C1R, GC, C1S, ...
GO:0005796	Golgi lumen	2.11	0.00	HSPG2, SOD3, MUC5AC, BGN, MMP14, MUC1, SDC1, GPC1, SDC4, APP, WNT5B, VTN, GPC4, PODXL2, DEFA3, GPC6, MUC13, WNT4, DCN, WNT5A,

ID	Term	NES	Adj. P-Value	Genes
				CSPG4, PROC, MMP16, PCSK5, PPIL2, ...
GO:0098644	complex of collagen trimers	2.17	0.00	COL4A2, COL1A2, COL5A1, COL1A1, COL27A1, COL3A1, COL5A2, COL4A1
GO:0032994	protein-lipid complex	2.16	0.00	APOE, APOB, SAA1, APOC1, MSR1, PEX3, APOA1, LSR, APOA2, PLTP, DBI, APOC3, HDLBP, PON1
GO:0005911	cell-cell junction	1.58	0.00	CLDN1, CDH1, CLDN4, PKP3, CDCA3, GRHL2, RASIP1, CLDN12, CDK4, CDC42BPB, KRT8, DLG5, TNKS1BP1, KRT18, PARD3, NFASC, ESAM, VEGFA, DES, SYNM, ATP1B1, CLDN7, OBSL1, TMEM47, TRPV4, ...
GO:0036454	growth factor complex	2.00	0.00	IGFBP5, IGFBP6, IGFBP3, VEGFA
GO:0016942	insulin-like growth factor binding protein complex	1.83	0.00	IGFBP5, IGFBP6, IGFBP3
GO:0034358	plasma lipoprotein particle	2.10	0.01	APOE, APOB, SAA1, APOC1, MSR1, APOA1, LSR, APOA2, PLTP, APOC3, HDLBP, PON1
GO:1990777	lipoprotein particle	2.10	0.01	APOE, APOB, SAA1, APOC1, MSR1, APOA1, LSR, APOA2, PLTP, APOC3, HDLBP, PON1

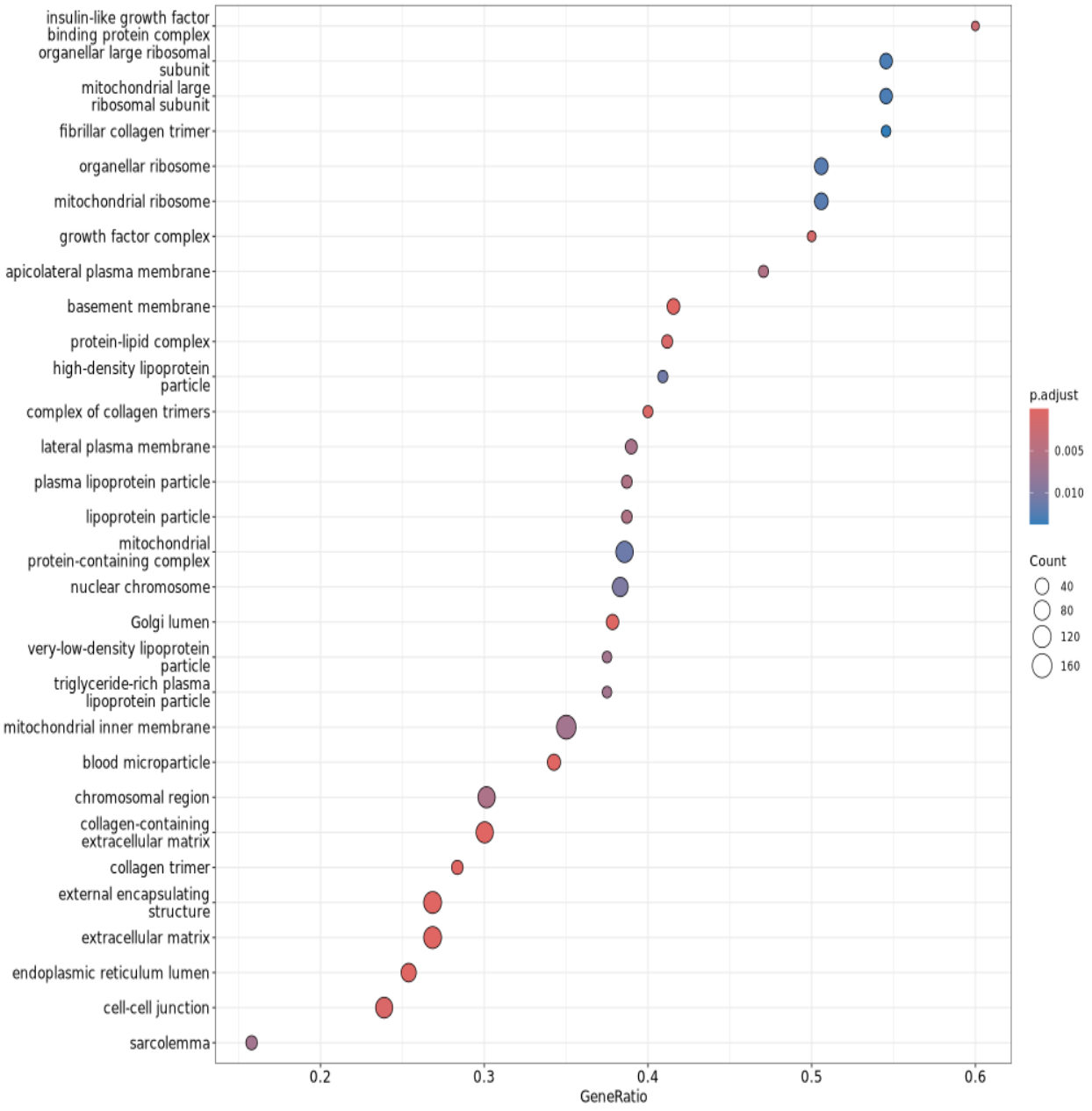

Figure K.9. Dotplot of *GO Cellular Component* enriched pathways. Dots represent enriched pathways, with size indicating gene count and colour showing significance (e.g., red = lower and blue = higher adjusted p-value.

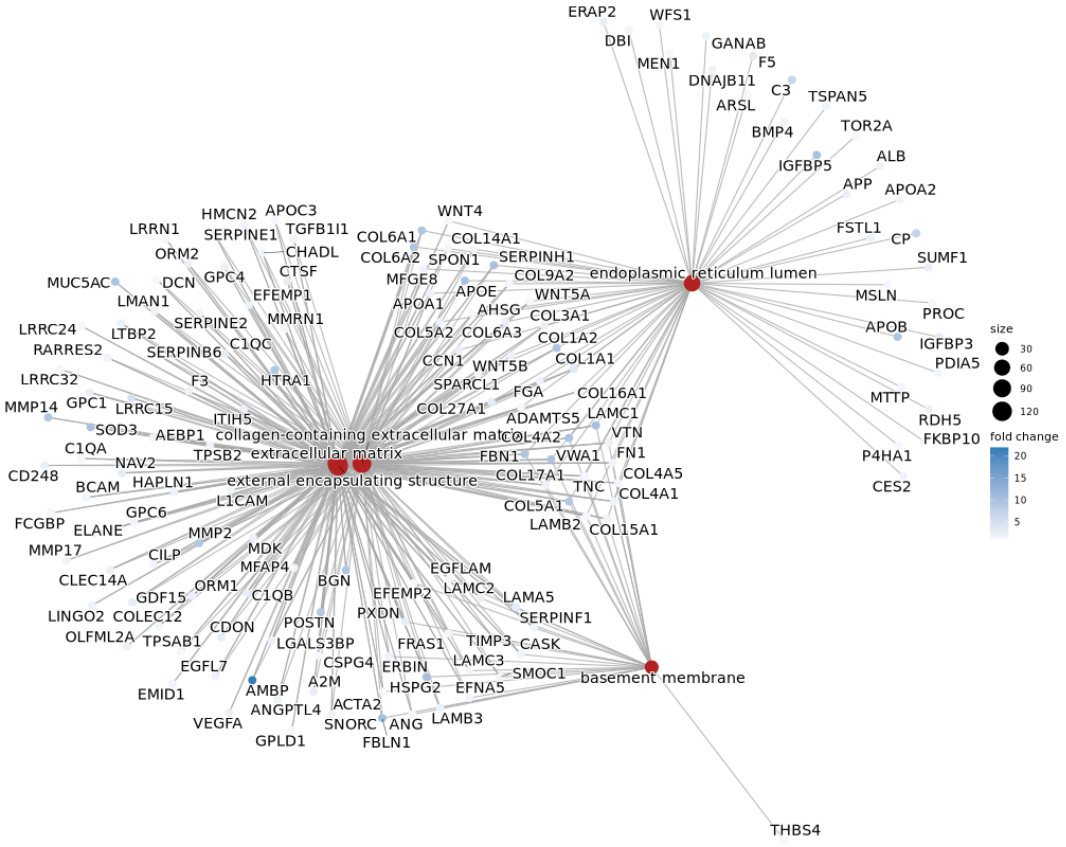

Figure K.10. Cnetplot of *GO Cellular Component* gene-pathway relationships. Pathways and their associated genes are connected, with node size and edge thickness indicating enrichment and shared genes.